# Seawater Systems for Sustainable Development: Evaluation of a Marine Microalgal Strain as Biomass Feedstock for Hypersaline Bioethanol Production

A thesis submitted in fulfilment of the requirements for the degree of

Doctor of Philosophy

May 2018

Quang Cong Doan

Faculty of Engineering, Computer and Mathematical Sciences

School of Chemical Engineering


THE UNIVERSITY of ADELAIDE

Australia

(This page intentionally left blank)

*"One can see from space how the human race has changed the Earth. Nearly all of the available land has been cleared of forest and is now used for agriculture or urban development. The polar icecaps are shrinking and the desert areas are increasing. At night, the Earth is no longer dark, but large areas are lit up. All of this is evidence that human exploitation of the planet is reaching a critical limit. But human demands and expectations are ever-increasing. We cannot continue to pollute the atmosphere, poison the ocean and exhaust the land. There isn't any more available."*

Stephen Hawking

*"We cannot solve a problem by using the same kind of thinking we used when we created them."*

Albert Einstein

*"Rethink tomorrow"*

Novozymes A/S

(This page intentionally left blank)

# Executive Summary

The potential of microalgal biomass as a feedstock for bioethanol fermentation has been widely considered alongside the mix of other bioenergy streams. Yet only a modest level of research has been reported in this area compared to other renewable feedstock for bioethanol. Use of marine microalgae from seawater systems provides greater sustainability at the scale required for biofuels to circumvent reliance on fresh water, but presents processing challenges associated with fermentation of hypersaline biomass. The marine microalgae *Tetraselmis* sp. strain MUR-233 was selected based on biomass productivity as part of a broader Australian Research Council Linkage Project (ARCLP 100200616) to assess the diversification of energy streams from microalgae. Detailed carbohydrate analysis was conducted on monoculture isolates of this strain to assess its potential as a bioethanol feedstock. MUR-233 when cultivated for biomass productivity had a total carbohydrate content that ranged from 6.8 % to 11 % ash free dry weight (afdw). The cell wall carbohydrates of MUR-233 were composed primarily of 3-deoxy-manno-2-octulosonic acid and galactose, present at respective quantities of up to 63.1 % and 19.3 % molar ratio of cell wall carbohydrates. Accumulated intracellular starch was the key variant with biomass total carbohydrate composition, and could be enriched to an average of 47 % afdw when MUR-233 was cultured under continuous illumination at 7 % salinity in hypersaline seawater. Glucose from starch was determined to be the primary substrate from MUR-233 biomass for ethanologenic conversion. For utilising the starch-enriched hypersaline MUR-233 biomass, the filamentous fungus *Rhizopus oryzae* NRRL 1526 was found to possess sufficient facultative halotolerance for simultaneous saccharification and fermentation of the material in its undiluted hypersaline state. Performance tests on NRRL 1526 had determined that in nutrient rich control medium it was able to survive, grow and produce ethanol in hypersaline submersed culture at up to 10.5 % salinity in sea salt, although increasing salt concentrations had a negative impact on fungal growth and ethanol production. Starch enzymatic hydrolysis by the fungus was not impacted up to 7 % salinity, indicating that the native starch degrading enzymes of NRRL 1526 were halotolerant. It was found

that although this fungal strain was capable of producing up to 26.1 $g \cdot L^{-1}$ ethanol with an 84.8 % conversion efficiency (or percent yield), when fed with hypersaline MUR-233 biomass there was a shift in carbon flux towards other metabolic products. At 7 % salinity ethanol was still the major product of NRRL 1526 from assimilation of MUR-233 biomass, ranging between 9.62 $g \cdot L^{-1}$ to 11.24 $g \cdot L^{-1}$, but the percent ethanol yield was reduced to as low as 44.8 %. Under these conditions, lactic acid was also produced. The studies conducted herein addressed a knowledge gap about whether hypersaline *Tetraselmis* marine microalgal biomass produced in seawater could be fermented to ethanol through selective use of a halotolerant microorganism, confirming that such an approach was possible. However, the dilute aqueous nature of MUR-233 biomass and its fermentable substrates presents significant challenges to the feasible use of this alternative biomass feedstock for microbial bioethanol production.

# Declaration

I certify that this work contains no material which has been accepted for the award of any other degree or diploma in my name, in any university or other tertiary institution and, to the best of my knowledge and belief, contains no material previously published or written by another person, except where due reference has been made in the text. In addition, I certify that no part of this work will, in the future, be used in a submission in my name, for any other degree or diploma in any university or other tertiary institution without the prior approval of the University of Adelaide and where applicable, any partner institution responsible for the joint-award of this degree.

I acknowledge that copyright of published works contained within this thesis resides with the copyright holder(s) of those works.

I also give permission for the digital version of my thesis to be made available on the web, via the University's digital research repository, the Library Search and also through web search engines, unless permission has been granted by the University to restrict access for a period of time.

I acknowledge the support I have received for my research through the provision of an Australian Government Research Training Program Scholarship, and a Joint Research Engagement (JRE) Engineering Cadetship Grant provided by the Australian Government Department of Education and Training.

This research was supported under Australian Research Council's (ARC) Linkage Projects funding scheme (Project ARCLP 100200616) with industry partner SQC Pty Ltd, and the Australian Renewable Energy Agency (ARENA) advanced biofuels investment readiness program funding agreement number Q00150. The views expressed herein are mine and are not necessarily those of the ARC or ARENA.

Signature of Candidate: Date:

(This page intentionally left blank)

# Acknowledgements

On my original mission to save the planet from the terror of global warming, I ignored all seemingly extraneous suggestions that my biochemistry knowledge and industry experience might be better diverted to finding high-value products in algae. After all, recycling sequestrated carbon dioxide into biofuels from prolific marine microalgae would power our indispensable cars whilst saving more fresh water for our everyday lives and food production, pull the brakes on global greenhouse gas emissions and, most importantly, save the coral reefs. All it really took was an optimistic meeting with a resourceful academic named David Lewis, and my journey had begun.

Firstly, therefore, I would like to acknowledge and thank my supervisors Professor David Lewis and Dr Tommaso Liccioli Watson for sticking around on this journey. They have been invaluable in guiding me to the end, generous in sharing their insight and knowledge, and persistent with encouragement that was much needed at times. It really has been a long journey, and I hope that this thesis goes towards repaying their patience.

My work would not have been possible without the guidance and support of my unofficial collaborative supervisors. I would like to acknowledge and thank Emeritus Professor Geoff Fincher and Professor Rachel Burton from the ARC Centre of Excellence for Plant Cell Walls, and Professor Vladimir Jiranek from the School of Agriculture, Food and Wine for allowing me to spend time within their research groups to use their facilities and gain specific cross-disciplinary knowledge relevant to my studies. I am grateful for their generosity and patience in supporting my studies. Furthermore, I cannot thank enough all the team members in these research groups for everything from sharing their unique expertise to a laugh or warm smile every day.

I would like to thank Dr Navid Moheimani and Dr Alison Mastrangelo, who were my co-supervisors during the early stages of my studies, for their support and directive contributions.

There are so many aspects of my work where key knowledge was provided by individuals along the way. Mr Steven Amos deserves a special mention for sharing my journey whilst providing a

fastidious and steadfast technical fountain of knowledge in just about every chemical engineering aspect of my research. Thanks to Dr Kenneth Yongabi for pointing me in the direction of *Rhizopus* amongst all the curious microorganisms he suggested that I test. Thank you to Mr Jelle Lahnstein for demystifying high performance liquid chromatography for me, and teaching me how to fish for carbohydrates with bottles of solvent through finely packed beds. Thank you to Dr Marilyn Henderson for a gentle introduction and guidance through advanced microscopy. Thank you to Associate Professor David Jeffery for taking the complexity out of my mass spectrometry. Thank you also to Ms Jo Hugman for your patience in trying to show me that statistics could be fun – I think that was your take-home message.

I would like to acknowledge and thank all the staff and team at the School of Chemical Engineering for their support and friendship along the way. A special thought also goes to my crew at the School, particularly my original office buddies Mr Theo Kalaitzidis and Dr Cheng Hu, who were always around for support and the frequent banter. Thanks to Dr Andrew Lee, Dr Daniel Lane and Dr Andrew Ward for sharing my journey and also keeping me sane.

I acknowledge the facilities, and the scientific and technical assistance, of the Australian Microscopy & Microanalysis Research Facility at Adelaide Microscopy, The University of Adelaide. I am also grateful to our industry partner SQC Pty Ltd for their sponsorship of my work alongside the Australian Research Council.

Lastly, and most importantly, I am thankful and forever grateful for the love and support of my wife, Angela, who I have asked to sacrifice so much to allow this journey to happen. She has been a keystone to the happiness of our family. Thanks also to my daughter, Amelia, for putting up with a dad who always seems to be working or studying – it's finally time for a new day.

# Table of contents

# List of Tables

# List of Figures

(This page intentionally left blank)

# Related Publication

The publication (and related corrigendum) from work presented in this thesis:

Doan, QC, Moheimani, NR, Mastrangelo, AJ & Lewis, DM (2012), 'Microalgal biomass for bioethanol fermentation: Implications for hypersaline systems with an industrial focus', *Biomass and Bioenergy*, vol. 46, pp. 79-88.

Doan, QC, Moheimani, NR, Mastrangelo, AJ & Lewis, DM (2013), 'Corrigendum to "Microalgal biomass for bioethanol fermentation: Implications for hypersaline systems with an industrial focus" [Biomass Bioenergy 46 (2012) 79–88]', *Biomass and Bioenergy*, vol. 58, pp. 406-407.

Copies of these articles have been appended in Appendix B.

(This page intentionally left blank)

# Abbreviations

| | |
|---|---|
| 2-DOG | 2-deoxyglucose |
| 5OMeKdo | 3-deoxy-D-manno-5-O-methyl-2-octulosonic acid |
| afdw | ash free dry weight |
| AIR | alcohol insoluble residue |
| ANOVA | analysis of variance |
| Ara | arabinose |
| ARC CoE | Australian Research Council Centre of Excellence |
| AX-HPLC | anion exchange high performance liquid chromatography |
| CCUG | Culture Collection University of Göteborg, Sweden |
| $CO_2$·eq | carbon dioxide equivalent |
| CSLM | confocal scanning laser microscope |
| DAD | diode array detection |
| Dha | 3-deoxy-lyxo-2-heptulosaric acid |
| DIC | differential interference contrast |
| dw | dry weight |
| EJ | exajoule ($10^{18}$ joules) |
| ELSD | evaporative light scatter detection |
| FESEM | field emission scanning electron microscope |
| Fuc | fucose |
| rcf | relative centrifugal force |
| Gal | galactose |
| GalA | galacturonic acid |

| | |
|---|---|
| GHG | greenhouse gas |
| GL | gigalitre ($10^9$ litres) |
| Glc | glucose |
| Gt | gigatonne ($10^{12}$ kg) |
| Gul | gulose |
| ha | hectare ($10^4$ $m^2$) |
| HPAEC | high-pH anion exchange chromatography |
| HPLC | high performance liquid chromatography |
| IEC | ion-exclusion chromatography |
| ILUC | indirect land use change |
| I-MR | Individuals and Moving Range |
| Kdo | 3-deoxy-manno-2-octulosonic acid |
| KPP | Karratha pilot plant |
| LB | lysogeny broth |
| LUC | land use change |
| Man | mannose |
| MERG | Microalgae Engineering Research Group, School of Chemical Engineering, University of Adelaide, South Australia, Australia |
| Milli-Q | Type 1 ultrapure water |
| MOPS | 3-(N-Morpholino)propanesulphonic acid sodium salt |
| MUR-233W | washed preparation of *Tetraselmis* sp. MUR-233 with dissolved compositional Red Sea Salt diluted to < 0.1 % w/v |
| *m/z* | mass to charge ratio |
| n | sample size |
| *N* | normality or equivalent concentration per litre |

| | |
|---|---|
| NaCl | sodium chloride |
| NAD | nicotinamide adenine dinucleotide |
| $NAD^+$ | oxidized nicotinamide adenine dinucleotide |
| NADH | reduced nicotinamide adenine dinucleotide |
| NRRL | Northern Regional Research Laboratory, U.S. Department of Agriculture, Peoria, Illinois, USA |
| PAD | pulsed amperometric detection |
| PBR | photobioreactor |
| PBS | phosphate-buffered saline |
| PMP | 1-phenyl-3-methyl-5-pyrazolone |
| ppm | parts per million |
| PSA | phenol sulphuric acid (chromogenic assay for total carbohydrates) |
| psi | pounds (of force) per square inch (of area) |
| PVDF | polyvinylidene difluoride |
| Rha | Rhamnose |
| RID | refractive index detection |
| RO | reverse osmosis |
| ROA | carboxylic acids |
| RP-HPLC | reverse phase high performance liquid chromatography |
| RSS | Red Sea Salt |
| RT | retention time of peak in analytical chromatography |
| SD | standard deviation |
| sp. | species |
| spp. | species (plural) |

| | |
|---|---|
| t | tonne ($10^3$ kg) |
| TFA | trifluoroacetic acid |
| UOA | University of Adelaide |
| UNKN | unknown |
| UV | ultraviolet |
| Xyl | xylose |
| YEPD | yeast extract peptone dextrose |
| YEPS | yeast extract peptone starch |

# Definitions

| | |
|---|---|
| *Biomass* | Biomass is use to describe harvested *Tetraselmis* sp. MUR-233 cells. This is a multidiscipline body of work and includes cell culture of other microorganisms including *Rhizopus oryzae* NRRL 1526. However, in the context of this thesis, biomass refers exclusively to material that is produced as a feedstock for fermentation. |
| *Project* | In the context of this thesis, Project (capitalised) refers to this body of postgraduate research, experimentation and investigations undertaken in fulfilment of the requirements for the degree of Doctor of Philosophy (PhD). |
| *Reverse osmosis (RO) water* | Laboratory grade water purified using reverse osmosis filtration and deionised to a conductivity of ≤8 $mS \cdot cm^{-2}$. |
| *Salinity* | In the context of this thesis refers to the dissolved sea salt content of a solution. This is expressed as either a concentration ($g \cdot L^{-1}$) or percentage ratio (% w/v). |
| *Self-induced anaerobic fermentation* | A fermentation vessel (typically 250 ml in this thesis) sealed with a water-filled airlock in which the culture headspace is not pre-purged of air. The flask becomes anaerobic during the initial phases of fermentation as $CO_2$ is produced. |
| *Type 1 ultrapure water* | Analytical grade water purified and deionised to a resistance of 18.2 MΩ·cm at 25 °C (conductivity of 0.055 $\mu S \cdot cm^{-1}$) and passed through a 0.22 μm particulate filter. |

(This page intentionally left blank)

# Chapter 1
# Project introduction

## 1.1 Key objective

The purpose of this Project was to evaluate the potential for producing bioethanol from the biomass of an industrially relevant marine microalga. The studies herein focus on an important gap in knowledge regarding the challenging hypersaline nature of biomass harvested from marine microalgae. Additionally, the process application reported herein reveals key knowledge that has not typically been emphasised in the published literature and impacts on the feasibility assessment of microbial ethanolic fermentation using any microalgal biomass.

## 1.2 Industrial relevance

Global climate change concerns and the goal to mitigate fossil carbon emissions generated significant renewed interest and research on the use of biomass from microalgae for producing biofuels (Aikawa *et al.* 2013; Brennan & Owende 2010; Chernova & Kiseleva 2017; Chisti 2007; Milano *et al.* 2016; Sawayama *et al.* 1999; Sawayama & Tsukahara 2005; Schenk *et al.* 2008; Taher *et al.* 2011). High reported levels of organic carbon accumulated within microalgae as lipids, proteins and carbohydrates could provide raw substrates for conversion to energy products such as "green" crude, methane, diesel and ethanol. Key factors in evaluating the viability of biofuel feedstock development from microalgae would be feasible economics, environmental impact and net energy balance of accompanying processes. To this end, rigorous investigations into each potential product stream would provide the necessary data for any continued long-term development.

This Project forms part of a broader Australian Research Council Linkage Project (ARCLP 100200616), to assess the diversification of energy streams from microalgae (Lane *et al.* 2015; Lee *et al.* 2016; Ward & Lewis 2015; Ward *et al.* 2014). The specific focus here of this Project was to assess the potential for producing bioethanol from the biomass carbohydrates of the green

microalga *Tetraselmis* sp. strain MUR-233 (hereafter referred to as "MUR-233"). This microalga is of commercial interest to the Project's industry partner, SQC Pty Ltd (SQC), and has broader relevance to the incorporated joint venture start-up company Muradel Pty Ltd (Muradel) and an Australian Renewable Energy Agency (ARENA) advanced biofuels project (Q00150).

*Tetraselmis* is a genus of quadriflagellate photosynthetic green microalgae that is euryhaline, tolerant to a broad range of saline concentrations, and has typically been isolated from salt lakes and marine environments (Fon Sing & Borowitzka 2015; Kirst 1990). *Tetraselmis* is able to maintain osmoregulation and cytoplasmic ion homeostasis to adapt and grow in a wide range of environmental salt concentrations from 0.01 M to 1.2 M sodium chloride (NaCl) (Strizh *et al.* 2004). This euryhaline physiology is distinctly desirable for microbiologically competitive production of *Tetraselmis* biomass in open ponds using seawater. Such seawater production systems can be subject to frequent elevation in process salinity from the inevitable evaporative concentration of the culture environment to hypersaline levels. The ability of *Tetraselmis* to survive in a broad range of salinities provides a selective advantage over less adaptive microorganisms. Considering the vast diversity of microalgal varieties, the genus *Tetraselmis* has been important industrially because of its robustness in culture for producing protein rich biomass for mariculture. For this reason it has also been of interest for biofuel production since the 1980s (Laws & Berning 1991; Okauchi & Kawamura 1997; Thomas *et al.* 1984).

MUR-233 used in this Project was originally isolated by researchers at Murdoch University, Western Australia, and selected for halotolerance and high lipid production in outdoor cultures (Fon Sing 2010). It was one of several *Tetraselmis* candidates for potential third generation biofuel feedstock for a project known as AP6, funded by the Australian Federal Government to investigate the economic and technical feasibility of producing a biodiesel feedstock from marine microalgae under the Asia-Pacific Partnership (APP) on Clean Development and Climate, Project Number RDG 07-26 (Fon Sing & Borowitzka 2015). The robustness of this strain for biomass productivity

has been assessed in outdoor open raceway pond systems (Raes *et al.* 2013). Furthermore, during the later stages of this AP6 project, MUR-233 was selected as the most robust of the candidate *Tetraselmis* strains for pilot scale cultivation at the Muradel Pty Ltd facility at Karratha in the Pilbara region in Western Australia (Fon Sing *et al.* 2014).

## 1.3 Hypersaline challenge to development

A minimum salinity of 3.5 % weight per volume w/v would be expected for any microalgal biomass grown in open ponds using seawater, corresponding to the average saline concentration of the world's seawater which contains 24.5 $g \cdot L^{-1}$ of NaCl as shown in Table 31 (American Society for Testing and Materials International 2013). In the context of this Project, a hypersaline environment is defined as a sea salt salinity of greater than 4 % w/v, or a NaCl concentration greater than 28 $g \cdot L^{-1}$. For the work described in this thesis, the biomass from MUR-233 has been produced in cultures that were maintained within an elevated saline concentration more than twice that of average seawater (7-11 % w/v). This was based on previous work at Murdoch University, now published, on MUR-233 and other *Tetraselmis* spp. from saline lakes (Fon Sing 2010; Fon Sing & Borowitzka 2015) which determined that biomass productivities were highest at ≤ 7 % w/v NaCl salinities.

The downstream processing of hypersaline biomass presents a sustainability challenge. In a country like Australia, there is often limited local availability of fresh water, particularly in warmer arid or marginally arable regions with high solar radiance suited to the establishment of open pond systems utilising seawater. A process that requires washing or significant dilution of sea salt from biomass would demand continued capital investment in enormous quantities of fresh water, and directly compete with municipal and agricultural needs for this valued resource. For bioethanol production, it would be important to investigate halotolerant microbial systems that would facilitate the utilisation and fermentation of carbohydrates from the hypersaline biomass of MUR-233.

## 1.4 Thesis statement and hypothesis

The experimental work described within this thesis sought a solution in which MUR-233 biomass harvested from hypersaline production cultures could be biologically converted to produce ethanol. A focus on environmental sustainability for the process aimed to utilise MUR-233 biomass without removal of inherent salt by excessive washing with fresh water. Consequently, a hypothesis was proposed stating that:

> *"A halotolerant fermentative microorganism exists in nature that would provide a salt resistant bioprocess solution for utilisation of MUR-233 biomass produced in seawater as a viable alternative biomass feedstock for microbial bioethanol production under hypersaline conditions."*

Therefore, this thesis addresses a knowledge gap about whether bioethanol could be fermented from a hypersaline microalgal biomass produced in seawater, using hypersaline fermentative conditions through selective use of halotolerant microorganisms. To this end, the work herein covers the key findings from compositional profiling of MUR-233 biomass, its carbohydrates, and its subsequent bioconversion to ethanol under hypersaline conditions by the filamentous fungus *Rhizopus oryzae* NRRL 1526. Further understanding of this research area, resulting from detailed investigations to test both the hypothesis and current knowledge, has led to the development of a thesis statement that concludes:

> "*The filamentous fungus* Rhizopus oryzae *NRRL 1526 found in nature possesses sufficient facultative halotolerance to provide a salt resistant bioprocess to simultaneously saccharify and ferment starch-enriched MUR-233 biomass to bioethanol. However, the dilute aqueous nature of MUR-233 biomass and its fermentable substrates presents significant challenges to the feasible use of this alternative biomass feedstock for microbial bioethanol production."*

## 1.5 Thesis structure

The significant relevance and importance of this Project to the discovery of new knowledge for industrial application has been covered in Chapter 1. This will be followed by a literature review presented in Chapter 2, assessing current knowledge regarding the production of bioethanol from microalgae. General methodology details relevant to the Project are covered in Chapter 3 and Appendix A as referenced in the text. Experimental findings from this Project have been presented within the four key chapters, Chapter 4 to Chapter 7. Each of these experimental chapters includes an introductory section that, where needed, provides relevant background information to each respective chapter from either cited publications or in-house knowledge. The background information has been presented in this way rather than being combined within the literature review of Chapter 2 to allow more focus to the presentation of related experimental results. This has been partly due to the multi-discipline nature of the work conducted. The presentation of the Project herein is completed in Chapter 8 with conclusions and discussion relating to overall findings and potential future work and directions for building on the new knowledge gained.

## 1.6 Key findings

*Tetraselmis* sp. strain MUR-233 when cultivated for biomass productivity had a total carbohydrate content that ranged from 6.8 % to 11 % ash free dry weight (afdw). The cell wall carbohydrates of MUR-233 were composed primarily of 3-deoxy-manno-2-octulosonic acid (Kdo) and galactose. These major monosaccharides were present at up to 63.1 % (Kdo) and 19.3 % (galactose) of the molar ratio of cell wall carbohydrates. Other minor monosaccharides measured in MUR-233 cell wall included mannose, gulose, rhamnose, glucose, xylose, arabinose, fucose and galacturonic acid. Biomass glucose composition varied depending on the amount of accumulated starch, but only trace amounts of glucose, 0.32 % afdw, was measured in the cell wall. The starch content of MUR-233 could be enriched when cultured under continuous illumination at up to 250 $\mu mol \cdot photons \cdot m^{-2} \cdot s^{-1}$, accumulating to an average starch content of 47 % afdw.

A key consideration in the process development was the dilute nature of the MUR-233 biomass due to inherent seawater harvested with the microalgae. To minimise further dilution at the pretreatment stage, the filamentous fungus *Rhizopus oryzae* NRRL 1526 was used in a simultaneous saccharification and fermentation approach to converting MUR-233 starch to ethanol. NRRL 1526 displayed facultative halotolerance and was able to survive, grow and produce ethanol in hypersaline submersed culture at up to 10.5 % salinity in sea salt. However, increasing salt concentrations had a negative impact on fungal growth and ethanol production. Starch enzymatic hydrolysis by the fungus was tested up to 7 % salinity in hypersaline seawater with no impact to activity, indicating that the native starch degrading enzymes of NRRL 1526 were halotolerant. It was found that although this fungal strain could produce up to 26.1 $g \cdot L^{-1}$ ethanol with an 84.8 % conversion efficiency (or percent yield), when fed with hypersaline MUR-233 biomass there was a shift in carbon flux towards other metabolic products. In the hypersaline self-anaerobic conditions tested, ethanol was still the major product at 9.62 $g \cdot L^{-1}$ to 11.24 $g \cdot L^{-1}$ from assimilation of MUR-233 biomass, but the percent ethanol yield was reduced to as low as 44.8 %. Under these conditions, lactic acid was also produced.

A new method was also developed during this Project that provides a simple screening tool for creating axenic *Tetraselmis* or other green microalgae cultures. The method uses ultraviolet (UV) excitation at 330 nm to 385 nm and fluorescent detection at emission > 420 nm to visualise and distinguish surface bacteria by their autofluorescence against chlorophyll autofluorescence from the *Tetraselmis* cells.

# Chapter 2
# Literature review

The majority of this chapter has been published in the Journal of Biomass and Bioenergy (Doan *et al.* 2012, 2013). Updates have also been incorporated for inclusion of more recent studies and understanding in the relevant fields of research since the original publication. Some changes to units of measure have also been made for consistency with the broader thesis.

## 2.1 Introduction

Over the last decade, the value of developing alternative sources for renewable liquid transportation fuels has increasingly been recognised. Key drivers for renewable energy have been the concern over global climate change associated with greenhouse gas (GHG) emissions (Australian Academy of Science 2010), as well as the speculation regarding energy security based on assessments that the world has already reached peak oil production (Aleklett *et al.* 2010). To address the effective future mitigation of GHG emissions, the International Energy Agency (IEA) forecasted a 450 Scenario in their 2009 World Energy Outlook (WEO) to limit global increase in temperature to 2 °C. This forecast, in which atmospheric GHG would be stabilised at a volume fraction of 450 ppm carbon dioxide equivalent ($CO_2$·eq), estimated that by 2030 the world demand for transport biofuels would be 11.64 EJ and supply 9.2 % of total global transport fuels. This is equivalent to an annual production growth of 9.6 % from a 1.43 EJ global biofuel output in 2007 (International Energy Agency 2009). The current main focus of the IEA's current Energy Technology Perspectives (ETP) is the 2 °C Scenario (2DS) for an energy system deployment strategy with at least a 50% chance of extending the 450 Scenario's goal for a 2 °C global temperature increase limit by 2100 (2018b). Based on the 2DS forecast, biofuels would contribute 30 EJ into the energy mix towards an annual reduction in global emissions of 3.93 Gt·$CO_2$·eq by 2060 (International Energy Agency 2018a, 2018c). Two important transport biofuels are bioethanol and biodiesel. Of these, bioethanol has historically been produced in the largest

volumes; for example, the bioethanol component of worldwide biofuel production in 2007 was 1.06 EJ, equivalent to 50 GL (Sims *et al.* 2008). In the automotive industry, bioethanol emerged as the primary alternative renewable transport fuel to supplement and potentially replace gasoline (Balat & Balat 2009), and has also been considered as a low-blend additive to diesel (Pidol *et al.* 2012; Sayin 2010). In 2015, bioethanol contributed to two-thirds of an estimates 3 EJ global biofuel production, although current overall growth in this sector is significantly slower that pre-2010 levels (International Energy Agency 2017).

Bioethanol derived from photosynthetic organisms can mitigate the impact of GHG emissions through photoautotrophic conversion of atmospheric carbon dioxide to useful biomass. However, first generation bioethanol made from starch-rich agricultural produce have received widespread criticism for being unsustainable and socially irresponsible (Moore 2008a). These concerns have led to development of second generation bioethanol from more sustainable feedstocks, such as cellulosic biomass (Moore 2008b). Even so, proponents for the impact of global land use change (LUC) continue to question the overall benefit that biofuels, such as current bioethanol and biodiesel, derived from land vegetation will have on net global GHG emissions (Hill *et al.* 2010). Furthermore, there remains uncertainty as to how future governmental policies on biofuels might be impacted with regard to the consequences of indirect land use change (ILUC) and its associated costs (Kocoloski *et al.* 2009). Current regulatory modelling by the U.S. Environmental Protection Agency (EPA) and California Air Resources Board (CARB) to assess the overall environmental impact of ILUC have estimated a modest 20 % GHG reduction resulting from corn ethanol in comparison to gasoline, and to date the impact of corn ethanol on global food/feed market prices have still been small (Hoekman & Broch 2017). However, a key environmental concern remains regarding energy-intensive agricultural activities associated with corn cropping for ethanol production, and whether there is any net reduction in GHG emissions given that upstream GHG emissions are considerably higher for corn ethanol compared to gasoline (Hoekman *et al.* 2017).

The potential for producing third generation bioethanol from alternative biomass such as microalgae and macroalgae has generated significant interest. A comprehensive review of this topic by John *et al.* (2011) acknowledged a need for high salt tolerant microalgal species to improve utilisation of seawater. Marine or hypersaline algal species are desirable as sustainable sources of biomass; however, the fundamental aspect of hypersalinity inherent with such biomass is under-emphasised and has not been addressed in the majority of research reported in this area. Microalgae and macroalgae are often considered together when compared to terrestrial sources of biomass, yet they each present very different processing challenges from farming, production and conversion. Marine microalgae targeted for biofuels could be harvested from open or closed mass culturing systems, and most likely operated under hypersaline conditions to conserve water. Additionally, for both practical and economic reasons, marine microalgae as viable biofuel feedstocks cannot be completely dewatered and washed; hence, concentrates of harvested marine microalgal biomass would carry significant quantities of saline or hypersaline water. In contrast, marine macroalgae would commonly be harvested from their natural coastal environment, whether wild or farmed, and can be more easily dewatered and washed.

There has been significant progress in the fermentation of marine macroalgal biomass for biofuel production. For instance, an important breakthrough microbial platform has been engineered in *Escherichia coli* for simultaneous saccharification and fermentation (SSF) of alginate, and enhanced assimilation of mannitol and glucose to bioethanol from the brown macroalga *Saccharina japonica* (Wargacki *et al.* 2012). Additionally, there is now considerable research and commercial interest in developing marine macroalgae as a feedstock for biobutanol production through acetone butanol ethanol (ABE) fermentation with *Clostridia* spp. (Huesemann *et al.* 2012; Potts *et al.* 2012). The conversion of marine macroalgal biomass to bioethanol and biobutanol warrants review to assess the implications of recent developments; particularly for macroalgal biomass conversion to biobutanol which has a higher energy density and better gasoline engine compatibility than bioethanol (Dürre 2008). However, the review reported here will focus primarily on marine

microalgae as a feedstock for bioethanol in order to highlight the importance of hypersaline systems for consideration.

While the attention of many research groups has focused towards utilising marine microalgal biomass for sustainable energy supplies, there has been minimal research and development on biofuel production under hypersaline conditions. In many parts of the world where arable land and fresh water resources are limited due to marginal climate conditions or demands associated with population growth, hypersaline processes will likely be required for sustainable commercial biofuel production from microalgae, particularly at the scale needed to supplement or supply the world's insatiable appetite for liquid transportation fuels (Borowitzka & Moheimani 2013). The concerns around sustainable use of land and fresh water resources can be obviated through the development of marine based systems for producing biofuels. Photosynthetic marine microalgal production systems are well suited to this purpose as the microalgae can be cultured using seawater in arid locations that have no agricultural value. Microalgae are resilient organisms and include many culturable species rich in lipids and carbohydrates. They grow rapidly and are able to produce a daily average 20 $g \cdot m^{-2}$ ash free dry weight (afdw) biomass in open raceway pond systems, making them ideal biomass feedstock for producing biofuels (Borowitzka & Moheimani 2013). This average microalgal biomass productivity is equivalent to an annual yield of 73 $t \cdot ha^{-1}$ and is comparable to that of sugarcane crops, which have been reported at between 70 $t \cdot ha^{-1}$ to 77 $t \cdot ha^{-1}$; the largest energy crop harvested for bioethanol (Balat & Balat 2009; Gauder *et al.* 2011). Indeed, it is anticipated that microalgae will be an important biomass for third generation biofuels. Although almost all of the reported research on microalgal liquid biofuels is focused on the production of lipid for biodiesel (Fon Sing *et al.* 2011), the economic feasibility of generating biodiesel from a microalgal biomass feedstock may depend on the development of energy co-products such as methane, hydrogen, ethanol, butanol and aviation fuel (Stephens *et al.* 2010).

In the early 1980s, it was recognised that microalgae such as the genus *Dunaliella* had potential as

a rich, renewable biomass for use in the fermentative production of butanol and ethanol (Nakas *et al.* 1983). Furthermore, the increased global pressure on the resource sector to produce fuel from renewable and environmentally sustainable sources has led to ongoing research in methods to produce ethanol from microalgae since the late 1990s (Harun & Danquah 2011; Harun *et al.* 2010; Hirano *et al.* 1997; Hirayama *et al.* 1998; John *et al.* 2011; Nguyen *et al.* 2009; Shirai *et al.* 1998). As a result, a modest body of knowledge now exists that demonstrates the feasibility of two main approaches for producing ethanol from microalgae. One area gaining significant interest is the anaerobic fermentation of the microalgal biomass by solventogenic microorganisms, which can utilise and convert the microalgal carbohydrates to ethanol. Another field of research has demonstrated the direct synthesis of ethanol as a metabolite in strains of both naturally occurring and engineered microalgae. Some such processes are currently under commercial development (Ueda *et al.* 1996; Woods *et al.* 2010b), although bioethanol made from microalgae is not yet available on the market.

The main focus of this review is on the potential for fermentative production of bioethanol from marine and hypersaline microalgal biomass, as well as assessing developments in the general area of microalgal ethanol reported thus far and proposing industrially and environmentally relevant process considerations for future research. As cultivation of marine microalgae in seawater introduces a minimum salinity of 3.5 % w/v to the harvested biomass, particular emphasis is placed on the need for developing appropriate systems to operate under hypersaline conditions in order to minimise the environmental impact at commercial scale, thus achieving a sustainable biomass supply.

## 2.2 Fermentable substrates in microalgae

Commercially available ethanol biofuel is converted from fermentation of sugar-rich agricultural crops, with 80 % sourced from corn and sugarcane (Sims *et al.* 2008), and demonstration cellulosic ethanol refineries are also now in operation (Jones 2010; Lin & Tanaka 2006; Sims *et al.* 2008;

Sivakumar *et al.* 2010; Wyman 1999). The carbohydrates of microalgae have been studied since the mid-1900s (Archibald *et al.* 1960; Eddy *et al.* 1958; Hirst *et al.* 1972; Olaitan & Northcote 1962; Suzuki 1974; Wilkinson *et al.* 1950). While early studies did not focus on the fermentation potential of microalgal biomass, they did establish that many of today's commercially important microalgal groups, such as the chlorophyta green algae, contained starch-type storage carbohydrates similar to those found in vascular higher plants currently used as substrates for ethanol production (Balat & Balat 2009). The key storage carbohydrates of the main algal groups, which include unicellular microalgae and the cyanobacteria blue-green algae, are compared in Table 1.

Structurally, microalgal starch grains consist of amylose and branched amylopectin homopolysaccharides much like those of higher plants (Ball 2002), however, only green algae accumulate starch in the same way within the chloroplast through the assimilation of adenosine diphosphate (ADP) glucose. The floridean starch of red algae, as with similar cytosolic starch found in the cytoplasm and periplast of other algae groups (Table 1), is synthesised from uridine diphosphate (UDP) glucose much like glycogen from heterotrophic eukaryotes (Dauvillée *et al.* 2009). Other granular storage polysaccharides from this group of microorganisms include the α-1,4-glucan cyanophycean starch of cyanobacteria and the morphologically diverse paramylon, a β-1,3-polyglucan stored in the cytoplasm of euglenoids and chlorarachniophyta (Monfils *et al.* 2011). Additionally, the reserve polysaccharide chrysolaminaran in microalgae of the taxa heterokontophyta and haptophyta is soluble and stored in a cytoplasmic vacuole.

Aside from the polyglucan storage products, there is a diverse range of carbohydrates associated with both cellular structure and osmoregulatory function across different species of microalgae. For instance among chlorophytes, the cell wall of some *Chlorella* spp. comprises of α-cellulose and hemicelluloses (Northcote *et al.* 1958), whereas the more primitive *Chlamydomonas* spp. cell wall has hydroxyproline glycosides consisting of glucose, galactose and arabinose (Miller *et al.* 1972).

**Table 1: The diversity of main storage carbohydrates of algae groups**

| Division | Storage carbohydrate | Composition | Ref. |
|---|---|---|---|
| Cyanophyta (= Cyanobacteria) "*Blue-green algae*" | cyanophycean starch | α-1,4 polyglucan | [1], [4], [6] |
| Prochlorophyta (= Chloroxybacteria) | cyanophycean starch | α-1,4 polyglucan | [1], [4] |
| Glaucophyta | starch (in cytosol) | α-1,4 polyglucan; α-1,6 branches | [1], [2], [4], [5] |
| Rhodophyta, *"Red algae"* | floridean starch (in cytosol) | α-1,4 polyglucan; α-1,6 branches | [1], [2], [4], [5], [6] |
| Cryptophyta | starch (in periplast) | α-1,4 polyglucan; α-1,6 branches | [1], [4] |
| Heterokontophyta | chrysolaminaran (in vacuole) | β-1,3 polyglucan; β-1,6 branches | [1], [3], [4], [6] |
| Dinophyta | starch (in cytosol) | α-1,4 polyglucan; α-1,6 branches | [1], [2], [4], [6] |
| Haptophyta (= Prymnesiophyta) | chrysolaminaran (in vacuole) | β-1,3 polyglucan; β-1,6 branches | [1], [3], [4], [6] |
| Euglenophyta | paramylon (in cytosol) | β-1,3 polyglucan | [1], [4], [6] |
| Chlorarachniophyta | paramylon (in cytosol) | β-1,3 polyglucan | [1], [4] |
| Chlorophyta, "*Green Algae*" | starch (in chloroplast) | α-1,4 polyglucan; α-1,6 branches | [1], [2], [4], [5], [6] |

References:
[1] Bold and Wynne (1985) [3] Størseth *et al.* (2005) [5] Dauvillée *et al.* (2009)
[2] Ball (2002) [4] Barsanti *et al.* (2008) [6] Hirokawa *et al.* (2008)

Different again, the chlorophyte *Tetraselmis* spp. present 2-keto sugar acids as their major cell wall carbohydrate (Becker *et al.* 1991). In species such as *Botryococcus braunii* a large proportion of reported monosaccharides are secreted into the extracellular environment of the microalgae as exopolysaccharides (Allard 1990). The accumulation of sugar solutes can also provide an important osmoregulatory function in the salt tolerance of microalgae. Osmoregulation in the

green halophilic alga *Dunaliella* occurs through the synthesis and degradation intracellular glycerol in response to the salinity conditions of its external environment (Ben-Amotz & Avron 1973). In the euryhaline cyanobacteria, fresh water species are able to tolerate marginal hypersalinity of up to 4.5 % w/v sodium chloride (NaCl) through accumulation of the disaccharides sucrose and trehalose, and those species typically from marine or hypersaline environments that synthesise the compatible solute glucosylglycerol have shown halotolerance in the range of 6.0 % w/v to 10.0 % w/v NaCl (Mackay *et al.* 1984). Given the degree of carbohydrate diversity amongst microalgae, there remains a common group of monosaccharides that have been reported across different genera. These are summarised in Table 2 and in most cases, the reported monosaccharides from microalgae have generally been extracted from whole cells and are thus likely to represent both structural and physiological carbohydrates; additionally, their distribution between microalgae division, genera and species is diverse.

The total carbohydrate content of microalgae has been reported at up to 50 % to 60 % dry weight (dw) and includes both starch and monosaccharides derived from structural carbohydrates, such as mannose, galactose and arabinose (Choi *et al.* 2010; Matsumoto *et al.* 2003; Nguyen *et al.* 2009). However, the carbohydrate yield from biomass is dependent on both the selected microalgae and the cultivation conditions utilised. In one study, the total carbohydrate yields from *Dunaliella primolecta* were reported at 65 % dw, when grown under nitrogen-deficient conditions (Thomas *et al.* 1984). Furthermore, the study demonstrated that such conditions could lead to a five-fold increase in the carbohydrate yields from both *D. primolecta* and *Tetraselmis suecica*, and suggested potential applications in instances where carbohydrate rich biomass may be required for conversion to ethanol. It should be noted, however, that these improved carbohydrate levels were at the cost of reduced photosynthetic efficiencies and total biomass dw yields decreased 0.5-fold and 0.65-fold below the respective nitrogen-sufficient estimates. Nonetheless, a recent study outlined a two-stage cultivation of fresh water *Chlorella vulgaris* in which the biomass yields were optimised prior to nitrogen and iron deprivation, resulting in both improved biomass and high

intracellular carbohydrate yields. In fact, intracellular starch levels accumulated to 41 % dw, an amount almost 2-fold higher than those previously reported in other strains of *Chlorella* spp. (Dragone *et al.* 2011).

**Table 2: Reported monosaccharide species commonly found in microalgal biomass**

| Carbohydrate group | Monosaccharide | Selected references |
|---|---|---|
| pentose sugar | xylose ; ribose; fructose; arabinose | [2, 4, 5, 7, 8, 9, 10, 11, 12, 13] |
| hexose sugar | mannose; gulose; glucose; galactose | [2, 3, 4, 5, 7, 8, 9, 10, 11, 12, 13] |
| 6-deoxyhexose sugar | rhamnose; fucose | [2, 5, 8, 9, 10, 11, 12, 13] |
| sugar acid | galacturonic acid | [9, 11, 12, 13] |
| sugar alcohol | glycerol | [1, 6, 7] |

References:
[1] Nakas *et al.* (1983)
[2] Olaitan and Northcote (1962)
[3] Suzuki (1974)
[4] Miller *et al.* (1972)
[5] Allard (1990)
[6] Ben-Amotz and Avron (1973)
[7] Mackay *et al.* (1984)
[8] Brown (1991)
[9] Becker *et al.* (1989)
[10] Blumreisinger *et al.* (1983)
[11] Chiovitti *et al.* (2003)
[12] Dai *et al.* (2010)
[13] Gooday (1971a)

Amongst the storage, structural and physiological carbohydrates present in microalgae the types and quantities of basic monosaccharide components are potentially very suitable for conversion into ethanol. However, for optimal utilisation of such diverse carbohydrates new ethanologenic microorganisms may be required, although to date, the majority of studies in this area have utilised the standard strains of *Saccharomyces cerevisiae* (Table 3) with only a few that have assessed ethanologenic or solventogenic bacterial strains such as *Clostridium pasteurianum* (Nakas *et al.* 1983) and recombinant *Escherichia coli* (Lee *et al.* 2011). Certainly, the emerging processes for second generation bioethanol from cellulosic type biomass have demonstrated a need to identify or engineer alternative microorganisms that are able to utilised a variety of monosaccharides other than the hexose sugar glucose (Lin & Tanaka 2006). Furthermore, to exploit biomass derived from

marine microalgae cultivated in saline or hypersaline water, the identification of appropriate ethanologenic microorganisms that are halotolerant or halophilic may be necessary to facilitate industrial processing under conceivably hypersaline conditions.

## 2.3 Extraction of fermentable substrates

The structural carbohydrates of microalgal biomass consist of diverse monosaccharides. Although these have been analytically characterised, they are often components of complex cell walls in many marine microalgal species and may not easily be extracted or utilised. The conversion of microalgal sugars to bioethanol will depend on both the efficiency of their extraction, and the capacity of any chosen ethanologenic microorganism to utilise them. The extraction of fermentable sugars from microalgal biomass has been addressed by two groups in particular, using hydrothermal acid pretreatment with biomass from both *Chlamydomonas reinhardtii* UTEX 90 and *Chlorococcum humicola* (Harun & Danquah 2011; Nguyen *et al.* 2009). Using another approach, other researchers focused on enzymatic pretreatment of washed microalgal biomass with terrestrial cellulase, glucoamylase or α-amylose (Chen *et al.* 2010; Choi *et al.* 2010; Hirano *et al.* 1997; Shirai *et al.* 1998). Subsequent studies have continued to assess the effectiveness of both chemical and enzymatic hydrolysis pretreatments in microalgal carbohydrate extraction for bioethanol production (Ho *et al.* 2013), including the use of such methods with mixed microalgae biomass (Shokrkar *et al.* 2017). However, research by Matsumoto *et al.* (2003) suggests that enzymatic processes may be inherently limited or at the least incomplete when applied under saline conditions. In their work, this team demonstrated the feasibility of converting saline biomass from a total of 76 different marine microalgae to reduced sugars by saccharification with a marine amylase-producing bacterium, *Pseudoalterimonas undina* NKMB 0074. They reported poor hydrolysis to reducing sugars due to low amylase production by the bacterium, but interestingly observed that under saline conditions terrestrial amylase and glucoamylase were

completely inhibited and as such would be unsuited to industrial application for hydrolysing carbohydrates from unwashed marine biomass (Matsumoto *et al.* 2003).

There is an expanding body of knowledge on halophilic enzymes and microorganisms that have the potential to effectively treat marine biomass. A review of applications for halophilic microorganisms concluded that the industrial demand for salt-tolerant enzymes is limited (Oren 2010), though continued development of processes to generate biofuels from marine microalgae may provide future opportunities for such applications, for example, in the hydrolysis of hypersaline biomass. Potentially useful salt-tolerant enzymes have been isolated from a diverse population of marine and hypersaline microorganisms. The studies on many such salt-tolerant hydrolytic enzymes, including a number of halophilic amylases, from halophilic archaea and bacteria have been reviewed by Ventosa *et al.* (2005). Other examples include the marine *Streptomyces sp.* D1 which produces a moderately halophilic α-amylase (Chakraborty *et al.* 2008), and a highly stable but salt dependent halophilic α-amylase isolated from *Haloarcula hispanica* (Vasisht *et al.* 2005). Also, a glucoamylase able to hydrolyse both α-1,4 and α-1,6-glycosidic linkages of starch amylose and amylopectin has been discovered in the marine yeast *Aureobasidium pullulans* N13d (Duan *et al.* 2006), and a potentially very useful thermophilic and halophilic amyloglucosidase has been identified in *Halobacterium sodomense* with optimal activity at temperatures between 66 °C to 76 °C and molarities of 1.4 $mol \cdot L^{-1}$ to 3.9 $mol \cdot L^{-1}$ NaCl (Oren 1983). Additionally, it has been reported that some halophilic α-amylases, such as those from *Haloarcula* sp. strain S-1 and a particular strain of *Nesterenkonia* sp., are more tolerant to organic solvents than terrestrial amylases (Fukushima *et al.* 2005; Shafiei *et al.* 2011). Such enzymes may be especially suitable for hydrolysis of carbohydrates from hypersaline biomass.

## 2.4 Fermentation of microalgal biomass

In comparison to the development efforts into other biomass sources such as lignocellulosic residues, a review of the literature has shown minimal progress made in the past 30 years towards fermenting bioethanol from renewable microalgal biomass. As a result, research in this area is really in its formative stage and a long way from yielding a commercially viable product. The genus *Dunaliella,* which accumulates high concentrations of intracellular glycerol in hypersaline environments as a means of osmotic stabilisation, was assessed by Nakas *et al.* (1983) as a potentially rich renewable biomass for use in fermentation schemes aimed at producing neutral solvents. In this study, cultures of five *Dunaliella* species (*D. tertiolecta*, *D. primolecta*, *D. parva*, *D. bardawil*, and *D. salina*) were optimised for biomass glycerol content. A 300-fold concentrate of harvested biomass was successfully fermented to yield *n*-butanol, 1,3-propanediol and ethanol by the bacterium *Clostridium pasteurianum.* This bacterium produced peak levels of solvent in 1.0 % w/v NaCl but was totally inhibited in 3.0 % w/v NaCl. The concentrated *Dunaliella* biomass preparation used had a salinity below 1.0 % w/v but insufficient glycerol for solvent conversion to achieve yields comparable to those obtained utilising traditional substrates such as molasses or glucose. Despite its limited success, the study demonstrated that fermentation of microalgae biomass could indeed be realised. More importantly, Nakas *et al.* (1983) concluded that for large-scale applications the successful fermentation of a saline biomass would require either salt removal or the use of a solvent-producing halotolerant organism.

Since these early observations by Nakas *et al.* (1983), minimal work on assessing halotolerant or halophilic organisms for fermentative production of ethanol has been reported. It would appear that many researchers have concluded that fermentation using yeast had been thoroughly investigated and, as such, have prioritised research around developing efficient technologies for biomass pretreatment (Nguyen *et al.* 2009). A recent review of technological developments on the production of ethanol from microalgae alluded to the importance of using marine microalgae to

avoid commodity competition for fresh water (John *et al.* 2011), but also presented fermentation as a ready option, simply involving the use of processes similar to those currently established employing appropriate yeast strains. This seems to be the dominant view taken by those currently investigating approaches to utilising microalgal biomass for conversion to ethanol. To circumvent the salinity issues presented by the fermentation of marine biomass, the majority of studies undertaken to date have used microalgae grown in low saline medium or, alternatively, have implemented a wash step for salt removal.

Bioethanol has been produced using biomass substrates from the freshwater microalga *Chlamydomonas reinhardtii* UTEX 90 (Choi *et al.* 2010; Nguyen *et al.* 2009), the freshwater cyanobacteria *Arthrospira (Spirulina) platensis* (Aikawa *et al.* 2013), the marine microalgae *Chlorococcum* sp., *Chlorococcum humicola* and *Dunaliella* sp. (Harun & Danquah 2011; Harun *et al.* 2010; Shirai *et al.* 1998), and reported marine strains of *Chlorella vulgaris*, such as *Chlorella vulgaris* IAM C-534 (Hirano *et al.* 1997; Lee *et al.* 2011). The reported ethanol yields from these studies (Table 3) demonstrate varying levels of success across the different processes assessed. Shirai *et al.* (1998) had limited success fermenting biomass from a *Dunaliella* sp. that had been hydrolysed with a commercial glucoamylase, achieving ethanol yields of 0.011 $g \cdot g^{-1}$ dw biomass. In contrast, a study by Harun *et al.* (2010), which assessed both whole cell and lipid-extracted *Chlorococcum* sp. biomass in the absence of hydrolytic pretreatment, reported ethanol yields of up to 0.383 $g \cdot g^{-1}$ dw biomass. This study is of particular interest as it suggests that a lipid-extraction process may facilitate the release of fermentable sugars from microalgal biomass for conversion to ethanol. The yield differences observed in these various studies can be attributed to the available levels of fermentable sugars from the selected microalgae and to the effective ethanol conversion rate in the processes used. These reported studies are important in demonstrating a proof of concept for efficient conversion of marine microalgal carbohydrates to ethanol; furthermore, they highlight a need for sufficient extraction of fermentable carbohydrates from any microalgae

biomass used to be matched with optimal process conditions and microorganisms for fermentation.

**Table 3: Reported bioethanol yields from fermentation of microalgal biomass**
Ethanol yields have been calculated from data reported in each study.

| Microalga | Pretreatment(s) | Fermenting microorganism | Ethanol yield from total dw biomass ($g \cdot g^{-1}$) | Ref. |
|---|---|---|---|---|
| *Dunaliella* sp. | glucoamylase [b] | *Saccharomyces cerevisiae* IAM 4140 | 0.011 | [1] |
| *Chlorella vulgaris* IAM C-534 * | α-amylase & glucoamylase | *Saccharomyces cerevisiae* IFO 039 | 0.123 | [2] |
| *Chlamydomonas reinhardtii* UTEX 90 | dilute acid / heat | *Saccharomyces cerevisiae* S288C | 0.292 | [3] |
| *Chlamydomonas reinhardtii* UTEX 90 | α-amylase [c] | *Saccharomyces cerevisiae* S288C | 0.235 | [4] |
| *Chlorococcum* sp. | (no pretreatment) | *Saccharomyces bayanus* | 0.383 | [5] |
| *Chlorococcum humicola* | dilute acid / heat | *Saccharomyces cerevisiae* | 0.520 [a] | [6] |
| *Chlorella vulgaris* * | dilute acid / heat, cellulase [d] & cellobiase [e] | *Escherichia coli* SJL2526 | 0.400 [a] | [7] |
| *Arthrospira (Spirulina) platensis* | Lysozyme | *Saccharomyces cerevisiae* MT8-1δGS [f] | 0.439 | [8] |

* Both have been reported as marine strains of *C. vulgaris*.
[a] Calculated yield that is above stoichiometric limit for sugar-to-ethanol conversion; based on reported ethanol concentrations produced relative to percentage of carbohydrates biomass feedstock.
[b] Glucozym AF6 (Amano Pharmacy Co. Ltd.); [c] Termamyl (Novozymes A/S); [d] Celluclast (Novozymes A/S); [e] Novozymes 188 (Novozymes A/S); [f] recombinant amylase-expressing yeast strain.

References:
[1] Shirai *et al.* (1998)
[2] Hirano *et al.* (1997)
[3] Nguyen *et al.* (2009)
[4] Choi *et al.* (2010)
[5] Harun *et al.* (2010)
[6] Harun and Danquah (2011)
[7] Lee *et al.* (2011)
[8] Aikawa *et al.* (2013)

The limited available studies on conversion of microalgal biomass to ethanol emphasises a need for further verification of published studies, especially where ethanol yields above what would be considered stoichiometric limits have been reported (Table 3). Under ideal conditions, a theoretical stoichiometric ethanol yield of 0.51 $g \cdot g^{-1}$ glucose (see Section 7.1.1) is produced from typical yeast fermentation, where one mole of glucose yields two moles each of ethanol and carbon dioxide (Balat & Balat 2009). Considering the complexity of microalgal carbohydrates, it is unlikely that all carbohydrate groups would be efficiently utilised, particularly when using *Saccharomyces cerevisiae*. Additionally, substrate to product mass balances should account for other dry weight components in the microalgae such as lipids and proteins that cannot be converted to ethanol. For instance, a reported ethanol yield of up to 0.52 $g \cdot g^{-1}$ dw from *Chlorococcum humicola* biomass appears to exceed twice the stoichiometric maximum of 0.224 $g \cdot g^{-1}$ expected based on the reported total 43.8 % dw input of carbohydrate and starch (Harun & Danquah 2011). Likewise, it was reported that an *Escherichia coli* SJL2526 fermentation of *Chlorella vulgaris* biomass yielded ethanol at 0.40 $g \cdot g^{-1}$ dw from feedstock containing 27 % dw total sugars; a quantity which appears to be almost 3-fold higher than stoichiometric limits (Lee *et al.* 2011). New studies to ratify existing data are essential before assessments can be made regarding the actual net energy return from current reported processes.

The knowledge base required for process scale-up of bioethanol fermentation using marine microalgal biomass is incomplete. In particular, the issue of hypersalinity within the marine biomass has been overlooked which, in turn, has led to the seemingly prevalent opinion that the fermentable sugars from the biomass of marine microalgae can be easily converted to ethanol using existing processes. A trend in many existing studies has been to wash saline microalgal biomass feedstocks with deionised water for salt removal and improved compatibility with the selected downstream processes. For example, such a process generated reduced salt conditions which then facilitated the use of commercial terrestrial α-amylases for investigations with harvested biomass from two *Chlorella vulgaris* strains and a *Dunaliella* sp. (Hirano *et al.* 1997; Lee *et al.* 2011; Shirai *et*

*al.* 1998). Ultimately, when considering industrial scale marine microalgae production, methods such as desalting with fresh water are unlikely to be viable, and practical process solutions to deal with hypersalinity will be a key factor for successful commercial implementation. In this type of setting, terrestrial hydrolytic enzymes and halosensitive ethanologenic microorganisms such as some *Saccharomyces cerevisiae* and *Escherichia coli* may prove to be ineffective.

## 2.5 Direct ethanol synthesis in microalgae

A lateral development path for producing ethanol from microalgae has been pursued by a number of research groups. Rather than harvesting microalgal biomass as a fermentation substrate, these researchers have selected or engineered microalgae that can directly produce ethanol as a secreted metabolite. In nature, some microalgae and cyanobacterium undergo self-fermentation through utilisation of their intracellular starch in dark and light anaerobic environments. Under these conditions, the production of ethanol has been reported in the *Chlamydomonas reinhardtii* strains F-60 and UTEX2247, *Chlamydomonas sp.* YA-SH-1, *Chlorococcum littorale* and *Cyanothece* PCC 7822 (Gfeller & Gibbs 1984; Heyer & Krumbein 1991; Hirano *et al.* 1997; Hirayama *et al.* 1998; Ueno *et al.* 1998; van der Oost *et al.* 1989). However, anaerobic self-fermentation via the Embden-Meyerhof-Parnas (EMP) metabolic pathway in naturally occurring microalgae produces much lower levels of ethanol in comparison to reported yields from yeast fermentations. For example, in a dark fermentation process, *Chlorococcum littorale* produced an ethanol yield of 0.021 $g \cdot g^{-1}$ dw biomass with a conversion ratio of 0.27 $g \cdot g^{-1}$ glucose (Ueno *et al.* 1998), whereas lipid-extracted *Chlorococcum sp.* biomass, when used as a substrate for yeast fermentation, allowed for a more efficient conversion of available sugars with an ethanol yield of 0.383 $g \cdot g^{-1}$ dw biomass (Harun *et al.* 2010). Furthermore, unless axenic microalgal cultures are used in dark fermentation systems, any ethanol secreted at such low titres may provide a nutrient source of carbon for contaminant heterotrophic organisms, thus limiting process efficiency (Puig *et al.* 2007).

In order to be practical, processes using microalgae under dark fermentation to produce ethanol require the selection of strains capable of high ethanologenic productivity. More productive dark fermentation studies have been reported utilising the marine microalgae *Chlamydomonas reinhardtii* UTEX2247 and *Chlamydomonas sp.* YA-SH-1 with respective ethanol yields of 0.08 $g \cdot g^{-1}$ and 0.154 $g \cdot g^{-1}$ dw biomass (Hirano *et al.* 1997; Hirayama *et al.* 1998). These studies required the maintenance of a viable microalgal culture for dark fermentation after harvesting by centrifugation, and form the basis for a US patent (Ueda *et al.* 1996), which also lays claims for its utilisation with the genera *Chlamydomonas*, *Chlorella*, *Spirulina*, *Oscillatoria* and *Microcystis*. However, aside from the need to maintain axenic cultures, there may be limitations for processes based on dark fermentation relating to intracellular substrate usage and starch-to-ethanol conversion efficiencies. Such metabolic limits were observed in an investigation of 37 cyanobacterial strains by Heyer and Krumbein (1991), who concluded that the rates of dark fermentation were minimal and geared towards cell maintenance; most metabolites like ethanol were produced at much lower levels than what would be acceptable for fuel production. In regard to substrate availability, the ethanol producer can only utilise its intracellular supply. In fact, the data presented in the studies by Hirano *et al.* (1997) and Hirayama *et al.* (1998) suggests that conversion of carbohydrate reserves to ethanol ceases well before substrate exhaustion. In contrast, a fermentation system where exogenous substrate is provided to encourage growth and production can be more readily optimised through process design to yield higher producer densities and product titres.

A review of algal-based ethanol processes concluded that future developments should focus on the metabolic engineering of ethanol-producing microalgal strains and the design of appropriate photobioreactor (PBR) systems (John *et al.* 2011). Early research in this area produced limited results when a fresh water cyanobacteria, *Synechococcus* sp. strain PCC 7942, was metabolically engineered to produce ethanol under oxygenic photoautotrophic conditions and gave yields much lower than those generally obtained during commercial production of ethanol by yeast fermentations (Deng & Coleman 1999). Despite the early limitations in this approach to producing

ethanol, commercial development in this area is ongoing; in fact, Algenol Biofuels Inc. claim to have developed a commercially applicable process using a genetically modified (GM) strain of ethanol-producing autotrophic cyanobacteria (Duhring *et al.* 2010; Woods *et al.* 2010a; Woods *et al.* 2010b) in a non-conventional PBR system. An industrial scale up of typical closed PBR designs currently in use for cultivating microalgae would incur prohibitively high infrastructure costs in construction, operation and maintenance (Borowitzka 1999), therefore, the viability of PBR systems for industry depends on significant improvements on plant design, operation and construction materials (Davis *et al.* 2011). The Algenol Biofuels Inc. patented process utilises a new PBR design to minimise downstream processing by allowing for direct, continuous ethanol collection from evaporative condensate of their ethanologenic cultures.

## 2.6 Industrial outlook towards sustainable biomass

In 2007, an estimated arable land area of 4,300,000 ha was used in Brazil to cultivate sugarcane crops for the production of 25 GL of bioethanol, or 5,817 $L \cdot ha^{-1}$ (Gauder *et al.* 2011), with the majority of bagasse from this feedstock being utilised for process heat (Soccol *et al.* 2010). Furthermore, it has been proposed that if discarded sugarcane trash was instead collected and used to supplement process heat generation, then 50 % of the bagasse could be made available as feedstock for cellulosic bioethanol production and potentially account for an additional 4,000 $L \cdot ha^{-1}$ of bioethanol (Soccol *et al.* 2010). The net benefit of this improved biomass usage would be a 0.41-fold reduction in the required land area for producing 0.69-fold more bioethanol, yet even so, the total yearly production would be insufficient for the challenging biofuel targets set under the 2009 WEO's 450 Scenario. If sugarcane bioethanol remained as Brazil's primary biofuel and production was to increase at the IEA's required annual rate of 9.6 % to 2030, Brazil would still need to expand the cultivation of biofuel crops over a further 4-fold of the existing arable land area allocated for this purpose. A study by Gauder *et al.* (2011) provided data to suggest that, in balance with domestic food production needs, Brazil may have sufficient arable land to sustainably expand

its bioethanol capacity to 76.7 GL by 2020, which is within 94 % of the production growth rate required under the 450 Scenario for this period. However, the world's population is expected to exceed 9 billion people by 2050 (United Nations 2007), and responsible use of arable land on a global level should be an important consideration. Indeed, it has been suggested that future population growth will have a considerably greater impact on land and water resources for food production than will other factors such as economic or technical developments, and that the global capacity for food production may be significantly limited by government policies which drive increased bioenergy usage (Schneider *et al.* 2011).

The land use for commercial scale biofuel crop cultivation is well beyond the capacity of any current microalgal based system; in fact, the largest commercial microalgae open pond system is currently only 750 ha (Borowitzka & Moheimani 2013). Nonetheless, biomass productivities by unit area per annum from saline or hypersaline microalgal open pond farms can be comparable to those of commercial biofuel crops such as sugarcane (Table 4), and hence, such farms could supply feedstock towards bioenergy production without competing with food production for arable land and drinking water. However, to date, there have been no reports on the biomass productivity of marine microalgae selected for carbohydrate enrichment and cultured over long-term growth studies in large-scale open ponds. Additionally, the microalgal biomass described in many of the laboratory scale studies for ethanol fermentation contained significantly higher compositions of fermentable sugars than those currently assessed for lipid production in large-scale open pond systems. Therefore, to compare potential biofuel yields from marine microalgal biomass against data from commercial sugarcane bioethanol production (Gauder *et al.* 2011), a set of hypothetical large scale open pond farms have been constructed, as shown in Table 4. The compositional carbohydrate and lipid data for the microalgae presented was extracted from the literature (Brown 1991; Hirano *et al.* 1997; Liu *et al.* 2008), and an assumption made that realistic average daily biomass productivities of 20 $g \cdot m^{-2}$ afdw could be achieved (Borowitzka & Moheimani 2013) in cultures of the marine microalgae selected. Furthermore, it was assumed that the reported cellular

glucose or starch content in the microalgae would be fully converted to ethanol and, for the purposes of this example, any unresolved process limitations in relation to biomass harvesting and hypersaline fermentation systems were ignored. The biomass productivity of marine microalgae in open pond farms compares well against the yearly 77.5 $t \cdot ha^{-1}$ production of Brazilian sugarcane crops, which averages to a daily 21 $g \cdot m^{-2}$.

**Table 4: Comparison of potential yields from hypothetical large scale marine microalgal farms to reported yield from sugarcane energy crop**

| Biomass | Available sugar or starch (% dw) | Lipid (% dw) | Annual biomass production ($t \cdot ha^{-1}$) | Annual potential ethanol conversion ($L \cdot ha^{-1}$) | Productivity of ethanol production ($L \cdot t^{-1}$) | Additional lipid production ($L \cdot t^{-1}$) |
|---|---|---|---|---|---|---|
| Sugarcane | 11.8 [c] | - | 77.5 [c] | 5,890 | 76 [c] | - |
| *Dunaliella tertiolecta* [a] | 10.4 [d] | 15 | 73 [g] | 4,898 | 67 [h] | 167 |
| *Isochrysis galbana* [a] | 9.9 [d] | 23 | 73 [g] | 4,636 | 63 [h] | 256 |
| *Tetraselmis chui* [a] | 10.2 [d] | 17 | 73 [g] | 4,804 | 66 [h] | 189 |
| *Nannochloris atomus* [a] | 0.154 [d] | 21 | 73 [g] | 7,245 | 99 [h] | 233 |
| *Chlorella vulgaris* [b] | 37 [e] | 7.8 [f] | 73 [g] | 17,343 | 238 [h] | 87 |

[a] Hypothetical scenario where microalgae species has been selected for lipid content. Carbohydrate and lipid data used from Brown (1991).
[b] Hypothetical scenario where microalgae species has been selected for carbohydrate content.
[c] Annual production data for sugarcane energy crops from Brazil in 2008 (Gauder *et al.* 2011). Available sugar from sugarcane is calculated based on reported biomass and ethanol productivity data (Gauder *et al.* 2011) using theoretical maximum yield of 54 %.
[d] Glucose calculated from reported carbohydrate and monosaccharide quantities provided in Brown (1991).
[e] Starch content used from the reported marine Chlorella vulgaris strain IAM C-534 from Hirano *et al.* (1997).
[f] Lipid content used from a reported marine Chlorella vulgaris (Liu *et al.* 2008).
[g] Calculated based on daily average biomass productivity of 20 $g \cdot m^{-2}$ afdw for microalgae grown in open pond systems (Borowitzka & Moheimani 2013).
[h] Ethanol productivities calculated based on theoretical maximum mass fraction yield of 0.51 achieved from reported quantities of either glucose or total starch.

Only glucose and starch content were considered as fermentable carbohydrates in the microalgae assessed, yet even so, the potential ethanol yield from *Dunaliella tertiolecta*, *Isochrysis galbana* and

*Tetraselmis chui* biomass was, on average, 86 % of the reported yield from sugarcane. The glucose composition in these species would be considered as typical of microalgae at an approximate 10 % dw, and *Nannochloris atomus* biomass, with 15.4 % dw of glucose, demonstrated the potential to yield 30 % more ethanol per weight of biomass than sugarcane. These four species are perhaps representative of the saline and marine microalgae that could be considered in lipid production for bioenergy, yet would still provide residual biomass suitable for ethanol fermentation yields able to match that of terrestrial sugarcane crops. Conversely, if a microalgawas to be selected for production of fermentable sugars, for example the marine strain of *Chlorella vulgaris* IAM-C534 with a starch content of 37 % dw of biomass, the potential ethanol yield could, in theory, be over three-fold higher than what could be produced from sugarcane while still yielding a significant proportion of lipid for other bioenergy products such as biodiesel.

## 2.7 Conclusion

In today's environmental and economic climate, ethanol has emerged as an important liquid transportation biofuel. The potential of marine or saline microalgal biomass to be cultivated as a sustainable substrate feedstock in ethanol fermentation is evident; however, there are still many technical challenges in both the early development and scale up stages. There has only been a modest level of investigation into the fermentation of marine microalgal biomass, and significant scope exists for improvement, particularly in the area of process sustainability. A consideration of the desired industrial outcomes should guide early development research objectives. For instance, hypersalinity should be a key factor in process design and optimisation, given that seawater is the most feasible and sustainable environment in which to produce microalgal biomass for bioenergy. Additionally, the cultivation of saline microalgae over millions of hectares of land with annual productivities equivalent to 73 $t \cdot ha^{-1}$ should direct downstream processing away from environmentally costly steps such as the desalting of saline biomass.

The limited number of reports in the published literature suggests that few research groups have addressed the issue of process hypersalinity. Yet there are clear advantages to developing a process for treating and fermenting hypersaline biomass, particularly in view of the extensive ongoing global development of marine microalgal systems for producing lipids for biofuels. Whether the end biomass is sourced from open raceway ponds or closed PBR systems there is likely to be an abundant supply of potentially fermentable lipid-extracted residue marine biomass for conversion to ethanol if a sustainable process can be developed. Even microalgal biomass with minimal fermentable sugar content of approximately 10 % dw could be utilised to produce significant yields of bioethanol. However, in many instances, existing fermentation research may not be applicable for use with a sustainable marine or hypersaline biomass. Further investigation into halotolerant and halophilic enzymatic hydrolysis would address the need for more appropriate biochemical pretreatment of hypersaline biomass for extraction of fermentable sugars. Priority should also be given to developing improved microbial systems for effective ethanologenic or solventogenic conversion of hypersaline biomass, as a hypersaline fermentation system reduces the requirement for fresh water during production. Non-agricultural feedstock like marine microalgae may provide a solution to sustainable biomass supply.

This review does not cover the economic feasibility of producing bioethanol from hypersaline microalgal biomass. Nor has it assessed the comparative costs with existing processes that use agricultural crops. Additionally, the process engineering challenges associated with a hypersaline process have not been reviewed. Although the sole focus has been on bioethanol as the end product, the principle consideration for use of a hypersaline biomass remains the same regardless of the eventual end product. Indeed, there is likely significant value in other energy products such as butanol that may be similarly converted.

# Chapter 3
# General materials and methods

## 3.1 Field samples

### 3.1.1 MUR-233 from Karratha

*Tetraselmis* sp. strain MUR-233 biomass from field cultures was sourced from the Muradel Pty Ltd pilot plant at Karratha, Western Australia (Fon Sing *et al.* 2014). This material was provided as a concentrated slurry following harvest by electro-flocculation and centrifugation. For greater sample consistency only biomass that had been directly harvested by flotation or settling during the electro-flocculation process were analysed. All biomass samples were excluded which had been collected from settling tanks 1 to 2 days after an electro-flocculation step.

## 3.2 Microalgae cultivation

### 3.2.1 Modified f medium culture media

The culture media used to grow *Tetraselmis* sp. strain MUR-233 was a hypersaline modified f medium (Guillard & Ryther 1962) without vitamin supplementation, and containing ($L^{-1}$): 70 g Red Sea Salt (Red Sea Fish Pharm Ltd, Eilat, Israel), 150 mg $NaNO_3$, 10 mg $NaH_2PO_4.2H_2O$, 8.72 mg $Na_2EDTA$, 6.3 mg $FeCl_3.6H_2O$, 0.36 mg $MnCl_2.4H_2O$, 0.044 mg $ZnSO_4.7H_2O$, 0.02 mg $CoCl_2.6H_2O$, 0.0196 mg $CuSO_4.5H_2O$, and 0.0126 mg $Na_2MoO_4.2H_2O$. Appendix A.2 details the composition of Red Sea Salt (RSS) relative to natural seawater (NSW) and the ASTM standard for substituted ocean water. Appendix A.3 provides details of hypersaline modified f medium preparation.

### 3.2.2 Preparation of modified f medium agar culture plates

Culture plates were used which contained the marine f medium, described in Section 3.2.1, with 1 % w/v agar and up to 20 $\mu g \cdot ml^{-1}$ of the antibiotic carbenicillin. A specific preparation method was required for this solid agar medium because autoclaving of hypersaline seawater media containing RSS resulted in irreversible hydrothermal precipitation of salts from the media. For this method a 1.5 times concentrated 0.22 µm filter sterilised media solution was prepared containing

($L^{-1}$): 105 g RSS, 225 mg $NaNO_3$, 15 mg $NaH_2PO_4.2H_2O$, 13.08 mg $Na_2EDTA$, 9.45 mg $FeCl_3.6H_2O$, 0.54 mg $MnCl_2.4H_2O$, 0.066 mg $ZnSO_4.7H_2O$, 0.03 mg $CoCl_2.6H_2O$, 0.0294 mg $CuSO_4.5H_2O$, 0.0189 mg $Na_2MoO_4.2H_2O$, and between 7.5 mg to 30 mg carbenicillin. This media solution and a solution of melted sterile 3 % w/v agar were temperature equilibrated to 37 °C then mixed at a 2:1 ratio prior to pouring onto sterile Petri dishes. The carbenicillin variation on plates was a result of incremental increases from 5 $\mu g \cdot ml^{-1}$ to 20 $\mu g \cdot ml^{-1}$ over the course of experimentation.

### 3.2.3 Microalgal single colony selection on solid media

The solid growth medium was prepared as described in Section 3.2.2. A flame sterilised sample loop was used at a 45° angle to streak the Karratha sample onto the prepared plates using a four-quadrant streak pattern for selection of single colonies. Plates were then incubated for 21 days at a constant 24 °C ambient temperature under 55-60 $\mu mol \cdot photons \cdot m^{-2} \cdot s^{-1}$ white fluorescent light (Osram Lumix Daylight L36W/865, 6500K) and 12-hour light/dark cycling until microalgae growth was visibly abundant for manual sampling. The morphologically dominant colony type was aseptically picked with a flame sterilised sample loop under a stereo microscope (Olympus SZ, Olympus America Inc., Melville, USA; Zeiss Stemi 2000-C, Carl Zeiss AG, Oberkochen, Germany) and mixed into 500 µL of 35 $g \cdot L^{-1}$ RSS solution. The sample in solution was then mounted onto a covered glass slide for confirmation of *Tetraselmis* sp. morphology using an Olympus CH light microscope (Olympus America Inc., Melville, USA). Once colony morphology was matched to *Tetraselmis*, single colonies were selected using the stereo microscope streaked for single colonies as above onto new plates until visibly separated from contaminating organisms. Two colonies from monoculture plates were selected and each transferred into sterile antibiotic-free 16 ml liquid cultures for propagation (Section 3.2.2).

### 3.2.4 Bench scale microalgal growth and maintenance

MUR-233 was cultured autotrophically in the laboratory in volumes up to 600 ml using modified f medium in Milli-Q water (Section 3.2.1) under 48-80 $\mu mol \cdot photons \cdot m^{-2} \cdot s^{-1}$ white fluorescent light

(Osram Lumix Daylight L36W/865, 6500K) with 12-hour light/dark cycling at an ambient temperature of 24 °C. Culture volumes were kept at a maximum 1/3 of culture vessel volume to allow efficient surface aeration by orbital shaking at 110-120 rpm on a Ratek platform mixer (Ratek Instruments Pty Ltd, Boronia, Australia). The bench scale apparatus for cultivation of MUR-233 is shown in Figure 1.

**Figure 1: Bench scale setup for cultivation of MUR-233**

Typically, cultures were seeded to cell densities between $2\times10^5$ to $4\times10^5$ cells·ml$^{-1}$ into Erlenmeyer flasks as shown below in Table 5. Where required, media was filter sterilised using 0.22 µm sterile filters into flasks that had been pre-sterilised by autoclave. Cultures were maintained in semicontinuous growth in which 80 % of total culture volume was removed at regular time intervals (typically every 3 to 4 days) and replaced with an equal volume of fresh medium, whereby culture nutrient concentrations were replenished and cell concentration diluted five-fold.

**Table 5: Flask volumes and agitation settings for *Tetraselmis* bench scale cultures**

| CULTURE VOLUME (ml) | FLASK VOLUME (ml) | ORBITAL AERATION (rpm) |
|---|---|---|
| 16 | 50 | 110 |
| 160 | 500 | 120 |
| 300 | 1,000 | 120 |
| 600 | 2,000 | 120 |

### 3.2.5 Calculations for microalgal growth

The specific growth rate of cultures was calculated as the growth rate ($\mu$) during exponential phase determined by plotting cell counts on a natural log scale against time.

Culture growth rate ($\mu$) was calculated as:

$$\mu = ln\left(\frac{N_2}{N_1}\right) \times \left(\frac{1}{t_2 - t_1}\right) \quad \textbf{Equation 1}$$

where $N_2$ and $N_1$ are the number of cells at times $t_2$ and $t_1$.

The specific growth rates ($\mu_{log}$) of cultures were calculated as the growth rates ($\mu$) during exponential phase determined by plotting cell counts on a natural log scale against time.

Divisions per day (Div·day$^{-1}$) was calculated as:

$$\text{Div} \cdot \text{day}^{-1} = \frac{\mu}{\ln 2} \quad \textbf{Equation 2}$$

Generation time (Gen't) was calculated as:

$$\text{Gen}'\text{t} = \frac{1}{\text{Div} \cdot \text{day}^{-1}} \quad \textbf{Equation 3}$$

### 3.2.6 Photobioreactor microalgal growth and maintenance

MUR-233 was cultured in air bubble photobioreactors (PBR) under 210-250 µmol·photons·$m^{-2}$·$s^{-1}$ white fluorescent light (Philips TL-D LIFEMAX Super 80, TL-D 58W/840 1SL, 4000K), and 12-hour light/dark cycling within an ambient temperature range of 20 °C to 24 °C. The PBRs were mixed with compressed air supplied at 6 bar and with a flow rate of 9.2 ± 0.3 L·$min^{-1}$. The PBRs were of approximate dimensions 52 cm circumference and 115 cm height, and constructed from 200 µm low density flexible polyethylene.

**Figure 2: Photobioreactor setup for cultivation of MUR-233**

Culture volumes varied between 5 L and 25 L per PBR and were grown autotrophically using modified f medium in Milli-Q water (Section 3.2.1). Level markings on the PBRs were used to

maintain culture salinities by volume re-adjustments. The PBR apparatus for cultivation of MUR-233 is shown in Figure 2.

## 3.3 Microalgae culture analysis

### 3.3.1 Cell counting

Culture sample was prepared by staining and immobilisation with a 1:100 addition of 5 % v/v Lugol's solution containing 10 % v/v acetic acid (Table 40), and aliquoted onto a 0.1 mm depth Neubauer Improved haemocytometer (ProSciTech Pty Ltd, Kirwan, Australia) for counting. Where cell numbers were less than 10 cells·mm$^{-3}$ the sample was recounted using a 0.2 mm depth Fuchs-Rosenthal haemocytometer (ProSciTech Pty Ltd, Kirwan, Australia). Cell counts were performed using an Olympus IX50 inverted microscope (Olympus America Inc., Melville, USA) at ×10 magnification.

### 3.3.2 Cell measurement by digital imaging

An Olympus IX50 inverted microscope (Olympus America Inc., Melville, USA) was used to capture culture image digitally at ×4 magnification. Each culture sample was stained and immobilised with a 1:100 addition of 5 % v/v Lugol's solution containing 10 % v/v acetic acid (Table 40), then mounted on a 0.1 mm depth Neubauer Improved haemocytometer for counting. Image captures were taken of both grids of the haemocytometer for each prepared sample. Image analysis software, analySIS LS Research v2.6 Build 1175 (Olympus Soft Imaging Solutions GmbH, Münster, Germany) was used to determine the image threshold range for MUR-233 cell size (40 to 220 μm$^2$) to exclude sample artefacts such as cell debris (below threshold) and also cell clusters (above threshold) from analysis. Culture images were then analysed to determine dimensions of each individual cell.

### 3.3.3 Cell density enumeration by digital imaging

Culture images were captured as described in Section 3.3.2 above. Each captured image was representative of a 0.3596 μL sample (2.19 x 1.64 x 0.1 mm). Cell enumeration of the captured

images was automated using image analysis cell counting software, CellC v1.2 (Tampere University of Technology, Tampere, Finland) with built-in algorithms for dividing cell clusters into single cells and automatic removal of over/undersized cells. Cell density was determined by the CellC software from the counted cell populations, based on the average count from two images of each sample:

$$cell\ density\ (\text{cells} \cdot \text{ml}^{-1}) = \frac{mean\ count}{0.3596} \times 1000 \qquad \textbf{Equation 4}$$

### 3.3.4 Fluorescence microscopy for microalgae surface bacteria

A live MUR-233 culture sample (cell density $8\times10^5$ cells·ml$^{-1}$) was mounted onto a covered glass slide and analysed with an Olympus BX51 fluorescence microscope (Olympus America Inc., Melville, USA) at Adelaide Microscopy (University of Adelaide, Australia). Cells were visualised under oil immersion at ×100 magnification with ultraviolet (UV) excitation at 330 nm to 385 nm and fluorescent detection at emission >420 nm. Excitation and emission wavelength selection were based on Dalterio *et al.* (1987) for bacterial detection.

### 3.3.5 Confocal imaging for microalgae surface bacteria

A live MUR-233 culture sample (cell density $8\times10^5$ cells·ml$^{-1}$) was mounted onto a covered glass slide and analysed with a Leica TCS SP5 confocal scanning laser microscope (CSLM) (Leica Microsystems, Wetzlar, Germany) at Adelaide Microscopy (University of Adelaide, Australia). Cells were visualised under oil immersion at ×100 magnification, a scan velocity of 400 Hz, diode laser excitation at 405 nm, and fluorescent detection with dual emission filters at 410 nm to 440 nm and 613 nm to 703 nm. Excitation and emission wavelength selections were based on Dalterio *et al.* (1987) for bacterial detection and Iwai *et al.* (2010) for chlorophyll autofluorescence.

### 3.3.6 Scanning electron microscopy of microalgae culture

Cells from a 3 ml MUR-233 culture sample (cell density $1.5\times10^6$ cells·ml$^{-1}$) were collected on a 0.22 µm syringe filter membrane then fixed in 1.25 % v/v glutaraldehyde, 4 % v/v

paraformaldehyde, 4 % w/v sucrose in PBS, pH 7.2 for 1 hour. The fixed sample was washed in PBS containing 4 % w/v sucrose for 5 minutes, and then post-fixed in 2 % w/v osmium tetroxide for 30 minutes. The sample was dehydrated as follows: 1 change of 10 minutes in 70 % v/v ethanol; 1 change of 10 minutes in 90 % v/v ethanol; and 3 changes of 10 minutes in 100 % v/v ethanol. This was followed by preparation for drying critical-point; the sample was immerse for 10 minutes in a 1:1 mix of hexamethyldisilazane and 100 % v/v ethanol, transferred to and evaporated in hexamethyldisilazane, then mounted on a 12 mm diameter stub. The sample was critical-point dried, platinum coated to prevent charging under the electron beam, and examined on a Philips XL30 field emission scanning electron microscope (FESEM) at an accelerating voltage of 10 kV.

## 3.4 Analytical sample preparation

### 3.4.1 Large volume biomass harvesting by chemical flocculation

This method was employed for harvesting PBR cultures. MUR-233 cultures were transferred into a conical bottom harvesting tank, either 15 L or 100 L, then flocculated by flash mixing with the addition of 5 ml of 38.96 $g \cdot L^{-1}$ aluminium sulphate octadecahydrate ($Al_2(SO_4)_3 \cdot 18H_2O$) per litre of culture. This was equivalent to 100 $mg \cdot L^{-1}$ alum or aluminium sulphate ($Al_2(SO_4)_3$) for the coagulation process. In instances where large sample volumes (e.g. 1 L) were collected during trials, Imhoff cones were used for settling. The microalgal floc was settled for 60 minutes, then excess medium removed by decanting. This settling/decanting step was repeated, then the remaining slurry was collected, heat sealed in 200 μm low density flexible polyethylene bags, and stored at -20 °C.

The use of alum was not considered problematic for the analytical testing performed during the experimental studies. In the high performance liquid chromatography methods used, alum would elute with other inorganic salts well before analyte peaks and would not carry through to any peak fractions collected for further analysis. Furthermore, where alcohol insoluble residues of

harvested biomass were prepared, alum would have been effectively removed along with other salts during wash steps.

### 3.4.2 Freeze-drying of biomass

A standard procedure for preparing biomass with consistent water content was required for analytical purposes as explained in Section 5.2. Harvested MUR-233 biomass was pelleted in 50 ml centrifuge tubes at 3,200 rcf using a bench scale Eppendorf Centrifuge 5810R (Eppendorf AG, Hamburg, Germany), the bulk supernatant discarded by decanting and residual supernatant removed using a 100-1000 µL micropipette. The retained pellet was snap-frozen with liquid nitrogen and dried in a Labconco FreeZone 6 freeze-dry system (Labconco, Kansas City, USA).

### 3.4.3 Mechanical grinding of freeze-dried biomass

Access to intracellular starch for enzymatic procedures was facilitated by mechanical cell disruption of biomass. Freeze-dried MUR-233 biomass was mechanically ground with a 4 mm diameter stainless steel ball bearing in a plastic capsule for 15 seconds at 4300 oscillations per minute using a CapMix™ capsule mixing device (3M, St Paul, USA). The grind setting for MUR-233 material was initially verified by light microscopy for effectiveness in disrupting cell structure. An aliquot of ground sample was suspended in Milli-Q water with a 1:100 addition of 5 % v/v Lugol's solution containing 10 % v/v acetic acid (Table 40), mounted onto a covered glass slide, and visually assessed by light microscopy at ×20 to ×40 magnification using an Olympus IX50 inverted microscope (Olympus America Inc., Melville, USA).

### 3.4.4 Preparation of alcohol insoluble residue

Alcohol insoluble residues (AIR) of biomass were prepared to remove soluble free sugars and allow more accurate assessment of structural carbohydrates. Depending on particular experimental requirements for the AIR preparations, these were either made using freeze-dried or fresh wet biomass. For freeze-dried biomass, 10 mg to 20 mg of material was weighed on a Shimadzu AUW220D analytical balance (Shimadzu Corporation, Kyoto, Japan). Fresh biomass was a pooled

pellet from 4 ml to 8 ml of *Tetraselmis* strain MUR-233 culture harvested at 16,000 rcf for 5 minutes using an Eppendorf 5415D microcentrifuge (Eppendorf AG, Hamburg, Germany). Biomass was washed twice in 1 ml 70 % v/v ethanol for 10 minutes each then twice in 1 ml 100 % v/v ethanol for 10 minutes each with all washes initial mixed using a Ratek VM1 vortex mixer (Ratek Instruments Pty Ltd, Boronia, Australia).

### 3.4.5 Acid hydrolysis of biomass

Typically, preparations of AIR as per Section 3.4.4 were used for analysis. These were hydrolysed using 1 ml 1 M sulphuric acid ($H_2SO_4$) or 2 M trifluoroacetic acid (TFA) at 100 °C in a SEM oven (S.E.M. (SA) Pty Ltd, Adelaide, Australia). For extraction of reducing monosaccharides the hydrolysis time was 180 minutes, but for optimal release of Kdo as discussed in Section 5.3.3 the hydrolysis time was 45 minutes.

### 3.4.6 Buffer conditioning for PMP-derivatisation

Hydrolysates were diluted 1/20 using MilliQ water to 50 mM sulphuric acid or 100 mM TFA. Where a more concentrated sample was required for analysis, a 100 µL aliquot of TFA hydrolysate was dried using a Speed Vac SC110 with RVT100-240V condenser (Savant Instruments, Farmingdale, USA), washed and re-dried twice in 100 µL methanol then resuspended in 100 µL 50 mM $H_2SO_4$. Diluted samples were stored at -20 °C until used.

### 3.4.7 Dilution and neutralisation of biomass Kdo extracts

After 45 minutes hydrolysis samples were diluted to 1/20 using MilliQ water and neutralised with a 1/60 addition of 1 M ammonium hydroxide ($NH_4OH$). Diluted samples were stored at -20 °C until used.

## 3.5 Analytical chemistry

### 3.5.1 Determination of total solids and ash-free solids

Total solids and ash-free solids were determined using ceramic crucibles dried to a constant weight at 550 ± 25 °C in a Carbolite VMF muffle furnace (Verder Scientific, Haan, Germany), and pre-weighed. All weights for this procedure were measured to the nearest 0.1 mg using an A&D GR-200 analytical balance (A&D Company Ltd, Tokyo, Japan). For solids determination of wet biomass 5 ml of material was used and transferred using a pipette. Wet slurry too thick for accurate liquid handling was diluted with ultrapure water. Where the biomass had been freeze-dried, between 100 mg and 500 mg of material was used. Biomass was dispensed into tared crucibles and initial weight recorded then dried at 105 °C in a SEM Qualtex Solidstat oven (S.E.M. (SA) Pty Ltd, Adelaide, Australia) for 24 hours. The crucible containing oven dried biomass was recorded then baked at 550 ± 25 °C for 24 hours, after which time the weight of crucible and remaining ash was recorded.

Depending on the starting state of biomass to be analysed a sample weight was calculated as:

$$sample\ weight = weight_{crucible\ plus\ air\ dry\ sample} - weight_{crucible} \quad \textbf{Equation 5}$$

$$sample\ weight = weight_{crucible\ plus\ wet\ sample} - weight_{crucible} \quad \textbf{Equation 6}$$

Total solids or dry weight (dw) was calculated as:

$$dw = weight_{crucible\ plus\ oven\ dry\ sample} - weight_{crucible} \quad \textbf{Equation 7}$$

Total ash-free solids or ash-free dry weight (afdw) was calculated as:

$$afdw = dw - (weight_{crucible\ plus\ ash} - weight_{crucible}) \quad \textbf{Equation 8}$$

The percent of total solids, moisture, and ash-free solids were calculated using:

$$\%\ total\ solids = \frac{dw}{sample\ weight} \times 100 \qquad \textbf{Equation 9}$$

$$\%\ moisture = 100\ \% - \%\ total\ solids \qquad \textbf{Equation 10}$$

$$\%\ total\ ash\ free\ solids = \frac{afdw}{sample\ weight} \times 100 \qquad \textbf{Equation 11}$$

The percentage of ash on a dw basis was calculated as:

$$\%\ ash = \frac{weight_{crucible\ plus\ ash} - weight_{crucible}}{dw} \times 100 \qquad \textbf{Equation 12}$$

### 3.5.2 Analysis of total carbohydrates

A 96-well microplate variation of the Dubois *et al.* (1956) phenol sulphuric acid (PSA) method was used (Masuko *et al.* 2005). Hydrolysates were prepared as per Section 3.4.5, diluted with ultrapure water typically from 1/5 to 1/20, and analysed against a D-glucose (Sigma-Aldrich Pty Ltd, Sydney, Australia) standard curve in the concentration range of 5 µg·ml$^{-1}$ to 150 µg·ml$^{-1}$ (Figure 3).

The standard dilutions were prepared from a 2 mg·ml$^{-1}$ glucose stock and 50 µL of each dilution added in triplicate to each 96-well assay plate for standard amounts 0, 1, 2.5, 5, 10, 20 and 35 µg glucose per well. Diluted 50 µL samples were added in triplicate, followed by careful addition of 150 µL 98 % w/v concentrated $H_2SO_4$ and then 30 µL 5 % w/v phenol in ultrapure water. The plates were tapped (light lateral) for mixing, incubated in a 90 °C oven (Xtron HI 2002, Bartelt Instruments Pty Ltd, Heidelberg West, Australia) for 30 minutes, and absorbance read at 490 nm with an initial 3 seconds shaking in a Tecan Infinite M200 Pro spectrophotometer (Tecan Group Ltd., Männedorf, Switzerland). Mean absorbances were corrected against the mean blank (0 µg·well$^{-1}$) background values.

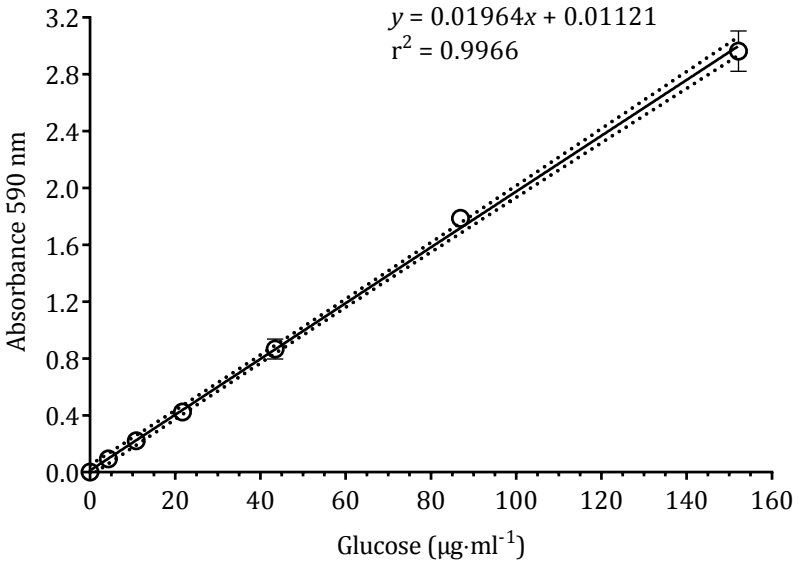


**Figure 3: Glucose standard curve for total carbohydrate assay**
An example of the linear dilution range for the high throughput microplate PSA method. Mean ± SD plotted (n = 3).

### 3.5.3 Analysis of derivatised reducing monosaccharides

Reducing monosaccharides were derivatised with 1-phenyl-3-methyl-5-pyrazolone (PMP) prior to analysis by reversed phase high performance liquid chromatography (RP-HPLC). Monosaccharides and PMP were sourced from Sigma-Aldrich Pty Ltd, Sydney, Australia. The method for pre-column labelling and analysis was as described by Comino *et al.* (2013), however, preparation of samples varied depending on the nature of hydrolysates analysed. For correct pH buffering in the PMP-derivatisation step, all sample dissolutions or dilutions were prepared to 50 mM $H_2SO_4$ or equivalent (see Section 3.4.5).

The PMP reagent was prepared by mixing 37 µL 1 M ammonium hydroxide ($NH_4OH$) with 40 µL 0.5 M PMP in methanol per reaction with each 20 µL of sample. For an internal standard (ISTD) 20 µL 0.5 mM 2-deoxyglucose in 50 mM $H_2SO_4$ was also added to each reaction. Samples with ISTD were derivatised in PMP reagent at 70 °C for 60 minutes then each reaction terminated with the addition of 20 µL 10 M formic acid (HCOOH). Excess PMP was solvent extracted twice from each

derivatised sample. For each extraction, unbound PMP was separated from the aqueous phase containing PMP-monosaccharides using an emulsion with 1 ml dibutyl ether then discarded with the dibutyl ether extractant after the phases were separated by pulse centrifugation.

The PMP-derivatisation of external standards was performed in the same manner as the sample derivatisation. Two monosaccharide standard mixtures were used depending on the expected nature of biomass samples: 10MS-VG at concentrations suitable for vegetative material low in starch; and 10MS-GR at concentrations suitable for starch rich material, e.g. grain or starch enriched biomass (Table 6 and Table 7).

**Table 6: Monosaccharide concentrations in 10MS-VG external standard solutions**

| Monosaccharide | Low standard (mM) | Medium standard (mM) | High standard (mM) |
|---|---|---|---|
| D-mannose | 0.008 | 0.04 | 0.2 |
| D-ribose | 0.008 | 0.04 | 0.2 |
| L-rhamnose | 0.008 | 0.04 | 0.2 |
| D-glucuronic acid | 0.008 | 0.04 | 0.2 |
| D-galacturonic acid | 0.008 | 0.04 | 0.2 |
| D-glucose | 0.04 | 0.2 | 1 |
| D-galactose | 0.008 | 0.04 | 0.2 |
| D-xylose | 0.008 | 0.04 | 0.2 |
| L-arabinose | 0.008 | 0.04 | 0.2 |
| L-fucose | 0.008 | 0.04 | 0.2 |

RP-HPLC analysis of PMP-monosaccharides was performed with a Phenomenex Kinetex 2.6 µm C18 100 Å 100 × 3 mm column (Phenomenex Inc., Torrance, USA) on an Agilent 1200LC system (Agilent Technologies, Santa Clara, USA), using eluent buffers: (A) 10 % v/v acetonitrile, 40 mM ammonium acetate, pH 6.8; and (B) 70 % v/v acetonitrile. Typically, 15 µL of sample was injected

and separated over a 12-minute gradient from 8 % to 16 % buffer B, at a flow rate of 0.6 ml·min$^{-1}$ and 30 °C, with diode array detection (DAD) at 250 nm. Example elution profiles of the 10MS-VG and 10MS-GR external reference standards are shown in Figure 49 of Appendix A.7.

**Table 7: Monosaccharide concentrations in 10MS-GR external standard solutions**

| Monosaccharide | Low standard (mM) | Medium standard (mM) | High standard (mM) |
|---|---|---|---|
| D-mannose | 0.012 | 0.06 | 0.3 |
| D-ribose | 0.012 | 0.06 | 0.3 |
| L-rhamnose | 0.012 | 0.06 | 0.3 |
| D-glucuronic acid | 0.012 | 0.06 | 0.3 |
| D-galacturonic acid | 0.012 | 0.06 | 0.3 |
| D-glucose | 0.16 | 0.8 | 4 |
| D-galactose | 0.012 | 0.06 | 0.3 |
| D-xylose | 0.012 | 0.06 | 0.3 |
| L-arabinose | 0.012 | 0.06 | 0.3 |
| L-fucose | 0.012 | 0.06 | 0.3 |

Agilent ChemStation software (Agilent Technologies, Santa Clara, USA) was used for system control, multilevel calibration of external standards, internal standard normalisation of samples, and peak integration. Integrated PMP-monosaccharide peaks were quantified by comparison with the calibrated curves of their corresponding monosaccharide standard. Peaks corresponding to unknown components were quantified using the calibration curve for mannose. A typical example of these calibration curves is shown in Figure 4. A complete set of examples for calibrations curves for the 10MS-VG / 10MS-GR standards and are provided in Appendix A.6.

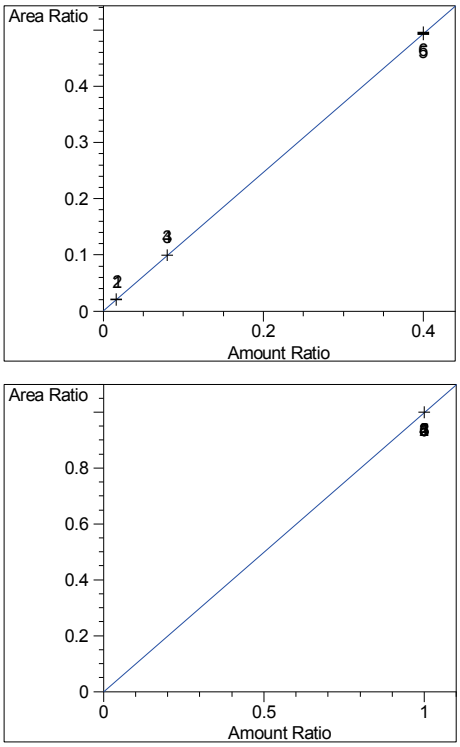


PMP-D-mannose at exp. RT: 4.177
DAD1 A, Sig=250,4 Ref=off
Correlation: 0.99999
Residual Std. Dev.: 0.00128
Formula: y = mx + b
m: 1.23380
b: 8.89973e-4
x: Amount
y: Area




PMP-2-DOG at exp. RT: 9.454
DAD1 A, Sig=250,4 Ref=off
Correlation: 1.00000
Residual Std. Dev.: 0.00000
Formula: y = mx + b
m: 1.00000
b: 0.00000
x: Amount
y: Area

**Figure 4: Example calibration curve for a 10MS-VG external mannose standard and the internal standard 2-deoxyglucose**

### 3.5.4 Separation of acid sugars by anion-exchange chromatography

Anion-exchange high performance liquid chromatography (AX-HPLC) for biomass hydrolysates was performed with a normal-phase Prevail™ Carbohydrate ES 5 µm 150 × 4.6 mm column (Grace Davison Discovery Sciences, Deerfield, USA) on an Agilent 1200LC system (Agilent Technologies, Santa Clara, USA), using eluent buffers: (A) MilliQ water; and (B) 300 mM ammonium acetate ($CH_3COONH_4$). For gradient testing, sample volumes of 25 µL were injected and separated over a 10-minute gradient from 40 % to 60 % buffer B, at a flow rate of 0.6 ml·min$^{-1}$ and 20 °C, with evaporative light scatter detection using an Alltech® ELSD 800 (Grace Davison Discovery Sciences, Deerfield, USA). Sample separation was followed by 3 minutes wash with 100 % B and 2 minutes re-equilibration to 40 % B.

### 3.5.5 Analysis of Kdo

High-pH anion exchange chromatography with pulsed amperometric detection (HPAEC–PAD) was conducted using a Dionex ICS5000 (Thermo Fisher Scientific Australia Pty Ltd, Scoresby, Australia). A Kdo standard series (2-keto-3-deoxyoctonate ammonium salt, Sigma-Aldrich Pty Ltd, Castle Hill, Australia) was diluted to concentrations (µM): 0.625, 1.25, 2.5, 5 and 10. An example elution profile of the Kdo external reference standard is shown in Figure 50 of Appendix A.8.

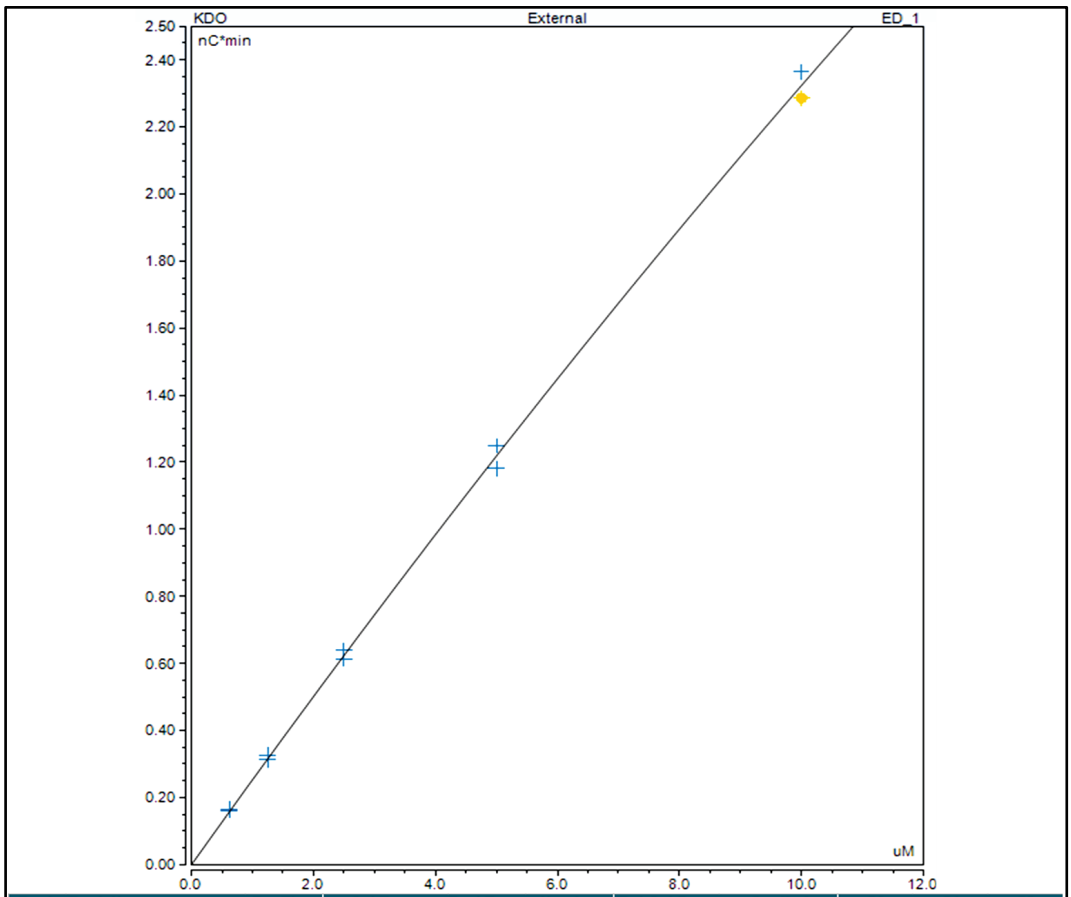


| Peak No. | Peak Name | Ret.Time min | Cal.Type | Eval.Type | Number of Points | Rel.Std.Dev. % | Coeff.of Determination | C0 (Offset) | C1 (Slope) | C2 (Curve) |
|---|---|---|---|---|---|---|---|---|---|---|
| *1* | *KDO* | *7.609* | *Quad* | *Area* | *10* | *2.9265* | *0.99904* | *0.0000* | *0.2553* | *-0.0023* |
| 2 | GalacturonicAcid | 10.017 | Quad | Area | 10 | 0.9203 | 0.99991 | 0.0000 | 0.3911 | -0.0011 |
| 3 | GlucuronicAcid | 11.067 | Quad | Area | 10 | 2.2750 | 0.99943 | 0.0000 | 0.5129 | -0.0040 |
| Maximum | | | | | | 2.9265 | 0.99991 | | | |
| Minimum | | | | | | 0.9203 | 0.99904 | | | |

**Figure 5: An example HPAEC calibration curve for Kdo**

Typically, for biomass extractions a 1:160 dilution in Milli-Q water was required. A 25 µL aliquot of each diluted sample was injected onto a Dionex CarboPAC PA-20 column (3×250 mm) with guard (3×50 mm) kept at 30 °C and operated at a flow rate of 0.5 ml·min$^{-1}$. The eluents used were (A) 0.1 M sodium hydroxide and (B) 0.1 M sodium hydroxide with 1 M sodium acetate. The multi-step gradient used was 1 % to 20 % B over 9.5 minutes followed by a 1.5 minute wash with 100 % B and re-equilibration at 1 % B. The detector was kept at 20 °C and data collection was at 2 Hz. The Gold Standard PAD waveform for carbohydrates (std. quad. potential) was used. The integrated peak areas were compared to a Kdo external standard curve, an example of which is provided in Figure 5.

### 3.5.6 Monosaccharide nominal mass confirmation by LC-ESI-MS and MS/MS

Nominal mass analysis by liquid chromatography electrospray ionization mass spectroscopy (LC-ESI-MS) and tandem mass spectrometry (MS/MS) was performed in the positive ion mode, using a LCQ Deca XP Plus ion trap mass spectrometer (ThermoFinnigan, San Jose, USA) fitted with an ESI source and interfaced with a Surveyor® HPLC (ThermoFinnigan, San Jose, USA), and PDA detector recording at 190 to 600 nm. The HPLC was equipped with an Alltima 5 µm C18 10 Å 250 × 2.1 mm column (Grace, Deerfield, USA) for separation of 10 µL sample loads, with 0.5 % v/v formic acid as solvent A and 0.5 % v/v formic acid in acetonitrile as solvent B delivered at a flow rate of 0.2 ml·min$^{-1}$ at 25 °C. For PMP-derivatised RP-HPLC fractions the gradient profile was 5 minutes isocratic at 25 % B, a linear increase to 33 % B at 10 minutes, a linear increase to 95 % B at 20 minutes, followed by 5 minutes isocratic, and a return to 25 % B at 26 minutes, followed by 10 minutes isocratic to re-equilibrate. The gradient profile for AX-HPLC fractions was 5 minutes isocratic at 1 % B, a linear increase to 90 % B at 15 minutes, followed by 4 minutes isocratic, and a return to 1 % B at 20 minutes, followed by 10 minutes isocratic to re-equilibrate. The MS analysis of PMP-derivatised RP-HPLC fractions was performed using a sheath gas flow rate of 55 units, an auxiliary gas flow rate of 20 units, an applied source spray voltage of 4.5 kV with source current at 80 µA, a capillary voltage of 20 V and the heated capillary maintained at 250 °C. A full scan analysis

from $m/z$ 50-1000 in the positive ion mode was followed by data-dependent MS/MS on the most intense ion identified using an isolation width of m/z 2.0, a normalised collision energy of 35 %, an activation Q of 0.250, an activation time of 30 ms, and a charge state of 1. For analysis of AX-HPLC fractions the capillary voltage was changed to 14 V, the full scan analysis increased to $m/z$ 50-2000 and the normalised collision energy to 50 % for MS/MS.

### 3.5.7 Low volume total starch assay

Total starch was determined using AIR preparations of 20 mg ground freeze-dried biomass (see Sections 3.4.2, 3.4.3 and 3.4.4) with an amyloglucosidase/α-amylase digestion method based on the Megazyme Total Starch Assay Kit (K-TSTA, Megazyme International Ireland, Wicklow, Ireland) and modified for low volume application. An AIR preparation of 20 mg standardised regular maize starch control (provided with the K-TSTA kit) which contained 96 % w/w starch was used with each assay. Specimens were wet with 80 µL 80 % v/v ethanol then suspended in 60 U thermostable α-amylase in 600 µL 50 mM MOPS, 5 mM calcium chloride at pH 7.0. The suspensions were mixed using a Ratek VM1 vortex mixer (Ratek Instruments Pty Ltd, Boronia, Australia), capped and incubated in a 100 °C water bath (make, city, country) for 12 minutes with mixing every 4 minutes. Following α-amylase digestion, specimens were transferred into a 50 °C water bath for 5 minutes to temperature equilibrate then 66 U amyloglucosidase in 820 µL 200 mM sodium acetate at pH 4.5 was added. Specimens were mixed and incubated at 50 °C in the water bath for 30 minutes. On completion of amyloglucosidase digestion, specimens were mixed and centrifuged at 16,000 rcf for 10 minutes using an Eppendorf 5415D microcentrifuge (Eppendorf AG, Hamburg, Germany). Supernatant samples, 900 µL, were diluted to 6 ml with ultrapure water then 50 µL of each dilution transferred to a 96-well deep well plate along with triplicates of 50 µL 1 mg·ml$^{-1}$ glucose standards and 50 µL ultrapure water blank samples. Each well was mixed with 1.5 ml GOPOD reagent (Megazyme International Ireland, Wicklow, Ireland) containing glucose oxidase plus peroxidase and 4-aminoantipyrine. The plate was then incubated at 50 °C for 20 minutes using an Eppendorf Thermomixer comfort with attached MTP microplate block (Eppendorf AG, Hamburg, Germany).

After incubation, 500 µL from each assay well was diluted 1:2 with 500 µL ultrapure water, then 250 µL of each assay sample was transferred into a 300 µL 96-well microplate and read at 510 nm on a µQuant microplate spectrophotometer (BioTek Instruments Inc., Winooski, USA).

Starch content of specimens were determined as follows:

$$starch,\ \% = \Delta_A \times F \times \frac{V_{final}}{V_{test}} \times D \times M \times \frac{100}{afdw_{initial}} \times 0.9 \qquad \textbf{Equation 13}$$

where:

$\Delta_A$ = Absorbance (reaction) read against the reagent blank

F = Conversion from D-glucose absorbance to µg = $\frac{0.05\ (\text{mg of glucose})}{\text{absorbance for 0.05 mg of glucose}}$

$V_{final}$ = Final volume of sample = 6 ml

$V_{test}$ = Volume of sample analysed = 0.05 ml

D = Dilution factor before read = 2

M = Multiplication factor to account for total digest volume = $\frac{1.5\ (\text{ml total digest})}{0.9\ (\text{ml digest used})} = 1.667$

$\frac{100}{afdw_{initial}}$ = Factor to express "starch" as a percentage of sample afdw

$afdw_{initial}$ = The ash free dry weight in milligrams of sample analysed

0.9 = Adjustment from free D-glucose to anhydro D-glucose (as occurs in starch) = $\frac{162}{180}$

### 3.5.8 Total residual nitrogen

Culture media samples were filtered using 0.45 µm PVDF filters (Millipore Corporation, Billerica, USA) and analysed for total residual nitrogen using the Total Nitrogen by persulphate-hydrazine colourimetric standard method 4500-NC (Eaton *et al.* 1998). The persulphate method uses a combination of digestion and colourimetric procedures to determine total nitrogen by oxidation of all nitrogenous compounds to nitrate. An anhydrous potassium nitrate ($KNO_3$) standard (Sigma-

Aldrich Pty Ltd, Sydney, Australia) series in the range 0 to 1.4 mg-N·L$^{-1}$ was prepared in a 70 g·L$^{-1}$ Red Sea Salt solution to adjust for the effect of sample salinity (Figure 6).

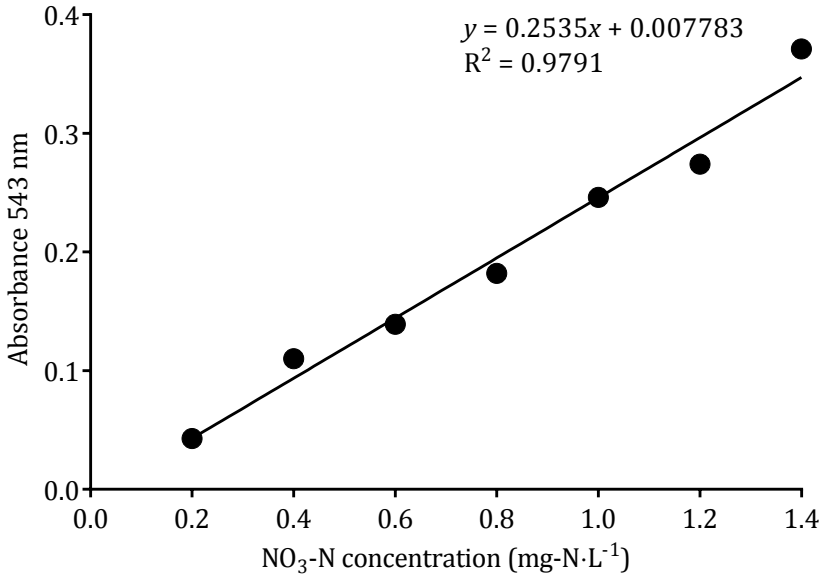


**Figure 6: Standard curve for total nitrogen assay**

### 3.5.9 Analysis of fermentation substrates and products

Standard analysis of fermentation samples was performed by HPLC using ion-exclusion chromatography (IEC) with a Phenomenex Rezex™ RFQ Fast Acid 8% cross-linked H+ 8 µm 100 × 7.8 mm column (Phenomenex Inc., Torrance, CA, USA) on an Agilent 1100LC system (Agilent Technologies, Santa Clara, USA), and 5 mM sulphuric acid ($H_2SO_4$) eluent buffer. This column was used to track glucose conversion to ethanol by refractive index detection (RID), and calibrated using a glucose-ethanol calibration standard mixture as detailed in Table 8. For organic acid analysis a Biorad HPX-87H ROA H+ (8%) column was used with the analytes measured by diode array detection (DAD) at 210 nm and calibrated against a ROA calibration standard mixture and a separate fumaric acid standard as detailed in Table 9.

**Table 8: Fermentation glucose-ethanol external standard solutions**

| Compound | Low standard ($g \cdot L^{-1}$) | Medium standard ($g \cdot L^{-1}$) | High standard ($g \cdot L^{-1}$) |
|---|---|---|---|
| Glucose | 0.3 | 3 | 30 |
| Glycerol | 0.1 | 1 | 10 |
| Lactic acid | 0.1 | 1 | 10 |
| Acetic acid | 0.1 | 1 | 10 |
| Ethanol | 0.3 | 3 | 30 |

**Table 9: Fermentation fumaric acid and ROA external standard solutions**

| Organic acid | Low standard ($g \cdot L^{-1}$) | Medium standard ($g \cdot L^{-1}$) | High standard ($g \cdot L^{-1}$) |
|---|---|---|---|
| Citric acid | 0.1 | 0.5 | 1 |
| Tartaric acid | 0.1 | 0.5 | 1 |
| Malic acid | 0.1 | 0.5 | 1 |
| Succinic acid | 0.1 | 0.5 | 1 |
| Lactic acid | 0.2 | 1 | 2 |
| Fumaric acid * | 0.001 | 0.05 | 0.1 |
| Acetic acid | 0. 1 | 0.5 | 1 |

* Prepared as a separate external standard to the ROA external standard.
Note: ROA external standard was a wine standard used in the Jiranek laboratory so also contained ($L^{-1}$): 0.1 g to 1 g glucose, 0.1 g to 1 g fructose, 1 g to 10 g glycerol and 10 g to 100 g ethanol. Most of these (with the exception of glycerol that had a weak absorbance at 210 nm) could only be detected by refractive index.

Dilutions for samples and standards were in Milli-Q water. Each sample and standard was filtered through a Phenex-NY 0.45 µm 4 mm syringe filter prior to loading. Typically, 20 µL of sample was injected and separated over either an extended 8-minute (for glucose and ethanol) or 30-minute (for organic acids) isocratic elution at a flow rate of 1.0 $ml \cdot min^{-1}$ and 60 °C that also facilitated column re-equilibration.

Agilent ChemStation software (Agilent Technologies, Santa Clara, USA) was used for system control, multilevel calibration of external standards, and peak integration. Integrated analyte peaks were quantified by comparison with the calibrated curves of their corresponding standard compound. A typical example of the glucose-ethanol fermentation calibration curves is shown in Figure 7. The complete set of examples for calibrations curves for all fermentation standards are provided in Appendix A.9. Examples of elution profiles for the fermentation standards are also provided in Appendix A.10.

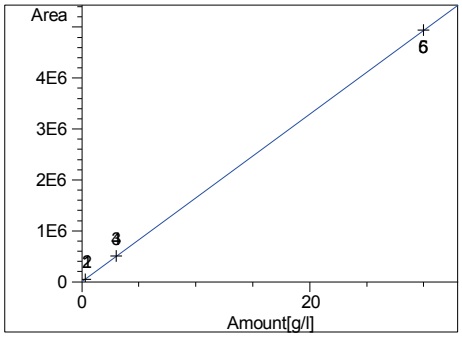


```
glucose at exp. RT: 2.125
RID1 A, Refractive Index Signal
Correlation:           1.00000
Residual Std. Dev.: 4783.48876
Formula: y = mx + b
      m: 164676.38272
      b:   3641.84661
      x: Amount
      y: Height
```

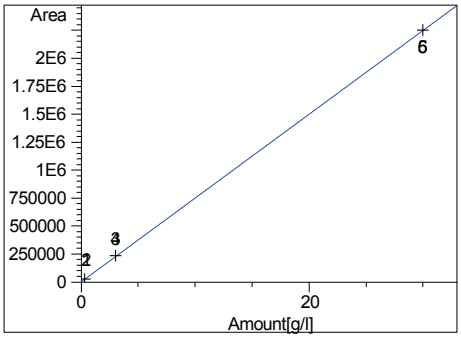


```
ethanol at exp. RT: 4.733
RID1 A, Refractive Index Signal
Correlation:           0.99999
Residual Std. Dev.: 3807.74696
Formula: y = mx + b
      m:  74948.09546
      b:   4336.71887
      x: Amount
      y: Height
```

**Figure 7: Example calibration curves for fermentation standard**
Calibration for glucose and ethanol IEC standards measured by RID.

## 3.6 Fermentation

### 3.6.1 Preparation MUR-233 biomass feedstock for fermentation studies

Production 20 L batches of MUR-233 were cultivated in PBRs following the procedure described in Section 3.2.6. Alum present at 100 mg·$L^{-1}$ or 0.29 mM concentration in harvested biomass was not expected to be problematic for fungal growth and metabolism. This alum concentration was well below levels reported as inhibitory to fungal mycelial growth (Kolaei *et al.* 2013) and also provided aluminium ions ($Al^{3+}$) at levels found to promote considerable production of antibacterial substances from *Rhizopus* strains, with beneficial implications to mycelial growth and physiology (Morita *et al.* 2004). In total five 20 L batches of MUR-233, each cultivated over 17 to 24 days were harvested by chemical flocculation and settling as described in Section 3.4.1 then stored at -20 °C. These were eventually freeze-thawed and pooled into a 50 L conical-bottomed settling tank as a single source biomass for fermentation studies. The pooled biomass was mixed and settled at room temperature for 3 hours. Excess supernatant was decanted from above the settled biomass bed and discarded. The settled biomass slurry was collected and stored in a 2-8 °C cold room. In total 5.5 L of biomass was produced at a slurry concentration of 6.7 ± 0.2 % afdw, based on analyses described in Section 3.5.1.

### 3.6.2 The fungal strain

*Rhizopus oryzae* NRRL 1526 was obtained from the Agricultural Research Service (ARS) Culture Collection, Bacterial Foodborne Pathogens and Mycology Research Unit (Request Number 2013-00000019, United States Department of Agriculture, Peoria, USA). The strain was maintained at pH 5.6 on modified Saboraud agar slants containing ($L^{-1}$): 10 g peptone, 40 g glucose, and 15 g agar and stored at 4 °C. The Saboraud agar slants were prepared as detailed in Appendix A.4.

### 3.6.3 Inoculum preparation

The experimental transfer and handling of *R. oryzae* NRRL 1526 was conducted in a Class II biosafety cabinet. A mycelium sample was transferred using a sterile loop from a *R. oryzae* stock

slant into liquid yeast extract peptone dextrose (YEPD) medium containing ($L^{-1}$): 20 g peptone, 10 g yeast extract, and 20 g glucose and incubated at 28 °C under self-induced anaerobic conditions with 120 rpm shaking for 6 days until a ball of mycelium was formed. The YEPD medium was prepared as detailed in Appendix A.4. Working liquid cultures of the fungus were maintained in the same growth conditions for use during the course of fermentation trials by inoculating individual liquid YEPD subcultures with a 3 mm mycelial plug, equivalent to 2 ± 0.2 mg fungal dry weight, from a day 4 parent culture. Mycelial plugs were produced using a flame-sterilised stainless steel punching cylinder apparatus with push piston as shown in item B of Figure 8.

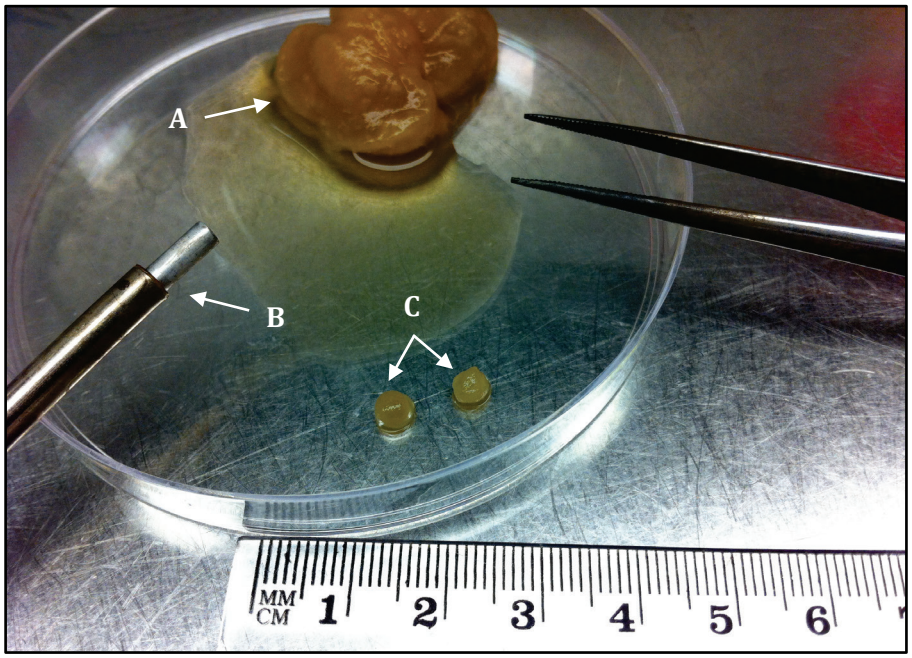


**Figure 8: Apparatus for inoculum preparation**
Image shows (A) congealed *R. oryzae* mycelial biomass, (B) stainless steel plug tool, and (C) mycelial plugs.

### 3.6.4 Preparation of salt-removed (washed) MUR-233 biomass slurry

This method was used to produce a salt-removed control by sequential dilution of separated liquid from apportioned amounts of pooled MUR-233 biomass from Section 3.6.1. MUR-233 biomass in

2 × 200 ml of harvested slurry was separated from saline background medium in 250 ml centrifuge bottles at 3,200 rcf using a bench scale Eppendorf Centrifuge 5810R (Eppendorf AG, Hamburg, Germany). The bulk of supernatant was discarded by decanting and residual supernatant removed using a 25 ml pipette. The removed supernatant was replaced with RO water, and biomass was mixed back into a slurry to dilute residue saline liquid. This process was repeated until the initial 7 % w/v RSS in the biomass was diluted to < 0.1 % w/v as shown in Table 10; the final salinity was estimated at 0.046 % w/v RSS. Salt-removed or washed MUR-233 biomass prepared using this method will be referred to as MUR-233W.

**Table 10: Dilution steps for biomass salt removal**

| Step | Volume exchanged from 2 × 200 ml (ml) | Volume ratio removed | Sequential dilution factor | Approximate final salinity (% w/v RSS) |
|---|---|---|---|---|
| 1 | 2 × 136 | 0.68 | 1/3.125 | 2.240 |
| 2 | 2 × 146 | 0.73 | 1/3.704 | 0.605 |
| 3 | 2 × 152 | 0.76 | 1/4.167 | 0.145 |
| 4 | 2 × 136 | 0.68 | 1/3.125 | 0.046 |

### 3.6.5 Preparation of acid hydrolysate fermentation feedstock

This method was used only for preparation of acid hydrolysates of washed MUR-233 biomass for preliminary fermentation trials. MUR-233W aliquots (2 × 50 ml) were pelleted in 50 ml centrifuge tubes at 3,200 rcf using a bench scale Eppendorf Centrifuge 5810R (Eppendorf AG, Hamburg, Germany), the bulk supernatant discarded by decanting and residual supernatant removed using a 100-1000 µL micropipette. The retained pellets were resuspended into 0.6 M sulphuric acid to a final 100 ml volume, then pooled into a 250 ml Schott bottle and autoclaved at 121 °C (1.06 bar) for 20 minutes to hydrolyse in an AMA250N autoclave (Astell Scientific Ltd, Sidcup, United Kingdom). The hydrolysed biomass was then re-neutralised to pH 6.5 using 5 M potassium

hydroxide. As this hydrolysate would be used as a fermentation media, re-neutralisation was done under and aseptic environment inside a Class II biosafety cabinet with pH test was conducted by pipetting 100 µL samples onto pH indicator strips.

### 3.6.6 Preparation of starch fermentation broth

This method was used to both disrupt MUR-233 cell structure to release starch, and to prepare solubilised starch dispersions in mixtures for fermentation studies. These included treatment of broths of salt-removed and standard MUR-233 biomass preparations, and yeast extract peptone starch (YEPS) control medium (Table 11). Soluble starch (analytical reagent grade, BDH Laboratory Chemicals, Poole, England) was used for the control medium preparation.

Each type of prepared broth was dispensed into a Schott bottle then autoclaved at 121 °C (1.06 bar) for 20 minutes in an AMA250N autoclave (Astell Scientific Ltd, Sidcup, United Kingdom). The final fermentation broths containing solubilised starch dispersions were then equilibrated to ambient room temperature prior to use in fermentations. A sample (1 ml) of each MUR-233 biomass broth was tested for release of starch using a 0.2 % iodine solution (Table 41) added at a 1:50 sample ratio. Broth samples stained blue where starch had been released and solubilised, in comparison to control samples of biomass suspension in which only cells stained blue.

**Table 11: Nutrient rich starch fermentation medium (YEPS)**

| Component | Standard ($g \cdot L^{-1}$) | Hypersaline NaCl * ($g \cdot L^{-1}$) | Hypersaline RSS ** ($g \cdot L^{-1}$) |
|---|---|---|---|
| Yeast extract | 10 | 10 | 10 |
| Peptone | 20 | 20 | 20 |
| Starch | 50 | 50 | 50 |
| Sodium chloride | - | 27 or 54 | - |
| Red Sea Salt | - | - | 42 or 70 |

* Medium used in Section 7.2.5
** Medium used in Section 7.3

### 3.6.7 Bench scale fermentation

Submerged fermentation studies (in liquid culture) using NRRL 1526 were conducted under sterile conditions to ensure that the experimental observations for biological substrate usage and ethanolic conversion could only be attributed to NRRL 1526. Process temperature was maintained at 28 °C in a temperature-regulated room, and cultures were mixed on orbital shakers at 120 rpm. All fermentations were self-induced anaerobic in which the culture vessel was sealed, not pre-purged of air, but becomes anaerobic during the initial phases of fermentation as $CO_2$ is produced. The typical vessel volumes and types for fermentations are shown in Table 12.

For fermentations in 50 ml cone-bottomed polypropylene tubes, the fermentation broths were sterilised separately then dispensed into the sterile tubes. The tubes were inoculated then sealed with screw caps and during fermentation the gas pressure from accumulated $CO_2$ was vented when individual tubes were opened for analytical sampling. Typically, daily 1 ml samples were taken.

**Table 12: Vessel volumes and types for *R. oryzae* NRRL 1526 bench scale fermentations**

| Fermentation volume (ml) | Vessel volume (ml) | Vessel type |
|---|---|---|
| 30 | 50 | Cone-bottomed tube |
| 100 | 250 | Conical flask |

Fermentations in 250 ml glass conical flasks were sealed with water-filled airlocks and septum sealed sampling ports (Figure 9). The fermentation broths were sterilised by autoclave in situ with each flask apparatus at 121 °C for 20 minutes. Sterile water was added to the airlocks after apparatus was sterilised. During fermentation, daily 1 ml samples were taken using a 1 ml syringe equipped with a 21-gauge needle. The needle and syringe were sterilised with absolute ethanol then rinsed three times with sterile water before and after sampling.

**Figure 9: Bench scale setup for NRRL 1526 fermentations**

A theoretical ethanol yield of fermentations (Equation 14) was determined based on the available glucose and a maximum stoichiometric ratio of 0.51, as explained in Section 7.1.1. A percent yield (Equation 15) was then calculated as the actual yield of ethanol produced divided by the theoretical yield, and expressed as a decimal percentage.

$$theoretical\ ethanol\ yield\ (g \cdot L^{-1}) = \ measured\ glucose\ (g \cdot L^{-1}) \times 0.51 \qquad \textbf{Equation 14}$$

$$percent\ ethanol\ yield\ (\%) = \frac{actual\ measure\ ethanol\ (g \cdot L^{-1})}{theoretical\ ethanol\ yield\ (g \cdot L^{-1})} \times 100\ \% \qquad \textbf{Equation 15}$$

A maximum ethanol volumetric productivity (Equation 16) was calculated based on a linear correlation between the start and end time-points corresponding to the greatest degree of change in ethanol concentrations measured for fermentations. It was not possible to measure specific

ethanol productivity ($g \cdot g \cdot day^{-1}$) because the growth profile of *R. oryzae* could not be determined during fermentations.

$$maximum\ ethanol\ volumetric\ productivity = \frac{\Delta\ ethanol\ (g \cdot L^{-1})}{\Delta\ time\ (day)} \quad \textbf{Equation 16}$$

## 3.7 Statistical analysis

The results of this Project were analysed using Minitab Statistical Software version 17.0 (Minitab Inc., State College, PA) and GraphPad Prism 7.02 software (GraphPad Software, Inc., La Jolla, CA). Unless specifically stated, data values reported with a measure of variability have been calculated as the mean (average value) with variance shown as the standard deviation (±SD).

### 3.7.1 Normality test

When data groups were tested for normality, the Shapiro-Wilk normality test was used with a significance level ($\alpha$) of 0.05 applied to a null hypothesis ($H_0$) stating that the data set follows the standard normal distribution.

### 3.7.2 Two sample testing

Standard data comparisons were performed using two-sample testing. First F for equal variance followed by t for equal means.

### 3.7.3 One-way analysis of variance (ANOVA)

Comparisons of multiple groups of data were performed using one-way analysis of variance (ANOVA). For these analyses, the Dunnett test was used when comparing the means every group in a data set to the mean of a control group, and the Tukey test used when comparing all the means of groups within the analysed data set with each other.

# Chapter 4
# Monoculture isolation from Karratha outdoor ponds

## 4.1 Introduction

This chapter describes the steps undertaken to isolate and establish a working monoculture of *Tetraselmis* sp. MUR-233 for use in experimental studies for this Project.

### 4.1.1 Biomass selection

At the inception of this Project, the proposed biomass resource for fermentation studies was a robust *Tetraselmis* sp. production strain MUR-233 cultured at Muradel's original pilot plant at Karratha in the Pilbara region of Australia. This was one of four *Tetraselmis* strains screened and selected for lipid productivity, which had been transferred to Muradel from Murdoch University. Due to its robustness in the local Karratha environment (latitude of 20°44'11.81"S and longitude of 116°50'48.35"E, or -20.736615 and 116.846765 respectively), MUR-233 proved to be the primary candidate in the timeframe of this Project for up-scaled culture to assess biomass productivity and lipid yields for biodiesel (Fon Sing *et al.* 2014; Isdepsky 2015).

A culture sample of MUR-233 was provided by Muradel from an open raceway pond at Karratha and transferred for subcultivation and further propagation in the Microalgae Engineering Research Group (MERG) laboratories within the School of Chemical Engineering at the University of Adelaide (UOA). In part, this transfer was necessitated by concerns around biomass supply after the commencement of this Project due to unforeseen delays in the biomass production at Karratha. Another aspect to this culture transfer was that at the time it was believed that *Tetraselmis* sampled from Karratha would be a more appropriate source than the original culture collection at Murdoch University to capture potential differences resulting from evolutionary biological adaptation to environmental conditions specific to the field. Later studies (not covered in this Project) by research conducted in the MERG team would also allude to the importance of symbiotic microflora

in maintaining MUR-233 culture health, and exposure to the Karratha environment may have also changed the microfloral composition of the MUR-233 culture.

### 4.1.2 Requirement for MUR-233 monoculture

In consideration of co-energy products from this biomass, knowledge on the carbohydrate composition was critical to determining its potential for fermentation to bioethanol. As will be discussed in later chapters there is a degree of general knowledge on the typical carbohydrates found in various species of the *Tetraselmis* genus. However, a full taxonomic study has yet to be undertaken for MUR-233 to enable reliance on the literature, and there was limited available information within Muradel and its joint venture partners on the carbohydrate profile of MUR-233. Some of this information has since been published (Fon Sing & Borowitzka 2015), but a significant gap in knowledge outside the body of work described in this Project still exists on the precise carbohydrate composition of MUR-233. Hence, the important first step of this Project was to characterise this carbohydrate composition to both verify existing knowledge and determine the potential for microbial conversion to ethanol.

The exposure of the Karratha outdoor pond to environmental factors such as the unfiltered seawater used in cultivation presented difficulties to maintaining a true monoculture of MUR-233, and instances of contamination with other microalgae species had been reported during the commissioning of the raceway pond cultures. In order to study the specific carbohydrates of MUR-233 it was necessary to isolate this production strain from the sample received from Karratha prior to further studies in the Adelaide laboratories. A monoculture was needed for the carbohydrate characterisation studies on MUR-233 discussed in Chapter 5 to ensure that the quality (specific composition) of the experimental data would not be compromised by contaminant microorganisms. Another key reason for transferring the production strain to a laboratory monoculture was to enable lifecycle screening to determine the suitability of biomass produced from this microalga as a bioethanol feedstock.

### 4.1.3 "Cleaning" rather than purification of MUR-233

Methods which have been employed to purify microalgae and obtain axenic cultures include clonal isolation by micropipetting or streaking for single colonies, and effective removal of background bacteria has been achieved with combinations of antibiotics applied in actively growing microalgae cultures (Andersen 2005). However, the purification of a microalgae culture to the extent of being truly axenic is very difficult and the term "axenic", in practice, usually refers to a culture that is demonstrably free of any contaminant prokaryotic or eukaryotic organisms (Barsanti & Gualtieri 2006). There are a number of reasons for this difficulty in purifying cultures. Background bacteria may go undetected because they do not respond to standard nutrients required by microalgae in culture. In some instances, bacteria are attached to the microalgae cell surface (Rosowski 1992) and may prove difficult to dislodge and remove. Additionally, microalgae culture survival may also be dependent on coexisting bacteria through obligate symbiotic relationships and the removal of such bacteria would be detrimental to culture health (Barsanti & Gualtieri 2006).

For the purpose of characterising the carbohydrate composition of MUR-233, a truly axenic culture was not necessary. The aim was to isolate a MUR-233 monoculture and ensure that background microbial populations carried over from the seawater used at Karratha would be removed to the extent that no significant heterogeneous biomass would be co-produced in MUR-233 cultures to obscure the specific analytical characterisation of this strain.

## 4.2 MUR-233 culture from Karratha

A field sample taken at the Karratha pilot plant (KPP) and transferred to MERG was expanded into a 500 ml liquid culture in modified f medium as described in Section 3.2.4 prior to clean up of the MUR-233 culture. A visual qualitative assessment of the expanded culture was conducted under an inverted light microscope (Olympus IX50, Olympus America Inc., Melville, USA) to determine the extent of biological heterogeneity with other organisms.

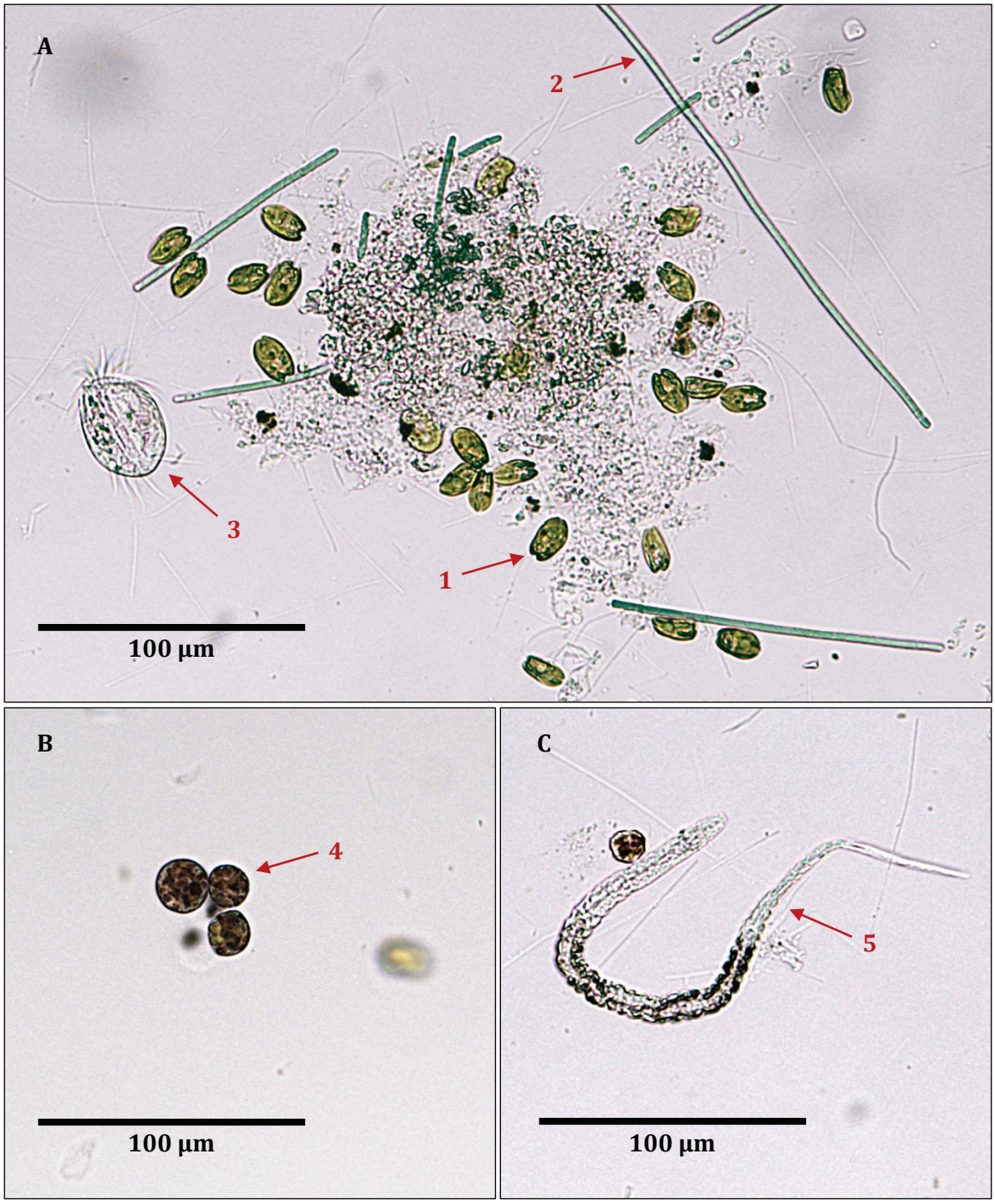


**Figure 10: Culture expanded from Karratha field sample**
Olympus IX50 Inverted light microscope slide mount (×20 magnification) images showing: (1) *Tetraselmis* sp. strain MUR-233; (2) filamentous cyanobacterium; (3) ciliate protozoa; (4) red microalgae; and (5) nematode.

The observed *Tetraselmis* sp. were assumed to be strain MUR-233 and found to be actively motile. Although MUR-233 was the most dominant species, the assessment revealed a polyculture of microorganisms (Figure 10). Ciliate protozoa resembling the genus *Euplotes* were observed, often in the vicinity of masses of microalgae cell debris. Such invasive grazers are commonly detected in outdoor microalgae cultures and have the potential to decimate biomass yields if left untreated (Day *et al.* 2012). Based on an observed frequency of one grazer per 40 µL of culture mounted onto slides (n = 6), the concentration of grazers was estimated to be 25 cells·ml$^{-1}$, a ratio of approximately 1 per 32,000 MUR-233 cells. Also present were red microalga with morphology similar to *Porphyridium* sp. and filamentous cyanobacterium, each with their respective phycoerythrin and phycocyanin pigments distinctively visible. Nematodes were also observed in the culture. A complete assessment of the exact nature and variety of contaminant organisms present was not essential to this Project, and only a rudimentary search of the literature was conducted for the purpose of this qualitative comparison.

## 4.3 MUR-233 isolation on solid media

Isolation of microalgal cells on solid agar media can be an effective method for directly establishing axenic cultures without further purification treatment, especially for *Tetraselmis* spp. which are known to grow on agar (Andersen 2005). It also effectively serves to eliminate against species of microalgae that are unable to grow on such media. Hence, the expanded culture from Karratha was transferred onto solid modified f medium agar (preparation described in Section 3.2.2) for single colony selection and propagation as described in Section 3.2.3.

As no genetic markers were available for MUR-233, isolated *Tetraselmis* cultures from the field sample could not be verified as strain MUR-233. It was assumed, therefore, that only one *Tetraselmis* strain was present in the culture and that the clonal isolates were MUR-233. The selection of a single colony for study would at least ensure that subsequent culture expansions would be derived from a clonal isolate to eliminate the possibility or likelihood of having multiple

strains or even species of *Tetraselmis* present in the working culture. Another assumption was made that biological observations in this Project on the culture derived from the isolated clone would be representative of the dominant *Tetraselmis* sp. present in the original MUR-233 Karratha sample.

The *Tetraselmis* sp. dominant polyculture derived from Karratha was successfully transferred to solid growth media. Green microalgal colonies were visible on agar plates after 7 days of cultivation. However, the plate colonies required up to 21 days of growth to achieve a more suitable size for sample transfer by a flame-sterilised loop. Visual assessment and manipulation of the plate cultures were conducted under a stereo microscope (Section 3.2.3). To achieve clonal isolation for MUR-233, a total of three sequential serial colony transfers onto subculture plates were required.

The first series of agar culture plates contained 5 $\mu g \cdot ml^{-1}$ carbenicillin, and showed a variable degree of biological heterogeneity. Observed *Tetraselmis* colonies were emerald green, as confirmed after morphological assessment on a wet slide mount under a light microscope (Section 3.2.3). However, on some plates the colonies appeared more olive green due to the presence of brown diatoms. Sections of a number of plates were also populated with darker blue-green cyanobacteria with filamentous colony structures. On all plates, colonies of an undetermined pink coloured microbial contaminant were also extensively distributed.

The visually cleanest *Tetraselmis* colonies were selected and subcultured onto a second agar plate series with carbenicillin concentration increased to 10 $\mu g \cdot ml^{-1}$. As shown in Figure 11-A and Figure 11-B, on these plates the colonies of the unknown microbial contamination were reduced but remained within close proximity to the *Tetraselmis*. Diatoms were only observed on one plate and cyanobacteria contamination was no longer visibly evident.

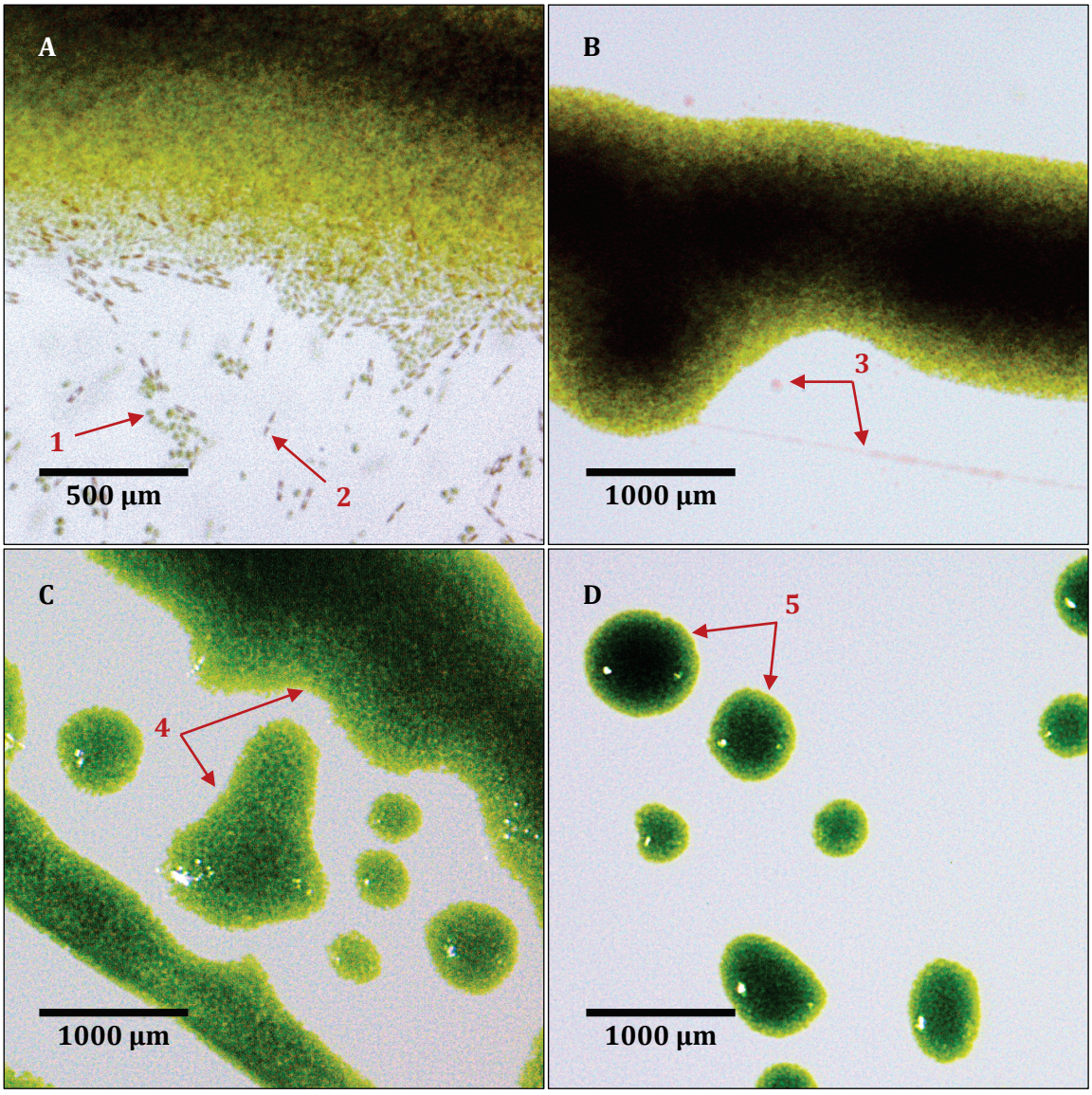


**Figure 11: *Tetraselmis* colonies on f medium agar plates**
Images captured under stereo microscope (Zeiss Stemi 2000-C). Second subcultured plate series (A) and (B) showing: (1) MUR-233 cells, (2) diatom cells, and (3) unknown microbial contaminant colonies. Third subcultured plate series (C) and (D) showing homogeneous purified MUR-233 in (4) mixed and (5) single colonies with no visible contamination from other microorganisms.

*Tetraselmis* colonies were selected and subcultured onto a third agar plate series containing 20 µg $ml^{-1}$ carbenicillin. The colonies on these plates were uniform in colouring with no further visual evidence of contamination, as shown in Figure 11-C and Figure 11-D. Subsequent MUR-233 cultures used for the laboratory studies in this Project were derived from a single colony on this

third agar plate series. To allow for experimental redundancy, initially two visually healthy colonies from the plates were transferred and expanded into liquid media, but ultimately only one clonal isolate was use once the *Tetraselmis* monocultures had been established.

## 4.4 "Cleanliness" assessment of isolated MUR-233

### 4.4.1 Assessment of potential background microbial contamination

The isolated MUR-233 was initially transferred back into 0.2 µm filter sterilised antibiotic-free liquid modified f medium, and cultured in 50 ml Erlenmeyer flasks as described in Section 3.2.4. Aside from visual assessments under light microscopy to confirm removal of the heterogeneous populations in the Karratha culture as discussed in Section 4.2, the isolated MUR-233 cultures were also checked for the background presence of bacteria and yeast contamination. A basic growth test was performed using lysogeny broth (LB) and yeast extract peptone dextrose (YEPD) media with and without added 70 $g \cdot L^{-1}$ RSS (Appendix A.4). A 100 µL volume of each sterile MUR-233 culture was inoculated into 20 ml of each different medium and incubated for 9 days at 37 °C then checked for background microbial growth by light microscopy. This test determined that no background microbial contamination was present. Once it was established that there was no background microbial carry-over from Karratha, the working MUR-233 cell line was expanded into non-sterile cultures in 500 ml shake flasks (Section 3.2.4) for further assessment.

### 4.4.2 A new method for detecting cell surface bacteria on green microalgae

There have been very few studies on bacterial attachment to microalgae cell walls. For *Tetraselmis*, one particular study showed three bacterial strains from the genera *Pseudomonas*, *Acinetobacter* and *Ruegeria* to be closely associated with *Tetraselmis indica* cell walls, in particular the shed cell wall material (Arora *et al.* 2012). The experimental results described in Section 4.4.1 showed no evidence of bacteria in the MUR-233 culture environment directly after clonal isolation. However, with the expansion of the clonal isolate into a working culture, there remained a likelihood that bacteria on the cell surface may have carried over or that other halotolerant bacteria could be

present in replacement non-sterile saline growth medium. Typically the autotrophic MUR-233 culture conditions would not be favourable for bacterial proliferation, however the carbohydrate rich cell walls of MUR-233, as expected in the genera *Tetraselmis* (Becker *et al.* 1998), could provide a nutrient source for bacterial growth (Arora *et al.* 2012). A simple method was required to determine the presence of bacteria on the cultured MUR-233 cell surfaces.

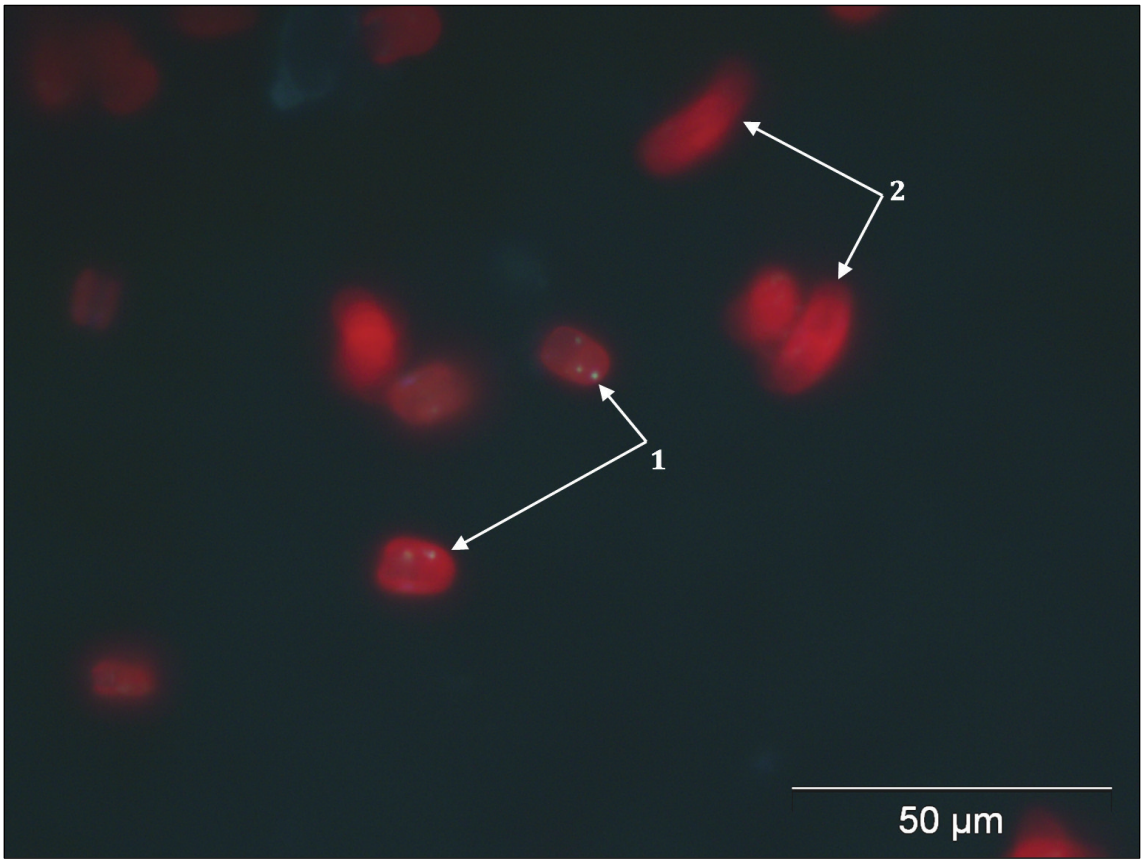


**Figure 12: Chlorophyll fluorescing purified *Tetraselmis* MUR-233 culture**
Olympus BX51 microscope (oil immersion ×100 magnification) images of culture sample. (1) Bluish white fluorescing points can be seen on non-motile cells. (2) Motile cells appear as blurred fluorescent streaks. Image was brightness adjusted by +10 %.

Intrinsic fluorescence in bacteria under UV light has been attributed to endogenous fluorophores such as some amino acids, reduced nicotinamide adenine dinucleotide (NADH), pteridines,

structurally related flavins, and pyridine coenzymes (Ammor 2007; Dalterio *et al.* 1987; Doddema & Vogels 1978). Although no bacteria had been visibly evident under light microscopy in the media of the MUR-233 working cultures, it was hypothesised that perhaps the presence of bacteria on the cell surface could be observed through fluorescence detection using UV excitation wavelengths consistent with the aforementioned studies. This was assessed as described in Section 3.3.4, and a MUR-233 culture image with red chlorophyll autofluorescence from the green microalgae is shown in Figure 12 in which distinct bluish white points were evident and indicative of possible cell surface bacteria. Bluish white fluorescence at the 330 to 385 nm excitation wavelength range used was consistent with findings from Doddema and Vogels (1978) who used an excitation wavelength at 350 nm. However, unlike this earlier study which assessed methanogens, any bacteria present on the MUR-233 cells were unlikely to be methanogenic anaerobes given the moderately aerated growth conditions of the shake flask cultures and the microalgal photosynthetic production of oxygen into the surrounding environment.

To verify this finding, the same MUR-233 culture was then assessed using confocal scanning laser microscopy (CSLM) as described in Section 3.3.5 as this would allow improved image depth of field for determining the location of what appeared to be surface bacteria fluorescence. Differential interference contrast (DIC) images from the CSLM are shown in Figure 13, including separately defined focal plane images with blue bacterial autofluorescence and red chlorophyll autofluorescence. Axial z-scanning of the MUR-233 specimen revealed that the two points of blue autofluorescence were present in the focal planes above those from which chlorophyll autofluorescence was observed, and indicated that their origin was external to the microalga cell and most likely on the cell surface. The DIC images from the CSLM revealed a considerably greater degree of structural detail for the MUR-233 cell than the previous wide-field fluorescence microscopy, and clearly showed autofluorescent chlorophyll internalised to the cell structure.

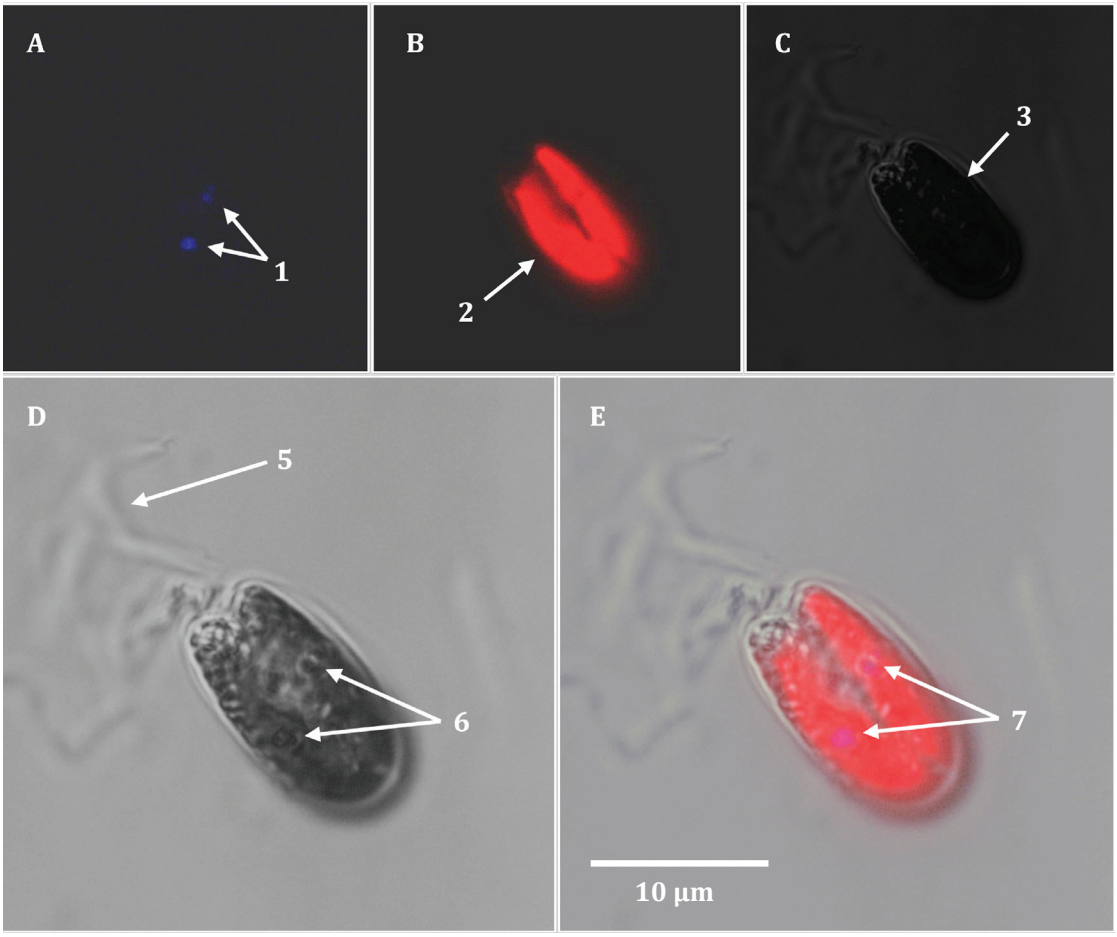


**Figure 13: CSLM images of a *Tetraselmis* MUR-233 cell**
Confocal scanning laser microscope (Leica TCS SP5, ×100 magnification) image captures of a live MUR-233 cell line using: (A) emission filter, 410 to 440 nm; (B) emission filter, 613 to 703 nm; (C) & (D) Black-and-white differential interference contrast (DIC) illuminance. (E) Overlay of images A, B & C. Image brightness adjustments: A, B & C by +10 %, D & E by +60 %. (1) & (7) bacterial autofluorescence; (2) MUR-233 chlorophyll autofluorescence; (3) MUR-233 cell DIC image; (5) motile flagella DIC image; and (6) surface bacteria DIC image as correlated with (1).

Following the CSLM observation of the likely presence of cell surface bacteria on individual cells of the MUR-233 working culture, scanning electron microscopy was conducted as described in Section 3.3.6 to verify the presence of the bacteria and validate the use of simple fluorescence microscopy for detection of cell surface bacteria on live microalgae. The resulting electron micrographic images (Figure 14) confirmed the presence of surface bacteria associated with cell membranes of MUR-233. The observed bacteria displayed cocci and coccobacilli morphology, and were attached to both whole MUR-233 cells and cell debris. The observed bacterial morphology

was consistent with that of both *Acinetobacter* sp. (typically coccobacillary shaped) and *Ruegeria* sp. (reported as spherical shaped) bacteria previously isolated from *Tetraselmis indica* cultures (Arora *et al.* 2012). That study reported that *T. indica* showed increased growth in xenic cultures with the *Acinetobacter* sp., and the combination of *Acinetobacter* sp. and *Ruegeria* sp. in xenic cultures resulted in prolonged microalgal survival. Interestingly, Arora *et al.* (2012) also reported the presence rod-shaped (bacilli) *Pseudomonas* sp. and associated with decreased microalgal growth. No bacterial with rod-shaped morphology were observed in the field emission scanning electron microscopy (FESEM) samples for the MUR-233 working culture.

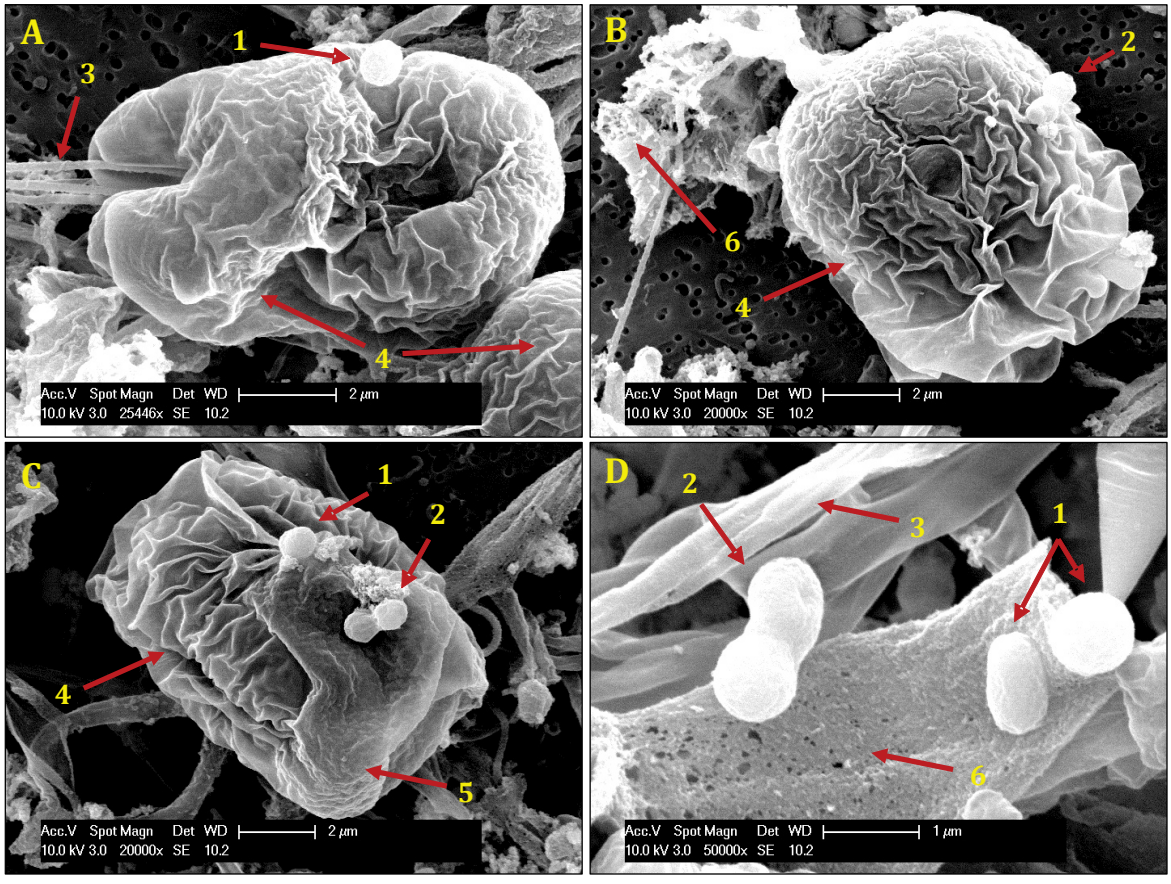


**Figure 14: FESEM images of *Tetraselmis* MUR-233 and surface bacteria**
Images (A), (B) and (C) show (4) MUR-233 cells one of which has attached (3) flagella. Surface bacteria including (1) cocci and (2) coccobacilli types attached to (4) MUR-233 cells and (6) cell debris. (5) Shows a section of scaled *Tetraselmis* cell surface that has not been affected by structural collapse from sample dehydration.

In Figure 14, MUR-233 cells in the prepared FESEM sample appeared to have wrinkled and collapsed structures, most likely a result of osmotic shock during sample preparation. Some sections of uncollapsed cell surface for the *Tetraselmis* can be seen with a scaled appearance typical to the genus. In Figure 14-C, "coli flour" structures adjacent to the coccus and coccobacillus cells may be indicative of partial digestion of the MUR-233 cell wall by secreted bacterial carbohydrases. For instance, the *Acinetobacter* sp. reported by Arora *et al.* (2012) were found to produce carbohydrases specific to polysaccharides generally present in the cell wall of *T. indica* such as glucans, galactans, galactomannans and pectins.

The experimental results determined that bacteria remained in the MUR-233 working microalgal monoculture with some attached to cell membranes, however, the level of contamination was deemed negligible. Also, much of the bacteria were found on cell debris so could potentially be controlled through the regular subculturing dilution in the semicontinuous culture maintenance of the MUR-233 working culture. The FESEM observations on bacteria morphology and potential carbohydrase activity aligned with bacteria that could potentially be beneficial to the health of the MUR-233 working culture. Hence, no further action was taken to remove the cell surface bacteria from the working culture.

A key development was the fluorescence microscopy approach described here for detecting surface bacteria on microalgae that has not previously been reported. This method has since become a useful tool in determining the effectiveness of antibiotic treatment in purifying axenic MUR-233 cultures for genomic sequencing through collaborative work with the ARC Centre of Excellence (CoE) for Plant Cell Walls (not covered in this Project).

## 4.5 MUR-233 working culture

The MUR-233 monoculture was expanded to a working culture and maintained in a 2,000 ml vessel as described in Section 3.2.4 with non-sterile media for the period of this Project. A visual qualitative assessment of the expanded and cleaned up monoculture was conducted by inverted light microscopy (Figure 15).

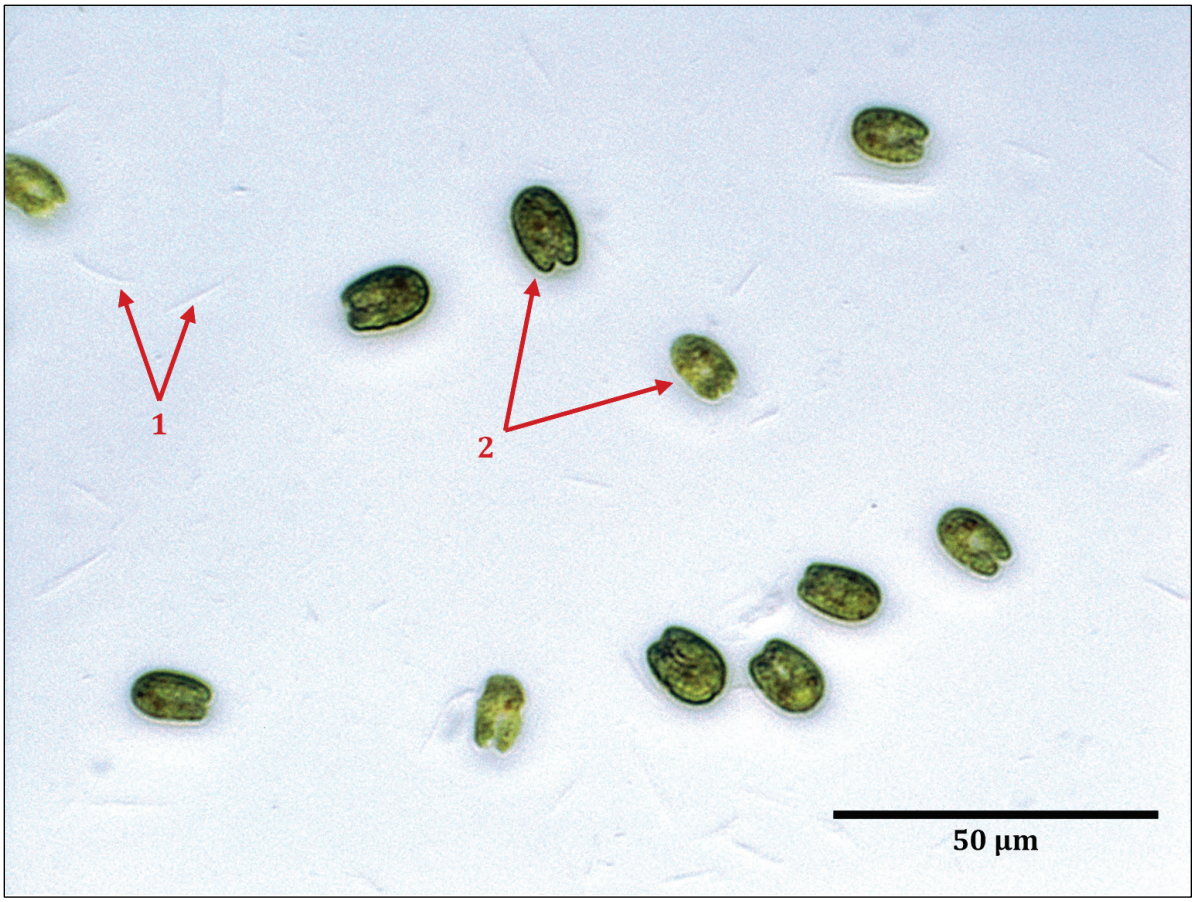


**Figure 15: Cleaned up MUR-233 culture**
Inverted light microscope (Olympus IX50, ×40 magnification) image of culture sample immobilised with 0.2 % v/v acetic acid showing (1) flagella and (2) MUR-233 cells.

The examined culture was motile with no visible benthic or cystic cells. The immobilised ellipsoid *Tetraselmis* cells are shown in Figure 15 with shed flagella resulting from treatment with

0.2 % v/v acetic acid to facilitated image capture and cell morphology assessment. Digital imaging was used to enable quantification of cell dimensions as described in Section 3.3.2, but due to the variance in cell size and shape non-normal distributions were observed for cell length, width and sphericity ($p > 0.05$). Nevertheless, as shown in Table 13 the respective medians for these cell measurements were in close agreement to the means, indicating a symmetrical distribution of cell size. This method determined that the MUR-233 working culture at day 4 before subculture displayed a size of 15.66 × 10.91 µm with 0.48 sphericity. The mean size was somewhat larger than measurements made under FESEM, as would be expected given the collapsed cell morphology observed in the FESEM images. The cell size was, however, consistent with the 10 × 13 µm measurements for *Tetraselmis* isolates reported in Fon Sing (2010), and also the revised data indicating sizes 10 × 15 µm and 15 × 20 µm reported by Fon Sing and Borowitzka (2015).

**Table 13: MUR-233 dimensional image analysis yields**
Cell measurement, including sphericity as a measure of cell roundness, at culture day 4 as determined by digital imaging of individual *Tetraselmis* cells from 3 separate cultures (n = 783).

| Cell measurement | Unit | Maximum | Minimum | Mean | Median |
|---|---|---|---|---|---|
| Length | µm | 20.99 | 8.75 | 15.66 | 15.81 |
| Width | µm | 15.67 | 4.96 | 10.91 | 11.05 |
| Sphericity * | - | 0.70 | 0.22 | 0.48 | 0.48 |

* A sphere has a sphericity of 1, and any particle which is not a sphere would have sphericity less than 1.

The laboratory bench scale growth conditions used in this Project were similar to original screening studies (Fon Sing 2010; Fon Sing & Borowitzka 2015) from which MUR-233 was subsequently selected as a candidate strain for Muradel. A key difference was the use of RSS here for salinity adjustment rather than natural seawater with added NaCl. As such the 7 % w/v salinity

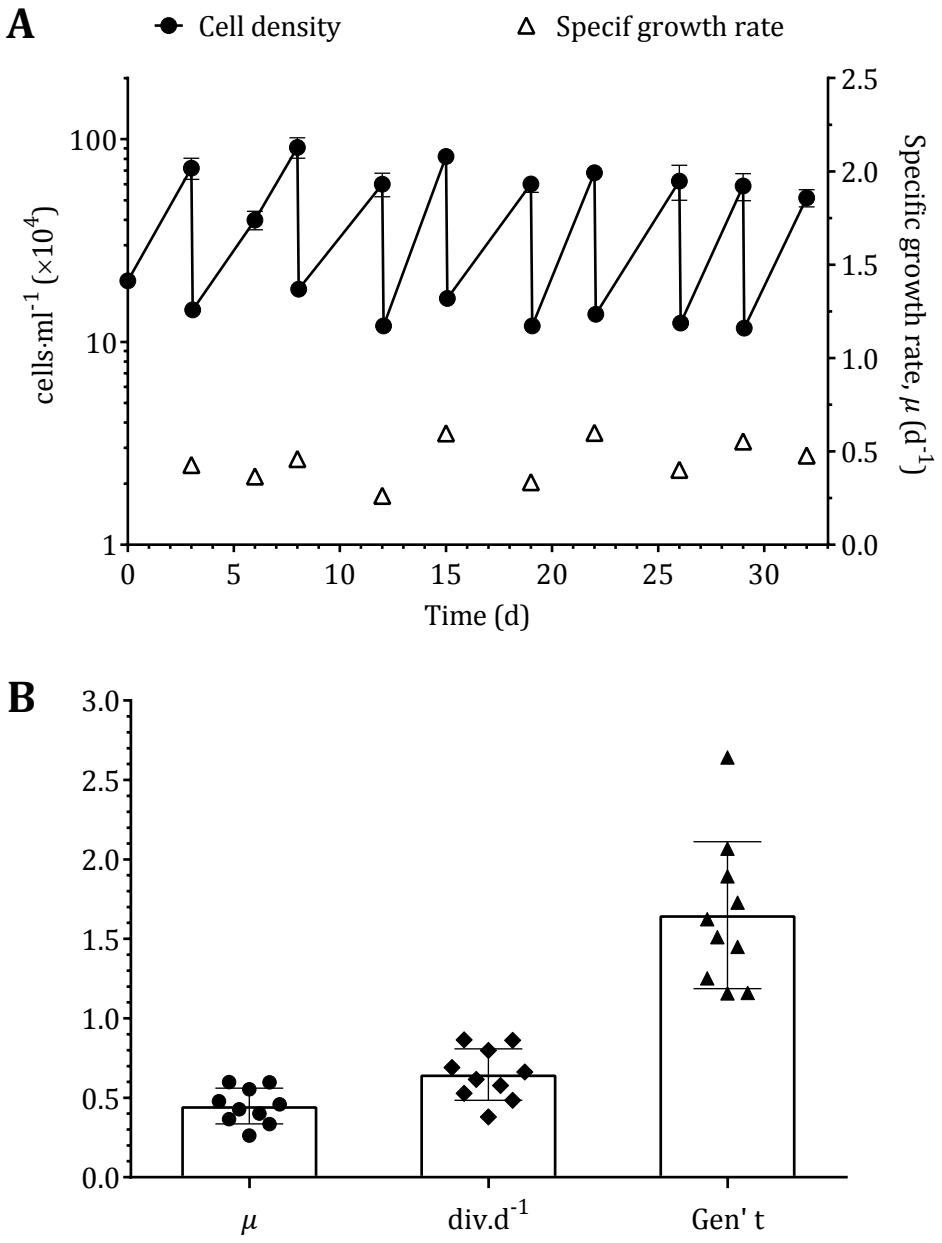


**Figure 16: Semicontinuous bench scale propagation of MUR-233**
Growth performance of the MUR-233 working culture. Data from cell counts (n = 9) at harvest points every 3 to 4 days. (A) Semicontinuous growth over a 32 days, showing cell concentrations (closed circle) and specific growth rate (open triangle) at harvest points. (B) Mean ± standard deviation values for the semicontinuous MUR-233 working culture growth rate ($\mu$), divisions per day (div.d$^{-1}$), and generation time (Gen' t).

of modified f medium in this study had an equivalent NaCl content of approximately 5 % w/v. The stabilised growth of the semicontinuous MUR-233 working culture is shown in Figure 16-A with cell counts determined as described in Section 3.3.1. During the semicontinuous growth an 80 % culture dilution rate was applied every 3 to 4 days, and cell densities were maintained between $1.36\times10^5 \pm 0.14\times10^5$ and $6.73\times10^5 \pm 0.79\times10^5$ cells·ml$^{-1}$. Between each subculture the growth media remained well buffered in the RSS base solution at pH 8.4 to 8.6.

The purpose of this culture was to confidently establish an effective and low input approach to maintaining a motile MUR-233 working culture so that a consistent inoculum would be available for experimental work and biomass production batches on an as needed basis. The specific growth rate ($\mu$) for MUR-233 in laboratory culture at 5 % w/v NaCl has previously been reported at 0.5 (Fon Sing & Borowitzka 2015). In comparison, as shown in Figure 16-B this working culture displayed a reduced $\mu$ of 0.45 ± 0.11 d$^{-1}$ with 0.65 ± 0.16 div·d$^{-1}$, and 1.65 ± 0.46 Gen' t. Overall, however, both the reduced $\mu$ and relatively broad statistical standard deviation across the growth metrics on culture performance was acceptable and reflective of the low input approach to the culture maintenance.

## 4.6 Concluding remarks

A working monoculture of the *Tetraselmis* sp. strain MUR-233 was established with stabilised semicontinuous growth and low input culture maintenance requirements. Visual and growth assessments confirmed that the *Tetraselmis* cells in the culture were motile and displayed quadriflagellate morphology, an average size of 15.7 × 10.9 µm, and an average specific growth rate ($\mu$) of 0.45 d$^{-1}$ that were consistent with MUR-233. The working monoculture was important for enabling carbohydrate profiling of MUR-233 as well as providing seed cultures for producing biomass for fermentation trials.

During this undertaking to clean up a field sample of the Karratha pilot plant and isolate MUR-233, a new qualitative method for detecting cell surface bacteria on green microalgae was developed

using fluorescence microscopy. This method uses ultraviolet (UV) excitation at 330 nm to 385 nm and fluorescent detection at emission >420 nm to visualised and distinguish surface bacteria by their autofluorescence against chlorophyll autofluorescence from the *Tetraselmis* cells. The method provides a simple approach to assess for effective removal of surface bacteria in instances where axenic *Tetraselmis* or other green microalgae cultures may be desirable.

# Chapter 5
# Structural carbohydrates of biomass

## 5.1 Introduction

The working monoculture isolated in Chapter 4 enabled cultivation of a homologous biomass for analytical characterisation. This following chapter covers experimental work undertaken to verify and quantify the available structural monosaccharides present in MUR-233 biomass. The findings will be compared to what has been reported in the literature for various *Tetraselmis* species. Experimental work assessing biomass glucose in relation to starch will be presented in Chapter 6.

The physicochemical properties of the genus *Tetraselmis* were investigated during the mid to late 1900s amongst numerous other studies of green microalgae in relation to the evolutionary origin of land plants (Lewis & McCourt 2004). Hence, there is a small existing body of knowledge on the carbohydrate composition of various *Tetraselmis* species. However, at the outset of this Project the species identity for MUR-233 was unknown and remains unverified, necessitating investigations to determine the exact biomass carbohydrate profile.

### 5.1.1 Carbohydrate ultrastructure of *Tetraselmis*

The *Tetraselmis* genus of green microalgae displays a scaly morphology common to Prasinophytes, but it is now understood that *Tetraselmis* sits as an evolutionary intermediate between Prasinophyceae and the more advanced class Chlorophyceae, and is classified under Chlorodendrophyceae to reflect a mitotic physiology similar to the Chlorophyceae group of microalgae (Domozych *et al.* 1981). Initial studies of Prasinophycean scales included those on *Tetraselmis* cell ultrastructure (internal and surface characteristics) and cell wall chemical composition (Becker *et al.* 1991; Melkonian 1979; Norris *et al.* 1980; Parke & Manton 1965). Incorporation studies using radio-labelled glucose in *Tetraselmis subcordiformis* indicated the cell wall composition would be high in carbohydrates with glucans from starch and exogenous glucose transported to the Golgi apparatus during cell growth to be transformed to precursors for the

synthesis of the cell wall polysaccharides (Gooday 1971b). However, despite the glucose utilisation in producing these cell wall polysaccharides the composition of *Tetraselmis* cell walls consist of very little neutral monosaccharides.

### 5.1.2 Cell wall (theca) carbohydrates of *Tetraselmis*

The genus *Tetraselmis* has an amorphous cell wall or theca which was originally thought to be pectin-like with galactose and uronic acids as major components (Lewin 1958). Investigations with *Tetraselmis marinus* found that, even during division, cells were always covered with at least one theca (Parke & Manton 1965). Quadriflagellate motile *Tetraselmis* cells have only a single theca whereas resting or benthic cells (cysts) may have multiple thecal layers. The thecae of *Tetraselmis* spp. are characteristically covered in coalesced (fused) scales and rich in carbohydrates, consisting up to 82 % w/w of the theca dry weight (dw) with a predominance of acidic polysaccharides (Becker *et al.* 1998; Melkonian *et al.* 1991).

In *Tetraselmis striata* and *Tetraselmis tetrathele*, 3-deoxy-D-manno-2-octulosonic acid (Kdo) was found to be the major structural monosaccharide component (Becker *et al.* 1991; Melkonian *et al.* 1991). Kdo is an acid labile 2-keto-sugar acid (Becker *et al.* 1998; Kiang *et al.* 1997) that is also found in bacterial lipopolysaccharides (Müller-Loennies *et al.* 2003) and pectic polysaccharides of some plant cell walls (York *et al.* 1985). Becker *et al.* (1998) proposed that for *T. striata* the thecae consisted of a highly branched polysaccharide core structure of scales to which was attached $\alpha$-2,4-linked poly-Kdo with mono- and disaccharide galacturonic acid side chains (Figure 17). Other key cell wall acidic sugars included 3-deoxy-D-manno-5-O-methyl-2-octulosonic acid (5OMeKdo) and 3-deoxy-lyxo-2-heptulosaric acid (Dha). In total, the 2-keto-sugar acids (Kdo, 5OMeKdo and Dha) formed 60 % of the dry weight of the cell wall. In this study, gulose and galactose were also identified as key monosaccharides in the thecal scales. Earlier work by Becker *et al.* (1989) also detected low levels of glucose and arabinose in *T. striata* cell walls; approximately 1 % molar ratio or less of the total carbohydrates in the cell wall.

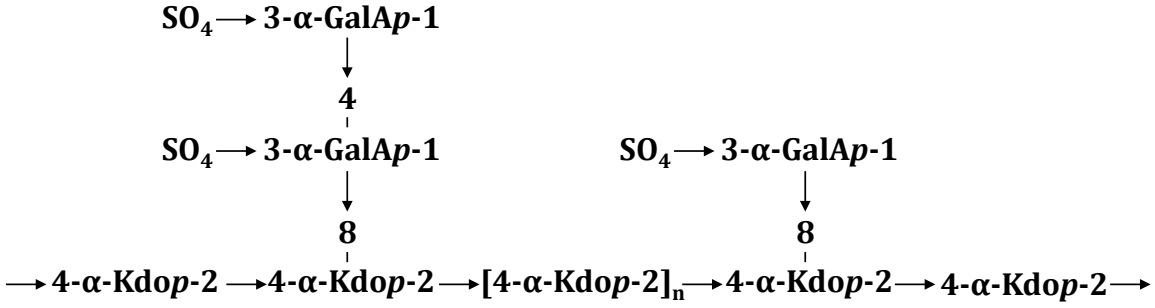


**Figure 17: Proposed cell wall polysaccharide of *Tetraselmis striata***
The relative amount of GalA and Kdo containing di- and trisaccharides in partial hydrolysates indicated that about 70 % to 80 % of side chains are trisaccharides, and based on periodate oxidation and methylation analysis the average distance between attached side chains (n) is about 4 Kdo units.

Reference: Becker *et al.* (1998). Source figure reproduced under a John Wiley and Sons license for print and electronic formats in a thesis/dissertation (RightsLink Printable License Number 4344301119821).

### 5.1.3 *Tetraselmis* cell wall carbohydrates compared to other green microalgae

Aside from the salinity challenges discussed in Section 1.3, the acidic monosaccharides in *Tetraselmis* cell walls also present significant challenges for fermentation with organisms such as *Saccharomyces cerevisiae*, which typically convert neutral sugars to ethanol. Suitability as fermentable feedstock varies between different green microalgae that often have complex cell wall carbohydrates unlike cellulosic structures of land plants that are used to feed second-generation bioethanol processes. An analytical comparison of *Tetraselmis* cell wall monosaccharides conducted by Becker *et al.* (1991) against a number of other green algae species is presented in Table 14. Similarly, other studies have shown significant diversity in the types of carbohydrate structures found in cell walls of different taxa of green microalgae, especially in comparison to the Chlorodendrophyceae taxon in which *Tetraselmis* is grouped. These studies have been previously summarised by Domozych *et al.* (2012) and are presented here in Table 15.

**Table 14: Monosaccharide composition of cell walls or of complex glyco-conjugates isolated from the culture medium of various species**

A. Neutral sugars, expressed in mol % of total carbohydrate.

| Taxon | Material | Ara | Rha | Xyl | Fuc | Gul | Gal | Man | Glc |
|---|---|---|---|---|---|---|---|---|---|
| *Tetraselmis striata* | Theca | 1 | – | – | – | 4 | 7 | – | – |
| *Tetraselmis tetrathele* | Theca | 1 | – | – | – | 3 | 7 | – | – |
| *Scherffelia dubia* | Theca | 1 | 1 | 2 | – | 4 | 7 | – | – |
| *Mantoniella squamata* | Scales | 4 | 3 | 6 | 6 | 14 | 4 | ? | 6 |
| *Pyramimonas amylifera* | Scales | 6 | 4 | 6 | – | 6 | 6 | – | 10 |
| *Mesostigma viride* | Scales | 13 | – | 4 | – | 6 | 6 | – | – |
| *Nephroselmis olivacea* | Scales | 15 | 2 | 4 | – | 6 | 4 | – | 9 |
| *Micromonas pusilla* | EtOH * | – | – | (+) | (+) | – | – | – | – |
| *Chlamydomonas reinhardtii* | Cell wall | 22 | 14 | 2 | – | 5 | 26 | 23 | 8 |
| *Chlamydomonas reinhardtii* | EtOH | 32 | 16 | 4 | – | – | 32 | 8 | 8 |
| *Dunaliella bioculata* | EtOH | 4 | 28 | 4 | – | – | 19 | 26 | 29 |
| *Dunaliella primolecta* | EtOH | 7 | 17 | 19 | – | – | 7 | 24 | 33 |
| *Asteromonas gracilis* | EtOH | 7 | 10 | 16 | 7 | – | 16 | 21 | 18 |
| *Hafniomonas reticulate* | EtOH | 7 | 10 | 16 | 7 | – | 16 | 21 | 18 |
| *Monomatix* sp. | EtOH | 36 | – | 17 | – | – | 21 | (+) | 25 |
| *Pedinomonas tuberculate* | EtOH | 36 | 8 | 6 | – | – | 20 | 10 | 15 |

B. Acidic sugars, expressed in mol % of total carbohydrate.

| Taxon | Material | GalA | Kdo | 5OMeKdo | Dha | Glc NAc | Kdo in acetic acid extracts ** |
|---|---|---|---|---|---|---|---|
| *Tetraselmis striata* | Theca | 21 | 54 | 4 | 8 | – | ND |
| *Tetraselmis tetrathele* | Theca | 20 | 58 | 4 | 7 | – | ND |
| *Scherffelia dubia* | Theca | 18 | 60 | 4 | 6 | – | ND |
| *Mantoniella squamata* | Scales | 5 | 13 | 15 | 25 | ? | + |
| *Pyramimonas amylifera* | Scales | 4 | 20 | 24 | 16 | – | + |
| *Mesostigma viride* | Scales | (+) | 24 | 16 | 28 | – | + |
| *Nephroselmis olivacea* | Scales | 3 | 15 | 10 | 32 | – | + |
| *Micromonas pusilla* | EtOH * | – | – | – | – | – | – |
| *Chlamydomonas reinhardtii* | Cell wall | (+) | – | – | – | – | – |
| *Chlamydomonas reinhardtii* | EtOH | (+) | – | – | – | – | – |

| Taxon | Material | GalA | Kdo | 5OMeKdo | Dha | Glc NAc | Kdo in acetic acid extracts ** |
|---|---|---|---|---|---|---|---|
| *Dunaliella bioculata* | EtOH | – | – | – | – | – | – |
| *Dunaliella primolecta* | EtOH | – | – | – | – | – | – |
| *Asteromonas gracilis* | EtOH | – | – | – | – | 6 | – |
| *Hafniomonas reticulate* | EtOH | – | – | – | – | 3 | – |
| *Monomatix* sp. | EtOH | – | – | – | – | – | – |
| *Pedinomonas tuberculate* | EtOH | – | – | – | – | 5 | – |

* EtOH medium polymers precipitated with ethanol.
** +/– = indicates the presence/absence in acetic acid extracts of whole cells; ND = not determined. Ara = arabinose; Rha = rhamnose; Xyl = xylose; Fuc = fucose; Gul = gulose; Gal = galactose; Man = mannose; Glc = glucose; GalA = galacturonic acid; Kdo = 3-deoxy-D-manno-2-octulosonic acid; 5OMeKdo = 3-deoxy-D-manno-5-O-methyl-2-octulosonic acid; Dha = 3-deoxy-lyxo-2-heptulosaric acid; GlcNAc = N-acetylglucosamine; (+) = trace; ? = questionable; – = not detectable.

Reference: Becker *et al.* (1991).

**Table 15: Summary of the composition of extracellular coverings in green algae**

| Taxon | Covering type | Biochemical composition |
|---|---|---|
| Prasinophyceae | "Scales," coatings | 2-Keto acid sugars, mannans, glycoproteins |
| Chlorodendrophyceae | Wall of fused scales | 2-Keto acid sugars, proteins |
| Trebouxiophyceae | Cell walls | Cellulose, algaenan, β-galactofuranan |
| Chlorophyceae | Crystalline glycoprotein walls; fibrillar cell walls | Hyp-rich glycoproteins, cellulose pectins, AGP, extensin |
| Ulvophyceae | Cell walls | Cellulose, β-mannans, β-xylans, sulphated (sometimes pyruvylated) polysaccharides or sulphated rhamnogalacturonans, AGP, extensin |
| Charophyceae-early divergent clades | Scales, cell walls | 2-Keto acid sugars, cellulose, homogalacturonans, 1,3 β-glucans, AGP |
| Charophyceae-late divergent clades | Cell walls | Cellulose, homogalacturonans, RG-I xyloglucans, mannans, xylans, mixed linkage glucans, 1,3 β-glucans, AGP, extensin, lignin |

AGP = arabinogalactan proteins; Hyp = hydroxyproline.

Reference: Domozych *et al.* (2012)

### 5.1.4 Whole of biomass carbohydrate quantification

The quantification of specific monosaccharides in MUR-233 biomass is important for determining the amount of available sugar substrate for fermentation to ethanol. Typically, the phenol-sulphuric acid (PSA) analytical method has been used for measuring carbohydrates in MUR-233 (Fon Sing 2010; Fon Sing & Borowitzka 2015; Isdepsky 2015). This approach for determining total sugar concentration in a sample is based on the original methodology developed by Dubois *et al.* (1956) which provides reliable estimates of sugar content in pure solutions. The method uses strong acidic conditions to transform carbohydrates to furfural compounds by dehydration, and then condenses these with aromatic compounds such as phenol (or anthrone in other similar methods) to produce chromogens. Masuko *et al.* (2005) showed that there were differences in chromogenic responses between sugars, even though at 490 nm most sugars can be measured at or near their absorption maxima (Figure 18). However, the relative absorbance of analysed samples to that of the reference standard would in some instances limit the usefulness of this method, where some sugars such as glucosamine and *N*-acetylneuraminic acid would produce negligibly low responses to this assay. Despite these approximations, an adapted high throughput variant of the PSA method (Masuko *et al.* 2005) has been used in this Project to enable comparison of results to the previously mentioned studies on the MUR-233 strain. Yet as will be later discussed in this Chapter, the expected 2-keto-sugar acid rich content of *Tetraselmis* cell walls would limit the accuracy of the PSA methodology, requiring consideration of alternative analytical approaches that would be more suited for accurate quantification of the MUR-233 biochemical composition.

Based on the literature at the time of this Project's inception, insufficient information was available to determine the amounts of different *Tetraselmis* cell wall monosaccharides as proportions of the total cell dry weight. Previous studies including those discussed above which characterised specific thecal monosaccharides would typically only quantify these relative to the total detected monosaccharides or polysaccharide fractions. To date, only one published study has reported on

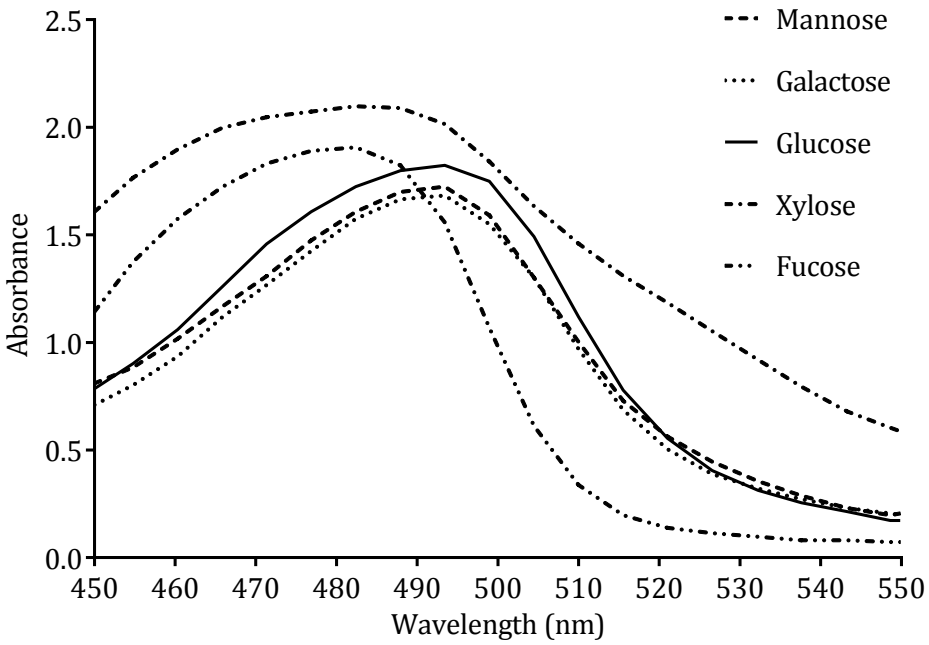


**Figure 18: Variances in PSA chromogenic responses of different reducing monosaccharides**
Absorption spectra of color products from mannose, galactose, glucose, xylose and fucose with peaks at 491, 491, 493, 486 and 482 nm, respectively.

Reference: Masuko *et al.* (2005). Source figure reproduced under an Elsevier license for print and electronic formats in a thesis/dissertation (RightsLink Printable License Number 4315151343263). Graph was digitized using GetData Graph Digitizer software.

the quantity of selected *Tetraselmis* cell wall monosaccharides relative to total cell weight (Kermanshahi-pour *et al.* 2014). That study determined *Tetraselmis suecica* UTEX LB 2286 consisted of 5 % w/w Kdo on a dry weight basis of microalgae alongside the finding that the cell wall monosaccharide composition consisted of 54 % Kdo, 17 % Dha, 21 % galacturonic acid and 6 % galactose. These results inferred that the remaining cell wall monosaccharide proportions on a dry weight basis in the microalgae were 1.6 % Dha, 1.9 % galacturonic acid and 0.6 % galactose such that 9.1 % of the total cell dry weight consisted of cell wall carbohydrates. However, even this study does not provide monosaccharide quantification on a total cell ash-free dry weight basis for the marine microalgae. The carbohydrate characterisation conducted in this Project seeks to

bridge this gap in knowledge in relation to monosaccharide quantities specific to MUR-233, using quantitative methodology relevant for application to biofuel production.

## 5.2 Specific requirements for analytical sample preparation

This Project involved significant analytical experimentation on MUR-233 biomass samples, typically of wet concentrated cells harvested by direct centrifugation, flocculation and settling or flotation, or a combination of these. Development of a standardised methodology was required, which would provide a consistent sample preparation for analysis regardless of the sample source.

A standard concentration method for microalgae cultures involves filtration onto glass fibre filters (Moheimani *et al.* 2013). Samples prepared in this way can be used for gravimetric analysis to determine culture productivity based on dw and afdw. For hypersaline cultures (such as MUR-233) this method also includes an ammonium formate wash before drying to remove adhering salts and in some instances precipitous carbonates without breaking cells open. Such filtration would typically be used for culture concentration prior to extraction steps in measuring microalgae composition, including the analysis of total carbohydrate content.

However, despite being a rapid cell harvesting method, filtration presented a number of undesirable limitations to the requirements of this Project. Primarily, the Project required a method to collect samples at a standard concentration in which all solids would be retained, including dissolved solids from the culture media. When the MUR-233 biomass is used as a process feedstock it carries with it co-harvested saline water and all the constituent salts. Understanding the liquid content of the biomass with its dissolved solids was therefore also important, yet much of this would be removed with filtration, particularly if followed by an ammonium formate wash. Also, a suitable sample preparation method must be applicable to all available MUR-233 source material whether from a dilute culture or concentrated slurry. The collection of biomass from concentrated slurries onto filters would be cumbersome without dilution of the material and consequently the dissolved solids contained within.

Another key consideration was the versatility of a sample preparation that would be stable over long-term storage at ambient temperature, and would enable ease of aliquoting for accurate compositional quantification in low volume assays. These sample characteristics were important to reduce experimental sampling requirements and allow a single sample preparation to be analysed across a variety of methodologies (such as for carbohydrates and total solids) with accurate correlation between the different assays. Furthermore, use of low volume assays would enable higher throughput replicate testing of material for improved precision. Samples collected by filtration are typically stored at -20 °C for long-term stability, requiring further care with freeze-thaw handling at the point of use; such samples are also difficult to separate from the bulk of the filter matrix to gravimetrically aliquot for use in low volume assays.

Section 3.4.1 describes a standard sample concentration and preservation method for biomass used in this Project. Centrifugation with a standard centrifugal force of 3,200 rcf was used to achieve a suitable sample endpoint. The remaining pellet would have a consistent packed cell density with liquid in the interstitial space between cells that would be representative of the decanted liquid in the original sample volume. This enables all the representative solids to be retained when the pellet is freeze-dried; a process that retains the chemical integrity of the sample in a dewatered state that can be stored over long term under ambient conditions. The moisture content in freeze-dried samples stored under ambient conditions on the bench was determined to be between 8 % and 10 % by mass (Section 3.5.1, Equation 10).

## 5.3 Kdo measurement in biomass hydrolysates

### 5.3.1 Potential interference in total carbohydrate assay

The PSA method quantifies carbohydrates against a glucose reference standard and minor quantitative variances result from the chromogenic responses of different monosaccharides to this assay. However, the presence of significant quantities of Kdo in *Tetraselmis* relative to other reported monosaccharides may limit the accuracy the PSA method for testing MUR-233 biomass.

Free 3-deoxyaldulosonic acids are unstable under acidic conditions (BeMiller *et al.* 1993), and Kdo would be severely degraded in the PSA method which uses the strong acid to dehydrate aldoses to furfural derivatives.

The chromogenic response of Kdo in a dilution series (1:50, 1:20, 1:10, 1:5, 1:2 and neat) prepared from a 1.86 mg·ml$^{-1}$ Kdo standard stock (2-keto-3-deoxyoctonate ammonium salt, Sigma-Aldrich Pty Ltd, Castle Hill, Australia) was tested using the low volume high throughput PSA method (Section 3.5.2), and compared to the relative chromogenic response from the glucose reference standard. The PSA assay absorbance comparison at 490 nm between glucose and Kdo is shown in Figure 19 with the chromogenic response of Kdo reduced by a factor of 6.98 against the glucose standard. Additionally, due to its known acid lability, the remaining portion of Kdo measured in the assay reaction was likely much less than the initial added concentrations. Nevertheless, if present in the MUR-233 samples Kdo would potentially contribute to an unquantifiable absorbance response with the PSA assay and elicit an inaccurate total carbohydrate quantity.

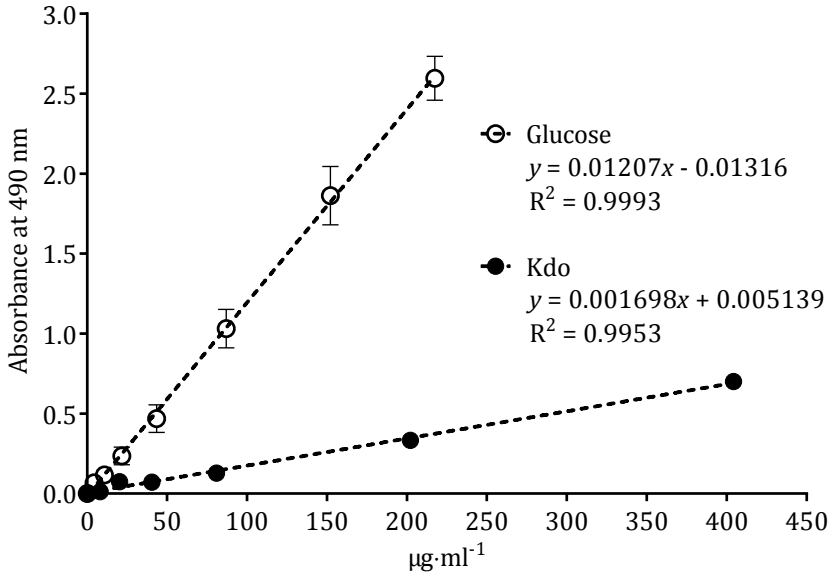


**Figure 19: Glucose and Kdo absorbances at 490 nm**
Chromogenic response for both sugars plotted as mean ± SD (n = 3).

### 5.3.2 Project limitations for Kdo analysis

Studies by Becker *et al.* (1989) and Kermanshahi-pour *et al.* (2014) used gas-liquid chromatography and gas chromatography both in combination with mass spectrometry (GLC-MS and GC-MS) to analyse 2-keto-sugar acids in methods based on trimethylsilyl (TMS) derivatives of methanolysates of *Tetraselmis* theca and whole cells. Alongside Kdo, these other studies also quantified the Dha and, in the case of Becker *et al.* (1989), 5OMeKdo content in *Tetraselmis*.

This Project, however, is limited to Kdo analysis by high-pH anion exchange chromatography with pulsed amperometric detection (HPAEC-PAD) as the only available method suitable for detecting Kdo. Mass spectroscopy was only used to verify the nominal mass of liquid chromatography peak fractions, and was not a component of the standard analytical method. Although a purified 2-keto-3-deoxyoctonate ammonium salt was purchased for use as a Kdo reference standard, appropriate analytical standards for 5OMeKdo and Dha were not commercially available. An alternative course of action was to conduct prep-scale chromatographic isolation and purification of probable 5OMeKdo or Dha from MUR-233 to produce in-house analytical reference standards. However, such an exercise would have been excessively time consuming and divergent from the main objective of this Project.

### 5.3.3 Hydrolysis strategy for quantification

Consistency in sample preparation was a key criterion for analytical work conducted in this Project. In this way, a single sample preparation could be tested across different methodologies. However, for quantitative Kdo estimations, severe conditions with very strong acids for complete cleavage of glycosidic bonds of cell wall polysaccharides to release Kdo could result in complex changes to the molecule (BeMiller *et al.* 1993). The hydrolysis conditions described in Section 3.4.5 using 1 M $H_2SO_4$ or 2 M TFA enable comparable extraction of monosaccharides from MUR-233 biomass. For the acid labile Kdo the use of TFA (p$K_a$ = -0.3) was preferred over $H_2SO_4$ (p$K_a$ = -3/2); the former being a weaker acid whilst at the concentrations used provides the same number of $H^+$

protons for hydrolysis. A study by Kiang *et al.* (1997) demonstrated that Kdo degradation during hydrolysis with 2 M TFA at 100 °C was similar to the more commonly used 1 % acetic acid treatment at 100 °C for release of Kdo from lipopolysaccharides.

The degradation effect for acid hydrolysis on Kdo in 2 M TFA was tested (see Figure 20) with results comparable to findings from the literature (Kiang *et al.* 1997). For this timecourse study 1 mM aliquots of the Kdo reference standard were hydrolysed in 2 M TFA for 120 minutes at 100 °C. Sacrificial sampling was implemented at 15, 30, 45, 60, 90 and 120 minutes with the time-point samples neutralised (Section 3.4.7) to ensure reaction termination for HPAEC analysis as per Section 3.5.5. It is clear that Kdo degrades significantly under the acid-catalysed hydrolysis conditions used to release other biomass carbohydrates from the MUR-233 cell wall matrix for analysis. After 45 minutes under the hydrolysis conditions approximately 46 % of Kdo was lost at which point the rate of degradation also reduced. It is uncertain why Kdo degradation slowed at

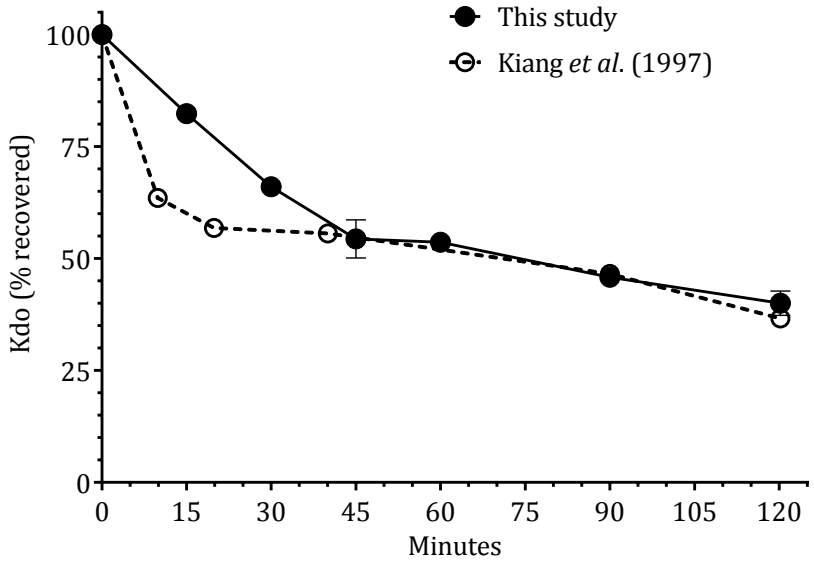


**Figure 20: Acid degradation profile for Kdo reference standard**
A comparison of timecourse hydrolyses in 2 M TFA at 100 °C from this Project against published data. For this study, mean values ± SD plotted (n = 2).
Reference: Kiang *et al.* (1997). Graph was digitized using GetData Graph Digitizer software.

this point, however, this phenomenon had no bearing on the final methodology adopted for quantification of Kdo.

A hydrolysis study was also conducted on MUR-233 to determine the release and degradation profile of Kdo extraction from the biomass. Samples of ground freeze-dried material, 20 mg each, were gravimetrically weighed, de-starched using α-amylase and amylogucosidase (Section 3.5.7) with solids recovered by 10 minutes centrifugation at 16,000 rcf. AIR preparations of the solids were acid hydrolysed in 1 ml of 2 M TFA at 100 °C. As with the reference standard timecourse study, triplicate sample groups were neutralised at time-points 15, 30, 45, 60, 75, 90, 120 and 180 minutes from commencement of hydrolysis (Section 3.4.7) then analysed by HPAEC, as described in Section 3.5.5. The broad hydrolysis timeline was matched to the standard 180 minutes of a typical sample preparation. However, more frequent sampling was conducted during the early stages of hydrolysis to ensure that an optimal hydrolysis time for Kdo quantification could be established.

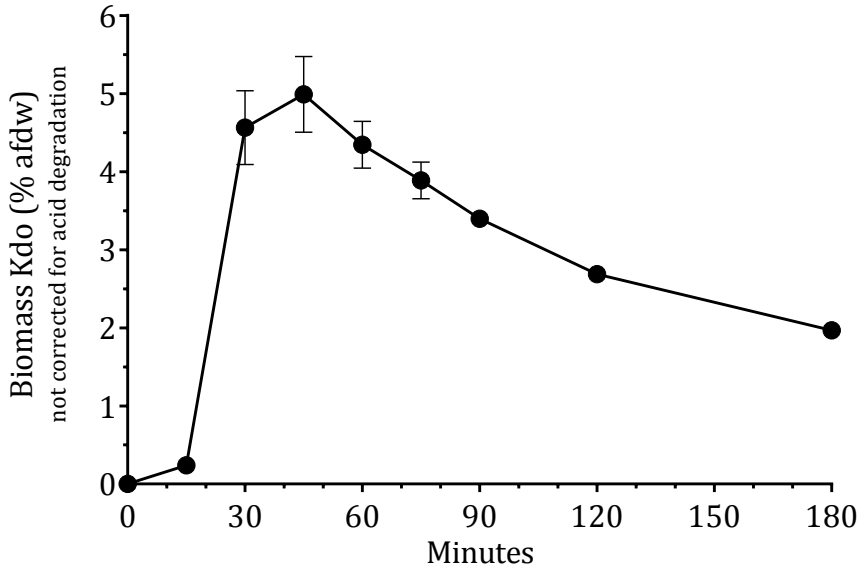


**Figure 21: Hydrolysis profile for Kdo in MUR-233**
Timecourse analyses of Kdo release and degradation in 2 M TFA at 100 °C. Mean values ± SD plotted (n = 3).

The measured Kdo recovered from MUR-233 biomass over the different hydrolyses time-points are shown in Figure 21. The study indicated that minimal Kdo was released from the MUR-233 biomass in the first 15 minutes of hydrolysis. Rapid Kdo release was then evident by 30 minutes, peaking at 45 minutes after which a concentration decline was suggestive of Kdo degradation in the samples. An assumption was made that at the point of decline Kdo was fully released from the biomass. This formed the basis for the standard Kdo hydrolytic extraction method and calculation for analytical Kdo quantification used in this Project (Section 3.4.5). An example chromatogram is provided in Figure 22, showing release of Kdo from de-starched MUR-233 biomass after

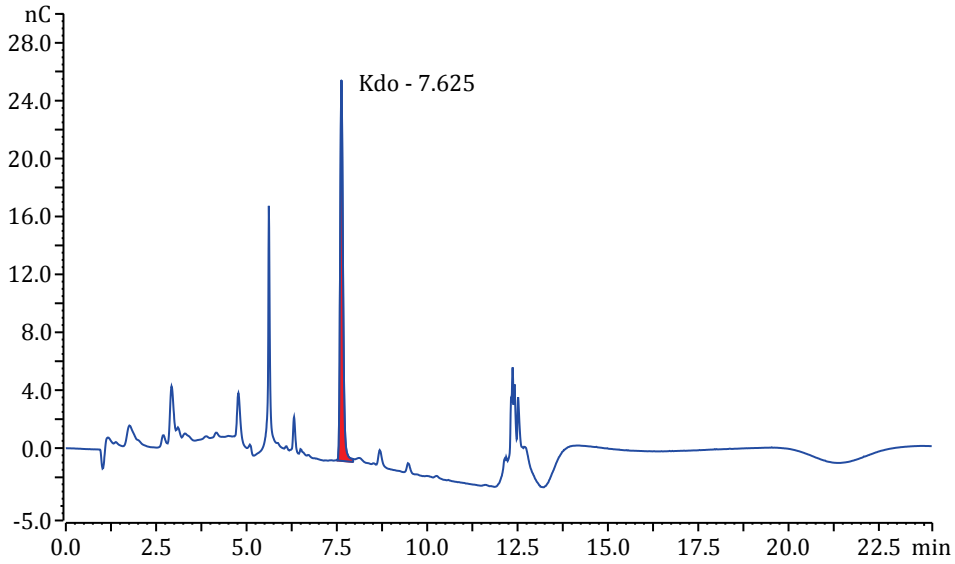


**Figure 22: HPAEC chromatogram of Kdo from MUR-233**
A 45 minute hydrolysate of de-starched biomass separated on a PA-20 column. Kdo elutes at RT 7.625 minutes.

45 minutes of hydrolysis. For quantification using this extraction method, the Kdo value obtained from HPAEC-PAD measurement was corrected for Kdo degradation during hydrolysis. The initial hydrolysis study on Kdo reference standard found that only 54 % of material was recovered after

45 minutes of hydrolysis in 2 M TFA at 100 °C (Figure 20). The correction for Kdo quantity in acid hydrolysates under these conditions is therefore calculated as:

$$\text{Corrected Kdo quantity} = \frac{\text{Kdo value by HPAEC}}{0.54} \qquad \textbf{Equation 17}$$

Where, 0.54 = the mass fraction of expected recoverable Kdo

## 5.4 Cell wall composition

### 5.4.1 Identification of compositional monosaccharides

The identification of monosaccharides in MUR-233 was confirmed using liquid chromatography electrospray ionization mass spectroscopy (LC-ESI-MS) and tandem mass spectrometry (MS/MS). To improve analyses by the above methods, the individual monosaccharides needed to be separated as much as practical. MUR-233 was cultivated to a cell density of $1.5\times10^6$ cells·ml$^{-1}$ to generate material for analysis. The culture was harvested and freeze-dried (Section 3.4.1) then mechanically ground (Section 3.4.3). A portion of this biomass was de-starched using the enzymatic steps described in Section 3.5.7 with the exception that the residual solids were recovered by 10 minutes centrifugation at 16,000 rcf. AIR preparations of these residual solids and also of remaining ground biomass were made (Section 3.4.4).

The sensitivity of the HPAEC system is effective for analytical separation of Kdo. However, the Dionex ICS5000 system had inherent load volume and flow path limitations that prevented inline adaptation for fraction collection. An alternative method for separating Kdo in biomass hydrolysates was required to facilitate sample collection for nominal mass determination. Hence, a method using anion-exchange high performance liquid chromatography (AX-HPLC) as described in Section 3.5.4 was developed to separate acidic sugars for the purpose of collecting Kdo peak fractions. This method was optimised for qualitative separation and was not used for Kdo quantification, as it was less sensitive than the already established HPAEC method.

The AIR preparations of the de-starched solids were hydrolysed for Kdo release (Section 3.4.5) and neutralised (Section 3.4.7) prior to AX-HPLC. The sample load volume was increased to 100 µL to increase peak concentrations for final fraction collection. Evaporative light scatter detection (ELSD) was used to develop and optimise the method, however this detection method is destructive in nature so once the procedure was established the ELSD was taken offline to enable fraction collection. Fractions were manually collected at 20-second intervals between 5 minutes and 11 minutes runtime.

The elution chromatogram for the MUR-233 hydrolysate with peak positions relative to reference standards for Kdo, glucuronic acid (GlcA) and GalA is shown in Figure 23. A primary peak 2 corresponds to Kdo at retention time (RT) 7.2 minutes with an unknown pre-peak 1 at RT 6.3 minutes and late tailing peak 3 at RT 10.5 minutes. In total 18 fractions were collected. An aliquot of each was re-analysed by AX-HPLC with the ELSD inline to determine the peak fractions. In total

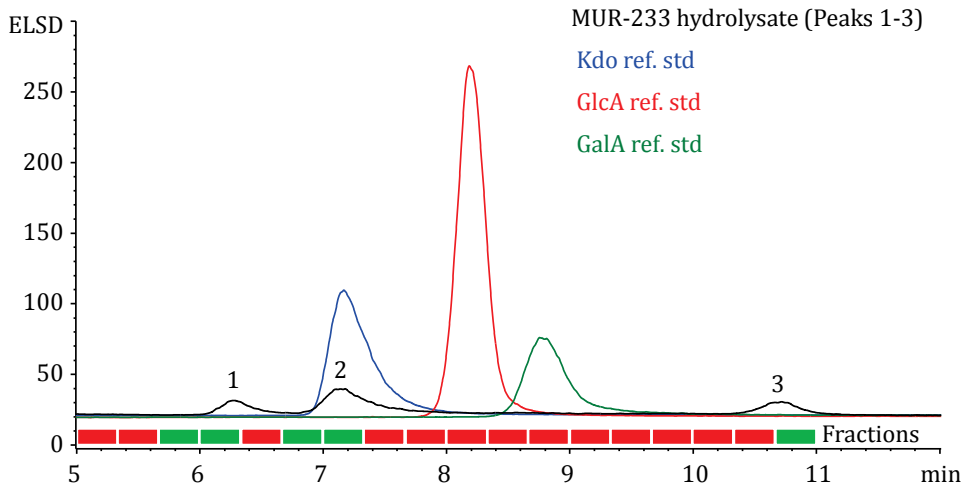


**Figure 23: AX-HPLC chromatogram overlays for Kdo fractionation**
MUR-233 hydrolysate peaks 1-3 (black) relative to reference standards. Boxes (red/green) indicated the approximate time intervals for manually collected fractions with the green boxes representing peak containing fractions retained for LC-ESI-MS. See Table 16 for identities of peaks 1 to 3.

**Table 16: Nominal mass determined for AX-HPLC peak fractions**

| Peak | Carbohydrate (CH) | CH mass ($g \cdot mol^{-1}$) | Extracted ion chromatogram (XIC) RT (min) | Predicted \| Detected $[M+NH_4]^+$ *m/z* | Detected MS/MS fragment ions of matched relative abundance to ref. standards *m/z* |
|---|---|---|---|---|---|
| 1 | 5OMeKdo* | 252.08 | 3.47 | 270.12 \| 270.07 | - |
| 2 | Kdo | 238.07 | 3.28 | 256.10 \| 256.08 | 113.03\| 184.81\| 192.89\| 202.77\| 220.77\| 237.93\| 238.77 |
| 3 | Single-charged monomer of Kdo* | 220.12 | 3.79 | 238.14 \| 238.16 | - |

* No reference standards available.
M+ = molecular ion of carbohydrate with attached ammonium ion.

five fractions were retained for LC-ESI-MS: pre-peak 1 was collected in fractions 3 and 4; peak 2 corresponding to Kdo was collected in fractions 6 and 7; and the tail peak 3 was collected in fraction 18. The RT of peaks in the collected fractions was skewed compared to the predicted RTs during method development. This was likely a result of the 4-fold larger load volume used to maximise peak collection. Despite movement in RT for peaks, the fractions collected were representative of clean single peaks.

Derivatisation using with 1-phenyl-3-methyl-5-pyrazolone (PMP) provides derivatives of reducing sugars that separate well by RP-HPLC for diode array detection (DAD). To verify the identification of reducing monosaccharides present in MUR-233, AIR preparations were made for both whole freeze-dried biomass and de-starched biomass. These were then hydrolysed using 1 M $H_2SO_4$ as per Section 3.4.5 then derivatised and run on the RP-HPLC method (Section 3.5.3) with the exception that 100 µL load volumes were used to maximise on fraction collection. Fractions were manually collected at approximate 1-minute intervals, but primarily based on the position of peaks of interest visible by DAD during elution. The 10MS-VG reference standard mix was also derivatised and run in the same way with fractions collected for use as standards for LC-ESI-MS

and MS/MS. All fractions collected from the RP-HPLC runs were acidified with 10 M formic acid at a 1:100 sample ratio.

The collected fractions for whole and de-starched biomass hydrolysates are shown in Figure 24 in relation to corresponding monosaccharide peaks at various RT. The positions of reference standards have also been overlayed for comparison. Peak 16 is the internal reference standard 2-deoxyglucose (2-DOG), and its uniformity was indicative of consistent sample preparation and elution on the column. A list providing the known and unknown identities of corresponding sugars for peaks 1 to 15 is provided in Table 17.

All retained fractions from AX-HPLC and RP-HPLC separations were dried using a Speed Vac SC110 with RVT100-240V condenser (Savant Instruments, Farmingdale, USA) and stored at -20 °C. For confirmation of MUR-233 monosaccharides by nominal mass, stored peak fractions from AX-HPLC

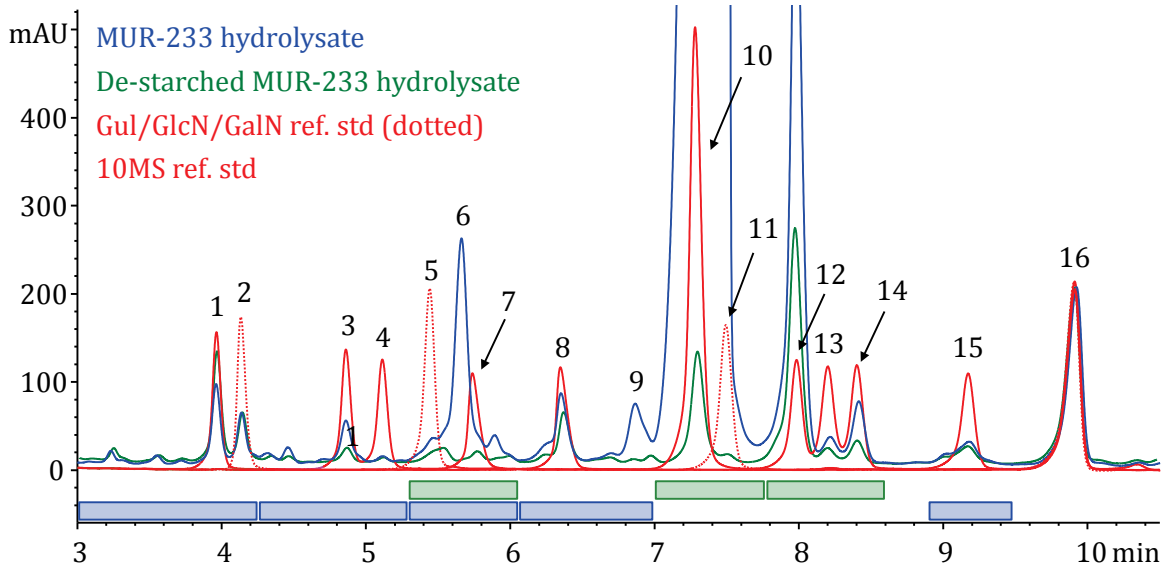


**Figure 24: RP-HPLC chromatogram overlays for reducing monosaccharide fractionation**
Overlay shows peaks for PMP-derivatised sugars for MUR-233 hydrolysate (blue), de-starched MUR-233 hydrolysate (green), and reference standards (red/dotted red). Boxes indicate fractions for LC-ESI-MS with blue fractions collected from MUR-233 hydrolysate, and green fractions collected from de-starched MUR-233 hydrolysate. Peak 16 is the internal standard (2-deoxyglucose). See Table 17 for identities of peaks 1 to 15.

**Table 17: Nominal mass determined for RP-HPLC peak fractions**
MS/MS fragment ions in blue are related to PMP (see Figure 26).

| Peak | Carbohydrate (CH) | CH mass ($g \cdot mol^{-1}$) | Extracted ion chromatogram (XIC) RT (min) | Predicted \| Detected $[M+H]^+$ *m/z* | Detected MS/MS fragment ions with matched relative abundance to ref. standards *m/z* |
|---|---|---|---|---|---|
| 1 | mannose | 180.16 | 8.81 | 511.22 \| 511.35 | 175.20\| 241.16\| 271.09\| 283.14\| 319.09\| 337.01\| 373.20\| 493.09 |
| 2 | gulose* | 180.16 | 9.13 | 511.22 \| 511.35 | - |
| 3 | ribose | 150.13 | 11.20 | 481.21 \| 481.30 | 175.20\| 187.16\| 241.14\| 271.16\| 289.14\| 307.00\| 373.14\| 463.13 |
| 4 | rhamnose | 164.16 | 11.89 | 495.22 \| 495.30 | 175.20\| 241.17\| 285.15\| 303.05\| 321.04\| 373.20\| 477.13 |
| 5 | glucosamine* | 179.17 | 6.16 | 510.23 \| 510.28 | - |
| 6 | hexose disaccharide | 342.32 | 8.12 | 673.36 \| 673.42 | - |
| 7 | glucuronic acid | 194.14 | 12.51 | 525.20 \| 525.18 | 175.22\| 241.17\| 271.15\| 315.14\| 333.11\| 351.05\| 373.19\| 507.15 |
| 8 | galacturonic acid | 194.14 | 13.13 | 525.20 \| 525.27 | 175.19\| 241.18\| 271.06\| 315.05\| 332.90\| 350.99\| 373.18\| 507.14 |
| 9 | hexose disaccharide | 342.32 | 9.37 | 673.36 \| 673.25 | - |
| 10 | glucose | 180.16 | 12.30 | 511.22 \| 511.28 | 175.20\| 241.16\| 271.10\| 283.13\| 318.99\| 337.05\| 373.20\| 493.16 |
| 11 | galactosamine* | 179.17 | | 510.23 \| 510.24 | - |
| 12 | galactose | 180.16 | 12.41 | 511.22 \| 511.30 | 175.20\| 241.15\| 271.09\| 283.10\| 319.04\| 337.02\| 373.19\| 493.13 |
| 13 | xylose | 150.13 | 13.54 | 481.21 \| 481.30 | 175.20\| 187.17\| 241.18\| 271.13\| 289.07\| 307.04\| 373.19\| 463.15 |
| 14 | arabinose | 150.13 | 14.67 | 481.21 \| 481.30 | 175.20\| 187.15\| 241.17\| 271.13\| 289.09\| 307.05\| 373.19\| 463.13 |
| 15 | fucose | 164.16 | 15.89 | 495.22 \| 495.30 | 175.19\| 241.18\| 285.06\| 303.05\| 321.05\| 373.21\| 477.13 |

* No reference standards tested at time of LC-ESI-MS.
$[M+H]^+$ = molecular ion of bis-PMP derivatised carbohydrate with attached hydrogen ion.

and RP-HPLC were dissolved in 0.5 % formic acid then analysed by LC-ESI-MS as described in Section 3.5.6. Results for the AX-HPLC fractions are provided in Table 16. A Kdo reference standard sample was also prepared in 0.5 % formic acid and analysed for comparison. Peak 2 matched Kdo with a mass-to-charge ratio (*m/z*) of 256.08 and similar tandem mass spectroscopy (MS/MS) ion fragmentation. All fractions collected from the AX-HPLC had an attached *m/*z 18.04 ammonium salt on the LC-ESI-MS due to the original ammonium acetate mobile-phase. This was also the case for the Kdo reference standard which was a 2-Keto-3-deoxyoctonate ammonium salt. A comparison of the MS/MS fragmentation between the detected Kdo and reference standard is shown in Figure 25, providing an example of how MS/MS was used to identify other monosaccharides with available reference standards.

Peak 1 from the AX-HPLC had a detected *m/z* 270.07 equivalent to a molecular mass of 252.03 after removal of ammonium. This mass corresponds to a methylation addition to Kdo and would be the expected mass for 5OMeKdo (chemical formula: $C_9H_{16}O_8$) which has been reported by other research groups studying *Tetraselmis* cell coverings (Becker *et al.* 1989; Kermanshahi-pour *et al.* 2014). The AX-HPLC peak 3 fraction had a smaller mass than Kdo at *m/z* 220.12 with ammonium excluded. This mass is too small for Dha (222.07 g·mol$^{-1}$) reported elsewhere for *Tetraselmis*. Also, the MS/MS ion fragments for this peak were of similar mass to those of Kdo with the exception that no fragments were detected at *m/z* 238. This similar fragmentation to Kdo suggests that the peak was a related moiety, and possibly represents single-charged monomers of Kdo which would have an expected mass unit of 220.1. The finding is consistent with results from a study of lipidated poly-Kdo polysaccharides in which negative-ion electrospray ionization quadrupole time of flight mass spectroscopy (ESI-QTOF MS) produced lipid-free mono-, di-, tri-, and tetramers of Kdo with mass differences of 220.1 corresponding to single-charged monomer ions (Sharypova *et al.* 2006).

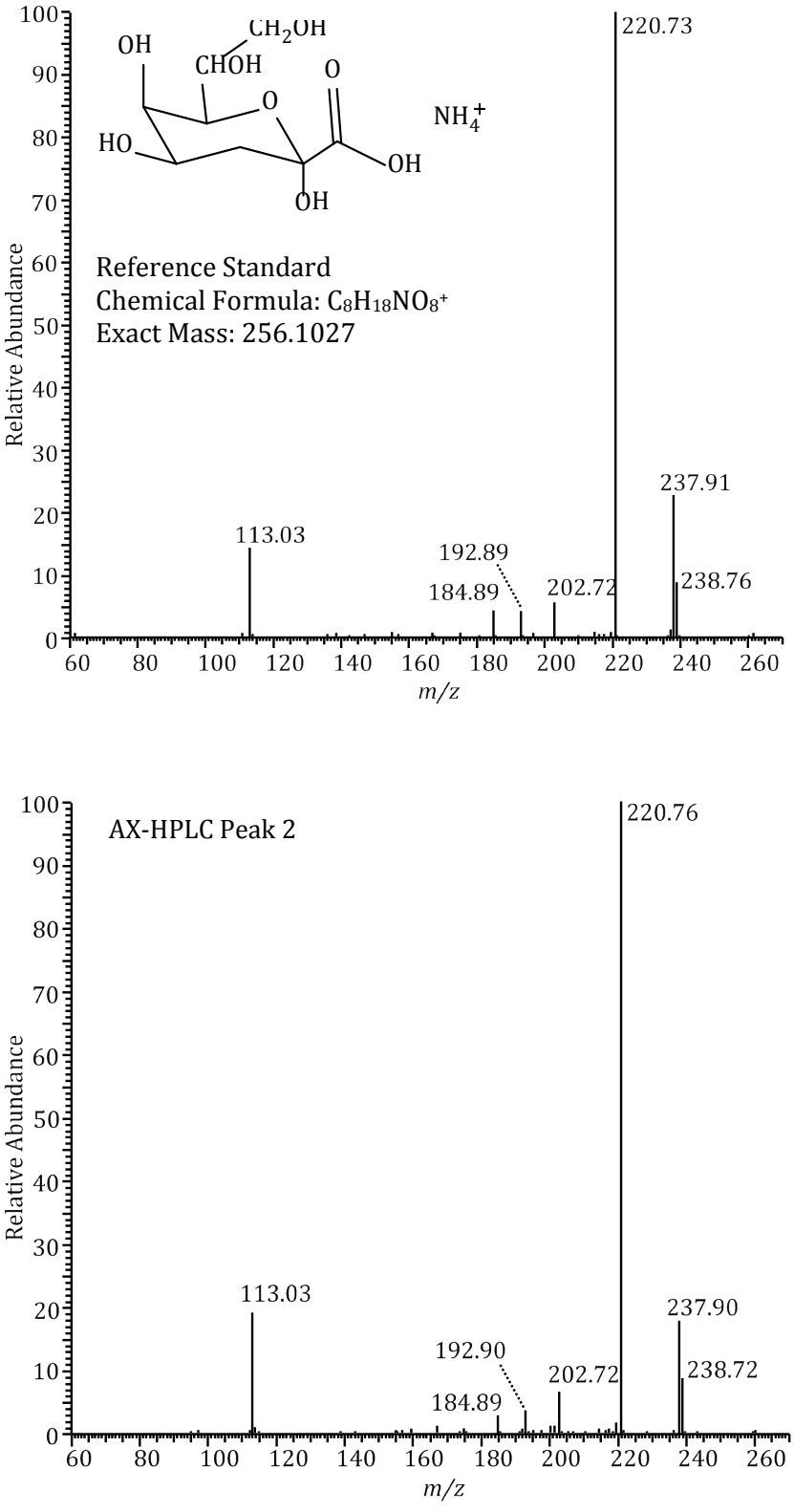


**Figure 25: MS/MS *m/z* 256 of 3-deoxyoctulosonic acid ammonium salt**
Identification of Kdo in MUR-233 peak 2 fraction from AX-HPLC by comparison of detected MS/MS fragment ions pattern and relative abundance against the Kdo reference standard.

The results from LC-ESI-MS analysis of RP-HPLC fractions of reducing monosaccharides derivatised with bis-PMP are shown in Table 17. Desktop analyses of the MS/MS fragment ions of samples determined that all detected compounds were attached to PMP or fragments of PMP. A consistent set of compounds in all MS/MS profiles represented only PMP, bis-PMP and fragments of these. The structure of these fragments are shown in Figure 26 with corresponding *m/z* coloured blue in Table 17 for each related known monosaccharide. Furthermore, all detected compounds carried an attached hydrogen ion (*m/z* 1) from the formic acid mobile-phase.

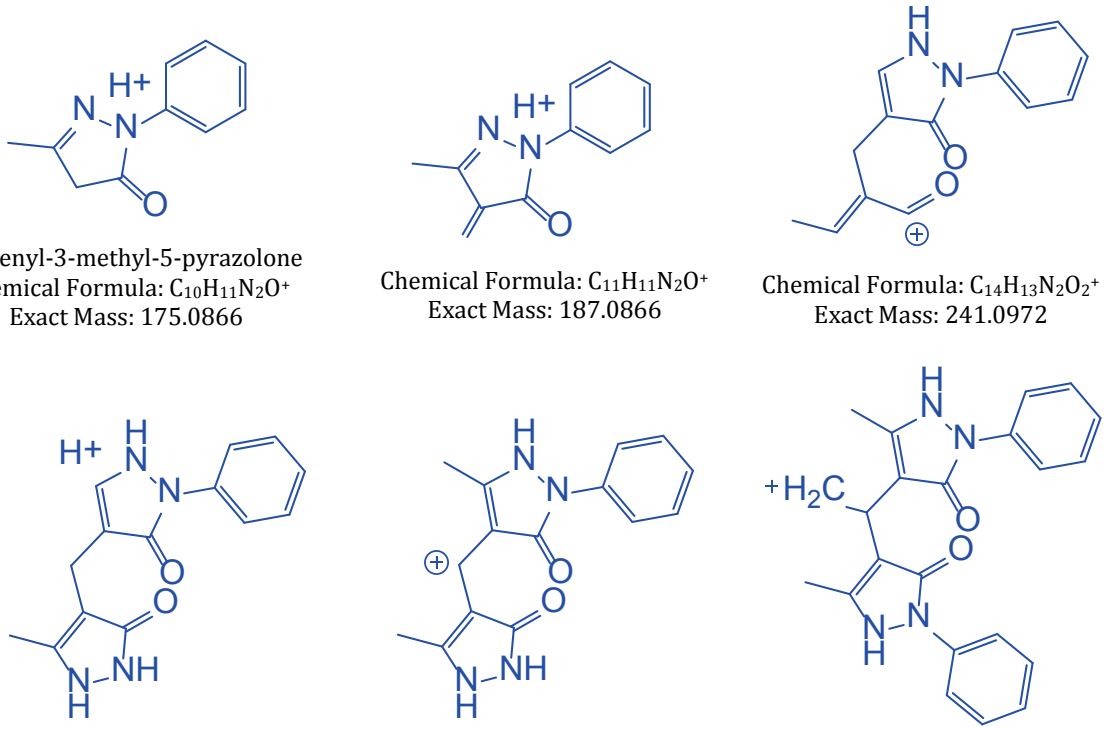


**Figure 26: Probable moieties of bis-PMP for common MS/MS fragments detected**

Monosaccharides with known reference standards were confirmed by comparison of MS/MS ion fragmentation patterns and relative abundance. All 10 monosaccharides from the 10MS-VG reference standard fractions were found to be present in MUR-233 biomass hydrolysate fractions.

The corresponding peaks for these as shown in Figure 24 include: the acidic sugars (7) glucuronic acid and (8) galacturonic acid; the hexose sugars (1) mannose, (10) glucose and (12) galactose; the pentose sugars (3) ribose, (13) xylose and (14) arabinose; and the deoxyhexose sugars (4) rhamnose and (15) fucose.

For unknown monosaccharides the, identification was more difficult because the LC-ESI-MS used a different chromatographic chemistry to the RP-HPLC method. This was necessary to ensure that only volatile buffers were injected into the electrospray ionisation chamber for MS. Consequently, the elution peak profiles between the two methods varied significantly. Significant unknown peaks in collected fractions were targeted and identified against major peaks in corresponding LC-ESI-MS profiles once known monosaccharide peaks had been eliminated. Key unknown peaks in the RP-HPLC profile were aligned with a probable corresponding *m/z*.

From the chromatogram shown in Figure 24, peak 2 adjacent to mannose was aligned with *m/z* 511.22 equivalent to a bis-PMP derivatised hexose sugar. A study by Yamamoto and Rokushika (2004) showed that, with bis-PMP derivatisation, gulose had a similar retention relative to mannose by RP-HPLC. *Tetraselmis* cell wall coverings is known to contain gulose, and the subsequent acquisition and analysis of a gulose reference standard using the method from Section 3.5.3 confirmed the identity of peak 2 as gulose. Rather than including gulose in the reference standard mix, this peak was quantified against the mannose reference standard in subsequent MUR-233 analysis.

Analysis of fractions from the de-starched biomass detected bis-PMP derivatised material in two fractions with *m/z* 510.23 indicative of hexosamine sugars. Subsequent tests with in-house reference standards identified corresponding trace peaks on the RP-HPLC elution profile as glucosamine and galactosamine. These peaks were of negligible quantity and were therefore excluded from specific consideration in the standard reducing monosaccharide analysis of MUR-233 biomass. Despite extended hydrolysis conditions utilised to liberate MUR-233

monosaccharides, the LC-ESI-MS analysis identified di-, and trisaccharides in the various fractions. Of these, two were aligned with significant peaks 6 and 9 in the RP-HPLC profile. Both had *m/z* 673 and fragmented to *m/z* 511 indicating hexose disaccharide compounds.

### 5.4.2 Relative proportions of cell wall monosaccharides

Analysis was conducted on MUR-233 biomass both from KPP and PBR cultures from the UOA laboratory. MUR-233 was cultivated in PBRs as described in Section 3.2.6 then harvested as described in Section 3.4.1 at day 2 during the growth phase of culture. Both of the KPP and UOA materials were processed by freeze-drying (Section 3.4.2), AIR preparation (Section 3.4.4), and acid hydrolysed with samples processed (Sections 3.4.5, 3.4.6, and 3.4.7) for analysis of both Kdo and reducing monosaccharides (Sections 3.5.3 and 3.5.5). The afdw of each biomass sample was determined (Section 3.5.1) to enable mass balance of analytical results.

The studies to be discussed in Chapter 6 determined that the non-starch glucose content of MUR-233 was 0.32 % afdw. Rather than de-starching all MUR-233 samples that were analysed, an assumption was made that this was the base amount of glucose in all MUR-233 cultures and related to cell wall material. The molar ratios of measured cell wall monosaccharides were determined by normalising glucose to this base amount; that is, any glucose above 0.32 % afdw was disregarded from the monosaccharide total. As previously discussed, the assessment of biomass carbohydrate based on cell wall molar proportion is inadequate for determining fermentable substrate quantities in potential process feedstock. Such an assessment, however, allows a useful comparison of MUR-233 against previously reported *Tetraselmis* sp.

The molar ratios of identified monosaccharides in MUR-233 cell wall or theca are presented in Table 18. Despite the conserved percentage of afdw in glucose for both KPP and UOA materials, its ratio as a percentage mole of total non-starch carbohydrates varied due to the relative proportion of other monosaccharides measured. Consistent to both cultures harvested from the KPP open

**Table 18: Monosaccharide composition as a molar percent of total non-starch carbohydrates**

A comparison of observed content in MUR-233 against other reported *Tetraselmis* excluding proportions relating to starch.

A. Neutral sugars

| Microalgae | Material | Monosaccharides (% mol) | | | | | | | | |
|---|---|---|---|---|---|---|---|---|---|---|
| | | Man | Gul | Rha | Glc | Gal | Xyl | Ara | Fuc | Ref. |
| KPP MUR-233 | WBA * | 4.4 | 2.3 | 0.3 | 3.6 | 19.3 | 2.1 | 2.6 | 2.4 | [1] |
| UOA MUR-233 | WBA * | 3.2 | 1.5 | 0.7 | 5.9 | 14.1 | 0.7 | 2 | 1 | [1] |
| *T. striata* | Theca | - | 4 | - | - | 7 | - | 1 | - | [2] |
| *T. tetrahele* | Theca | - | 3 | - | - | 7 | - | 1 | - | [2] |
| *T. suecica UTEX LB 2286* | PCW | NR | NR | NR | NR | 6 | NR | NR | NR | [3] |

B. Acidic sugars (and unknowns)

| Microalgae | Material | Monosaccharides (% mol) | | | | | |
|---|---|---|---|---|---|---|---|
| | | Kdo | 5OMeKdo | Dha | GalA | UNKN ** | Ref. |
| KPP MUR-233 | WBA * | 53.7 | NR | NR | 4.9 | 4.6 | [1] |
| UOA MUR-233 | WBA * | 63.1 | NR | NR | 3.8 | 4 | [1] |
| *T. striata* | Theca | 54 | 4 | 8 | 21 | NR | [2] |
| *T. tetrahele* | Theca | 58 | 4 | 7 | 20 | NR | [2] |
| *T. suecica UTEX LB 2286* | PCW | 54 | NR | 17 | 21 | NR | [3] |

WBA = whole biomass AIR; PCW = purified cell wall; NR = not reported; – = not detectable; KPP MUR-233 (n = 18); UOA MUR-233 (n = 3).
* The molar percentage of monosaccharides in AIR preparations have been normalised to exclude the starch component of biomass analysed.
** The molar percentage of unknown (UNKN) or non-quantifiable carbohydrates in AIR preparations have been calculated based on quantitation of non-characterised RP-HPLC peaks against a mannose standard calibration.

References: [1] This Project
[2] Becker *et al.* (1991)
[3] Kermanshahi-pour *et al.* (2014)

pond and UOA PBRs, the most abundant monosaccharide in the cell wall of MUR-233 was Kdo ($Kdo_{KPP}$ 53.7 % mol, and $Kdo_{UOA}$ 63.1 % mol) with the galactose also found in high quantities ($Gal_{KPP}$ 19.3 % mol, and $Gal_{UOA}$ 14.1 % mol). Small quantities of cell wall material for MUR-233 from both KPP and UOA also contained unknown bis-PMP derivatised components likely to be hexose di- and

trisaccharides as identified when the unknown peaks were previously analysed by LC-ESI-MS. When cultivated in a PBR, MUR-233 contained 8.8 % higher Kdo as a proportion of the AIR material analysed than the KPP MUR-233. Conversely, galactose was 5.2 % higher in the KPP material. In general, the KPP cell covering was marginally richer in hexoses and pentoses that are more readily fermented in conventional systems than the acidic sugars such as Kdo.

In all samples, ribose was also detected at moderate levels, but was excluded from the total molar calculations for cell wall monosaccharides. While assessing starch enrichment for MUR-233 (Section 6.3.3), measurements of ribose over the growth cycle of batch cultures found that ribose quantities peaked to 0.492 ± 0.008 % afdw at day 3 during exponential growth phase and declined to 0.077 ± 0.008 % afdw by stationary phase at day 16. Although an interesting trend, the quantities measured were not significant to the total fermentable substrates in MUR-233 biomass. Hence, this phenomenon was not investigated further. Nevertheless, preliminary data (not presented) for proximate analyses of the MUR-233 biomass carbon, hydrogen and nitrogen (CHN) has indicated that cellular nitrogen levels most likely representing intracellular protein displayed a similar profile to that observed with ribose. This leads to a proposal that the ribose detected in the AIR preparations of MUR-233 biomass is not likely a component of the MUR-233 cell wall structure, but was instead associated with elevated ribonucleic acid (RNA) activity related to protein expression.

The observed differences between KPP and UOA biomasses suggest that cultivation environments could affect biomass composition. The study by Fon Sing *et al.* (2014) provides details on the cultivation conditions for the KPP biomass. One environmental variation was the use of RSS at UOA rather than natural seawater supplemented with NaCl in the form of commercial grade pool salt (Lake Deborah Natural Australian Lake Salt). Another variable was the difference between the more controlled system in PBRs as opposed to the open raceway ponds at KPP that would have been subject to evaporative salinity changes and may have also carried less dominant

contaminating microalgae. Given the similarity in distribution of key monosaccharides found between KPP and more controlled UOA biomass, it was unlikely that any probable contaminating microalgae significantly affected the analyses. However, whilst salinity was maintained at 7 % w/v RSS in the PBRs with only minor daily fluctuation, in the open ponds it varied across harvests from 5.5 % to 12.5 % w/v NaCl. The provision of nutrient supplement to cultures also differed. Batch PBR cultures were provided with an initial 109.43 $mg \cdot L^{-1}$ of nitrate ($NO_3$) and 6.78 $mg \cdot L^{-1}$ of phosphate ($PO_4$), whereas in the semicontinuous KPP cultures these nutrients were dosed at respective daily concentrations of 35 $mg \cdot L^{-1}$ and 2 $mg \cdot L^{-1}$. Studies on *Tetraselmis subcordiformis* have shown that both salinity and nutrient limitation can affect the accumulation of starch (Yao *et al.* 2013a, 2013b; Yao *et al.* 2012). Although the monosaccharide molar ratios presented in this section have been normalised for starch variation they do not account for differences in potential changes in intracellular carbon flux between synthesis to starch in the pyrenoid (Ball 2002) or the transformation to cell wall polysaccharide precursors in the Golgi apparatus (Gooday 1971b).

A comparison of the analysed MUR-233 with *T. striata*, *T. tetrahele* and *T. suecica* is also provided in Table 18. As already mentioned, 5OMeKdo and Dha could not be verified or quantified for MUR-233 without available reference standards, and no comparison can be made other than the probable non-quantified presences of 5OMeKdo determined by LC-ESI-MS (Section 5.4.1) would affect the final molar ratios calculated for MUR-233. The cell wall quantities of Kdo varied but analysis of the MUR-233 samples here confirmed Kdo as the primary structural monosaccharide in agreement with other studies on *Tetraselmis*. A key difference to the other species compared here was the proportions of galacturonic acid and galactose in MUR-233. Galacturonic acid proposed in these other studies as a key structural polysaccharide component of *T. striata* (Figure 17) was 4-times lower in MUR-233, whereas galactose content was 2- to 3-times higher in MUR-233. The galactose observation is perhaps in line with a study by (Lewin 1958) on *Platymonas subcordiformis*, now reclassified as *T. subcordiformis*, which found that galactose and an unidentified uronic acid were the major sugars in cell wall extracts.

## 5.5 Available sugars in Karratha MUR-233 biomass

An essential component of this Project was to analyse KPP MUR-233 biomass once it became available as a potential fermentable feedstock. A total 18 samples were tested to profile the biomass produced at the Karratha pilot plant for monosaccharide composition and total available fermentable carbohydrate on an afdw basis as shown in Figure 27. A relative comparison to UOA PBR cultures is also provided in Table 19. Monosaccharide proportions in the cell walls as molar ratios have already been discussed for these samples in Section 5.4.2.

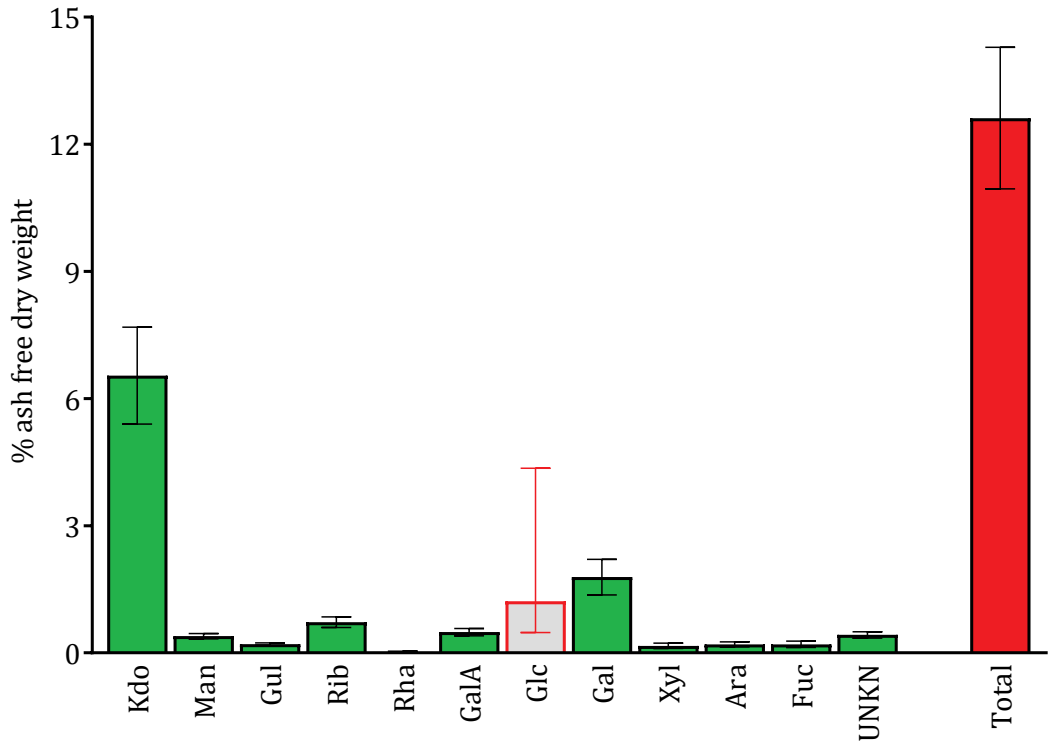


**Figure 27: Monosaccharide profile of MUR-233 from outdoor ponds at Karratha**
Compositional monosaccharides measured in biomass from a 56-day semicontinuous culture. Kdo was measured by HPAEC-PAD. Reducing monosaccharides and unknowns (UNKN) were measured by RP-HPLC-DAD. MUR-233 biomass from different harvests (n = 18): glucose (Glc) plotted as median with minimum and maximum range; all other values plotted as mean ± SD.

MUR-233 analysed from the Karratha pilot plant spanned 56 days of semicontinuous growth in open raceway ponds from 25 August to 21 October 2012. Harvested biomass showed significant variation in afdw that was consistent with findings from Karratha field trials (Fon Sing *et al.* 2014), ranging from 27.8 % to 49.7 % due to both the differences in sample salinity and also contaminants which resembled inorganic soil material from the outdoor environment. An average 12.62 ± 1.67 % afdw of total carbohydrates was observed across 18 harvests from the KPP semicontinuous culture. This was not significantly different to the 12.35 ± 0.32 % afdw total carbohydrate content of the UOA MUR-233 harvested at growth phase from PBRs (t-test, $p > 0.05$).

The data from KPP samples was grouped by monosaccharide types, and each group then tested for normality. With the exception of glucose (discussed further in Chapter 6), the measured quantities for each of the other monosaccharide and unknowns across the 18 different KPP harvests were normally distributed (Shapiro-Wilk, $p > 0.05$). On this basis, an assumption was made that the results were a true representation of a MUR-233 monosaccharide profile for KPP biomass. The quantities of monosaccharides as a percentage of afdw for KPP MUR-233 biomass are shown in Table 19 relative to those from UOA PBR cultures. Typically, the monosaccharides relating to cellular structure were present in greater proportion in the KPP MUR-233 biomass compared to UOA MUR-233 biomass. There were also significantly greater proportions of the key structural monosaccharides Kdo (+1.97 ± 0.68 % afdw) and galactose (+1.02 ± 0.25 % afdw) detected in KPP than in UOA biomass samples (t-tests, $p < 0.05$). Further analyses of the KPP MUR-233 cell wall monosaccharides using individuals-moving range control charts showed four instances of unusual variation in Kdo composition in the 18 harvests assessed. As the key structural monosaccharide synthesised during growth phase in preparation for cell division, Kdo composition would be a primary indicator for variations in the rate of cell wall precursor synthesis. Any such precursor polysaccharides would have also been retained in AIR preparations of analysed samples. It is possible that the measured Kdo reflects both integrated cell wall composition as well as precursor structures accumulated for cell division. The presence of such precursor structures

could also explain the instances of observed higher proportions of Kdo and structural monosaccharides. Without further information regarding the specific differences in cultivation variables between the harvested batches of KPP biomass, the cause of unusual Kdo variations observed could not be determined.

**Table 19: MUR-233 monosaccharide in semicontinuous and batch cultures**
Mean (± SD) monosaccharide quantity in MUR-233 whole biomass AIR preparations calculated as a percent of ash free dry weight.

| MUR-233 | Monosaccharides (% afdw) | | | | | | |
|---|---|---|---|---|---|---|---|
| | Kdo | GalA | Man | Gul | Rib | Rha | Glc |
| KPP MUR-233 (Semicontinuous) | 6.54 (± 1.07) | 0.49 (± 0.08) | 0.39 (± 0.06) | 0.2 (± 0.03) | 0.72 (± 0.12) | 0.02 (± 0.015) | 1.22* (1.06 - 1.54) |
| UOA MUR-233 (Batch) | 4.57 (± 0.44) | 0.23 (± 0.02) | 0.18 (± 0.005) | 0.08 (± 0.002) | 0.41 (± 0.02) | 0.03 (± 0.007) | 5.7 (± 0.41) |

| MUR-233 | Monosaccharides (% afdw) | | | | | |
|---|---|---|---|---|---|---|
| | Gal | Xyl | Ara | Fuc | UNKN** | Total |
| KPP MUR-233 (Semicontinuous) | 1.79 (± 0.42) | 0.17 (± 0.06) | 0.2 (± 0.06) | 0.2 (± 0.07) | 0.42 (± 0.07) | 12.62 (± 1.67) |
| UOA MUR-233 (Batch) | 0.77 (± 0.009) | 0.03 (± 0.005) | 0.09 (± 0.01) | 0.05 (± 0.01) | 0.22 (± 0.007) | 12.35 (± 0.32) |

* KPP MUR-233 glucose data was non-normal and shown as median with 95 % confidence interval.
** The unknown (UNKN) carbohydrates in AIR preparations were calculated as the sum of unknown RP-HPLC peaks that had been quantified against a mannose standard calibration.

The differences in the quantities of structural carbohydrates, in part attributed to proposed precursor structural components, between semicontinuous outdoor cultures and batch cultures in the laboratory were indicative of optimised culture conditions in Karratha for high biomass productivity. For instance, a key nutrient difference was the use of carbon dioxide for producing

KPP biomass (Fon Sing *et al.* 2014) which increases the carbon to nitrogen ratio and photosynthesis in the outdoor MUR-233 culture. Furthermore, the KPP biomass was also exposed to high solar irradiance of between 904 to 1,507 μmol·photons·$m^{-2}$·$s^{-1}$ in Karratha during the production period analysed (Bureau of Meteorology 2018). This irradiance for the open raceway ponds was also significantly higher than the artificial irradiance of 210 to 250 μmol·photons·$m^{-2}$·$s^{-1}$ white fluorescent light applied to PBR cultures in the laboratory.

The observed glucose variance between the KPP MUR-233 and UOA MUR-233 biomass will be further discussed in Section 6.3.1. Based on the structural monosaccharide results across 56 days of semicontinuous culture, it was evident that KPP MUR-233 biomass with the determined average carbohydrate composition would not be a suitable feedstock for conversion to bioethanol. Importantly, in the KPP MUR-233 the total carbohydrates consisted of 51.8 % Kdo that cannot be readily fermented by typical ethanologenic microorganisms such as *Saccharomyces cerevisiae* or *Zymomonas mobilis*.

## 5.6 Concluding remarks

A quantitative discrepancy was determined between the PSA method traditionally used in AP6 projects for total carbohydrate assessment and more specific methods using various HPLC techniques. This was particularly important in the quantitation of acid labile structural monosaccharides such as Kdo, and as a result, the HPLC methods were used in preference for both quantifying and characterising the carbohydrate composition of MUR-233.

The key monosaccharides in MUR-233 structural cell wall material were determined by RP-HPLC and HPAEC then verified by mass spectrometry. There was variance between the minor monosaccharides found in MUR-233 and those reported in the literature. The key difference was the relative abundance of galactose found here versus galacturonic acid reported in key studies on *Tetraselmis* spp. thecae. However, there have also been reports of significant proportions of galactose found in *T. subcordiformis* that may allude to the species identity of this strain that has

yet to be confirmed. However, Kdo content was in proportion to what has been found in other research papers in regards to both the 53.7 % to 63.1 % molar ratio in the cell structural carbohydrates and the 4.57 % to 6.54 % afdw in the biomass. By mass, Kdo constituted up to half of the carbohydrates in the MUR-233 cell wall structure.

With only trace amounts of glucose found in the cell wall (see Chapter 1), the results confirm that unlike typical lignocellulosic biomass that can be hydrolysed to glucose subunits for fermentation, the cell wall composition of MUR-233 is not feasible for providing glucose suitable to direct glycolytic conversion to pyruvate for alcoholic fermentation. The minor amounts of other reducing sugars present in the cell wall do not support additional work to identify microorganisms with suitable alternate metabolic pathways for their utilisation. Therefore, any application of MUR-233 biomass as an alternative feedstock for producing ethanol would be dependent on enrichment of intracellular starch content to provide a suitable a substrate for microbial conversion. In circumstances where MUR-233 is cultivated for biomass and lipid productivity such as in Karratha, a requirement for altered cultivation conditions for starch enrichment could eliminate opportunities to use recycled material such as lipid-extracted biomass for a bioethanol stream in a biofuel biorefinery

# Chapter 6

# Biomass starch assessment and enrichment

## 6.1 Introduction

The experimentation conducted in Chapter 5 to analyse MUR-233 biomass for structural carbohydrate composition also measured glucose as a key component of acid hydrolysed AIR sample preparations. This following chapter will describe work undertaken to determine the distribution on glucose between MUR-233 cell wall and stored starch polysaccharides. Earlier work on MUR-233 prior to this Project showed that the strain's total carbohydrate content ranged from 6 % to 12 % afdw (Fon Sing & Borowitzka 2015), and the work presented in this chapter alongside findings already discussed in Chapter 5 sought to verify and understand the variability around these findings. The work undertaken in this chapter also sought to establish a simple approach for producing starch-enriched hypersaline MUR-233 biomass as a suitable substrate for fermentation trials.

### 6.1.1 Starch as an energy reserve

Alongside other unicellular green microalgae, the polysaccharides of *Tetraselmis (Platymonas)* were studied in determining that photosynthetic microalgae stored starch as an energy reserve with similar amylose and amylopectin heterogeneity and biochemical composition to those of higher plants (Hirst *et al.* 1972; Suzuki 1974). Green microalgae synthesise starch around a Rubisco-rich pyrenoid and accumulate starch granules in their chloroplast stroma under varying environmental conditions such as high irradiance, high carbon dioxide saturation, and with nutrient limitation, depletion or starvation (Ball 2002). In general, the starch that green microalgae accumulate has analogous physicochemical properties to higher plant storage starch (Ball 2002). It is a storage polysaccharide containing exclusively α-1,4 linked and α-1,6 branched glucose residues with branching ratios of 1:20 for amylopectin and around 1:100 for amylose. The relative

amylose content of this starch is 15 % to 30 % with iodine interaction of 550 nm for amylopectin and > 620 nm for amylose identical to higher plant storage starch.

Glucose has been reported as a major component, 88.3 % w/w dw, of polysaccharides isolated from *Tetraselmis chui* (Brown & Jeffrey 1992). However, as previously discussed analyses of cell wall composition in *T. subcordiformis*, *T. striata* and *T. tetrathele* (Becker *et al.* 1989; Becker *et al.* 1991; Lewin 1958) have indicated that glucose is not an important component of the structural carbohydrates for this genus of microalgae, and leads to the supposition that any significant measure of glucose from *Tetraselmis* biomass would be derived from pyrenoidal or stored chloroplast stromal starch.

### 6.1.2 Relevant environment factors for starch accumulation

In a similar way to leaf cells in higher plants, carbon flows into the cytoplasmic sink of *Tetraselmis* through the degradation of starch to glucose for synthesis of cellular material. As previously discussed, this carbon flow has been tracked to cell wall polysaccharides from radio-labelled glucose derived carbon (Gooday 1971b). In microalgae the strength of this sink is driven by cell division (Ball 2002). Hence, environmental factors that influence cell division affect the carbohydrate profile of microalgal cultures (González-Fernández & Ballesteros 2012). In this Project for the cultured MUR-233 grown at consistent light and temperature with no inorganic carbon supply, the remaining key factors influencing cell division are nutrient depletion and high salinity.

It is well established that environmental nitrogen deficiency results in starch accumulation in *Tetraselmis* cultures (Bondioli *et al.* 2012; Lourenço *et al.* 1997; Thomas *et al.* 1984; Yao *et al.* 2012). Nitrogen-starvation causes the arrest of cell divisions in microalgal cultures and the recycling of cellular macromolecular components into starch and lipids (Ball 2002). A number studies on *T. suecica* have reported the shifting of photosynthetically fixed carbon to increase carbohydrate production to between 50 % and 67 % w/w dw in nitrogen deficient cultures (Bondioli *et al.* 2012;

Thomas *et al.* 1984; Utting 1985). However, the improvement of carbohydrate yields in *T. suecica* through nitrogen starvation also occurred at the expense of a significant reduction in biomass productivity and photosynthetic efficiency (Bondioli *et al.* 2012; Thomas *et al.* 1984). Also, under nitrogen replete conditions the type of nitrogen source may affect the carbohydrate profile of microalgae (González-Fernández & Ballesteros 2012). Edge and Ricketts (1977) observed that the carbohydrate content of nitrogen-starved *Platymonas striata* Butcher (*T. striata*) cells was approximately double that of nutrient replete cells, but that refeeding of nitrogen-starved cells with either nitrate or ammonium resulted in a significant reduction in the accumulated cellular carbohydrates. Furthermore, nitrogen-starved *T. striata* cultures seeded with ammonium-nitrogen assimilated cells accumulated more carbohydrate than comparable cultures grown from nitrate-nitrogen assimilated cells. Importantly however, *T. striata* biomass productivity was significantly reduced with ammonium-nitrogen assimilated cells.

The impact of culture salinity on *Tetraselmis* carbohydrates was an important consideration in this Project which used hypersaline growth conditions to produce biomass. Early studies to assess the impact of hyposalinity variances from 1 % to 3.5 % w/v salinity on the biochemistry of *T. suecica* focused on strategies to improve protein yields for shellfish food, but also produced data that showed only nominal changes to the carbohydrate content of cells (Utting 1985). There has been minimal research on the effect of high salinities on *Tetraselmis* carbohydrates. A study which assessed the manipulation of salinity to enhance starch production in short-term batch cultures of *T. subcordiformis* showed highest starch yields of 58.2 % w/w dw achieved under nitrogen deprivation at approximately 0.7 % w/v salinity, but reduced yields of 31 % w/w dw under hypersaline nitrogen replete growth (Yao *et al.* 2013b). Previous work at Murdoch University on MUR-233 and other *Tetraselmis* spp. from saline lakes, determined that the culture of the *Tetraselmis* spp. in excessive salinity at 11 % w/v NaCl resulted in significant impediments to growth and accumulation of intracellular storage products. This including an increase in total carbohydrates attributed to osmolytes such as mannitol (Fon Sing & Borowitzka 2015).

## 6.2 Glucose and starch

### 6.2.1 Glucose variability in harvested MUR-233 biomass

One of the earliest carbohydrate assessments conducted for this Project sought to test and verify the carbohydrate content in MUR-233 as reported in earlier research on this strain by Fon Sing and Borowitzka (2015). Biomass used for these tests were taken from available frozen stock at MERG which had been harvested from small scale 2 $m^2$ raceway ponds at culturing facilities at the KPP (four samples) and the UOA (two samples).

Samples were freeze-dried (Section 3.4.1) and ground to a homogenous powder (Section 3.4.3). For each sample total solids and ash-free solids were determined using 100 mg per sample (Section 3.5.1) to facilitate the mass balance according to the biomass content from the analytical results. For assay, 20 mg of each sample was gravimetrically aliquoted for preparation of Alcohol Insoluble Residues (AIR) (Section 3.4.4) and then acid hydrolysed (Section 3.4.5). Total carbohydrates were tested using a low volume high throughput variant of the PSA method (Section 3.5.2), and reducing sugars were determined by reverse phase high performance liquid chromatography (RP-HPLC) (Section 3.5.3).

The analytical results across the six MUR-233 samples tested are shown in Figure 28. Total carbohydrate content measured between 6.8 % and 11.0 % afdw, and total reducing sugar content between 4.5 % and 8.4 % afdw. It was evident that variations in carbohydrate and reducing sugar composition in each biomass sample could be attributed to differences in glucose content, which in these samples ranged between 0.2 % and 4.1 % afdw. When glucose was excluded, the mean ± SD reducing sugar content of all samples was 4.0 ± 0.4 % afdw. There was also a consistent quantification difference of 2.6 ± 0.2 % afdw (mean ± SD) between the total carbohydrates and total reducing sugar content measured in each sample. Assumptions regarding this difference have already been discussed in Section 5.3.1 in relation to interference to the PSA method from 2-keto-sugar acid content in MUR-233 samples.

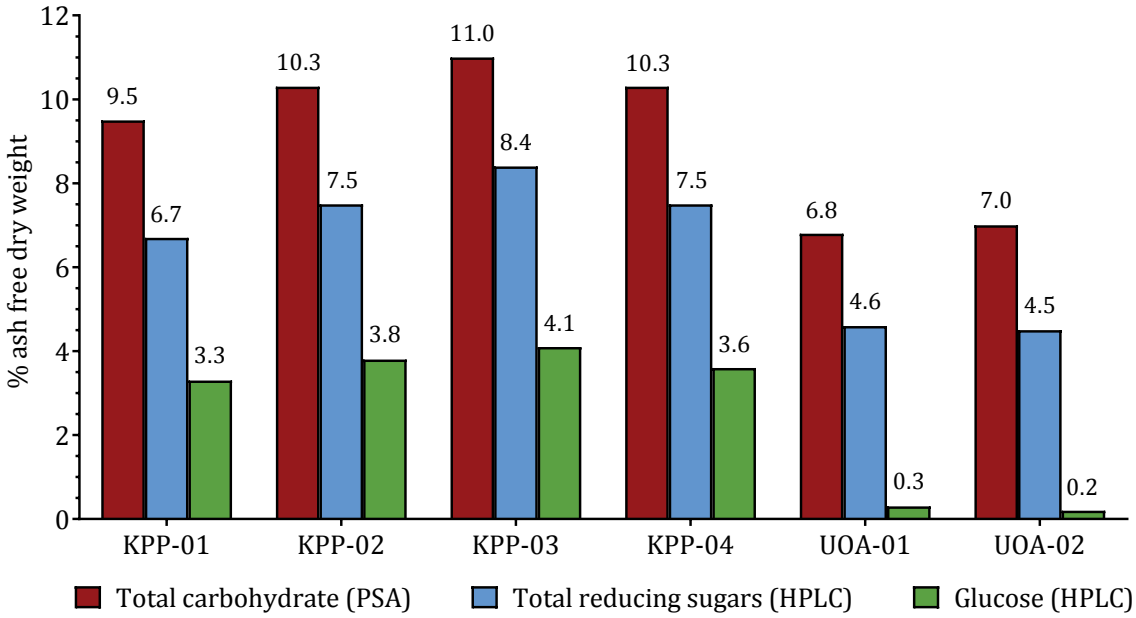


**Figure 28: Glucose as a key variable in MUR-233 carbohydrate quantification**
Preliminary screen of samples (n = 1) from outdoor open ponds: KPP = Karratha pilot plant (four samples, KKP-01 to KKP-04); UOA = University of Adelaide (two samples, UOA-01 and UOA-02); PSA = Analysed by phenol sulphuric acid assay; HPLC = Analysed by high performance liquid chromatography.

### 6.2.2 Starch component of measured glucose in MUR-233

The results shown in Figure 28 indicated glucose content in MUR-233 could be as low as 0.2 % afdw. This suggested that the cell structure of MUR-233 contained only minimal glucose relative to other monosaccharides. To verify the distribution of glucose between cell wall and starch polysaccharides, MUR-233 was batch cultured in a 2 L flask as described in Section 3.2.4 without passage or additional nutrient feed, and with continuous light to enable high levels of starch accumulation in cells (see Section 6.3.2). This was monitored by assessing culture samples (as per Section 3.3.1) every 7 days by light microscopy. Cells stain amber in the 5 % Lugol's solution, but the stain intensity increased to a solid dark violet as intracellular starch accumulated. After 21 days, approximately 500 mg dw of culture was harvested and freeze-dried (Section 3.4.2) of which

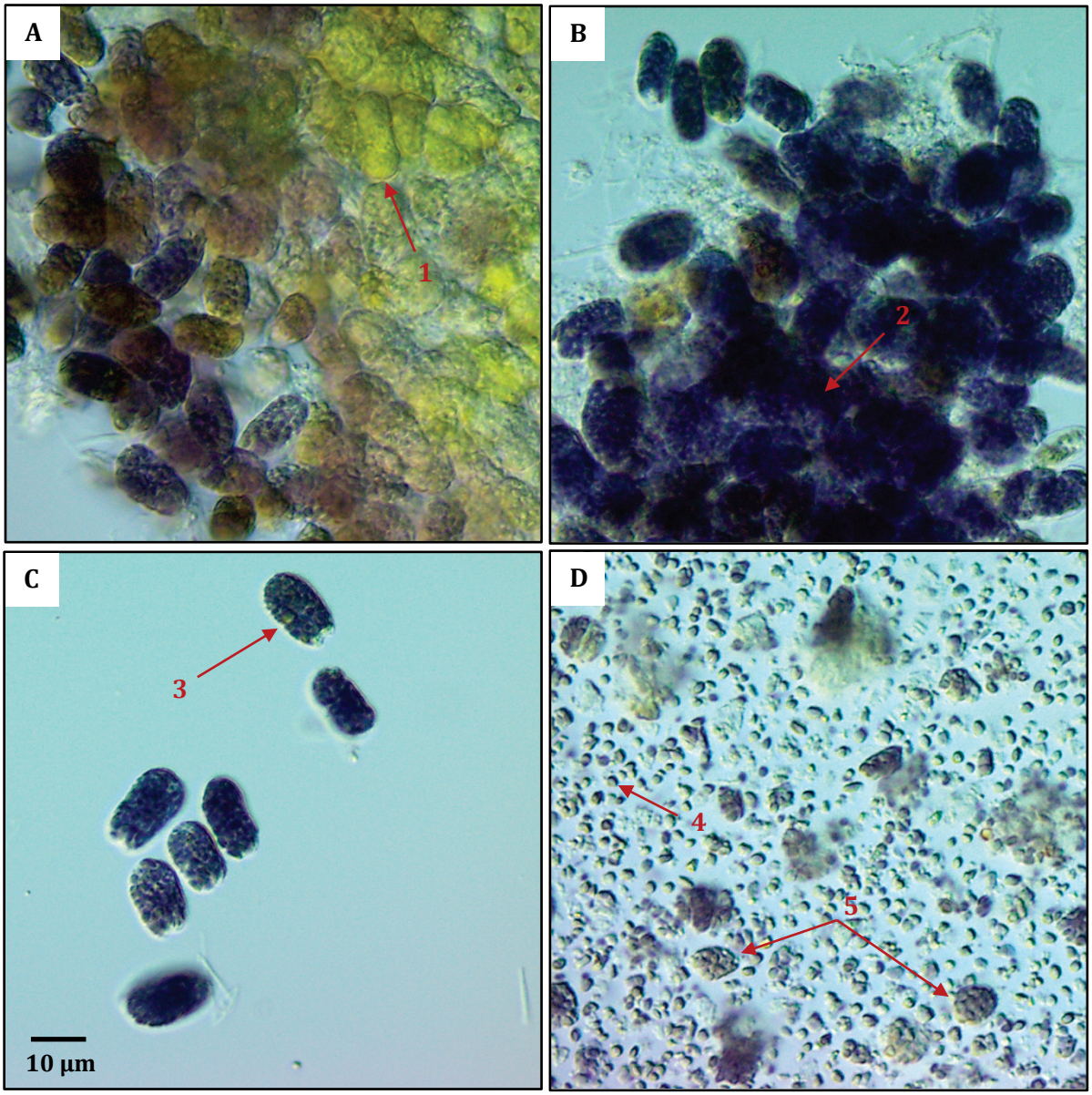


**Figure 29: Starch detection in MUR-233 using 0.8 % Lugol's iodine**
Images of freeze-dried MUR-233 biomass after 15 days continuous light culture with blue-stained microalgal starch: (A) image captured within 1 minute showing gradual penetration of stain solution into a floc still with unstained internal cells (1); (B) a floc with all internal cells completely stained after 5 minutes of elapsed time (2); (C) individual cells with visibly stained granular intracellular starch (3); and (D) ground biomass showing individual starch granules (4) in suspension and sections of disrupted cells (5).

50 % was mechanically ground (Section 3.4.3) for analysis. Suspension of samples of both whole and disrupted freeze-dried MUR-233 material in dilute 0.8 % Lugol's iodine solution stained the extant starch granules to enable clear visualisation under light microscopy. Microalgal starch

granules stained violet both within whole cells (Images A-C) and in suspension with disrupted cell material following mechanical grinding (Image D) are shown in Figure 29.

For determining the proportion of glucose attributable to starch in MUR-233, an enzymatic method specific to starch was complemented by RP-HPLC measurement of biomass glucose. The use of AIR preparations ensured that only glucose bound within alcohol insoluble cell structure and starch would be present prior to assay. Samples of the freeze-dried MUR-233 material were gravimetrically aliquoted for testing. AIR preparations were made from six 20 mg ground samples (as per Section 3.4.4), and afdw was determined using two 100 mg whole samples (as per Section 3.5.1). Three AIR preparations were acid hydrolysed (Section 3.4.5) and analysed for total glucose content by RP HPLC (Sections 3.4.6 and 3.5.3). Three AIR preparations were tested using an enzymatic low volume starch assay as described in Section 3.5.7. For each sample tested in the starch assay, the residual solids were recovered by centrifugation at 16,000 rcf for 10 minutes. AIR preparations of these were made to ensure removal of all free starch-glucose released through hydrolysis by α-amylase and amyloglucosidase. These AIR preparations were then acid hydrolysed (Section 3.4.5) and analysed for residual glucose content by RP HPLC (Sections 3.4.6 and 3.5.3).

Results from the complementary assays to compare total starch and total glucose are shown in Figure 30, revealing the distribution of glucose within the microalgal biomass. The low volume total starch assay measured the liberation of 33.8 ± 1.9 % afdw in glucose from the AIR preparations of cell disrupted material through the action of α-amylase and amyloglucosidase on the amylose and amylopectin structures within the samples. This was equivalent to 30.4 ± 1.8 % afdw of starch. Acid hydrolysis of AIR preparations of residual solids following starch digestion released only 0.32 ± 0.04 % afdw glucose based on RP-HPLC analysis. Total biomass glucose was found to be 33.5 ± 0.7 % afdw of the whole cells, and the difference between these RP-HPLC results provides estimated starch glucose of 33.2 % afdw and hence starch content of 29.9 % afdw, aligning closely to the digested quantity in the enzymatic assay. The results verified the preliminary

observations relating starch to the variable glucose content measured in MUR-233. It confirmed that glucose contributes to only a negligible proportion of the MUR-233 cell wall structure, and in this respect the strains is similar to other *Tetraselmis* reported in the literature (Becker *et al.* 1989; Becker *et al.* 1998).

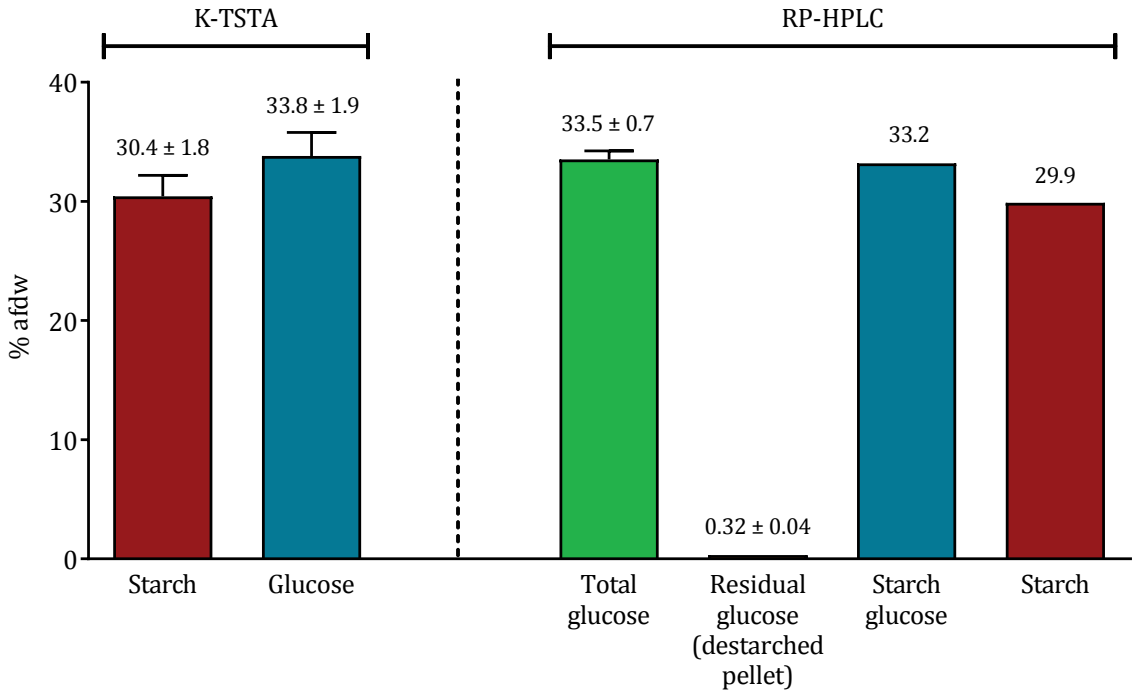


**Figure 30: Glucose distribution between starch and cell structure in MUR-233**
K-TSTA = Analysed by low volume total starch assay; RP-HPLC = Analysed by reversed phase high performance liquid chromatography measuring PMP-derivatised reducing sugars.

## 6.3 Starch-enrichment in MUR-233 biomass

### 6.3.1 Observed MUR-233 starch variance based on culture conditions

The differences in MUR-233 biomass monosaccharide composition between semicontinuous cultures optimised for biomass production and batch PBR cultures were shown in Table 19 from Section 5.5. The observed non-normal distribution of glucose in biomass harvested from KPP semicontinuous cultures was expected and reflective of variations in carbon flux into the

cytoplasmic sink whereby pyrenoidal starch would be utilised for synthesis of cell wall precursors. The starch content of biomass harvested from UOA PBRs was higher, indicating more favourable culture conditions for starch synthesis. This aligned with the expectation that batch conditions without continuous daily nutrient repletion would promote greater starch accumulation. A comparison of relative monosaccharide proportions to biomass afdw between semicontinuous and batch cultures further alludes to a change in intracellular carbon flux. The accumulation of starch would be expected to coincide with declining cell growth where the synthesis of precursors for new cell wall material for cell division would not be required. The observed increase in starch content with PBR batch cultures provides a potential option for carbohydrate enrichment in MUR-233 to produce a feedstock that would be more suitable for fermentation.

### 6.3.2 Approach to enhance starch accumulation

A simple approach was desirable for producing hypersaline biomass with sufficient starch for fermentation trials. Observed starch variance in MUR-233 related to differences in culture conditions suggested that laboratory batch cultures could be more favourable to higher starch accumulation, and other studies have shown enhancements in intracellular starch content in microalgae including *Tetraselmis* when cultivated using continuous light (Miranda *et al.* 2012; Suzuki 1974; Yao *et al.* 2012). For instance, a study of the carbohydrate effect of nitrogen refeeding on nitrogen-starved *P. striata* (*T. striata*) found that cells grown in continuous light accumulated 2 to 4 times more carbohydrates than those in an alternating light/dark regime (Edge & Ricketts 1977).

To test this approach, a small-scale assessment on the impact of continuous illuminance in batch cultures was conducted. Using the methodology described in Section 3.2.4, two groups (n = 3) of 300 ml MUR-233 batch cultures were seeded at $2\times10^5$ cells·ml$^{-1}$ from a log phase inoculum and grown over 5 days. The first group set up as the control used an unchanged methodology that provided 12-hour light/dark cycling to the cultures. The second group was subjected to continuous

illuminance over the test period. At day 5 all cultures were counted (Section 3.3.1) then harvested and freeze-dried (Section 3.4.2) for testing. For each culture, total solids and ash-free solids were determined using 100 mg per sample (Section 3.5.1) to facilitate the mass balance of the analytical results. AIR preparations were made using 20 mg of each sample (Section 3.4.4). These were then acid hydrolysed (Section 3.4.5) and tested for total glucose by RP-HPLC (Section 3.5.3). The starch content of each sample was calculated as per Equation 13 with 0.32 % afdw of the measured glucose excluded as an assumed level of non-starch glucose.

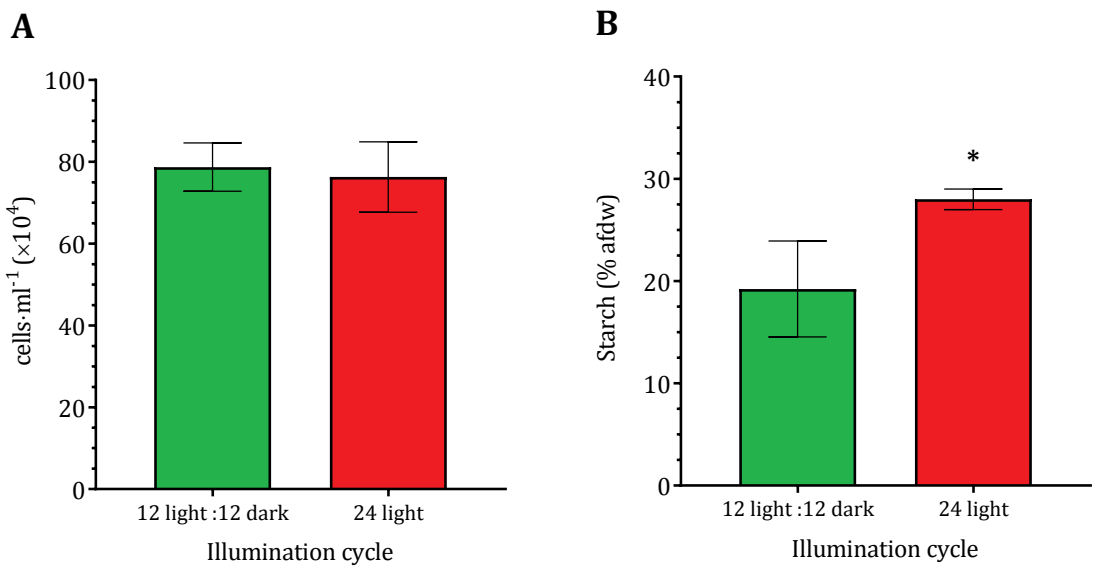


**Figure 31: Biomass and starch accumulation under different illumination cycles**
Results determined from cultures harvested (n = 3) at day 5. Cultures were grown with 12 hour light/dark cycling (green) and under continuous light (red). (A) Culture densities and (B) proportion of accumulated starch are shown as mean ± SD. Starch was calculated based on glucose measured by RP-HPLC of harvested biomass with the assumption that a 0.32 % afdw of the glucose measured was not starch related.

The impact of continuous illumination on starch accumulation is shown in Figure 31. Over a 5 day period, under a 12-hour light/dark illumination cycle MUR-233 reached a culture density of $7.87\times10^5 \pm 0.34\times10^5$ cells·ml$^{-1}$ and accumulated 19.22 ± 2.71 % afdw of starch. There was no

difference (t-test, $p > 0.05$) in the culture density of $7.63\times10^5 \pm 0.35\times10^5$ cells·ml$^{-1}$ for the second group when illumination was altered to a 24-hour continuous cycle, but a significant 8.77 ± 2.77 % afdw increase was observed in starch content to 27.99 ± 0.59 % afdw (t-test, $p < 0.05$). This result indicated a significant benefit for accelerating starch accumulation in the MUR-233 biomass through changing to continuous lighting in batch cultures.

### 6.3.3 Starch accumulation profile in batch PBR cultures

Based on the results presented above (Section 6.3.2), an approach was taken to produce MUR-233 biomass in batch cultures under continuous light to enhance carbohydrate production. No other changes were made to the nutrient composition previously established for autotrophic culture growth. The nutrient content would be replete at the start of each batch culture to minimise the impact on initial biomass production, and extension of culture time would provide nutrient depleted growth conditions. In this way, cultures could be grown to a higher cell density prior to the expected onset of starch accumulation to balance carbohydrate enrichment with biomass productivity.

A study was conducted to profile the accumulation of starch under the proposed growth conditions. Three 20 L MUR-233 batch cultures seeded at $2\times10^5$ cells·ml$^{-1}$ from a log phase inoculum were grown in PBRs as detailed in Section 3.2.6 with the exception that the light illuminance used was continuous over a 30-day period. Culture volumes were corrected daily for evaporative loss (based on the preceding day's volume level markings) with the addition of reverse osmosis (RO) water to maintain a consistent salinity at 7 % w/v RSS prior to analytical sampling. Daily samples (200 ml) were then taken from each culture to enable analysis of cell density (Section 3.3.3), total nitrogen of the culture media (Section 3.5.8), and monosaccharide content in the biomass for glucose quantitation to determine starch (Section 3.5.3). To enable accurate determination of total solids and ash-free solids (Section 3.5.1) additional samples of larger volume (1 L) were taken from each culture at days 2, 4, 6, 12, 14, 16, 22, 23 and 24. Culture volume levels were marked (with the air-

feed temporarily turned off for accuracy) after the final samples were taken on each day, and volumes were corrected using RO water back to the marked level of the previous day before each daily sample was taken. All samples were freeze-dried (Section 3.4.2) prior to analyses, and alum was used to harvest the 1 L samples (Section 3.4.1).

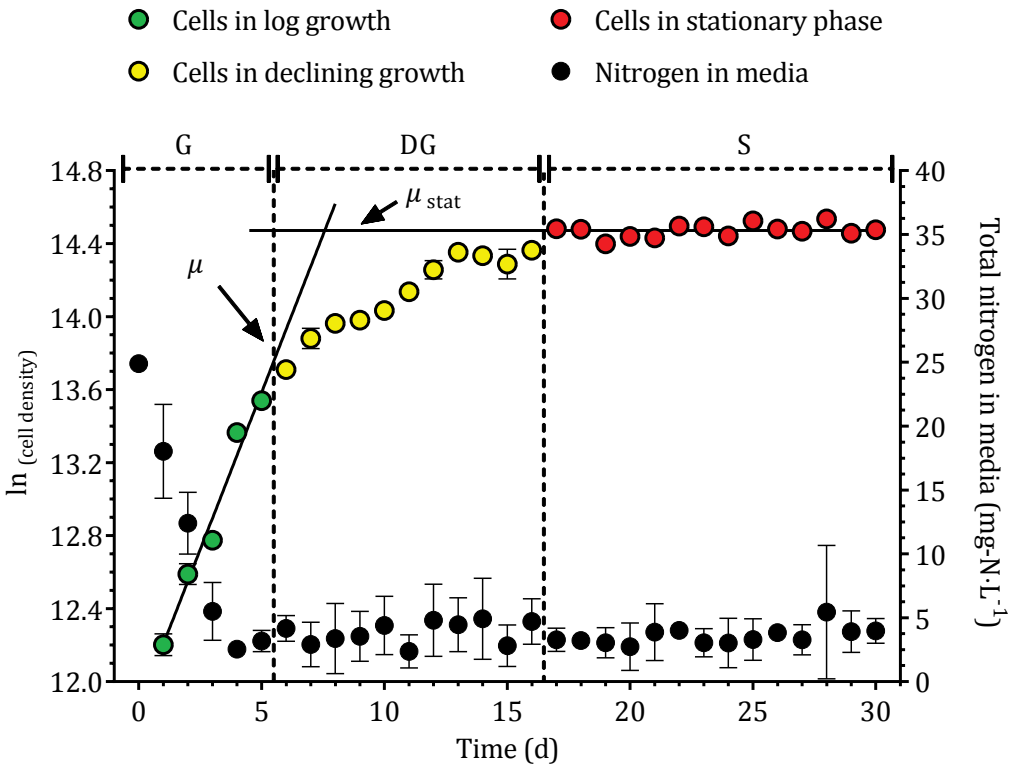


**Figure 32: MUR-233 culture profile under continuous illumination**
Analysis of natural log (ln) of cell density (open circles – green, yellow, red) and total residual nitrogen in growth medium (black circle) of samples from batch PBR cultures (n = 3) showing the mean ± SD for each measured quantity. Linear regression lines were fitted using GraphPad Prism software for culture exponential growth ($\mu$) and stationary ($\mu_{stat}$) phases. G = exponential growth phase, DG = declining growth phase, S = stationary phase.

The growth profile for MUR-233 in batch PBR cultures under continuous illumination is shown in Figure 32. Over the course of the study, the cultures experienced periodic salinity increases above the baseline 7 % w/v RSS due to evaporative loss in culture volume of approximately 1 L·d$^{-1}$,

requiring daily correction. Regression analysis was conducted using a linear model to determine that the cultures entered into stationary phase from day 17. For the purpose of analysis, stationary phase was defined as where the linear model would have a slope equal to zero to indicate a time-point through to day 30 from which no further change occurred in cell density. At stationary phase after 17 days of continuous irradiance in 7 % w/v RSS hypersaline f medium, the MUR-233 batch cultures yielded an average log increase ($\log 10 = 1$, $\ln 10 = 2.303$) in cell density to $1.93\times10^{6} \pm 0.16\times10^{6}$ cells·ml$^{-1}$. An average specific growth rate ($\mu$) of 0.34 ± 0.02 d$^{-1}$ was measured during exponential growth phase between day 1 and day 5, after which cultures began to decline in growth. This average specific growth rate is similar to average rates of 0.35 ± 0.02 d$^{-1}$ and 0.35 ± 0.04 d$^{-1}$ for continuous MUR-233 outdoor cultures (Fon Sing 2010; Fon Sing *et al.* 2014).

As expected, nutrient nitrogen was rapidly utilised in the first 3 days during culture exponential growth. However, after day 3 the total residual nitrogen in the media remained at an average 3.7 ± 2.0 mg-N·L$^{-1}$ between the three cultures. This observation suggested that there was restricted nitrogen uptake by the MUR-233 cells for the remainder of the 30-day culture period. The nitrogen to phosphorus (N:P) atomic ratio in f medium used is 12.5 and similar to the nutrient ratio used in field cultures, and in *Tetraselmis* spp. this approximate ratio has been shown to be optimal for biomass production at temperatures around 25 °C (Molina *et al.* 1991). However, optimal N:P utilisation is also linked with light intensity and for some microalgae a reduced N:P ratio may be required with saturated light intensities (Wynne & Rhee 1986). It is possible that the batch cultures of MUR-233 had become phosphorous limited when cultivated under continuous irradiance, resulting in cessation of nitrogen uptake.

Results for dry solids and ash content in collected 1 L culture samples are shown in Figure 33. The freeze dried samples had an average dry weight of 89.8 ± 0.7 % w/w with no significant difference observed in dry solids for each of the measured time-point samples up to day 24 when compared to day 2 (ANOVA, $p > 0.05$). This indicated that the freeze-dried samples retained an average

10.2 % moisture content when stored at ambient temperature. However, there was a clear significant reduction in sample ash content over the course of the culture (ANOVA, $p < 0.0001$). This change was gradual with no significant differences when adjacent sample groups were compared to each other (ANOVA, $p > 0.05$). Additionally, after day 12 no further change was observed across all sample groups analysed (ANOVA, $p > 0.05$). Nonlinear regression analyses were applied to the ash data set with curve comparisons conducted between exponential one-phase decay, two-phase decay and sigmoidal models to assess the suitability of fit for the observed ash profile. Based on these comparisons, the best-fit model chosen was an exponential one-phase decay model ($R^2 = 0.8822$) with a rate constant constraint of $K > 0$. The regression equation was then used with all the lower volume daily time-point samples taken to provide extrapolated ash contents for calculating respective biomass afdw.

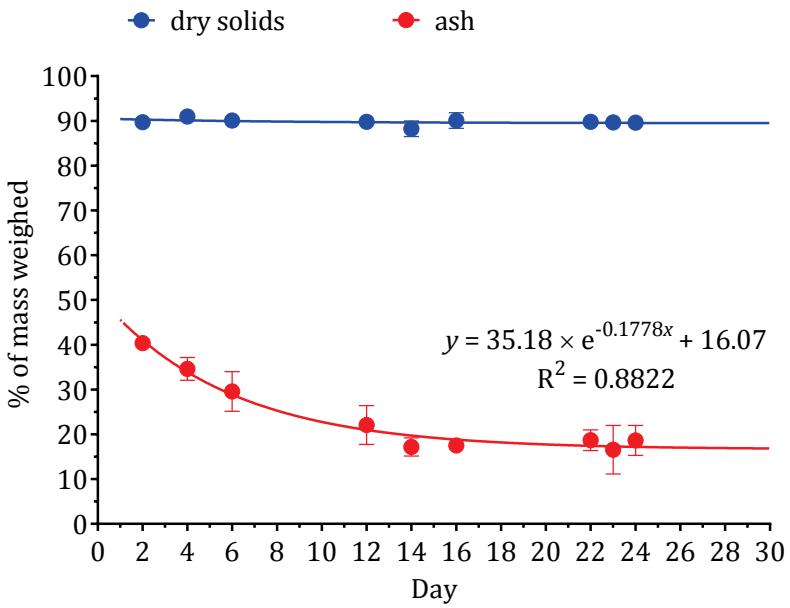


**Figure 33: Solids analysis on time-point samples of MUR-233 biomass in batch cultures**
Analysis of freeze-dried biomass from batch PBR cultures (n = 3) showing the mean ± SD for the percentage of total mass weighed for each treated sample. Individual times represent groups of samples, first processed for dry solids (blue) then ash content (red). Regression lines were fitted using GraphPad Prism software with the curve fit for ash with an exponential one-phase decay model, rate constant constraint of $K > 0$.

The profile for starch accumulation in relation to cell density over time is shown in Figure 34. As a percentage of the biomass afdw the starch concentration in cells began to increase from day 3, coinciding with nitrogen limitation. The measured average starch content in the PBR cultures of 28.42 ± 1.12 % afdw at day 5 was similar (t-test, $p > 0.05$) to that observed previously in the preliminary shake flask experiment. Comparisons of all culture samples grouped by day of harvest determined that from day 9 to the end of the batch trial at day 30 there was no further significant change in accumulated starch per afdw of biomass (ANOVA, $p > 0.05$). Over this period, the average starch content in the tested biomass was 46.37 ± 2.66 % afdw. However, at day 9 the culture cell density was only $1.19\times10^6 \pm 0.85\times10^6$ cells·ml$^{-1}$, approximately 60.2 % of the total average cell density achieved at stationary phase after day 17. As the starch concentration in cells remains constant after day 9, extending the culture time by at least eight days into stationary phase would potentially provide a 39.8 % harvest yield improvement. For production cultures, this would be a more time and cost effective option with no additional handling or input other than the correction to culture levels to maintain salinity at 7 % w/v RSS. Furthermore, the constant starch level maintained in the biomass up to at least 30 days provided for greater flexibility in harvest times. The results indicated that a harvest period between 17 and 30 days for starch-enriched cultures produced using these conditions would provide biomass with an average starch content of 47.01 ± 2.28 % afdw.

In comparison to the above yields, studies by Yao *et al.* (2012) and Yao *et al.* (2013a) reported starch-enrichment of between 42.2 % and 62.1 % dw in *T. subcordiformis* cultivated in artificial seawater under continuous light between 50 to 200 µmol·photons·m$^{-2}$·s$^{-1}$ in combination with a range of nutrient depleted conditions, starch content that were likely higher if considered in proportion to afdw. Although the light intensities used were in a similar range to that of MUR-233 cultures in this Project, the *T. subcordiformis* studies used 7.5- to 45-times higher seeding densities of $1.5\times10^6$ cells·ml$^{-1}$ to $9.0\times10^6$ cells·ml$^{-1}$. Furthermore, respective final culture densities of

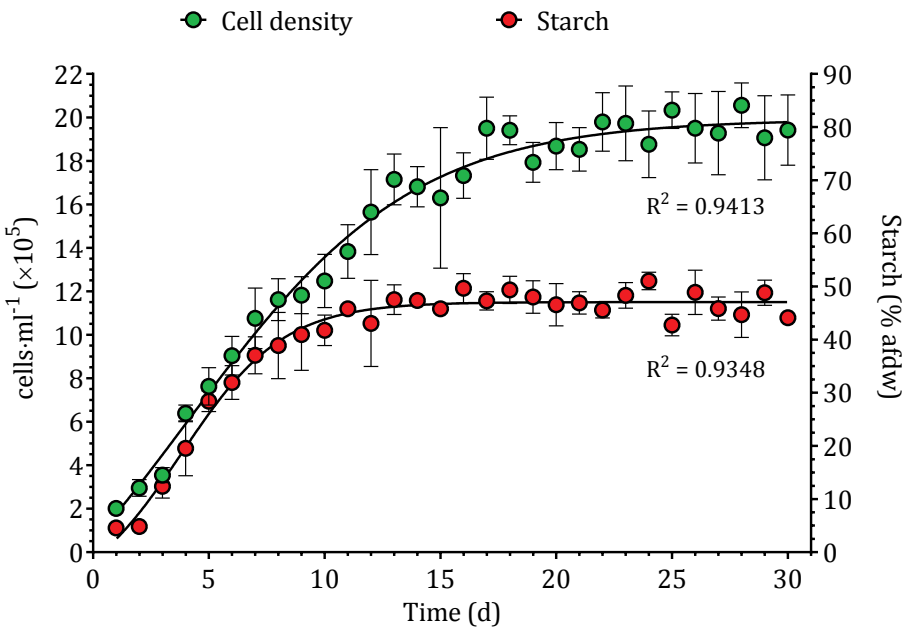


**Figure 34: MUR-233 starch accumulation under continuous illumination**
Analysis of cell density (green circle) and starch (red circle) of samples from batch PBR cultures (n = 3) showing the mean ± SD for each measured quantity. Regression lines were fitted to the data using GraphPad Prism software with the curve fit with sigmoidal dose-response (variable slope) models.

$5.7\times10^6$ cells·ml$^{-1}$ to $13.5\times10^6$ cells·ml$^{-1}$ were achieved after 4 days cultivation. For *Tetraselmis* species, these final culture cell densities seem extraordinary, especially when combined with nutrient depleted conditions, additional shading from the higher density cultures, and high starch content that indicate the cells should be trending towards growth arrest. Nevertheless, Yao *et al.* (2012) concluded that optimised photosynthetic activity and nutrient concentrations for the *T. subcordiformis* strain assessed were necessary to achieve a balance between high starch productivity and starch concentrations. Such aspects of MUR-233 cultivation could be assessed if future work is needed to optimised biomass from this strain.

## 6.4 Concluding remarks

MUR-233 cultured under conditions developed for biomass productivity had a total carbohydrate content that ranged from 6.8 % to 11 % afdw when tested by the PSA method, similar to earlier findings within the AP6 project referred to in Section 6.1. Experimental observations showed that variations in total carbohydrate content were primarily due to glucose quantities associated with intracellular starch accumulation, and that only 0.32 % afdw of glucose measured in the biomass related to cellular structure.

Based on observations of variance in glucose between semicontinuous and batch culture conditions, a simple process to enrich starch in MUR-233 biomass was determined for providing fermentable feedstock. Under continuous illumination in laboratory PBRs, the MUR-233 biomass accumulated an average starch content of 47 % afdw. An optimal time for culture harvest after 17 days was also determined. This aligned with the beginning of the culture stationary phase and allowed for a flexible timeframe for harvest, as the results showed that both starch and cell density did not change significantly if the culture was extended to 30 days.

This batch culture condition using continuous light is suitable for generating starch enriched MUR-233 biomass for laboratory studies on ethanologenic conversion. However, realistically to generate feedstock for a biofuel, the process will need to be scalable. As discussed in Chapter 2, the most likely scenario for feasible scale-up of microalgal biomass production is to use open outdoor production systems such as the raceway ponds used at Karratha. The significant increase of starch content, and hence carbon dioxide uptake, without additional nutrient expenditure could present opportunities for improved economics in carbon lifecycle. Further work would be needed to not only optimise such systems for producing starch-enriched biomass under natural diurnal light cycles, but also to assess the economic feasibility of the optimised process.

(This page intentionally left blank)

# Chapter 7
# Hypersaline conversion of biomass starch to ethanol

## 7.1 Introduction

The studies described in Chapter 5 and Chapter 6 quantified and characterised the carbohydrate composition of *Tetraselmis* sp. strain MUR-233, and verified that the key fermentable substrate within the biomass would be starch. A cultivation method was established for producing starch-enriched biomass as a feedstock for conversion to ethanol. To support some of the work described in this chapter, a pooled starch-enriched MUR-233 biomass was produced as described in Section 3.6.1. This chapter provides details on work conducted to investigate the suitability and halotolerance of the filamentous fungus *Rhizopus oryzae* NRRL 1526 (see Section 3.6.2) for converting the starch from this pooled MUR-233 biomass to ethanol under hypersaline conditions.

### 7.1.1 Anaerobic fermentation of ethanol

The microbiological production of ethanol through anaerobic fermentation is an ancient process that has been well studied and characterised (Mathews 1990). It is connected to essential cellular glycolysis (Figure 35) whereby metabolic energy is generated from carbohydrates through the conversion of one glucose molecule to two pyruvate molecules in the 10-step Embden-Meyerhof-Parnas (EMP) pathway common to a wide range of organisms. Glycolysis generates a net two adenosine triphosphate (ATP) molecules and two reduced nicotinamide adenine dinucleotide (NADH) molecules. ATP in biological systems acts as a store of free energy for cellular metabolism as it can undergo reactions with large negative free energy changes. Oxidised nicotinamide adenine dinucleotide ($NAD^+$) is a coenzyme crucial to the oxidation state of cells, but is converted to NADH during glycolysis and must be reoxidised to $NAD^+$ in order for cells to maintain homeostasis. Following glycolysis in anaerobic microorganisms, pyruvate decarboxylase catalyses the nonoxidative decarboxylation of pyruvate to acetaldehyde which is then converted to ethanol through a NADH-dependent reduction catalysed by alcohol dehydrogenase; this is one of numerous

processes that can facilitate the reoxidation of NADH to $NAD^+$. The balanced equation for alcoholic fermentation as shown in Equation 18 indicates a theoretical maximum 0.51 stoichiometric ratio for conversion of glucose to ethanol based on their respective atomic masses, 180.16 $g \cdot mol^{-1}$ and 46.07 $g \cdot mol^{-1}$.

$$\text{Glucose} + 2\text{ADP} + 2\text{P}_i + 2\text{H}^+ \rightarrow 2\ \text{ethanol} + 2\text{CO}_2 + 2\text{ATP} + 2\text{H}_2\text{O} \qquad \textbf{Equation 18}$$

where:

ADP = adenosine diphosphate

P*i* = inorganic phosphate dissociated from hydrogen phosphate ($HPO_4^{2-}$)

$H^+$ = hydrogen ion dissociated from $HPO_4^{2-}$

$CO_2$ = carbon dioxide

$H_20$ = water

### 7.1.2 Reasoning for a less conventional fermentation approach

In choosing a candidate microorganism for ethanol production, a key consideration was the physical nature of the biomass, which imposed limitations on feedstock concentration and handling. Starch enrichment in the MUR-233 pooled batch (Section 3.6.1) to be used for fermentation trials was calculated to be 54.8 ± 5.7 % afdw, based on acid hydrolysate (n = 3) glucose content measured using IEC-HPLC (Section 3.5.9). However, analyses of total solids and ash free solids (Section 3.5.1) determined that the biomass slurry harvested from the starch-enriched PBR cultures by chemical flocculation with alum and settling (Section 3.4.1) consisted of only 6.9 ± 0.2 % afdw. The remaining biomass slurry composition by weight was 85.2 ± 0.3 % water and 7.9 ± 0.1 % ash. This ash would be predominantly RSS as the salinity of the PBR cultures was 7 % w/v RSS. Furthermore, the starch in the MUR-233 biomass cannot be fermented by conventional yeasts such as *Saccharomyces* spp. without pretreatment to release its compositional glucose. However, pretreatment using established methods such as acid-based hydrolysis (Taherzadeh & Karimi 2007) with additional neutralisation steps would further dilute the

fermentable substrate, and methods that use enzymatic hydrolysis (Alvira *et al.* 2010) would be potentially cost prohibitive for large scale applications. As discussed in Section 2.3, there was also the possibility that commercially available terrestrial enzymes would not be effective under the hypersaline conditions presented by the MUR-233 biomass.

### 7.1.3 Halotolerance of filamentous fungi

The starch-enriched MUR-233 biomass slurry to be used as a fermentation feedstock retains a high salinity equivalent to the harvested PBR culture (Section 7.1.2). At the outset of this Project, it was hypothesised that the biomass could be converted to produce ethanol under hypersaline conditions, using a suitable halotolerant microorganism. Tolerance to high salinity by microorganisms is achieved through osmoregulation to adjust or accumulate intracellular compatible solutes or osmolytes. In response to dehydration effects caused by high salt concentrations external to the cells, the accumulated osmolytes act to exclude the external saline in the cells' surrounding environment. As discussed in Section 2.2, osmolytes in microalgae and cyanobacteria include glycerol, glucosylglycerol, sucrose and trehalose. Similarly, fungal species accumulate polyols in response to osmotic stress (Blomberg & Adler 1992); mainly glycerol, threitol, erythritol, ribitol, arabinitol, xylitol, sorbitol, mannitol and galactitol.

Filamentous fungi can be highly osmotolerant and have been demonstrated to be facultative halophiles, able to survive and reproduce in both non-saline and hypersaline environments. Mycodiversity studies of salt plains and hypersaline waters of solar salterns have isolated halotolerant soil filamentous fungi in salinities of 10 % to 32 % NaCl, including *Aspergillus*, *Eurotium*, *Penicillium*, *Anthrinium*, *Cladosporium*, *Fusarium*, and *Ulocladium* species (Butinar *et al.* 2005; Evans *et al.* 2013; Gunde-Cimerman & Zalar 2014). Under controlled conditions, *Eurotium amstelodami* and *Aspergillus wentii* were shown to synthesise glycerol for osmotic regulation to enable survival and growth at extremely low water potential in 10 % to 14 % sodium chloride (El-Kady *et al.* 1994). The required glycerol level for osmotic regulation depended on the

fungi species, and when grown in media containing 8 % NaCl, *A. wentii* accumulated 18 $g \cdot L^{-1}$ of glycerol whereas *E. amstelodami* only generated 8.7 $g \cdot L^{-1}$.

The effect of salinity on growth and productivity has also been assessed in industrially relevant species of filamentous fungi exploited for their ability to produce small-molecule metabolites. Common examples of such species include *Aspergillus niger* and *R. oryzae* (Lennartsson *et al.* 2014; Pena *et al.* 2012). Results from different studies indicate that the impact of salinity on growth and productivity varies depending on fungal strains. At 9 % NaCl salinity the vegetative growth of *A. niger* was similar to growth at < 1 % NaCl, but optimal vegetative growth occurred at 3 % NaCl with conidial (asexual reproductive spore) production optimal at 2 % NaCl (Mert & Dizbay 1977). Production of catalase and glucose oxidase in an *A. niger* AM-11, a mutant strain producing a high extracellular glucose oxidase, was found to peak at different salinities up to 7 % NaCl beyond which enzyme production ceased (Fiedurek 1998). The specific productivities for fructofuranosidase in *A. niger* SKAn 1015 and glucoamylase in *A. niger* AB1.13 were increased 18 times and 4.5 times, respectively, by adding NaCl to increase the osmolality of cultures by a factor of 10 with optimal productivities also correlating with changes to fungal morphology (Wucherpfennig *et al.* 2011). However, for *R. oryzae* ATCC 9363 increases in environmental salinity up to 4 % NaCl resulted in morphological changes, but reduced both growth and lactic acid production (Özer Uyar & Uyar 2016).

### 7.1.4 Simultaneous saccharification and fermentation

Today's industrial enzymes are derived from a wide range of microorganisms (Cherry & Fidantsef 2003), however in a majority of industrial applications, enzymes share the common function of hydrolytic degradation of natural biopolymers (Kirk *et al.* 2002). Amylases are an important biocatalyst in production of high-fructose syrups and ethanol, and the α-amylase gene promoter of filamentous fungi such as *Aspergillus oryzae* has been exploited for robust expression of recombinant industrial enzymes (Christensen *et al.* 1988; Kirk *et al.* 2002). The *Rhizopus* species

are common saprophytic fungi, and produce carbohydrases useful for the production of dextrose from starch (Food & Drug Administration 2017) as well as enzymes for breaking down other complex biopolymers such as lipids, pectins, proteins, and tannins (Canet *et al.* 2017; Ghosh & Ray 2011; Lennartsson *et al.* 2014).

The ability of filamentous fungi to saccharify complex carbohydrate substrates whilst simultaneously assimilate and ferment the extracted component sugars into valuable products has been widely exploited. For instance, *R. oryzae* is generally recognised as safe (GRAS) and has traditionally been an important industrial microorganism used to enhance value-added textures, flavours and nutritional characteristics in food production (Cantabrana *et al.* 2015; Londoño-Hernández *et al.* 2017). Filamentous fungi are also important for producing high value carboxylic acids as versatile precursor chemicals in the manufacture of products such as food additives, pharmaceuticals, cosmetics, agrichemicals, synthetic resins and biodegradable polymers (Ghosh & Ray 2011; Liu *et al.* 2017). Key carboxylic acids of commercial importance produced by *Rhizopus* and *Aspergillus* species include citric, fumaric, gluconic, itaconic, lactic and malic acids (Naude & Nicol 2017; Pimtong *et al.* 2017; Zhang *et al.* 2013). Furthermore, filamentous fungi are able to utilise sustainable carbon sources such as those from lignocellulosic biomass as production substrates (Dörsam *et al.* 2017). Biosynthesis of these carboxylic acids occur through the aerobic tricarboxylic acid (TCA) metabolic pathway in filamentous fungi (Figure 35), and is important to aerobic extraction of free energy from sugars and formation carboxylic components for other macromolecules (Lidén 2017), but under anaerobic conditions ethanol is biosynthesised as the primary metabolite in a fermentation pathway crucial to this Project (Section 7.1.1).

In the fuel-ethanol industry, simultaneous saccharification and fermentation typically refers to processes whereby commercially produced enzymes such as cellulases are added with an

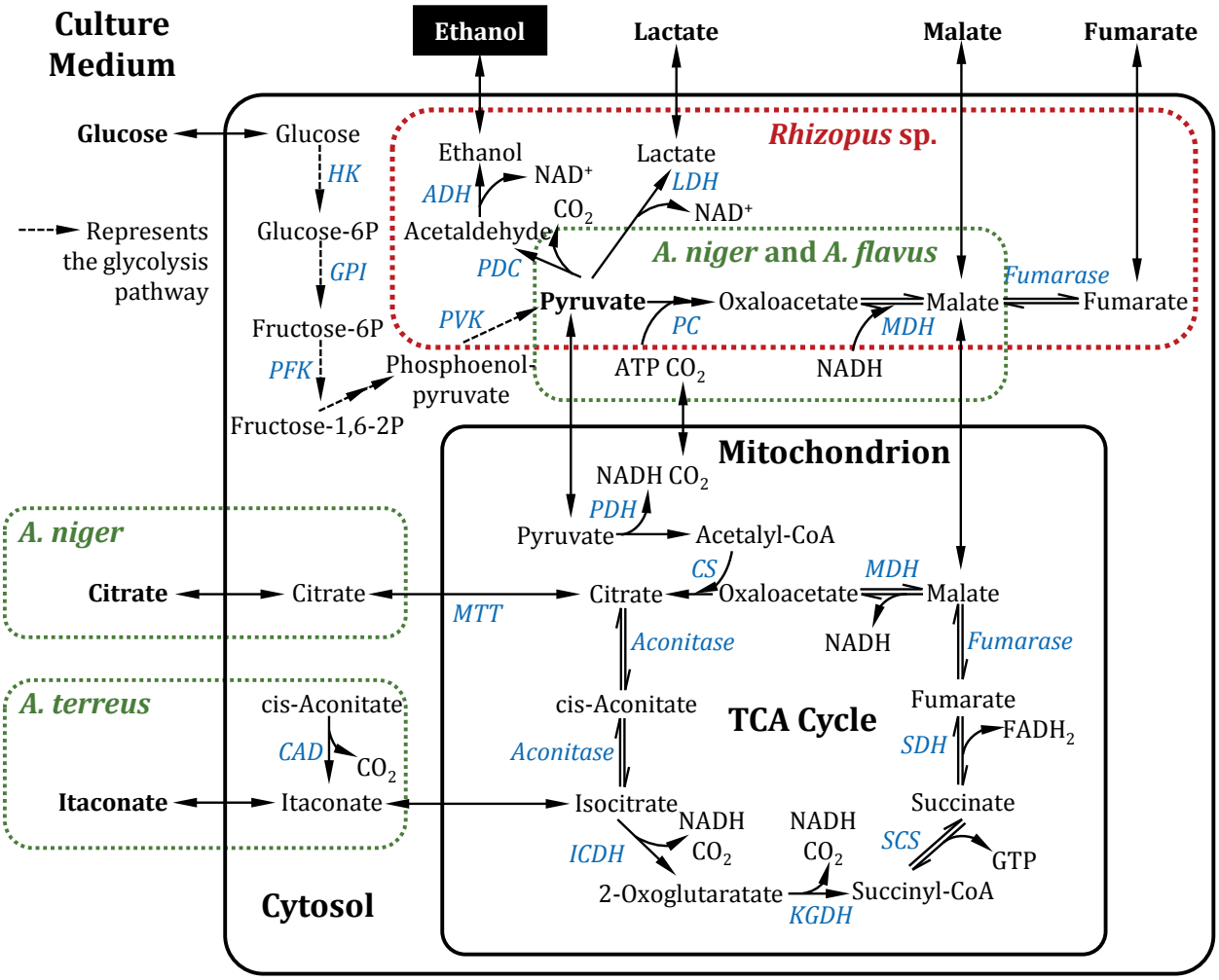


**Figure 35: Metabolic pathways in filamentous fungi for biosynthesis of ethanol and various carboxylic acids**
Dashed boxes indicate unique pathways found in particular fungal species.

| | | | |
|---|---|---|---|
| ADH | alcohol dehydrogenase | PC | pyruvate carboxylase |
| CAD | cis-aconitate decarboxylase | PDC | pyruvate decarboxylase |
| CS | citrate synthase | PDH | pyruvate dehydrogenase |
| GPI | phosphoglucose isomerase | PFK | phosphofructokinase |
| HK | hexokinase | PVK | pyruvate kinase |
| ICDH | isocitrate dehydrogenase | SCS | succinyl-CoA synthetase |
| KGDH | α-ketoglutarate dehydrogenase complex | SDH | succinate dehydrogenase |
| LDH | lactate dehydrogenase | | |
| MDH | malate dehydrogenase | | |
| MTT | mitochondrial tricarboxylate transporter | | |

Reference: Zhang *et al.* (2013). Source figure reproduced with minor edits and corrections under a John Wiley and Sons license for print and electronic formats in a thesis/dissertation (RightsLink Printable License Number 4315221225910).

ethanologenic yeast into dilute-acid pretreated lignocellulosic biomass for conversion to ethanol (Jørgensen *et al.* 2007; Varga *et al.* 2004). The cost of these commercial enzymes exerts economic pressure on the industry. Hence, there is an economic drive to develop both more efficient hydrolytic enzymes for extracting the fermentable sugars from biomass feedstock, and more cost effective processes for the production of such enzymes (Kirk *et al.* 2002). Processes that use more direct simultaneous saccharification and fermentation facilitated by filamentous fungi have previously been assessed as opportunities to combine enzymatic hydrolysis and ethanol conversion through a single naturally occurring microorganism for lignocellulosic ethanol production (Gong *et al.* 1981). However, the conversion of lignocellulosic biomass to ethanol by filamentous fungi alone is likely too slow for a competitive industrial process when compared to robust ethanol producers such as *Saccharomyces cerevisiae* (Hahn-Hägerdal *et al.* 2006). Nevertheless, there are current studies at demonstration scale to assess concepts for multiproduct distilleries or biorefineries that integrate the use of filamentous fungi such as *Neurospora intermedia* into first generation ethanol plants to improve ethanol yields and, at the same time, generate high value-added protein rich biomass for animal feed (Brancoli *et al.* 2017; Nair *et al.* 2017a; Nair *et al.* 2017b).

The target starch substrate in *Tetraselmis* sp. MUR-233 biomass prepared for ethanolic fermentation in this Project is enclosed within pectin-like polysaccharide cell structures composed of significant proportions of Kdo and galacturonic acid (see Chapter 5). Whilst this biomass is compositionally unsuitable for fermentation by *Saccharomyces cerevisiae* without hydrolytic pretreatment, the ability of filamentous fungi to degrade and assimilate diverse biopolymer substrates including starch, pectins and proteins should potentially enable such microorganisms to use the unmodified marine microalgae biomass as a nutrient source for growth and metabolism. Furthermore, *Aspergillus* and *Rhizopus* are two industrially important filamentous fungi with species that also display facultative halotolerance with potential to survive in the hypersaline conditions presented by the harvested MUR-233 biomass. In consideration of ethanologenic

capability, the accumulated concentrations of ethanol through anaerobic fermentation of glucose in liquid medium by different species of *Aspergillus* and *Rhizopus* filamentous fungi are shown in Table 20 (Oda *et al.* 2003; Skory *et al.* 1997). Calculations of percent ethanol yields based on these reported ethanol concentrations indicated that the *Rhizopus* species displayed a higher median percent ethanol yield of 79.2 % in comparison to 46.7 % for the *Aspergillus* species. These observations indicate that *Rhizopus* is a more suitable candidate microorganism than *Aspergillus* as an ethanol producer, and that *R. oryzae* was a species that frequently display high ethanologenic properties. Skory *et al.* (1997) and Oda *et al.* (2003) reported ethanol production of between 14.7 $g \cdot L^{-1}$ to 25.4 $g \cdot L^{-1}$ for *R. oryzae* from 50 $g \cdot L^{-1}$ glucose, the upper end of which indicates a percent ethanol yield close to 100 % based on maximum 0.51 stoichiometric yield (Oda *et al.* 2003; Skory *et al.* 1997). Additionally, ethanol yields of up to 32.3 $g \cdot L^{-1}$ were reported for some strains cultured in higher glucose concentrations of 100 $g \cdot L^{-1}$; a lower percent ethanol yield relative to available substrate that nevertheless may provide an upper titre limit guide for the species capacity for producing ethanol.

**Table 20: Ethanol production by filamentous fungi from 5 % w/v glucose**

| Fungus | Strain NRRL | Accumulated ethanol ($g \cdot L^{-1}$) | Percent ethanol yield (%) | Ref. * |
|---|---|---|---|---|
| *Aspergillus awamori* | NRRL 3112 | 7.2 | 28.2 | [1] |
| *Aspergillus awamori* | NRRL 4869 | 6.0 | 23.5 | [1] |
| *Aspergillus foetidus* | NRRL 337 | 5.2 | 20.4 | [1] |
| *Aspergillus niger* | NRRL 326 | 5.7 | 22.4 | [1] |
| *Aspergillus oryzae* | NRRL 694 | 24.4 | 95.7 | [1] |
| *Aspergillus oryzae* | NRRL 1989 | 16.1 | 63.1 | [1] |
| *Aspergillus oryzae* | NRRL 2220 | 15.9 | 62.4 | [1] |
| *Aspergillus oryzae* | NRRL 4799 | 16.2 | 63.5 | [1] |
| *Aspergillus sojae* | NRRL 1988 | 11.9 | 46.7 | [1] |
| *Aspergillus sojae* | NRRL 3351 | 8.0 | 31.4 | [1] |
| *Aspergillus sojae* | NRRL 5594 | 9.4 | 36.9 | [1] |

| Fungus | Strain NRRL | Accumulated ethanol ($g \cdot L^{-1}$) | Percent ethanol yield (%) | Ref. * |
|---|---|---|---|---|
| *Aspergillus sojae* | NRRL 5595 | 10.5 | 41.2 | [1] |
| *Aspergillus sojae* | NRRL 5597 | 10.6 | 41.6 | [1] |
| *Aspergillus sojae* | NRRL 6271 | 14.4 | 56.5 | [1] |
| *Aspergillus tamari* | NRRL 429 | 18.6 | 72.9 | [1] |
| *Aspergillus tamari* | NRRL 430 | 13.0 | 51.0 | [1] |
| *Aspergillus tamari* | NRRL 436 | 9.8 | 38.4 | [1] |
| *Aspergillus tamari* | NRRL 1654 | 15.5 | 60.8 | [1] |
| *Aspergillus tamari* | NRRL 13139 | 14.6 | 57.3 | [1] |
| *Rhizopus javanicus* | NRRL 13161 | 23.5 | 92.2 | [1] |
| *Rhizopus javanicus* | NRRL 13162 | 21.8 | 85.5 | [1] |
| *Rhizopus javanicus* | NRRL 2871 | 12.4 | 48.6 | [1] |
| *Rhizopus oryzae* | NRRL 1501 | 25.1 | 98.4 | [1] |
| *Rhizopus oryzae* | NRRL 2625 | 24.5 | 96.1 | [1] |
| *Rhizopus oryzae* | NRRL 3133 | 14.9 | 58.4 | [1] |
| *Rhizopus oryzae* | NRRL 6201 | 25.4 | 99.6 | [1] |
| *Rhizopus oryzae* | NRRL 6257 | 15.4 | 60.4 | [1] |
| *Rhizopus oryzae* | NRRL 13480 | 23.2 | 91.0 | [1] |
| *Rhizopus oryzae* | NRRL 395 | 19.3 | 75.7 | [1] |
| *Rhizopus oryzae* | IFO 4707 | 17.1 | 67.1 | [2] |
| *Rhizopus oryzae* | IFO 4716 | 20.2 | 79.2 | [2] |
| *Rhizopus oryzae* | IFO 5379 | 17.8 | 69.8 | [2] |
| *Rhizopus oryzae* | IFO 5384 | 14.7 | 57.6 | [2] |
| *Rhizopus oryzae* | IFO 9364 | 15.3 | 60.0 | [2] |
| *Rhizopus oryzae* | IFO 4726 | 21.0 | 82.4 | [2] |
| *Rhizopus oryzae* | IFO 4736 | 22.0 | 86.3 | [2] |
| *Rhizopus oryzae* | IFO 4747 | 22.6 | 88.6 | [2] |
| *Rhizopus oryzae* | IFO 4749 | 21.4 | 83.9 | [2] |
| *Rhizopus oryzae* | IFO 4754 | 21.7 | 85.1 | [2] |
| *Rhizopus oryzae* | ATCC 48005 | 18.1 | 71.0 | [2] |
| *Rhizopus oryzae* | ATCC 48006 | 16.5 | 64.7 | [2] |
| *Rhizopus oryzae* | ATCC 48007 | 17.5 | 68.6 | [2] |
| *Rhizopus oryzae* | ATCC 48008 | 16.1 | 63.1 | [2] |
| *Rhizopus oryzae* | ATCC 48009 | 20.4 | 80.0 | [2] |

* References: [1] Skory *et al.* (1997)
[2] Oda *et al.* (2003)

**Table 21: Ethanol production by *R. oryzae* from different biopolymer materials**

| Feedstock material | Pretreatment | *R. oryzae* strain | Percent ethanol yield (%) | Ref. * |
|---|---|---|---|---|
| Pure cellulose | enzymatic | CCUG 28958 | 80.4 | [1] |
| 20 g·L$^{-1}$ rice straw | dilute-acid | CCUG 28958 | 70.6 | [1] |
| 50 g·L$^{-1}$ rice straw | dilute-acid | CCUG 28958 | 66.7 | [1] |
| 100 g·L$^{-1}$ rice straw | dilute-acid | CCUG 28958 | 64.7 | [1] |
| Rice straw + cellulase | dilute-acid | CCUG 28958 | 73.6 | [2] |
| Wood forest residues | dilute-acid | CCUG 28958 | 80.4 | [3] |
| Wood forest residues | dilute-acid | CCUG 28958 | 66.7 | [3] |
| Cassava pulp hydrolysate | concentrated-acid | NRRL 395 (FC) | 68.6 | [4] |
| Cassava pulp hydrolysate | concentrated-acid | NRRL 395 (IC) | 54.9 | [4] |
| Cassava pulp hydrolysate | enzymatic | NRRL 395 (FC) | 94.1 | [4] |
| Cassava pulp hydrolysate | enzymatic | NRRL 395 (IC) | 60.8 | [4] |
| Paper pulp sulfite liquor | (no pretreatment) | CCUG 28958 | 73.3 | [5] |
| Wheat straw slurry | dilute-acid | CCUG 61147 | 78.4 | [6] |

FC = free cells; IC = immobilized cells

* Reference: [1] Abedinifar *et al.* (2009)
[2] Karimi *et al.* (2006)
[3] Millati *et al.* (2005)
[4] Thongchul *et al.* (2010)
[5] Taherzadeh *et al.* (2003)
[6] FazeliNejad *et al.* (2016)

*R. oryzae* has also been used in ethanolic fermentation of sugars derived from different biopolymer materials such as rice straw, wheat straw, cassava pulp, wood hydrolysates, and paper pulp sulphite liquor (Abedinifar *et al.* 2009; FazeliNejad *et al.* 2016; Karimi *et al.* 2006; Millati *et al.* 2005; Thongchul *et al.* 2010). The ethanol yields from these studies are summarised in Table 21. In these studies, native saccharification of the lignocellulosic feedstock materials by *R. oryzae* was assisted with a pretreatment step that used enzymatic or dilute-acid hydrolysis, or by the presence of readily available monosaccharides as was the case with paper pulp sulphite liquor and cassava pulp hydrolysate. A benefit of using *R. oryzae* for converting lignocellulosic hydrolysates, as is the case with some other filamentous fungi, is that they have demonstrated the ability to consume hydrolytic by-products such as furfural, acetic acid, and hydroxymethyl furfural (HMF) that are

typically inhibitors for yeast based processes (Millati *et al.* 2005). However, data from Millati *et al.* (2005) also indicated approximately 75 to 125 hours (3.1 to 5.2 days) lag time in *R. oryzae* fermentation of wood hydrolysates in comparison to fermentations with the same strains in a glucose medium. Interestingly, with rice straw and cassava pulp on which combinations of both acid and enzymatic treatments were trialled, the observed ethanol yields were higher with the enzymatic treatment relative to the corresponding material treated with acid. Unlike these reported studies, the aim of this Project's fermentation studies will be to feed starch-enriched MUR-233 biomass to *R. oryzae* NRRL 1526 without any prior chemical or enzymatic hydrolytic pretreatment, and assess the microorganism's native ability to degrade and assimilate the hypersaline marine biomass for ethanol production.

## 7.2 Preliminary studies for fermentation

An initial series of experiments on the filamentous fungus *R. oryzae* NRRL 1526 were conducted to assess key desirable physiological properties important for consumption of starch in MUR-233 biomass in the production of ethanol. These properties included:

- facultative halotolerance;
- anaerobic production of ethanol from glucose;
- utilisation of MUR-233 biomass as a growth and metabolic substrate; and
- hypersaline simultaneous saccharification and ethanolic fermentation of starch.

A working 30 ml liquid culture of NRRL 1526 was maintained in a 50 ml cone-bottomed tube as described in Section 3.6.3 to provide an inoculum source for seeding experiments. Prior to a fermentation experimental study the culture was passaged in duplicate by aseptic harvest and transfer of mycelial plugs (see Figure 8) to two fresh subcultures. One subculture was retained as the ongoing working culture, and the second subculture was harvested at day 4 for mycelial plugs used as fermentation inocula.

### 7.2.1 Ethanol production with salinity variance

The facultative halotolerance of NRRL 1526 to environmental salinity was investigated against varied concentrations of RSS in rich yeast extract peptone dextrose (YEPD) medium, prepared as described in Table 43 of Appendix A.5. In particular, the effect of increasing salinity on ethanol productivity was evaluated. NRRL 1526 ethanol production from 20 $g \cdot L^{-1}$ glucose in YEPD fermentation medium with RSS concentrations of 35, 70 and 105 $g \cdot L^{-1}$ were directly compared to a control group without RSS, using 30 ml liquid cultures (n =3). These salinities were representative of what could be expected in biomass derived from outdoor seawater culture systems such as raceway ponds, and were equivalent to NaCl concentrations 24, 48 and 72 $g \cdot L^{-1}$. The fermentations (n = 3) were conducted in 50 ml conical bottom tubes as described in Section 3.6.7 up to a period of 14 days. Each tube was inoculated with a 3 mm NRRL 1526 mycelial plug, equivalent to 2 ± 0.2 mg fungal dry weight. Daily samples of the fermentations were analysed on the same day of sampling for glucose, glycerol and ethanol by IEC-HPLC (Section 3.5.9) to monitor progress and completion. The experiment was considered complete when glucose concentrations were measured to be zero.

Effect of salinity on biomass growth and morphology is shown in Figure 36. In the absence of salt, the NRRL mycelium displayed a loose amorphous morphology that became denser with increasing salt, and at 10.5 % w/v salinity a tight mycelial pellet was formed (tube D). There was also a reduction in NRRL 1526 mycelium size with increasing salt, indicating a negative effect from salinity on fungal growth. A limitation to this and subsequent fermentation studies is that NRRL 1526 biomass growth, and hence the specific ethanol productivity, could not be measured during the course of fermentations as indicated in Section 3.6.7, particularly in subsequent studies where mycelia growth surrounded the MUR-233 cellular material.

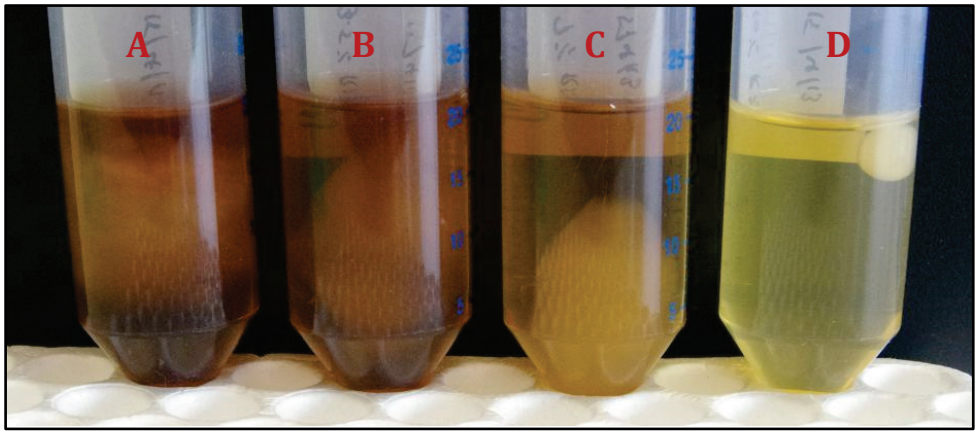


**Figure 36: NRRL 1526 morphology with salinity variance**
Growth morphology (day 14) in liquid YEPD fermentation medium containing different RSS concentrations: (A) 0 g·L$^{-1}$, (B) 35 g·L$^{-1}$, (C) 70 g·L$^{-1}$, and (D) 105 g·L$^{-1}$.

The measured experimental outcomes from this study are shown in Figure 37 and summarised in Table 22. Under the self-anaerobic conditions tested in variants of YEPD fermentation medium, NRRL 1526 produced ethanol as a primary metabolite from glucose utilisation, and higher salt was found to prolong fermentation time as evident between experimental groups with increasing salinity. For all fermentation groups, ethanol productivity declined and ethanol yields plateaued approximately 3 days before full glucose exhaustion. This plateau point was defined to be where all fermentations had achieved at least 90 % of their respective maximum ethanol yields, and was used as a reference end time-point for calculating maximum ethanol volumetric productivity (Equation 16). Fermentation time increased from 7 days in the control group to 14 days in cultures containing of 105 g·L$^{-1}$ RSS. Based on physical observations of mycelium growth and morphology, the prolonged fermentation time was likely a direct result of NRRL 1526 growth inhibition. Furthermore, these preliminary results indicate that ethanol volumetric productivity would be expected to peak at 8 days over a fermentation time of 11 days at 7 % w/v salinity such as found in the MUR-233 production batches pooled for this Project's fermentation trials.

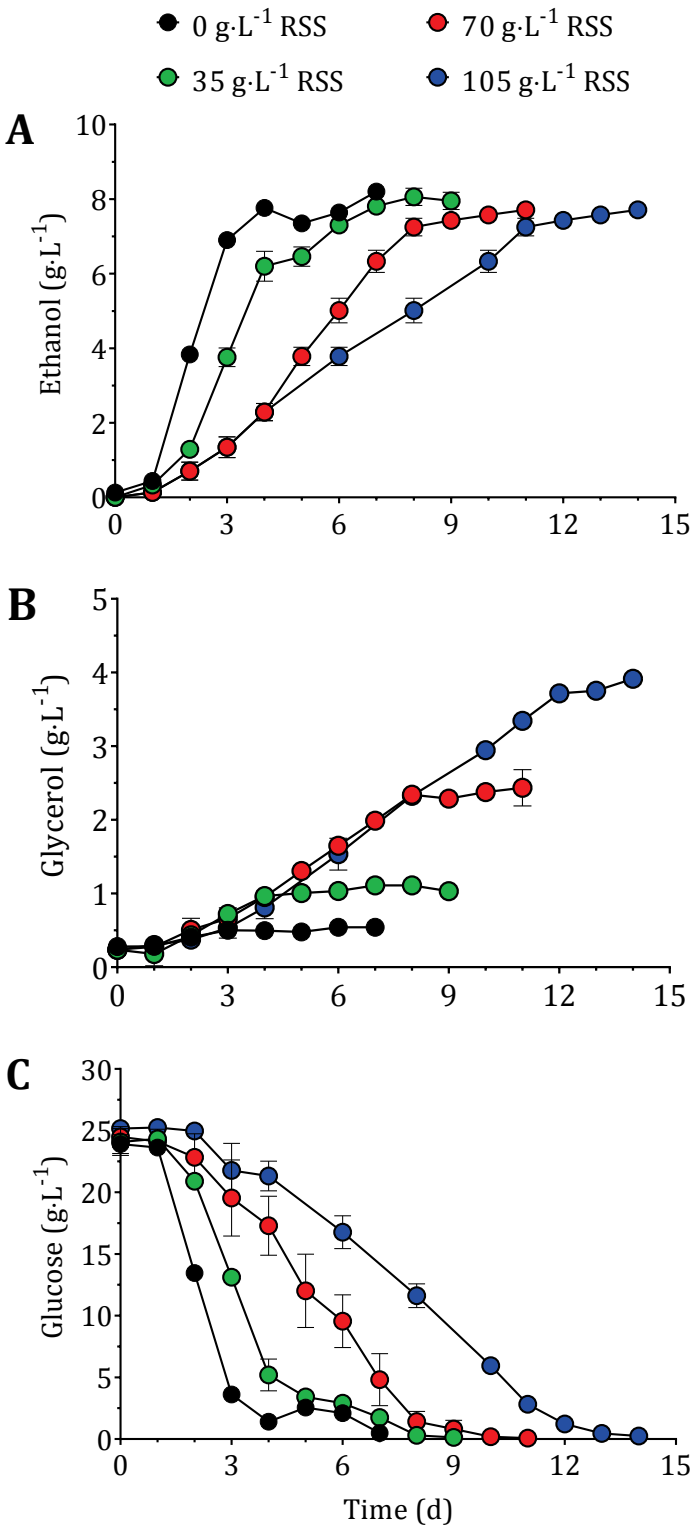


**Figure 37: Effect of salinity on metabolic production and substrate usage**
Formation of (A) ethanol and (B) glycerol, and consumption of (C) glucose by NRRL 1526 at different RSS concentrations: 0 g·L$^{-1}$ (black), 35 g·L$^{-1}$ (green), 70 g·L$^{-1}$ (red), and 105 g·L$^{-1}$ (blue). Plotted means ± SD (n = 3).

With increasing salt, the maximum ethanol volumetric productivity reduced by 4.6-times from 3.23 $g \cdot L^{-1} \cdot d^{-1}$ in the control group to as low as 0.7 $g \cdot L^{-1} \cdot d^{-1}$ at 10.5 % w/v salinity. In the absence of salt, the maximum ethanol yield was 8.2 ± 0.2 $g \cdot L^{-1}$ (mean ± SD) with a percent yield of 67 % based an initial 24 $g \cdot L^{-1}$ of available glucose as measured by IEC-HPLC. The relative difference in ethanol percent yield was only 4.1 % across the salinity range assessed, where the maximum ethanol yield was reduced to 7.7 ± 0.3 $g \cdot L^{-1}$ (mean ± SD) at higher salinities of 7 % w/v and 10.5 % w/v. In higher salt, the slightly lower final ethanol was possibly due to NRRL 1526 use of carbon substrate towards glycerol production as shown in plot B of Figure 37. Glycerol levels in this study were shown to increase up to 7.2-fold from quantities measured in the control group as growth medium salinity was increased to 10.5 % w/v. As previously mentioned, glycerol is a known osmolytes or compatible solute for filamentous fungi under salt stress conditions. Total depletion of glucose was observed at the end of all experimental groups (plot C of Figure 37), and a mass balance against actual yields of ethanol indicated that 7.9 $g \cdot L^{-1}$ to 8.9 $g \cdot L^{-1}$ of assimilated glucose was not converted to ethanol. This glucose was likely required for biomass survival and growth.

The conclusion of this preliminary study is that NRRL 1526 can ferment glucose to completion without loss of too much substrate to other pathways, but at lower ethanol production rates, under hypersaline conditions similar to those found in the MUR-233 biomass.

**Table 22: Summary of NRRL 1526 metabolite production with increasing salinity**

| Salinity (% w/v) | Maximum ethanol \| glycerol yields ± SD ($g \cdot L^{-1}$) | Percent ethanol yield * (%) | Maximum ethanol volumetric productivity ($g \cdot L^{-1} \cdot d^{-1}$) | Ethanol productivity decline (90 % max. yield) (d) | Glucose exhaustion (d) |
|---|---|---|---|---|---|
| 0 | 8.2 ± 0.21 \| 0.5 ± 0.06 | 67.0 | 3.23 ± 0.09 | 4 | 7 |
| 3.5 | 8.1 ± 0.40 \| 1.1 ± 0.06 | 66.2 | 2.46 ± 0.01 | 6 | 8 |
| 7 | 7.7 ± 0.30 \| 2.4 ± 0.24 | 62.9 | 1.27 ± 0.04 | 8 | 10 |
| 10.5 | 7.7 ± 0.30 \| 3.9 ± 0.10 | 62.9 | 0.70 ± 0.02 | 11 | 13 |

* Calculated against measured glucose in media

### 7.2.2 Utilisation of MUR-233 biomass by NRRL 1526

NRRL 1526 was able to survive and produce ethanol under hypersaline conditions with a YEPD nutrient rich background media. A further preliminary study was conducted to determine whether this *R. oryzae* strain would be able to grow and produce ethanol using only MUR-233 biomass without additional nutrient supplementation. The study used non-saline conditions to reduce stress on the fungus, and to facilitate this, salt was removed by washing from MUR-233 biomass as described in Section 3.6.4. NRRL 1526 was still untested, at this stage in the Project, for its ability or capacity to saccharify starch in a submersed culture. Therefore, whilst washed MUR-233 (termed MUR-233W) was tested to determine if microalgal starch could be accessed by the fungus for growth and metabolism, a MUR-233W acid hydrolysate group was also included to ensure an experimental condition that provided glucose as a known usable substrate for microbial uptake. An autoclave step was used to produce MUR-233W acid hydrolysate as described in Section 3.6.5, and indeed autoclaving was found to be an effective method for also disrupting the cell structure of MUR-233W biomass to release and solubilise starch as described in Section 3.6.6.

**Table 23: Dilutions of biomass slurries for fermentation**

| Biomass | Treatment | Dilution | % v/v of original broth |
|---|---|---|---|
| MUR-233W | autoclaved | 1:10 | 10 |
| | autoclaved | 1: 5 | 20 |
| | autoclaved | 1: 2.5 | 40 |
| MUR-233 acid hydrolysate | acidified & autoclaved | 1:10 | 10 |
| | acidified & autoclaved | 1: 5 | 20 |
| | acidified & autoclaved | 1: 2.5 | 40 |

For this preliminary study, prepared biomass broths were diluted in sterile Milli-Q water for the experimental groups, primarily to reduce exposure to excessive ionic residues from the acid and

re-neutralisation treatments of the hydrolysate slurry. Consistent biomass broth dilutions were used between both biomass treatments to facilitate comparative analysis (Table 23), and fermentations (n = 3) were conducted in 50 ml conical bottom tubes as described in Section 3.6.7 over a 14-day period. Each tube was inoculated with a 3 mm NRRL 1526 mycelial plug (2 ± 0.2 mg dw fungus). Daily samples were collected and stored at -20 °C then analysed together for glucose and ethanol by IEC-HPLC (Section 3.5.9).

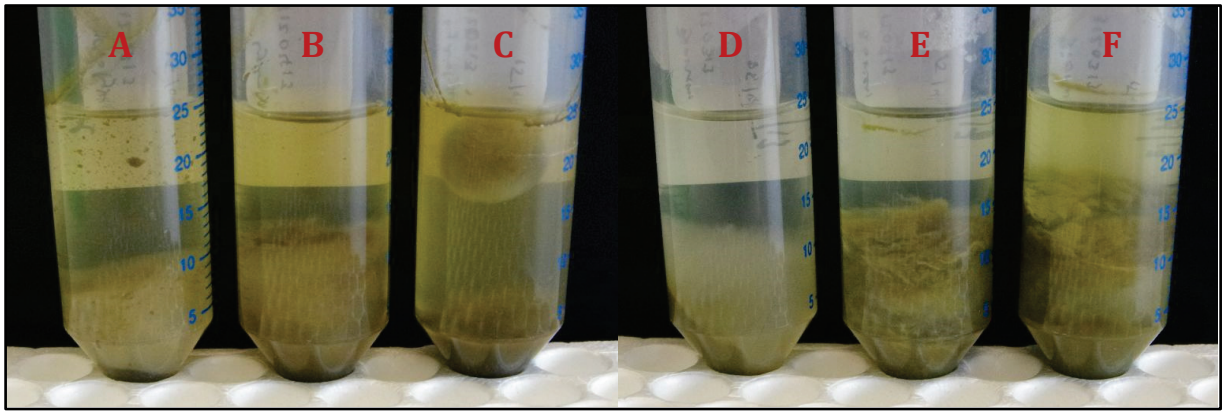


**Figure 38: NRRL 1526 morphology with MUR-233 biomass preparations**
Growth morphology (day 14) in fermentation preparations containing (A) 1:10, (B) 1:5 and (C) 1:2.5 diluted hydrolysate MUR-233W biomass; and (D) 1:10, (E) 1:5 and (F) 1:2.5 diluted MUR-233W biomass.

The study showed that NRRL 1526 was able to grow on MUR-233 biomass without additional nutrient supplementation, even when supplied at only 10 % v/v of the original broth concentration. Representative tubes from each fermentation group are shown in Figure 38. In each experimental group, the fungal mycelia mass was observed to internalise the microalgal biomass for both MUR-233W and MUR-233W acid hydrolysate, suggesting that NRRL 1526 accessed other biopolymers from the microalgae as well as glucose and starch as growth nutrients. As expected for a salt-removed biomass feedstock, the fungal morphology of most experimental groups was amorphous. However, tighter mycelia mass structures displayed in the hydrolysate groups,

including the formation of mycelial pellets in group C (Figure 38) which contained 40 % v/v of acid hydrolysate broth, was likely due to higher ionic stress from potassium and sulphate in these fermentations at up to 47 g·L$^{-1}$ and 57.6 g·L$^{-1}$, respectively, for the more concentrated biomass groups. These ions were introduced during biomass hydrolysis and re-neutralisation steps in the feedstock preparation.

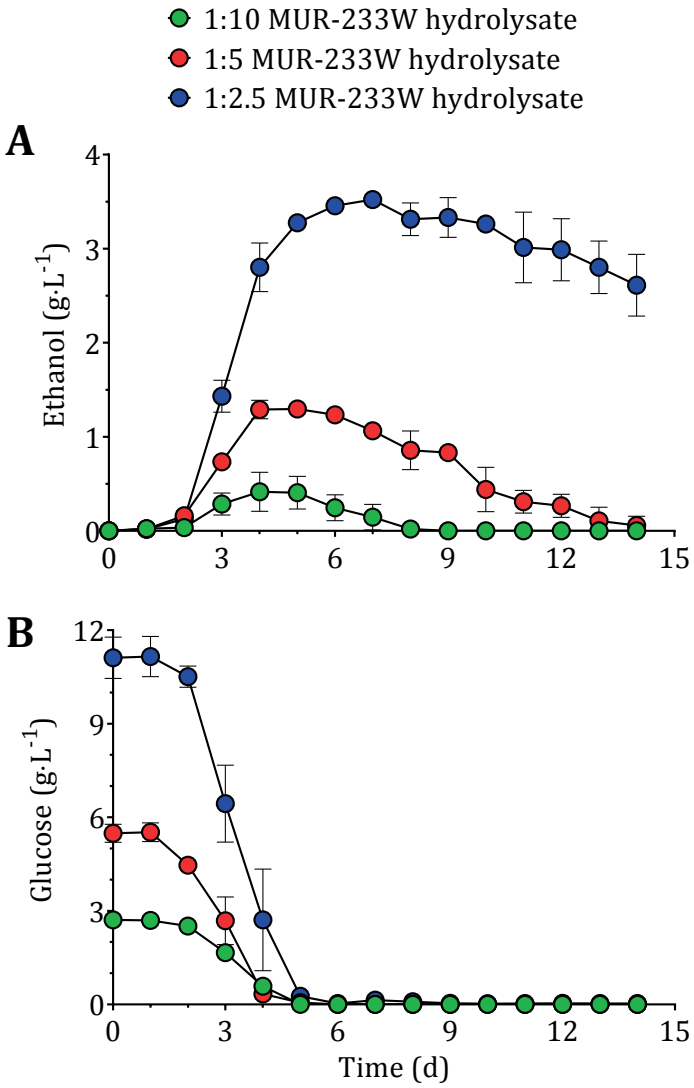


**Figure 39: NRRL 1526 metabolism of acid hydrolysate of washed MUR-33**
Formation of (A) ethanol and consumption of (B) glucose by NRRL 1526 in hydrolysate MUR-233W at biomass dilutions 1:10 (green), 1:5 (red), and 1:2.5 (blue). Plotted means ± SD (n = 3).

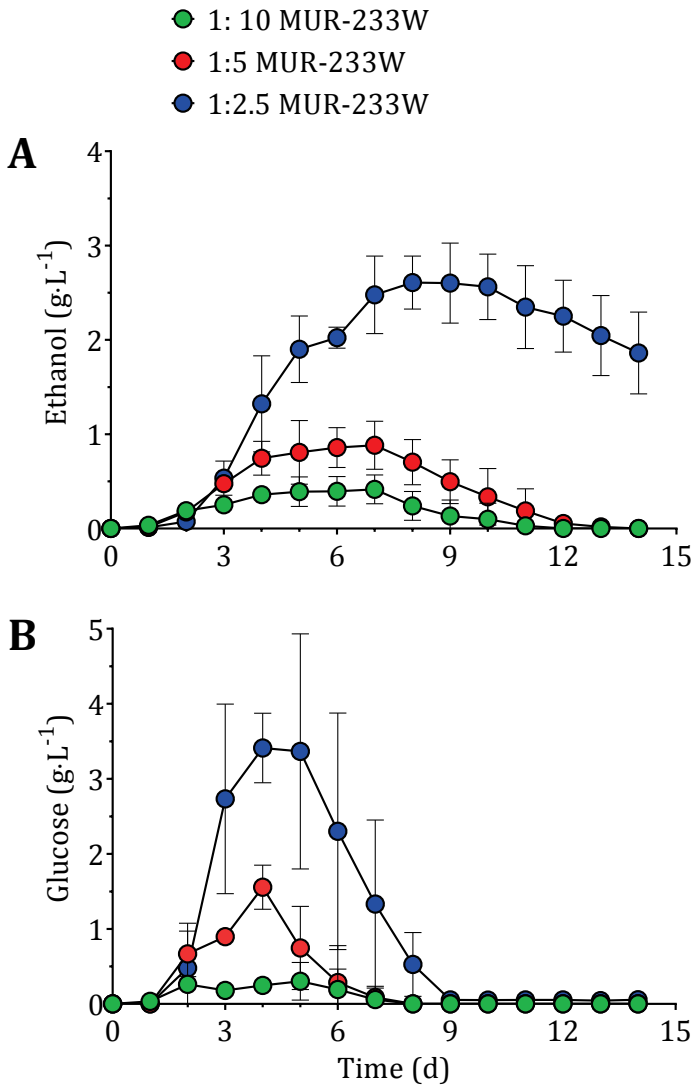


**Figure 40: NRRL 1526 metabolism of washed MUR-33**
Formation of (A) ethanol and consumption of (B) glucose by NRRL 1526 in MUR-233W at biomass dilutions 1:10 (green), 1:5 (red), and 1:2.5 (blue). Plotted means ± SD (n = 3).

The analytical results from this study for MUR-233W acid hydrolysate fermentations are shown in Figure 39 and in Figure 40 for fermentations of MUR-233W. Yield calculations for the study are summarised in Table 24. NRRL 1526 was able to utilise glucose from microalgal hydrolysate to produce ethanol, exhausting the available glucose and completing fermentation after 5 days. The percent ethanol yields at the higher hydrolysate dilutions of 1:10 and 1:5 were ≤ 46.1 %, however, improved to 62.1 % in the 1:2.5 hydrolysate broth. For all hydrolysate fermentations, the

concentrations of ethanol declined after maximum yields were reached and, for the less concentrated groups, both glucose and ethanol were completely consumed by the end of the study at day 14.

**Table 24: Summary of NRRL 1526 ethanol production from dilute washed biomass**

| Medium | Dilution | Maximum ethanol yield ± SD ($g \cdot L^{-1}$) | Percent ethanol yield (%) | Peak available glucose time-point (d) | Glucose exhaustion (d) |
|---|---|---|---|---|---|
| MUR-233W hydrolysate | 1:10 | 0.42 ± 0.21 | 30.1 | 0 | 5 |
| MUR-233W hydrolysate | 1:5 | 1.29 ± 0.10 | 46.1 | 0 | 5 |
| MUR-233W hydrolysate | 1:2.5 | 3.52 ± 0.05 | 62.1 | 0 | 5 |
| MUR-233W | 1:10 | 0.42 ± 0.15 | 30.1 * | 4 | 7 |
| MUR-233W | 1:5 | 0.88 ± 0.26 | 31.4 * | 4 | 7 |
| MUR-233W | 1:2.5 | 2.61 ± 0.28 | 46.1 * | 5 | 9 |

* Percent ethanol yield calculated based on initial glucose measured in equivalent dilutions of hydrolysate.

Saccharification of MUR-233 starch in the submersed fermentations was observed through the release of glucose into the fermentation broth over time as shown in Figure 40. Across the experimental groups with cell-disrupted biomass broth, peak glucose release was observed after 4 to 5 days. There were large replicate standard deviations were observed between glucose measurements in monitored samples that could have been attributed to differences in fungal growth, enzyme production, or glucose conversion. However, lower replicate standard deviations in measured ethanol accumulation from these same fermentations suggested that the glucose variance was not related to the rate of glucose conversion to ethanol. The requirement for NRRL 1526 to saccharify available starch before anaerobic fermentation of released glucose for ethanol conversion resulted in both extended fermentation times and lower ethanol yields. There was no lag difference between commencement of fermentations between acid hydrolysate and cell-

disrupted biomass groups, however, the fermentations in cell-disrupted biomass broth did not complete until day 7 for the in the higher 1:10 and 1:5 dilution groups, and day 9 for the 1:2.5 dilution group. Fermentations fed with 1:2.5 diluted cell-disrupted biomass took 2 days longer to complete and achieved a much lower percent ethanol yield (16 % less) than those with equivalent hydrolysate concentrations. At 1:2.5 dilution, there was a significant difference of 0.85 $g \cdot L^{-1}$ in maximum ethanol yields achieved between hydrolysate and cell-disrupted biomass fermentations (t-test, $p > 0.05$).

This study showed that NRRL 1526 could grow in MUR-233 biomass without supplementation, and produce ethanol from the carbohydrate substrates in MUR-233, including those within complex biopolymers such as starch. Ethanol production was more rapid with hydrolysate compared to cell-disrupted biomass. NRRL 1526 also produced enzymes that were able to saccharify MUR-233 starch. Furthermore, the extension to ethanol production times observed with simultaneous saccharification and fermentation appeared to be limited by the release of glucose from starch.

### 7.2.3 Ethanol production with excess glucose

Once it was established that NRRL 1526 could utilise either glucose from hydrolysate or starch from cell-disrupted MUR-233 to produce ethanol, an investigation was conducted to assess whether an upper limit existed for ethanol production by the *R. oryzae* strain that would restrict conversion of the available glucose in the starch-enriched MUR-233 biomass feedstock prepared in Section 3.6.1. This available glucose had been measured as 42 ± 4.4 $g \cdot L^{-1}$ from acid hydrolysates of the biomass using IEC-HPLC. In this study, NRRL 1526 ethanol production was compared for submerged cultures containing variable glucose supplied at concentrations 20 $g \cdot L^{-1}$ to 60 $g \cdot L^{-1}$ in a YEPD-based nutrient rich fermentation medium. The fermentations (n = 3) were conducted in 50 ml conical bottom tubes as described in Section 3.6.7 over a 9-day period. Each tube was inoculated with a 3 mm NRRL 1526 mycelial plug (2 ± 0.2 mg dw fungus). Daily samples were

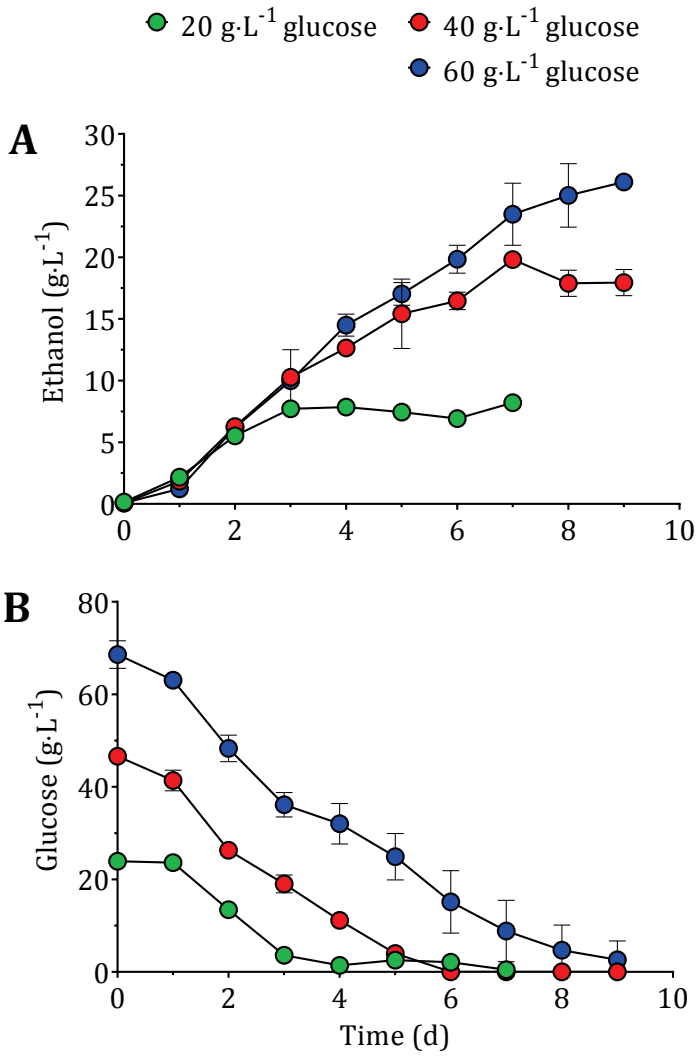


**Figure 41: NRRL 1526 ethanol production capacity**
Formation of (A) ethanol and consumption of (B) glucose over time by *R. oryzae* with varied initial glucose concentrations in growth medium: 20 g·L$^{-1}$ (green), 40 g·L$^{-1}$ (red) and 60 g·L$^{-1}$ (blue). Plotted means ± SD (n = 3).

collected and stored at -20 °C then analysed together for glucose and ethanol by IEC-HPLC (Section 3.5.9).

The ethanol production capacity of NRRL 1526 from glucose supplied in this study are shown in Figure 41 and summarised in Table 25. The measured glucose in samples showed a higher initial average concentration than what was gravimetrically prepared during the experimental setup, however, the quantified results to be discussed have been calculated based on measured amounts

from the IEC-HPLC assay. Over 9 days submerged culture, NRRL 1526 was substrate limited when supplied with 23.9 g·L$^{-1}$ glucose. In the cultures with highest mean glucose concentrations of 68.6 g·L$^{-1}$, the filamentous fungus was able to consume 66 g·L$^{-1}$ glucose to produce 26.1 ± 0.6 g·L$^{-1}$ ethanol. This was equivalent to 97 % of the total available substrate. The observed ethanol volumetric productivity increased with the availability of more glucose substrate; however, the percent ethanol yields were comparable (0.9 % difference) in cultures supplied with ≥ 46.6 g·L$^{-1}$ glucose with highest observed percent ethanol yield at 75.3 % when 46.6 g·L$^{-1}$ glucose was supplied. For this particular group, the maximum percent ethanol yield was based on day 9 quantities, and not the peak point observed at day 7 (plot A of Figure 41). This is because the sharp increase in ethanol concentration at day 7 was not consistent with glucose depletion observed in earlier day 6 samples for this experimental group, indicating that the day 7 ethanol measurement was likely to be inaccurate.

**Table 25: Summary of NRRL 1526 ethanol production with increasing salinity**

| Initial glucose | Maximum ethanol yield ± SD | Percent ethanol yield * | Ethanol volumetric productivity | Ethanol productivity decline (90 % max. yield) | Glucose exhaustion |
|---|---|---|---|---|---|
| (g·L$^{-1}$) | (g·L$^{-1}$) | (%) | (g·L$^{-1}$·d$^{-1}$) | (d) | (d) |
| 20 | 8.2 ± 0.21 | 67.3 | 3.23 ± 0.09 | 4 | 4 |
| 40 | 17.9 ± 1.06 ** | 75.3 ** | 3.35 ± 0.26 | 6 ** | 6 |
| 60 | 26.1 ± 0.62 | 74.6 | 3.61 ± 0.17 | 8 | 9 |

* Calculated against measured glucose in media.
** Based on measured ethanol at day 9.

The available glucose within MUR-233 starch has been quantified at 10 % less than the 46.6 g·L$^{-1}$ supply where the highest percent ethanol yield was observed in this study. This may limit the conversion efficiency of this filamentous fungus when supplied with MUR-233 biomass.

Nevertheless, the results from this study showed that NRRL 1526 could ferment to completion glucose supplied in excess of that available in MUR-233 biomass.

### 7.2.4 Enzymatic starch hydrolysis with salinity variance

As previously noted in Section 2.3, Matsumoto *et al.* (2003) found that under saline conditions terrestrial amylase and glucoamylase were completely inhibited and would be unsuitable for hydrolysing starch from unwashed marine biomass. To verify this report, an experiment was conducted with available thermostable α-amylase and amyloglucosidase (glucoamylase) sourced from the K-TSTA kit used in Section 3.5.7. These enzymes are, respectively, derived from B*acillus licheniformis* and *Aspergillus niger* (Megazyme 2018) which are both terrestrial microorganisms typically found in soils.

Separate AIR preparations (Section 3.4.4) were made from 3 × 300 mg dry potato starch and 3 × 7.9 ml autoclaved cell-disrupted MUR-233 biomass slurry (Section 3.6.1) which was equivalent to 3 × 300 mg microalgal starch based on a quantified hydrolysate glucose concentration of 42 $g \cdot L^{-1}$. For both sample types, the 300 mg AIR preparations were resuspended to 50 $g \cdot L^{-1}$ starch suspensions in 600 ml volumes with 100 mM sodium acetate, 5 mM calcium chloride, pH 5 buffer of different salinities. These included a no-salt control group and groups with dissolved RSS at 35 $g \cdot L^{-1}$ and 70 $g \cdot L^{-1}$. All the suspensions were heated at 90 °C for 30 minutes to solubilise constituent starch, and cooled to 50 °C at which point each 600 ml suspension was evenly mixed and split into 3 × 300 ml volumes. Thermostable α-amylase (6.6 U) and amyloglucosidase (7.3 U) were added to each 300 ml volume and incubated for 5 hours at 50 °C. Samples of each volume were taken at 2 hours and 5 hours, centrifuged at 16,000 rcf for 10 minutes then analysed for glucose by IEC-HPLC (Section 3.5.9).

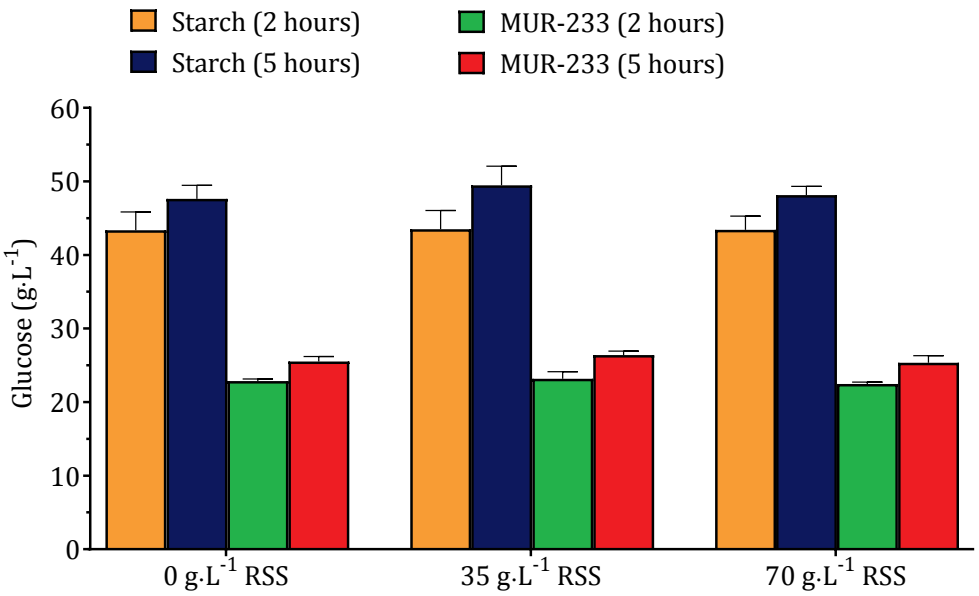


**Figure 42: Effect of variable salinity on enzymatic hydrolysis**
Release of glucose from 50 g·L$^{-1}$ potato starch and 50 g·L$^{-1}$ MUR-233 starch digested with α-amylase and amyloglucosidase in 100 mM sodium acetate, 5 mM calcium chloride, pH 5 buffer containing no salt (0 g·L$^{-1}$ RSS) and RSS at 35 g·L$^{-1}$ and 70 g·L$^{-1}$. Plotted means ± SD (n = 3).

**Table 26: Percentage of total starch glucose released at 5 hours digestion**

| Salinity (g·L$^{-1}$ RSS) | Starch (%) | MUR-233 (%) |
|---|---|---|
| 0 | 85.7 | 45.9 |
| 35 | 89.0 | 47.5 |
| 70 | 86.7 | 45.6 |

The results from this study are shown in Figure 42 and summarised as percentages of total starch glucose released from samples in Table 26. Thermostable α-amylase and amyloglucosidase were able to digest potato starch to release 85.7 % to 89 % of compositional glucose over a 5 hour incubation period. Individual comparisons of the different salinity groups at both the 2 hour and 5 hour sampling point determined that there was no significant difference (t-tests, $p > 0.05$) in the total released glucose between potato starch digests at RSS concentrations 0 g·L$^{-1}$, 35 g·L$^{-1}$ or

70 g·L$^{-1}$. Similar testing on experimental groups containing MUR-233 starch also determined no significant difference (t-tests, $p > 0.05$) in total glucose release between the difference salinity groups. However, only 45.6 % to 47.5 % of expected compositional glucose was released from MUR-233 starch preparations. It is possible that some glucose had been release during autoclave treatment of the biomass, in which case some free glucose may have been washed away in solution with ethanol during AIR preparations. It is also possible that some starch could have been trapped within semi-disrupted MUR-233 cell structure making enzyme accessibility difficult for digestion. Nevertheless, the results from this study showed that increasing salt within a salinity range of up to 7 % w/v RSS had no negative impact of hydrolytic enzyme activity. It is therefore expected that the 7 % w/v salinity found in the MUR-233 biomass for fermentation will not affect starch digestion by native α-amylase and amyloglucosidase of a terrestrial microorganism such as *R. oryzae*.

### 7.2.5 Simultaneous saccharification and fermentation with salinity variance

The preceding preliminary studies found that NRRL 1526 was able to ferment glucose to ethanol at 7 % w/v salinity. Furthermore, α-amylase and amyloglucosidase from some terrestrial microorganisms displayed uninhibited hydrolytic activity in releasing glucose from starch in solutions at this salinity. This next study combined these two factors to assess the salinity effect on ethanol production from starch by NRRL 1526 through simultaneous saccharification and fermentation. The saccharification of starch would not be assisted by addition of commercially produced enzymes. Instead, it would rely on natively secreted enzymes from NRRL 1526.

NRRL 1526 ethanol production from 50 g·L$^{-1}$ starch in 100 ml rich yeast extract peptone starch (YEPS) medium with NaCl concentrations of 27 g·L$^{-1}$ and 54 g·L$^{-1}$, prepared as described in Table 11 of Section 3.6.6, were directly compared to a control group without NaCl. The fermentations ($n = 3$) were conducted in 250 ml conical flasks with water-filled airlocks as described in Section 3.6.7 over a maximum 15 days. Each flask was inoculated with a 3 mm NRRL 1526 mycelial plug, equivalent to 2 ± 0.2 mg fungal dry weight. Daily samples were collected

and stored at -20 °C then analysed together for glucose and ethanol by IEC-HPLC (Section 3.5.9). Fermentations were considered complete when measured glucose concentrations reduced to zero.

The *Rhizopus* biomass formed mycelial pellets when grown in submersed liquid cultures in conical flasks with orbital mixing, and the effect of salinity on the morphology of these pellets is shown in Figure 43. As previously observed, mycelium morphology became more dense with higher salinity. Fermentation medium containing solubilised starch was in initially viscous at day 0, and clarified as saccharification progressed over the course of the experiment. When the experiment was terminated at day 15, the media in cultures with no salt and 27 g·L$^{-1}$ NaCl appeared clear with no viscosity. However, the fermentation medium of the 54 g·L$^{-1}$ NaCl group was opaque with starch still visibly in suspension (Figure 43-C), indicating incomplete substrate utilisation for fermentation.

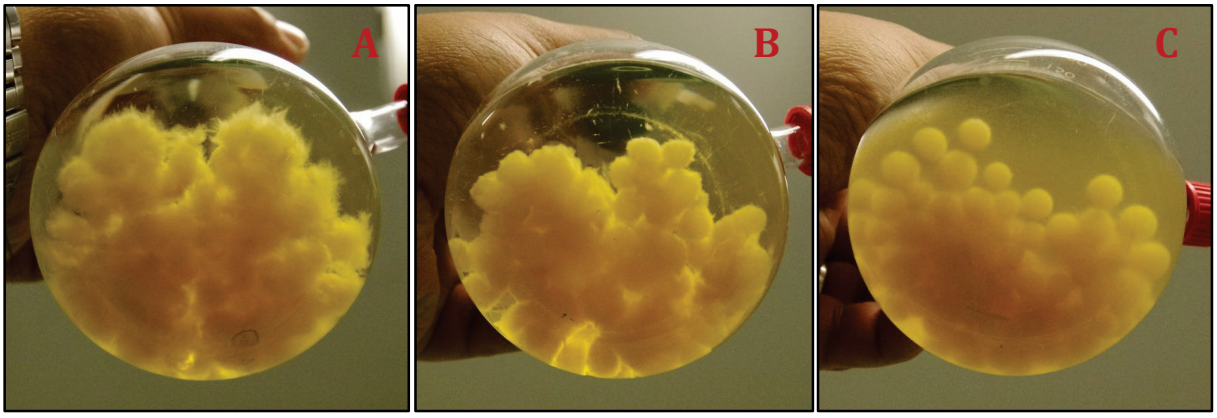


**Figure 43: NRRL 1526 morphology with salinity variance in shake flasks**
Growth morphology at day 15 in shake flask cultures in liquid YEPS fermentation medium containing different NaCl concentrations: (A) 0 g·L$^{-1}$, (B) 27 g·L$^{-1}$, (C), and 54 g·L$^{-1}$.

The impact of salinity on the ability of NRRL 1526 to simultaneously saccharify and ferment starch is shown in Figure 44, and yield calculations measuring this impact are summarised in Table 27. The rate of glucose release into the fermentation media was reduced with increasing salinity. This

was indicated by the peak time-point for available glucose measured in the media. A salinity increase of 27 g·L$^{-1}$ NaCl resulted in a 1-day delay to peak glucose release, and a 54 g·L$^{-1}$ NaCl increase extended this delay by an additional 2 days (Figure 44-B). However, in consideration of observations from Section 7.2.4 where salinity had no impact on enzymatic activity, the differences in glucose release rate in this study could be related to differences in the availability of hydrolytic enzymes produced by NRRL 1526 under variable saline conditions, where higher salinity would result in less available enzyme. It has already been shown that increasing salinity caused a reduction in biomass growth. Such a reduction would also effect the capacity of the biomass in culture to produce hydrolytic enzymes.

**Table 27: Summary of NRRL 1526 simultaneous saccharification and fermentation with varying salinity**

| NaCl salinity (g·L$^{-1}$) | Maximum ethanol yield ± SD (g·L$^{-1}$) | Percent ethanol yield (%) | Peak available glucose time-point (d) | Glucose exhaustion (d) |
|---|---|---|---|---|
| 0 | 24.0 ± 2.3 | 84.8 | 2 | 11 |
| 27 | 22.4 ± 1.4 | 79.2 | 3 | 12 |
| 54 | 19.1 ± 0. 5 | 67.3 | 5 | - |

Simultaneous saccharification and fermentation was observed with the production of ethanol commencing with the release of glucose, well before completion of starch saccharification. A maximum ethanol yield of 24 g·L$^{-1}$ was measured in the absence of salt, equivalent to a percent ethanol yield of 84.8 %. This result indicated that 8.4 g·L$^{-1}$ glucose was likely required for biomass growth and other metabolic processes, and is consistent with findings from the study described in Section 7.2.1. A salinity increase of 27 g·L$^{-1}$ NaCl resulted in a 5.6 % reduction in percent ethanol yield, which was reduced by an additional 11.9 % when salinity was increased to 54 g·L$^{-1}$ NaCl. However, the maximum and percent ethanol yields for the 54 g·L$^{-1}$ NaCl experimental group were

calculated based on analytical measurements at day 15, with glucose remaining in the media of some replicates of the experimental group (2.9 ± 3.2) g·L$^{-1}$ and starch still visible in media suspension.

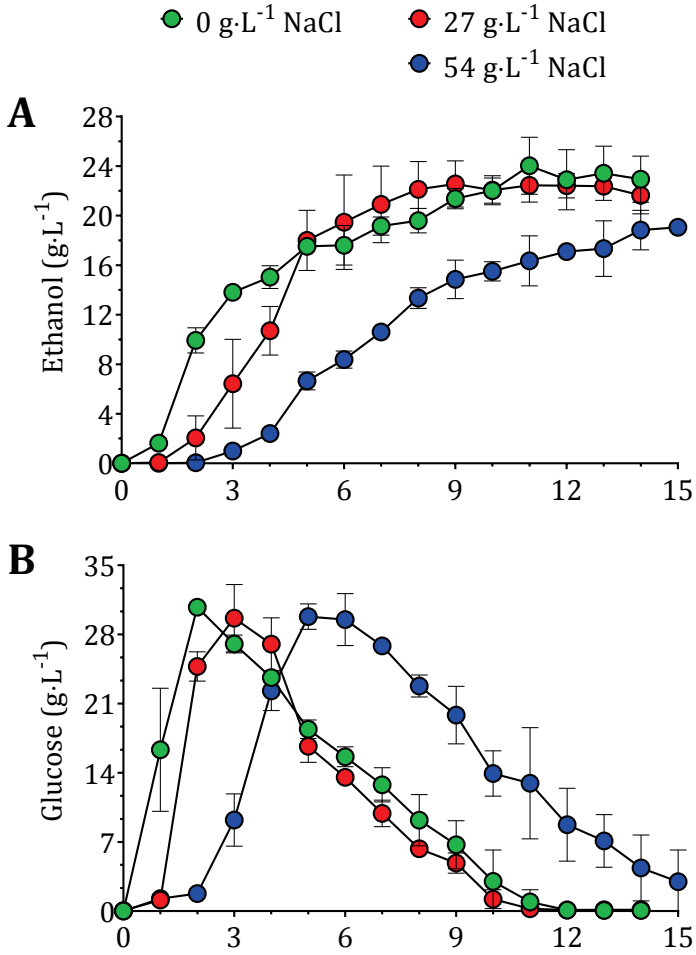


**Figure 44: Effect of NaCl concentrations on starch saccharification and fermentation**
(A) Ethanol production; (B) Glucose released and consumed from potato starch. Cultures at different NaCl concentrations: 0 g·L$^{-1}$ (green), 27 g·L$^{-1}$ (red), and 54 g·L$^{-1}$ (blue). Plotted means ± SD (n = 3).

The results of this study showed that the hydrolytic enzymes produced by NRRL 1526 were halotolerant and able to saccharify starch in saline conditions of up to 54 g·L$^{-1}$ NaCl. Reduced starch saccharification with increasing salinity could be related to less available enzyme due to salt

inhibition of biomass growth. There is potential to reduce this impact by increasing the inoculum amount in fermentations. Salt has a negative effect on ethanologenic production by NRRL 1526, with percent yield reductions of up to 17.5 % when fermentation medium salinity was increased to 54 $g \cdot L^{-1}$ NaCl. However, at this high salinity NRRL 1526 was still able to produce 19.1 $g \cdot L^{-1}$ ethanol.

## 7.3 Production of ethanol from hypersaline MUR-233 biomass

A final study was conducted, combining knowledge gained from the lead-up preliminary fermentation trials, to assess the effectiveness of NRRL 1526 in utilising harvested hypersaline MUR-233 biomass without supplementation to produce ethanol under self-anaerobic conditions. A pooled batch of starch-enriched MUR-233 biomass was produced for this study as described in Section 3.6.1. Previous experiments found that NRRL 1526 was able to simultaneously saccharify starch to glucose and ferment to ethanol under hypersaline conditions in NaCl concentrations higher than the typical 24.5 $g \cdot L^{-1}$ of seawater. However, delays in glucose release times could be attributed to a reduction in fungal growth at higher salinities and extend ethanol production times.

An approach was taken to increase the initial fungal mass and, hence, hydrolytic enzyme availability to reduce the process impact related to inhibited growth at higher salinities. The aim was to improve starch saccharification and glucose availability, and ultimately reduce the process time for converting available glucose to ethanol. For this purpose, a larger inoculum for experimental use was prepared in 2 litres of standard YEPS medium as described in Section 3.6.6. The inoculum was seeded with a 3 mm NRRL 1526 mycelial plug and cultivated over a 21-day period at 28 °C, using a 5-litre Schott bottle sealed with a water-filled airlock apparatus and mixed on a magnetic stirrer. Under this culture condition, the fungus grew as short loose elongated mycelial masses rather than pellets as previously observed with orbital mixing.

NRRL 1526 ethanol production from MUR-233 biomass was assessed at RSS salinities up to 7 % w/v. Blends of MUR-233 slurry for experimental groups were prepared as shown in Table 28.

A set of control fermentations in YEPS at equivalent RSS salinities were prepared and run in parallel to enable performance comparisons with previous studies. YEPS media for these control fermentations were prepared as described in Table 11 of Section 3.6.6. All fermentations (n = 3) were conducted in 100 ml biomass or control broths using 250 ml conical flasks with water-filled airlocks, as described in Section 3.6.7 over 14 days. Each flask was inoculated with a 1.5 ± 0.15 g of wet weight mycelium, equivalent to an average 127 mg of fungal dry weight. Samples were collected at days 0, 1, 3, 5, 7, 9, 11, 13 and 14 then stored at -20 °C. All samples were analysed for glucose and ethanol (Section 3.5.9). Day 14 samples were also analysed for other expected metabolites from *R. oryzae*: glycerol, citric acid, malic acid, lactic acid and fumaric acid (Section 3.5.9). Fermentations were considered complete when measured glucose concentrations reduced to zero.

**Table 28: Feedstock preparations for variable salinity MUR-233**

| Salinity (% w/v) | MUR-233W (% v/v) | MUR-233 (% v/v) |
|---|---|---|
| 0 | 100 | 0 |
| 4.2 | 40 | 60 |
| 7 | 0 | 100 |

The profiles for measured ethanol production and glucose release and consumption in fermentation broths of control YEPS and MUR-233 biomass at varying salinities are shown in Figure 45 and Figure 46, respectively. Key values from these results are also summarised in Table 29. The change in inoculum preparation resulted in more rapid release of glucose from starch in all fermentation broths. The rate of starch saccharification for glucose release, indicated by the peak available glucose time-point, for each fermentation was also comparable across all salinities with maximum glucose release typically observed between day 1 and day 3. Day 2 glucose levels

had not been measured, however, the observed glucose profiles suggested that peak glucose release might have occurred at this time-point. Improvements in saccharification was evident with the YEPS groups when compared to similar conditions assessed in Section 7.2.5 where differences

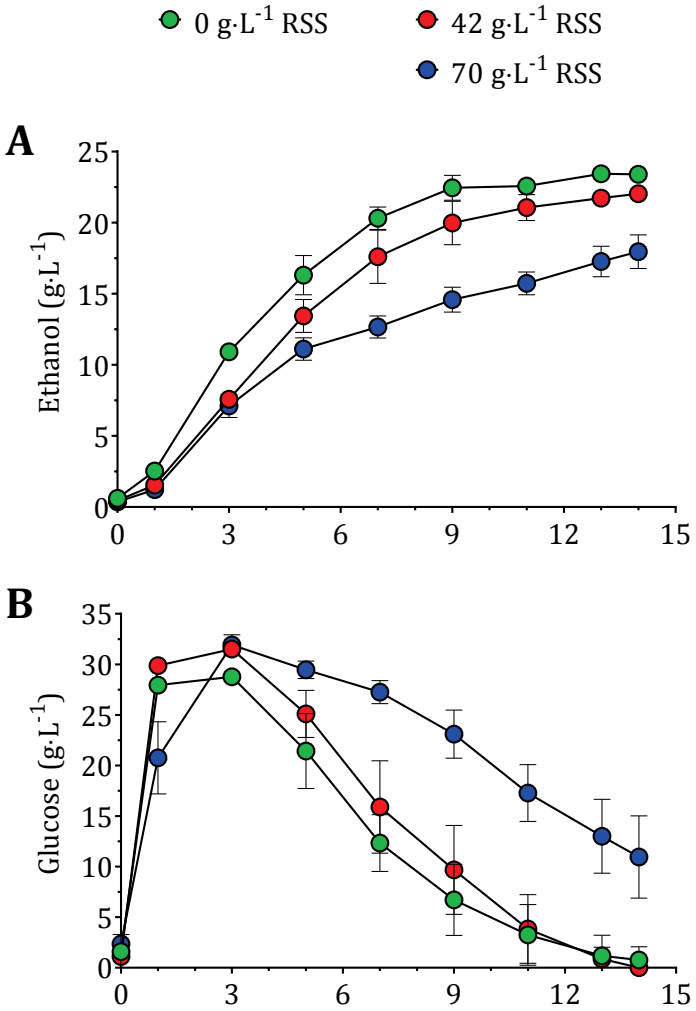


**Figure 45: Effect of RSS concentration on control potato starch saccharification and fermentation with increased inoculum mass**
(A) Ethanol production; (B) glucose released and consumed from potato starch by *R. oryzae* at RSS salinities: 0 % w/v (green), 4.2 % w/v (red), and 7 % w/v (blue). Plotted means ± SD (n = 3).

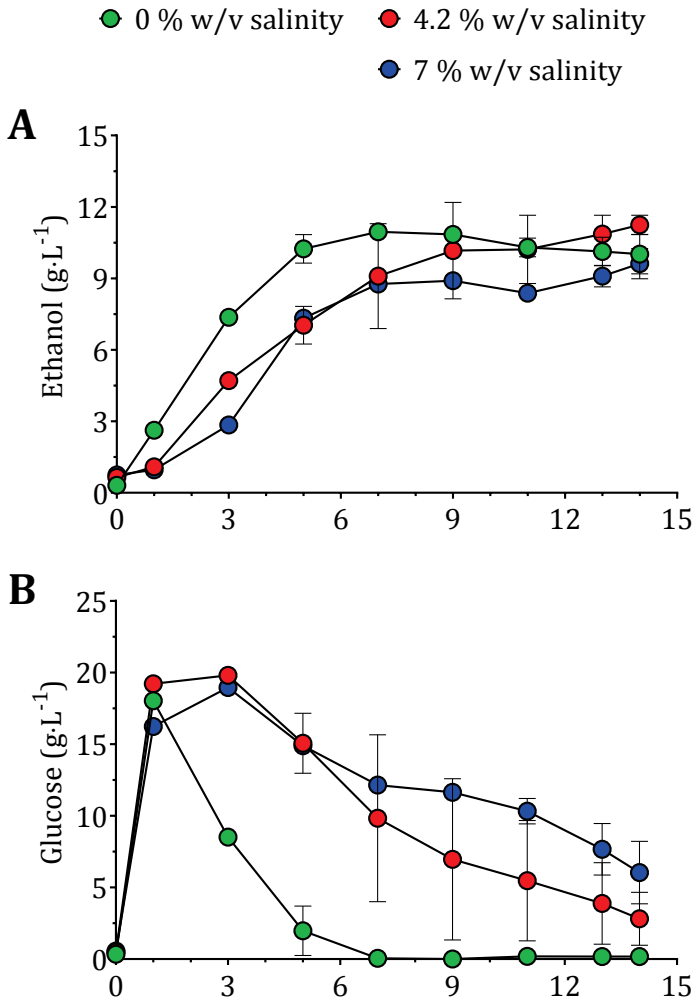


**Figure 46: Effect of RSS concentration on MUR-233 starch saccharification and fermentation with increased inoculum mass**
(A) Ethanol production; (B) glucose released and consumed from MUR-233 starch by *R. oryzae* RSS salinities: 0 % w/v (green), 4.2 % w/v (red), and 7 % w/v (blue). Plotted means ± SD (n = 3).

in glucose release of up to 4 days had been observed. Relative to the measure glucose quantities, the peak glucose release time-point also improved by 1 day in salt-free YEPS. The use of a larger amount of inoculating fungi was effective in improving the hydrolysis of starch in fermentation broths. This was likely a combination of both an increase enzyme proportionate to fungal mass increase, but perhaps also the presence of expressed hydrolytic enzymes in the residual transferred medium from the inoculum that was prepared in YEPS and required produce hydrolytic enzymes to access starch-bound glucose.

**Table 29: Summary of simultaneous saccharification and fermentation from starch and MUR-233 biomass at varying salinities**

| Medium | Salinity (% w/v) | Maximum ethanol yield ($g \cdot L^{-1}$) | Percent ethanol yield (%) | Residual glucose ($g \cdot L^{-1}$) | Peak available glucose time-point (d) | Glucose exhaustion (d) |
|---|---|---|---|---|---|---|
| YEPS * | 0 | 23.4 ± 0.35 | 82.3 | 0.77 ± 1.34 | 1-3 | 14 |
| | 4.2 | 22.02 ± 0.17 | 77.4 | 0 ± 0.0 | 1-3 | 14 |
| | 7 | 17.95 ± 1.19 | 63.3 | 10.95 ± 4.07 | 1-3 | - |
| MUR-233 ** | 0 | 10.02 ± 0.83 | 46.5 | 0.18 ± 0.04 | 1 | 7 |
| | 4.2 | 11.24 ± 0.41 | 52.2 | 2.81 ± 1.85 | 1-3 | - |
| | 7 | 9.62 ± 0.63 | 44.8 | 6.04 ± 2.19 | 1-3 | - |

Ethanol yields and residual glucose at day 14 presented as means ± SD (n = 3).
* Initial starch concentration 50.0 $g \cdot L^{-1}$ (glucose 55.6 $g \cdot L^{-1}$)
** Initial microalgal starch concentration 37.8 $g \cdot L^{-1}$ (glucose 42.0 $g \cdot L^{-1}$)

Ethanol production in the control YEPS groups was comparable to previous observations in Section 7.2.5 in relation to both maximum yields and percent yields. Under salt free conditions, a maximum 23.4 $g \cdot L^{-1}$ ethanol yield and percent yield of 82.3 % was achieved. In hypersaline conditions, the maximum ethanol yield was 22.02 $g \cdot L^{-1}$ in 4.2 % salinity and 17.95 $g \cdot L^{-1}$ when salinity was increased to 7 %. At the highest salinity, the percent ethanol yield was 19 % lower than in the absence of salt, although the replicate fermentations did not run to completion. However, ethanol production from NRRL 1526 in MUR-233 fermentation broth was very different to observations in the controlled YEPS groups. The highest ethanol production from MUR-233 biomass was observed at 4.2 % salinity with a maximum ethanol yield of 11.24 $g \cdot L^{-1}$ and percent yield of 52.2 %. The maximum ethanol yields from MUR-233 biomass with salt removed and at 7 % salinity were only 10.02 $g \cdot L^{-1}$ and 9.62 $g \cdot L^{-1}$, respectively. Furthermore, of the hypersaline fermentations assessed in MUR-233 biomass, only one replicate (from the 4.2% salinity group) ran close to completion with 0.74 $g \cdot L^{-1}$ residual glucose measured in the final broth. However, based on mean values across corresponding replicates it was found that fermentation of hypersaline MUR-233 biomass at both 4.2 % and 7 %

salinity did not complete in the provided experimental timeframe. Interestingly, glucose exhaustion occurred at day 7 in the fermentation group containing MUR-233W biomass and in the absence of salt, yet the percent ethanol yield achieved was only 46.5 %.

**Table 30: Yields of other metabolic products**

| | | Potato starch | | | MUR-233 biomass | | |
|---|---|---|---|---|---|---|---|
| | Salinity (% w/v) | 0 | 4.2 | 7 | 0 | 4.2 | 7 |
| Metabolic products ($g \cdot L^{-1}$) | glycerol | 1.03 (± 0.28) | 2.7 (± 0.05) | 3.31 (± 0.21) | 1.43 (± 0.84) | 2.05 (± 0.26) | 2.55 (± 0.2) |
| | citric acid | 0.73 (± 0.07) | 0.68 (± 0.02) | 0.6 (± 0.14) | 0.25 (± 0.15) | 0.22 (± 0.04) | 0.21 (± 0.03) |
| | malic acid | 1.39 (± 0.06) | 0.4 (± 0.03) | 0.3 (± 0.12) | 0.33 (± 0.05) | 0.16 (± 0.01) | 0.15 (± 0.04) |
| | lactic acid | 0.11 (± 0.09) | 0.15 (± 0.01) | 0.15 (± 0.01) | 0 (± 0.0) | 4.41 (± 0.07) | 6.05 (± 0.12) |
| | fumaric acid | 0.41 (± 0.03) | 0.44 (± 0.01) | 0.41 (± 0.05) | 1.75 (± 0.4) | 0.22 (± 0.01) | 0.24 (± 0.08) |

Yields of metabolic products at day 14 presented as means ± SD (n = 3).

The difference in percent ethanol yields from NRRL 1526 between fermentations in controlled nutrient rich YEPS medium and MUR-233 biomass can be explained to some extent through analyses of other metabolic products from NRRL 1526 formed during the fermentations. The measured yields for these other metabolic products are presented in Table 30. As expected, the production of glycerol in the fermentations increased with higher salinity. In nutrient rich YEPS medium across all salinities tested, ethanol was the primary metabolic product from NRRL 1526. Malic acid was also produced at levels 3.5- to 4.6-times higher in salt-free YEPS compared to hypersaline cultures, but the yield was still only 1.39 $g \cdot L^{-1}$. The key difference with MUR-233 biomass fermentations is that under hypersaline conditions the carbon flux for NRRL 1526 shifted

to also produce significant levels of lactic acid. Although ethanol was still the primary product, lactic acid was produced from MUR-233 biomass at 4.41 $g \cdot L^{-1}$ and 6.05 $g \cdot L^{-1}$ in respective 4.2 % and 7 % hypersaline conditions. However, fermentation of MUR-233W biomass did not produce lactic acid. Instead, malic acid was produced at 2.1-times and fumaric acid at 7.3- to 8-times the levels observed in hypersaline conditions. Fumaric acid produced from MUR-233W biomass was 1.75 $g \cdot L^{-1}$. Citric acid was produced as a minor metabolic product in all fermentations. The observed alteration of metabolic flux towards carboxylic acid production could be related to the difference in overall nutrient composition between YEPS and MUR-233 biomass; in particular, a difference in the carbon to nitrogen (C/N) ratio. The control fermentation medium YEPS had a C/N ratio of 3.1. However, the MUR-233 biomass cultivated to stationary phase and nitrogen limitation for starch enrichment had a significantly higher C/N ratio of 24.2 (experimental data not presented). Fermentation broths with excess carbon but limited nitrogen are favourable for production of carboxylic acids by filamentous fungi (Zhang *et al.* 2013). The C/N ratio is a process parameter that should be optimised in future ethanolic fermentation studies with NRRL 1526.

It should be noted that the results from the control set of fermentations in YEPS also indicated that the higher inoculum used, whilst improving saccharification rate, was not as efficient in converting available glucose to ethanol. For instance, ethanologenic fermentations took 2 to 3 days longer to complete in this study than previously observed in comparable conditions (Section 7.2.5). It is possible that the performance difference could be an indicator of reduced cell viability of the inoculum, resulting from the extended inoculum growth period required for generating sufficient fungal material for inoculation at higher mass quantities. The differences were not likely related to a change from NaCl to RSS as the salt-free YEPS group also displayed extended fermentation time. This reduced fermentation efficiency, would have contributed to extended fermentation times with MUR-233 biomass. However, the differences in NRRL 1526 metabolism between YEPS and MUR-233 biomass suggests that the microalgal biomass might present other limitations for the fungus to sufficiently convert available sugars to ethanol. Such limitations could include optimal

nutrient levels accessible to the filamentous fungus from MUR-233 biomass. Differences in nutrient composition and accessibility for the fungus could result in a shift of metabolism to other metabolic products needed as macromolecular building blocks. For instance, the provision of carboxyl groups for formation of peptides that might otherwise be assimilated from a nutrient rich YEPS medium. Further in-depth study on the interaction between this fungus and the algae biomass under these fermentation conditions should explain the observed discrepancy in the theoretical calculation for expected ethanol, particularly that observed with MUR-233W biomass fermentation, and additionally the differences observed the ethanologenic fermentation outcomes relative to the nutrient rich YEPS media.

## 7.4 Concluding remarks

The terrestrial filamentous fungus *Rhizopus oryzae* NRRL 1526 displayed facultative halotolerance and was able to survive, grow and produce ethanol in hypersaline submersed culture at up to 10.5 % salinity in sea salt. However, increasing salt concentrations had a negative impact on fungal growth and ethanol production.

Self-anaerobic fermentation with NRRL 1526 in nutrient rich salt-free medium with glucose had a volumetric ethanol productivity of 3.61 $g \cdot L^{-1} \cdot d^{-1}$ with an observed maximum ethanol yield of 26.1 $g \cdot L^{-1}$ and a percent ethanol yield of approximately 75 %. In such medium, the filamentous fungus could also be used for simultaneous saccharification and fermentation of starch to yield up to 24 $g \cdot L^{-1}$ ethanol with an 84.8 % conversion efficiency (or percent yield). Even when this medium contained sea salt at up 7 % salinity the fungal enzymes were able to hydrolyse starch to access glucose for production of 17.95 $g \cdot L^{-1}$ ethanol with a percent yield of 63.3 %. Experimental results also indicated that the activities of terrestrial enzymes such as α-amylase and amyloglucosidase were halotolerant and not inhibited when exposed to hypersaline conditions of up to 7 %.

NRRL 1526 was able to grow and utilise hypersaline MUR-233 biomass without supplementation. Ethanol was the dominant metabolic product for this fungus from assimilated MUR-233 biomass

during self-anaerobic fermentation. The highest percent ethanol yields was 52.2 % observed with a 4.2 % hypersaline MUR-233 feedstock, but at 7 % salinity the percent ethanol yield from biomass starch was reduced to 44.8 %. However, it was found that NRRL 1526 carbon flux shifted to producing more organic acids alongside ethanol when the fungus was fed with MUR-233 biomass. Fungal cultures utilising hypersaline MUR-233 biomass produced lactic acid as a key secondary metabolic product. Lastly, the ability of this *R. oryzae* strain to sufficiently convert available starch in hypersaline MUR-233 biomass to ethanol might be limited by other unknown factors such as accessibility to optimal nutrient requirements.

# Chapter 8
# Conclusions, discussion and future directions

## 8.1 Conclusions

The Project aimed to determine how biomass from *Tetraselmis* sp. strain MUR-233 harvested from hypersaline production cultures could be converted to produce ethanol under hypersaline conditions to minimise fresh water usage that should be directed towards municipal or food-growing agricultural needs. With this in mind, the following two key objectives were targeted and achieved:

1. to analyse MUR-233 biomass produced in seawater for suitable carbohydrate substrates and identify how these could be made available for microbial conversion to ethanol; and
2. to ascertain and select a halotolerant microorganism with the ability to assimilate and produce ethanol from minimally pretreated hypersaline MUR-233 biomass.

The primary and most abundant fermentable substrate in MUR-233 was verified to be intracellular starch that could be enriched to an average 47 % of the biomass ash free dry weight when cultivated in hypersaline seawater beyond nutrient limitation under continuous light. Furthermore, the filamentous fungus *Rhizopus oryzae* NRRL 1526 was found to possess facultative halotolerance with the ability to produce halotolerant enzymes that could digest starch from hypersaline MUR-233 biomass for assimilation and conversion to ethanol. However, optimal ethanol conversion efficiency for NRRL 1526 could not be achieved with the hypersaline MUR-233 biomass feedstock because assimilated glucose was also directed towards producing other metabolic products.

During the undertaking of this Project, other new knowledge and insights were also gained. Firstly, a new method was developed for detection of surface bacteria on microalgal cell walls, using fluorescence microscopy at 420 nm wavelength. Secondly, the handling and assessment of biomass slurries during this Project highlighted a critical consideration about the physical nature of

microalgal biomass that is poorly emphasised in the literature, yet imposes severe limitations on process feedstock concentration and production yields. Pointedly, regardless of the biomass carbohydrate or lipid enrichment or annual productivities that can be achieved from microalgae, the dominant component that constitutes 80 % to 90 % of any workable microalgal slurry that can be easily pumped or mixed will be water. Furthermore as indicated in Section 7.1.2, depending on dewatering methods utilised, in hypersaline systems the feedstock ash content could be as much as the process substrate concentration.

## 8.2 Discussion and future directions

This Project was established at the height of academic research and industry interest and optimism in microalgae biofuels to explore opportunities for diversifying energy streams from microalgal biomass. This thesis answers the knowledge gap about whether hypersaline *Tetraselmis* biomass produced in seawater could be fermented to ethanol through selective use of a halotolerant microorganism, confirming that such an approach was possible. Yet, despite changes to improve carbohydrate availability, the slow ethanol productivities and low yields achieved suggests this current process requires more development before its commercial feasibility can be assessed. Based on experimental results with the *Tetraselmis* biomass, further optimisation of the fermentation nutrient balance, particularly the C/N ratio, should improve process control over *R. oryzae* metabolic flux to enhance ethanol yield from biomass. It may be possible to improve microalgal starch production by the modifying open pond cultivation conditions used in Karratha. Perhaps changes to previous $C0_2$ supplementation profiles and microalgal growth times could provide a suitable C/N ratio for improved starch enrichment. However, it could also be argued that future direction of this work should assess the application *R. oryzae* and other filamentous fungi to different marine microalgae species that have more glucose-rich fermentable cell wall polysaccharides such as cellulose to reduce reliance on starch enrichment or to enhance overall usable carbohydrate yields. Ethanol production rates from glucose released by *R. oryzae* could also

be improved through investigations involving co-fermentation with robust ethanol producing yeast such as *Saccharomyces cerevisiae*. The filamentous morphology of *R. oryzae* also provides opportunities to use a more concentrated microalgal biomass for increased feedstock loading in solid-state fermentation systems, provided economically feasible processes for microalgae dewatering and harvest can be identified. The advantages relating to use of a facultative halotolerant microorganism such as *R. orzyae* with more concentrated biomass from seawater systems has yet to be thoroughly explored. However, current technical and economic challenges in critical areas such as industrial scale agricultural farming and harvesting of microalgae restricts serious progress in the microalgae biofuel space. This is evident in the evolution of the microalgae industry in recent years, and the new directions toward more high-value products taken by many original microalgae biofuel start-ups, confirming that it is not yet economically feasible to produce microalgae at the type of scale required for global biofuel demand (Wesoff 2017).

Nevertheless, there is an ongoing challenge to develop viable biofuel processes. As discussed in Chapter 2, biofuels are an essential component of the IEA's forward looking 2DS. The new knowledge generated from this thesis opens new opportunities in current developments on multiproduct distilleries or biorefineries (Section 7.1.4), where filamentous fungi are either integrated into first-generation ethanol plants or new second-generation ethanol plant designs to diversify value streams through generation of both ethanol and higher value-added protein-rich biomass for animal feed. *Rhizopus* and *Neurospora* are two such filamentous fungi already under consideration in such biorefineries (FazeliNejad *et al.* 2016; Nair *et al.* 2017b). The facultative halotolerance of *R. oryzae* and the halophilic activity of its enzymes observed in this Project could be exploited to introduce marine biomass such as macroalgae as additional feedstocks to biorefineries for ethanol and protein-rich biomass production, whilst also eliminating requirements for biomass pre-washing. There is an abundance of waste macroalgae biomass from both industry and naturally occurring tide phenomenon (Han *et al.* 2014) that could be diverted to biorefineries. For example, there is existing research to assess cellulose-rich seaweed waste

biomass from the carrageenan industry for use as a biofuels or biochemical feedstock (Uju *et al.* 2015). For biorefineries, future direction for investigations on *R. oryzae* NRRL 1526 or similar filamentous fungi could include the characterisation of halophilic enzymes produced by the fungi to enable more targeted application to marine biomass. Studies on fungi nutrient requirements for optimum ethanologenic production, in comparison to the nutritional value from different marine biomass, could also provide yield benefits in biorefinery applications. The halophilic enzymatic activity observed in the terrestrial NRRL 1526 strain indicates many industrial enzymes currently produced using filamentous fungi could be applicable in future investigations that involve enzymatic extraction of polymers from marine macroalgae biomass.

# Appendix A
# Supplementary material to methodology

## A.1 ASTM International specification for Substitute Ocean Water

The following table details the composition of substitute ocean water prepared in accordance with Section 6 of the ASTM International (previously American Society for Testing and Materials) standard issued under the fixed designation D1141 adopted in 1998 and reapproved 2008 (American Society for Testing and Materials International 2013). The chlorinity of this substitute ocean water is 19.38, and the pH after adjustment with0.1 *N* NaOH solution is 8.2.

**Table 31: Chemical composition of substitute ocean water**

| COMPOUND | SYMBOL | CONCENTRATION ($g \cdot L^{-1}$) |
|---|---|---|
| Sodium chloride | $NaCl$ | 24.53 |
| Magnesium chloride | $MgCl_2$ | 5.20 |
| Sodium sulphate | $Na_2SO_4$ | 4.09 |
| Calcium chloride | $CaCl_2$ | 1.16 |
| Potassium chloride | $KCl$ | 0.695 |
| Sodium bicarbonate | $NaHCO_3$ | 0.201 |
| Potassium bromide | $KBr$ | 0.101 |
| Boric acid | $H_3BO_3$ | 0.027 |
| Barium nitrate | $Ba(NO_3)_2$ | 0.0000994 |
| Manganese nitrate | $Mn(NO_3)_2$ | 0.0000340 |
| Copper(II) nitrate | $Cu(NO_3)_2$ | 0.0000308 |
| Zinc nitrate | $Zn(NO_3)_2$ | 0.0000096 |
| Lead nitrate | $Pb(NO_3)_2$ | 0.0000066 |
| Silver nitrate | $AgNO_3$ | 0.00000049 |

## A.2 Composition of Red Sea Salt

The following tables detail the elemental analysis of artificial seawater with a specific gravity of 1.025 (25 °C) produced with Red Sea Salt (RSS) compared with natural seawater (NSW) and the ASTM international standard composition of substitute ocean water. Specifically, nitrogen and phosphorus quantities are shown in Table 32, the quantities of major elements in Table 33, and the quantities of minor elements in Table 34. Elemental quantities for RSS were obtained from the manufacturer's product analysis sheet, which includes quantities for NSW derived from Spotte (1979), Bidwell and Spotte (1985), and Lide (2010). The ASTM quantities for supplemented ocean water were calculated based on ASTM standard D1141-98(2008) (American Society for Testing and Materials International 2013).

**Table 32: Nitrogen and phosphorus quantities**

| NUTRIENTS | ASTM ($mg \cdot L^{-1}$ or ppm) | NSW ($mg \cdot L^{-1}$ or ppm) | RSS ($mg \cdot L^{-1}$ or ppm) |
|---|---|---|---|
| N, as TAN | - | 0.005 - 0.05 | <0.03 |
| N, as Nitrate | 0.023 | 0.001 - 0.7 | <0.20 |
| P, as Phosphate | - | 0.001 – 0.42 | <0.05 |

**Table 33: Quantities of major elements**

| MAJOR ELEMENTS | SYMBOL | ASTM ($mg \cdot L^{-1}$ or ppm) | NSW ($mg \cdot L^{-1}$ or ppm) | RSS ($mg \cdot L^{-1}$ or ppm) |
|---|---|---|---|---|
| Chlorine | Cl | 19,902 | 19,400 | 18,772 |
| Sodium | Na | 11,031 | 10,800 | 10,692 |
| Magnesium | Mg | 1,351 | 1,280 | 1,180 |
| Calcium | Ca | 419 | 418 | 410 |
| Potassium | K | 398 | 380 | 360 |
| Sulphur | S | 923 | 884 | 820 |

**Table 34: Quantities of minor elements**

| MINOR ELEMENTS | SYMBOL | ASTM (mg·L$^{-1}$ or ppm) | NSW (mg·L$^{-1}$ or ppm) | RSS (mg·L$^{-1}$ or ppm) |
|---|---|---|---|---|
| Bromine | Br | 67.8 | 65 | 15 |
| Carbon | C (inorg.) | 28.7 | 28 | 30 |
| Strontium | Sr | 13.8 | 7.7 | 8 |
| Boron | B | 0.9 | 4.4 | 4.21 |
| Fluorine | F | 1.6 | 1.4 | 1.29 |
| Silicone | Si | - | 2.8 | >0.5 |
| Aluminium | Al | - | 0.001 | 0.0005 |
| Antimony | Sb | - | 0.0002 | 0.0002 |
| Arsenic | As | - | 0.002 | 0.002 |
| Barium | Ba | 0.05 | 0.05 | trace |
| Beryllium | Be | - | 0.000001 | trace |
| Bismuth | Bi | - | 0.0000001 | trace |
| Cadmium | Cd | - | 0.0001 | trace |
| Caesium | Cs | - | 0.002 | trace |
| Cerium | Ce | - | 0.0004 | trace |
| Chromium | Cr | - | 0.0004 | 0.00025 |
| Cobalt | Co | - | 0.00007 | 0.0001 |
| Copper | Cu | 0.0104 | 0.0002 | trace |
| Dysprosium | Dy | - | 0.0000009 | trace |
| Erbium | Er | - | 0.0000008 | trace |
| Europium | Eu | - | 0.00000002 | trace |
| Gadolinium | Gd | - | 0.0000007 | trace |
| Gallium | Ga | - | 0.0003 | trace |
| Germanium | Ge | - | 0.00005 | 0.00005 |
| Gold | Au | - | 0.00003 | 0.000009 |
| Hafnium | Hf | - | 0.000007 | trace |
| Holmium | Ho | - | 0.000008 | trace |
| Indium | In | - | 0.00003 | 0.00006 |
| Iodine | I | - | 0.06 | 0.055 |
| Iron | Fe | - | 0.0005 | 0.002 |
| Lanthanum | La | - | 0.0003 | trace |
| Lead | Pb | 0.0041 | 0.0004 | Trace |
| Lithium | Li | - | 0.178 | 0.163 |
| Manganese | Mn | 0.0104 | 0.0003 | 0.0005 |
| Mercury | Hg | - | 0.000005 | trace |

| MINOR ELEMENTS | SYMBOL | ASTM (mg·L$^{-1}$ or ppm) | NSW (mg·L$^{-1}$ or ppm) | RSS (mg·L$^{-1}$ or ppm) |
|---|---|---|---|---|
| Molybdenum | Mo | - | 0.001 | 0.0116 |
| Nickel | Ni | - | 0.0007 | 0.0003 |
| Niobium | Nb | - | 0.00001 | 0.00001 |
| Platinum | Pt | - | 0.0000006 | trace |
| Praesidium | Pr | - | 0.0000006 | trace |
| Radium | Ra | - | 0.0000000001 | trace |
| Rhenium | Re | - | 0.000004 | trace |
| Rubidium | Rb | - | 0.12 | 0.11 |
| Ruthenium | Ru | - | 0.0000007 | trace |
| Samarium | Sm | - | 0.00000005 | trace |
| Scandium | Sc | - | 0.00004 | trace |
| Selenium | Se | - | 0.004 | 0.004 |
| Silver | Ag | 0.00031 | 0.00002 | trace |
| Tantalum | Ta | - | 0.000007 | trace |
| Terbium | Tb | - | 0.0000001 | trace |
| Thallium | Th | - | 0.000002 | trace |
| Thulium | Tm | - | 0.0000002 | trace |
| Tin | Sn | - | 0.00003 | 0.000025 |
| Titanium | Ti | - | 0.0000001 | trace |
| Tungsten | W | - | 0.0001 | trace |
| Uranium | U | - | 0.00015 | trace |
| Vanadium | V | - | 0.0012 | 0.0018 |
| Ytterbium | Yb | - | 0.0000008 | trace |
| Yttrium | Y | - | 0.000013 | 0.00003 |
| Zinc | Zn | 0.0033 | 0.0005 | 0.009 |
| Zirconium | Zr | - | 1.4 | trace |

## A.3 Hypersaline modified f medium

A hypersaline f medium based on the Guillard and Ryther (1962) method and without vitamin supplementation was prepared by modifying the standard method provided in Andersen (2005). Details for stock solutions and media preparation are presented below.

### A.3.1 Preparation of chelated trace metals stock solution

Concentrated stock solutions (500 ml) of each trace metal were prepared in ultrapure water to the concentrations shown in Table 35. A chelating ferric-EDTA solution (1 L) was prepared to the concentrations shown in Table 36, by first dissolving EDTA in ultrapure water followed by the required amount of ferric chloride hexahydrate. Each concentrated trace metal solution was added to the 1 L ferric-EDTA solution in the quantities shown in Table 37.

**Table 35: Concentrated trace metals stocks**

| COMPOUND | SYMBOL | CONCENTRATION ($g \cdot L^{-1}$) | MOLARITY (M) |
|---|---|---|---|
| Manganese(II) chloride tetrahydrate | $MnCl_2.4H_2O$ | 360 | 1.82 |
| Zinc sulphate heptahydrate | $ZnSO_4.7H_2O$ | 44 | 0.15 |
| Cobalt(II) chloride hexahydrate | $CoCl_2.6H_2O$ | 20 | 0.08 |
| Copper(II) sulphate pentahydrate | $CuSO_4.5H_2O$ | 19.6 | 0.08 |
| Sodium molybdate dihydrate | $Na_2MoO_4.2H_2O$ | 12.6 | 0.05 |

**Table 36: Ferric-EDTA solution**

| COMPOUND | SYMBOL | CONCENTRATION ($g \cdot L^{-1}$) | MOLARITY (mM) |
|---|---|---|---|
| Disodium ethylenediaminetetraacetic acid | $Na_2EDTA$ | 8.72 | 23.4 |
| Ferric chloride hexahydrate | $FeCl_3.6H_2O$ | 6.30 | 23.4 |

**Table 37: Chelated trace metals stock solution**

| SOLUTION | QUANTITY ($ml \cdot L^{-1}$) | MOLARITY (mM) |
|---|---|---|
| Manganese(II) chloride stock | 1 | 1.82 |
| Zinc sulphate stock | 1 | 0.153 |
| Cobalt(II) chloride stock | 1 | 0.084 |
| Copper(II) sulphate stock | 1 | 0.0786 |
| Sodium molybdate stock | 1 | 0.052 |

### A.3.2 Preparation of macronutrient stock solutions

Macronutrient stock solutions (500 ml) were prepared in ultrapure water to the concentrations shown in Table 38.

**Table 38: Macronutrient stocks**

| COMPOUND | SYMBOL | CONCENTRATION ($g \cdot L^{-1}$) | MOLARITY (M) |
|---|---|---|---|
| Sodium nitrate | $NaNO_3$ | 150 | 1.76 |
| Sodium dihydrogen orthophosphate | $NaH_2PO_4.2H_2O$ | 10 | 0.0724 |

### A.3.3 Preparation of hypersaline modified f medium

Artificial 7 % w/v hypersaline seawater was prepared by dissolving 70 g $L^{-1}$ of RSS in RO water. The pH of this solution was 8.43 which was close to the buffering range of 8.2-8.4 at salinity 3.55 % w/v (3.55 ppt) specified by manufacturer. Modified f medium was prepared by addition of trace metals and macronutrients to the hypersaline seawater in the quantities shown in Table 39. The final N:P ratio of this modified f medium was 12.45, with a nitrogen content of 24.72 mg $L^{-1}$ and phosphorous content of 1.99 mg $L^{-1}$.

**Table 39: Modified f medium**

| SOLUTION | QUANTITY ($ml \cdot L^{-1}$) | MOLARITY (mM) |
|---|---|---|
| Chelated trace metals stock | 1 | n.d. |
| 150 g/L sodium nitrate stock | 1 | 1.76 |
| 10 g/L sodium dihydrogen orthophosphate stock | 1 | 0.0724 |

n.d. = not determined

## A.4 Lugol's and iodine solutions

The following solutions were used for staining of microalgae cells (Lugol's solution) and microalgae starch (iodine solution). For Lugol's solution, acetic acid was added to immobilise cells.

**Table 40: Lugol's solution**

| COMPONENT | Proportion of total volume | Amount in total volume |
|---|---|---|
| Iodine | 5 % w/v | 10 g |
| Potassium iodide | 10 % w/v | 20 g |
| Glacial acetic acid | 10 % v/v | 20 ml |
| Water | - | up to 200 ml |

**Table 41: Iodine solution**

| COMPONENT | Proportion of total volume | Amount in total volume |
|---|---|---|
| Iodine | 0.2 % w/v | 0.2 g |
| Potassium iodide | 2 % w/v | 2 g |
| Water | - | up to 100 ml |

## A.5 Bacterial, yeast and fungal growth media

The following media were used for growth of bacterial, yeast and fungus for experimental studies. Applications included tests for background bacterial and fungal/yeast in the isolated *Tetraselmis* cultures, growth of *R. oryzae* cultures, fermentation studies. Standard liquid media were sterilised by autoclave at 121 °C for 20 minutes. Hypersaline liquid media were filter sterilised using 0.22 µm syringe top units. Typically, a 20 ml to 30 ml medium volume was used per 50 ml cone-bottomed culture tube.

**Table 42: Lysogeny broth (Lennox)**

| COMPONENT | STANDARD ($g \cdot L^{-1}$) | HYPERSALINE ($g \cdot L^{-1}$) |
|---|---|---|
| Tryptone | 10 | 10 |
| Yeast extract | 5 | 5 |
| Sodium chloride | 5 | - |
| Red Sea Salt | - | 70 |

Reference: Lennox (1955).

**Table 43: Yeast rich medium (YEPD)**

| COMPONENT | STANDARD ($g \cdot L^{-1}$) | HYPERSALINE ($g \cdot L^{-1}$) |
|---|---|---|
| Yeast extract | 10 | 10 |
| Peptone | 20 | 20 |
| Glucose | 20 | 20 |
| Red Sea Salt | - | 35, 70 or 105 |

Reference: Treco and Lundblad (2001)

*R. oryzae* NRRL 1526 stock cultures were maintained on Sabouraud agar slants. To prepare these slants, the medium ingredient components shown in Table 44 at relative quantities for a 500 ml

final volume were combined in 450 ml of RO water, mixed until the peptone and glucose had dissolved, then adjusted to pH 5.6 with hydrochloric acid followed by a final volume adjustment to 500 ml with RO water. The prepared volume was autoclaved at 121 °C for 20 minutes, and 5 ml aliquots were poured into sterile 15 ml screw-capped tubes. The loosely capped tubes containing hot agar were tilted and cooled to solidify at a slanted position then sealed and stored at 2-8 °C ready for use.

**Table 44: Sabouraud agar**

| COMPONENT | AMOUNT ($g \cdot L^{-1}$) |
|---|---|
| Peptone | 10 |
| Glucose | 40 |
| Agar | 15 |

Reference: Hare (2008)

# A.6 Calibration curves for PMP-monosaccharide RP-HPLC analysis

**Figure 47: Typical 10MS-VG standard calibration curves**

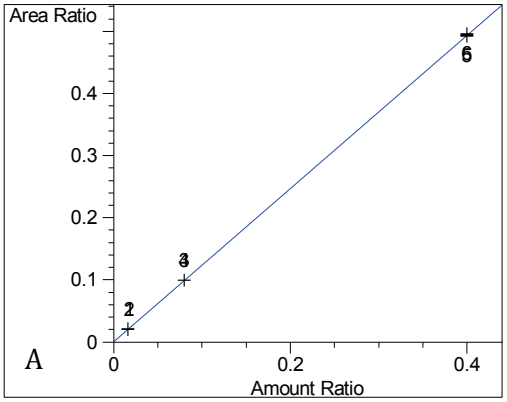


PMP-D-mannose at exp. RT: 4.177
DAD1 A, Sig=250,4 Ref=off
Correlation: 0.99999
Residual Std. Dev.: 0.00128
Formula: y = mx + b
m: 1.23380
b: 8.89973e-4
x: Amount
y: Area

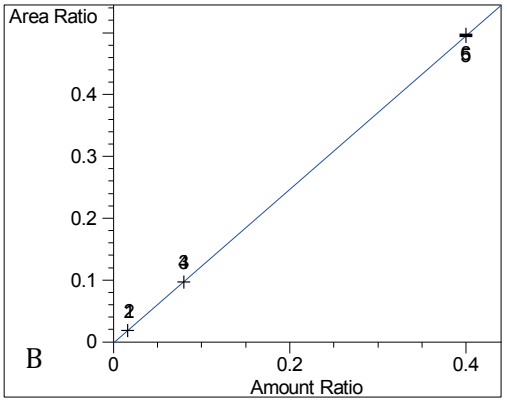


PMP-D-ribose at exp. RT: 5.115
DAD1 A, Sig=250,4 Ref=off
Correlation: 0.99998
Residual Std. Dev.: 0.00152
Formula: y = mx + b
m: 1.24281
b: -1.40312e-3
x: Amount
y: Area

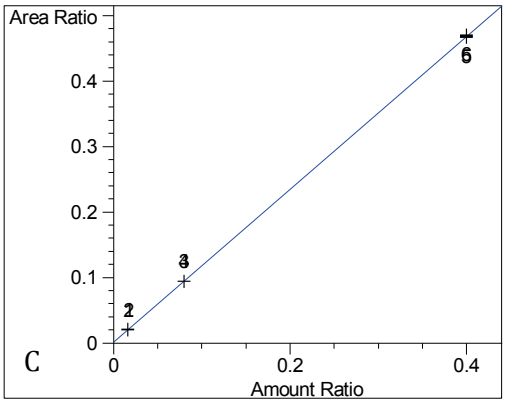


PMP-L-rhamnose at exp. RT: 5.380
DAD1 A, Sig=250,4 Ref=off
Correlation: 0.99999
Residual Std. Dev.: 0.00123
Formula: y = mx + b
m: 1.16872
b: 1.18102e-3
x: Amount
y: Area

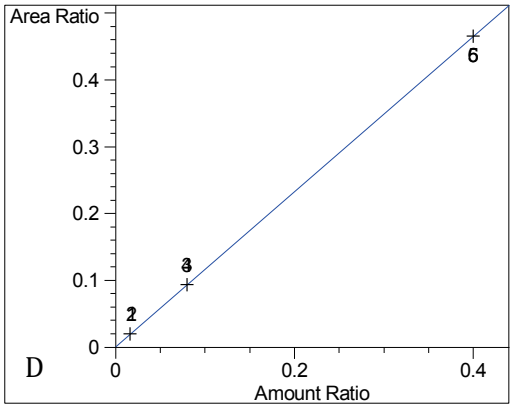


PMP-D-glucuronic acid at exp. RT: 6.062
DAD1 A, Sig=250,4 Ref=off
Correlation: 1.00000
Residual Std. Dev.: 0.00053
Formula: y = mx + b
m: 1.16294
b: 6.56756e-4
x: Amount
y: Area

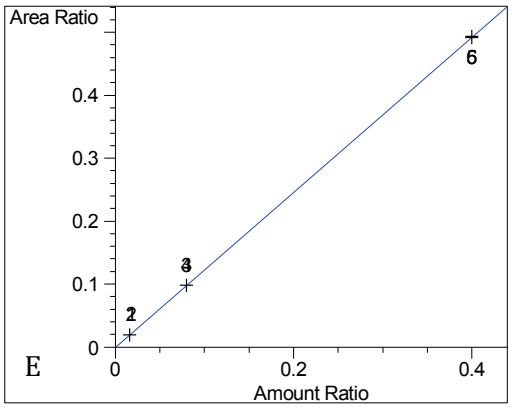


PMP-D-galacturonic acid at exp. RT: 6.689
DAD1 A, Sig=250,4 Ref=off
Correlation: 1.00000
Residual Std. Dev.: 0.00043
Formula: y = mx + b
m: 1.23200
b: -9.96307e-5
x: Amount
y: Area

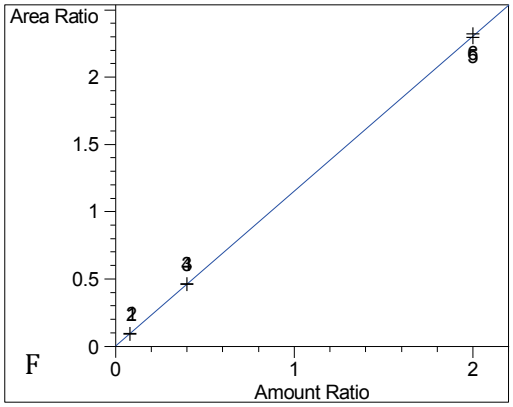


PMP-D-glucose at exp. RT: 7.577
DAD1 A, Sig=250,4 Ref=off
Correlation: 0.99997
Residual Std. Dev.: 0.00807
Formula: y = mx + b
m: 1.15449
b: 3.50149e-6
x: Amount
y: Area

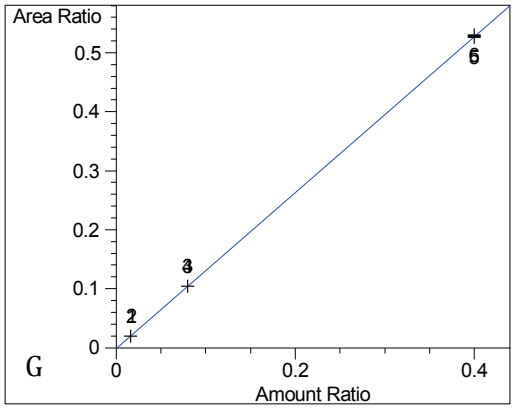


PMP-D-galactose at exp. RT: 8.264
DAD1 A, Sig=250,4 Ref=off
Correlation: 0.99998
Residual Std. Dev.: 0.00152
Formula: y = mx + b
m: 1.32347
b: -1.17544e-3
x: Amount
y: Area

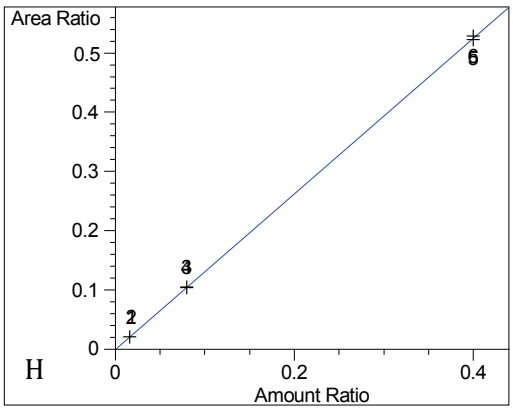


PMP-D-xylose at exp. RT: 8.485
DAD1 A, Sig=250,4 Ref=off
Correlation: 0.99998
Residual Std. Dev.: 0.00168
Formula: y = mx + b
m: 1.31557
b: -5.59686e-4
x: Amount
y: Area

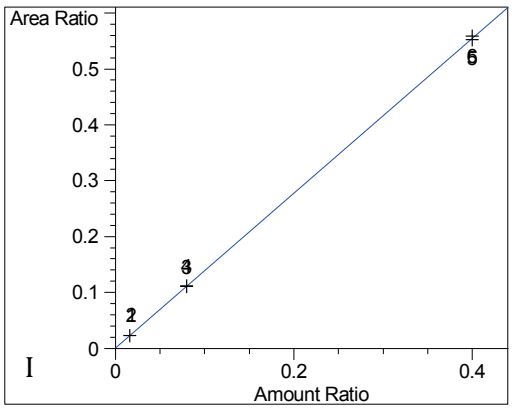


PMP-L-arabinose at exp. RT: 8.688
DAD1 A, Sig=250,4 Ref=off
Correlation: 0.99998
Residual Std. Dev.: 0.00191
Formula: y = mx + b
m: 1.38837
b: 4.80042e-4
x: Amount
y: Area

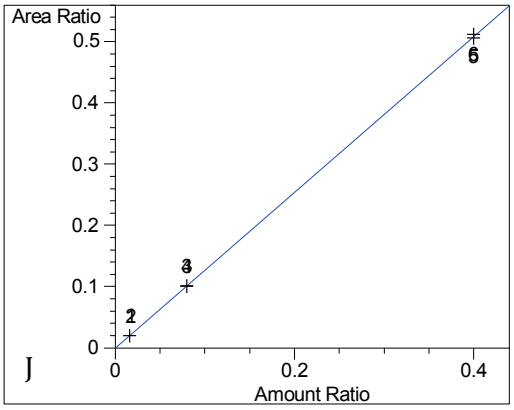


PMP-L-fucose at exp. RT: 9.467
DAD1 A, Sig=250,4 Ref=off
Correlation: 0.99997
Residual Std. Dev.: 0.00186
Formula: y = mx + b
m: 1.27438
b: -6.20938e-4
x: Amount
y: Area

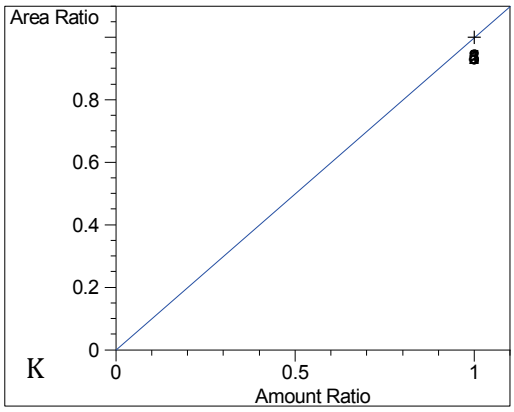


PMP-2-DOG at exp. RT: 10.180
DAD1 A, Sig=250,4 Ref=off
Correlation: 1.00000
Residual Std. Dev.: 0.00000
Formula: y = mx + b
m: 1.00000
b: 0.00000
x: Amount
y: Area

**Figure 48: Typical 10MS-GR standard calibration curves**

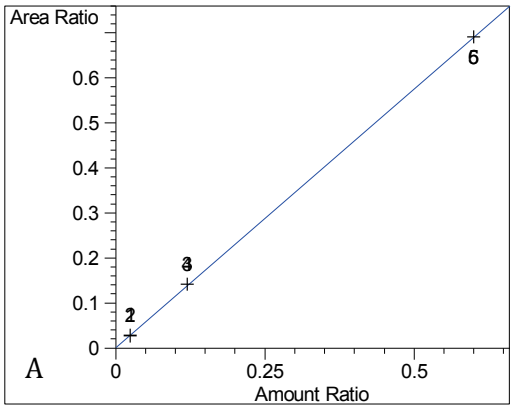


PMP-D-mannose at exp. RT: 3.766
DAD1 A, Sig=250,4 Ref=off
Correlation: 0.99998
Residual Std. Dev.: 0.00193
Formula: y = mx + b
m: 1.15004
b: 1.28931e-3
x: Amount
y: Area

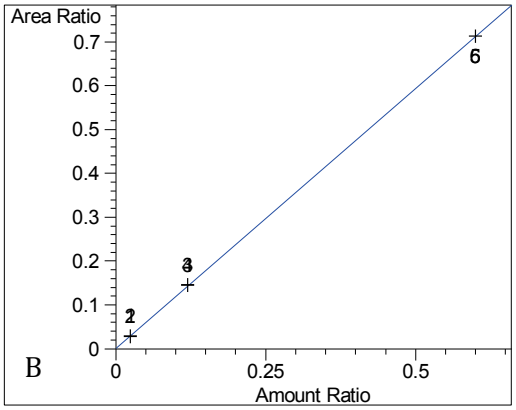


PMP-D-ribose at exp. RT: 4.628
DAD1 A, Sig=250,4 Ref=off
Correlation: 0.99999
Residual Std. Dev.: 0.00176
Formula: y = mx + b
m: 1.18721
b: 1.33902e-3
x: Amount
y: Area

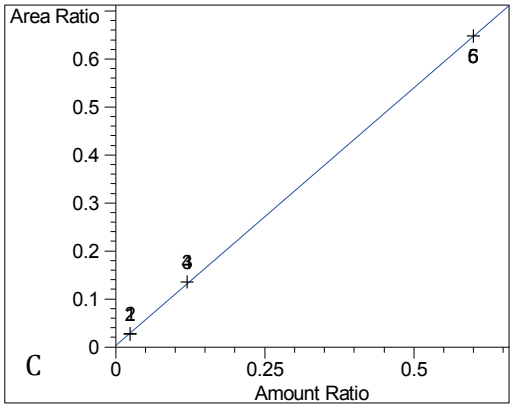


PMP-L-rhamnose at exp. RT: 4.877
DAD1 A, Sig=250,4 Ref=off
Correlation: 0.99996
Residual Std. Dev.: 0.00278
Formula: y = mx + b
m: 1.07582
b: 2.86219e-3
x: Amount
y: Area

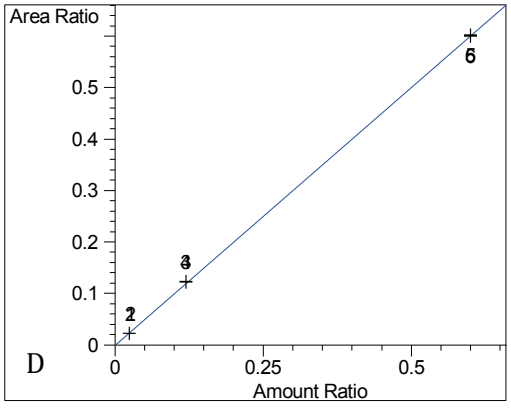


PMP-D-glucuronic acid at exp. RT: 5.376
DAD1 A, Sig=250,4 Ref=off
Correlation: 0.99998
Residual Std. Dev.: 0.00206
Formula: y = mx + b
m: 1.00224
b: -1.59954e-4
x: Amount
y: Area

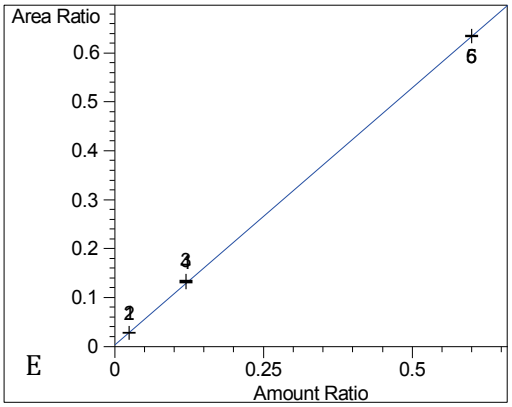


PMP-D-galacturonic acid at exp. RT: 5.954
DAD1 A, Sig=250,4 Ref=off
Correlation: 0.99995
Residual Std. Dev.: 0.00307
Formula: y = mx + b
m: 1.05281
b: 3.41680e-3
x: Amount
y: Area

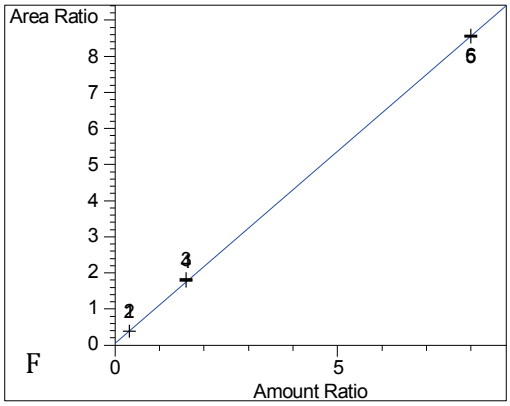


PMP-D-glucose at exp. RT: 6.772
DAD1 A, Sig=250,4 Ref=off
Correlation: 0.99994
Residual Std. Dev.: 0.04593
Formula: y = mx + b
m: 1.06473
b: 5.15696e-2
x: Amount
y: Area

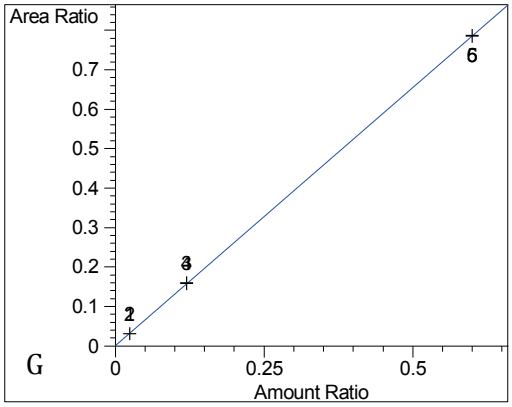


PMP-D-galactose at exp. RT: 7.575
DAD1 A, Sig=250,4 Ref=off
Correlation: 0.99999
Residual Std. Dev.: 0.00155
Formula: y = mx + b
m: 1.31143
b: 4.88211e-4
x: Amount
y: Area

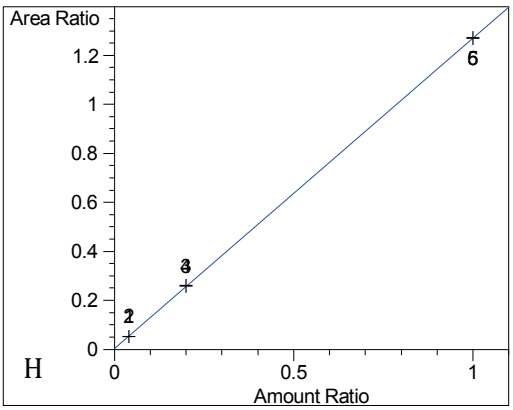


PMP-D-xylose at exp. RT: 7.794
DAD1 A, Sig=250,4 Ref=off
Correlation: 0.99999
Residual Std. Dev.: 0.00300
Formula: y = mx + b
m: 1.26932
b: 3.23169e-3
x: Amount
y: Area

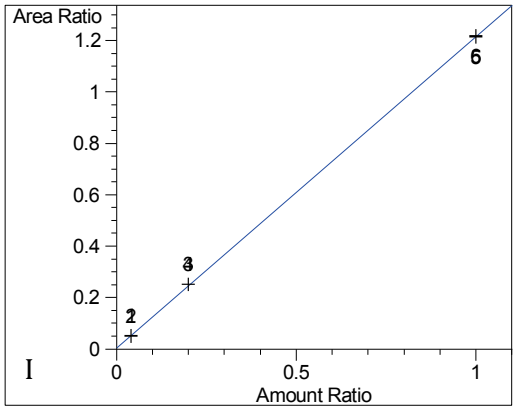


PMP-L-arabinose at exp. RT: 7.981
DAD1 A, Sig=250,4 Ref=off
Correlation: 0.99997
Residual Std. Dev.: 0.00428
Formula: y = mx + b
m: 1.21267
b: 4.29371e-3
x: Amount
y: Area

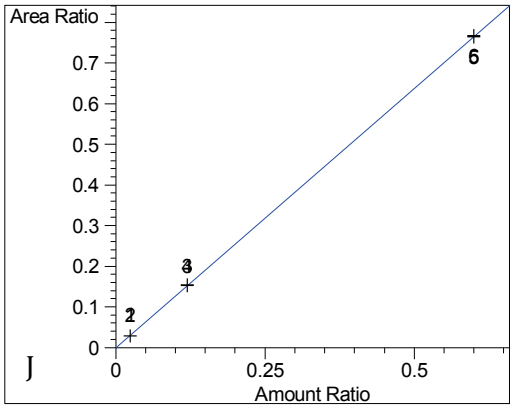


PMP-L-fucose at exp. RT: 8.739
DAD1 A, Sig=250,4 Ref=off
Correlation: 0.99999
Residual Std. Dev.: 0.00142
Formula: y = mx + b
m: 1.27813
b: -8.43649e-4
x: Amount
y: Area

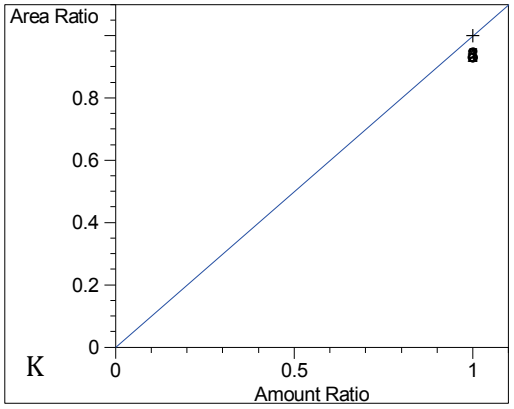


PMP-2-DOG at exp. RT: 9.454
DAD1 A, Sig=250,4 Ref=off
Correlation: 1.00000
Residual Std. Dev.: 0.00000
Formula: y = mx + b
m: 1.00000
b: 0.00000
x: Amount
y: Area

## A.7 Elution profiles for PMP-monosaccharide standards

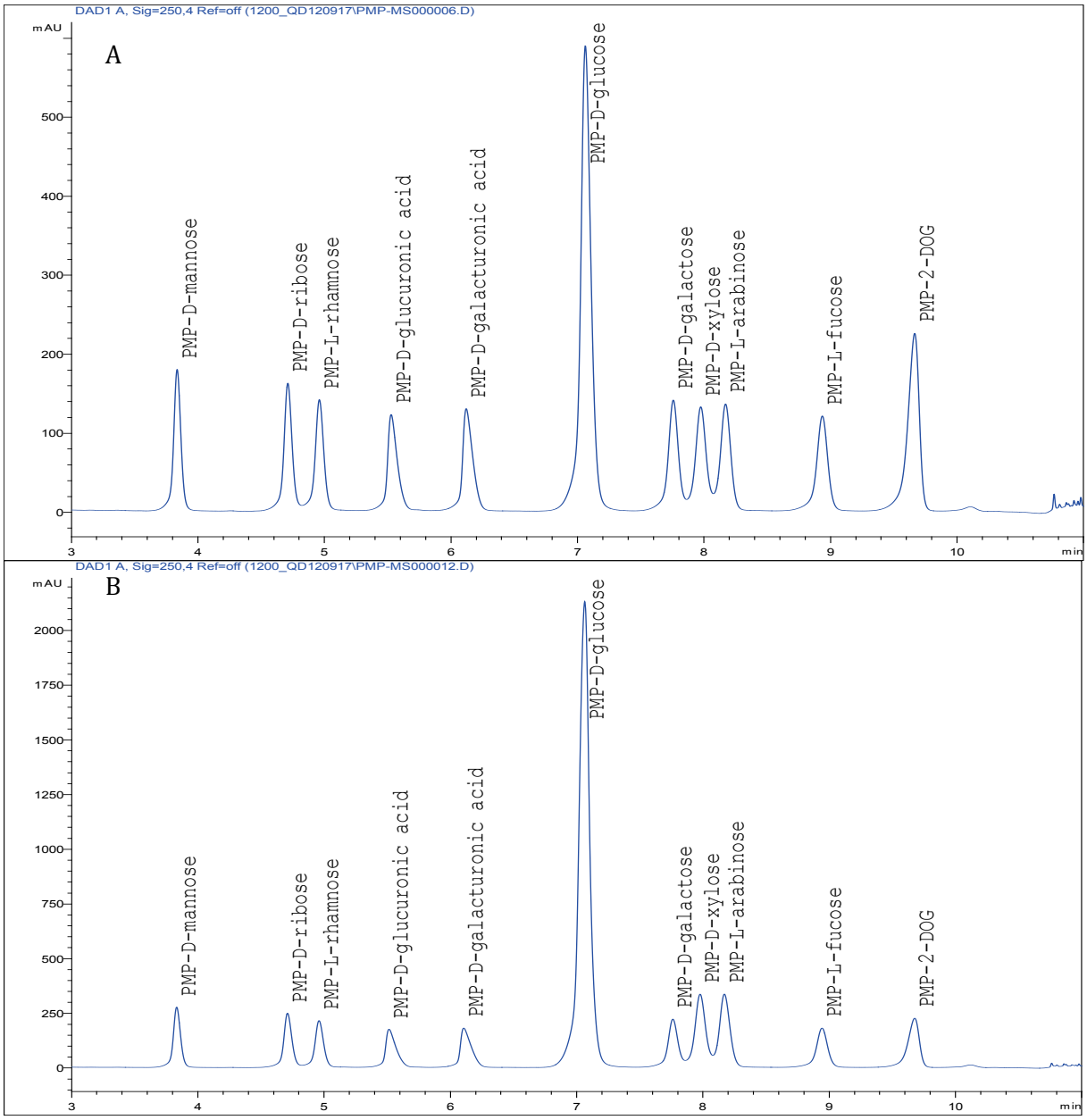


**Figure 49: Example elution profiles of RP-HPLC standards**
PMP-monosaccharide external standards under diode array detection (DAD): (A) 10MS-VG high standard and (B) 10MS-GR high standard.

## A.8 Elution profile for HPAEC standards

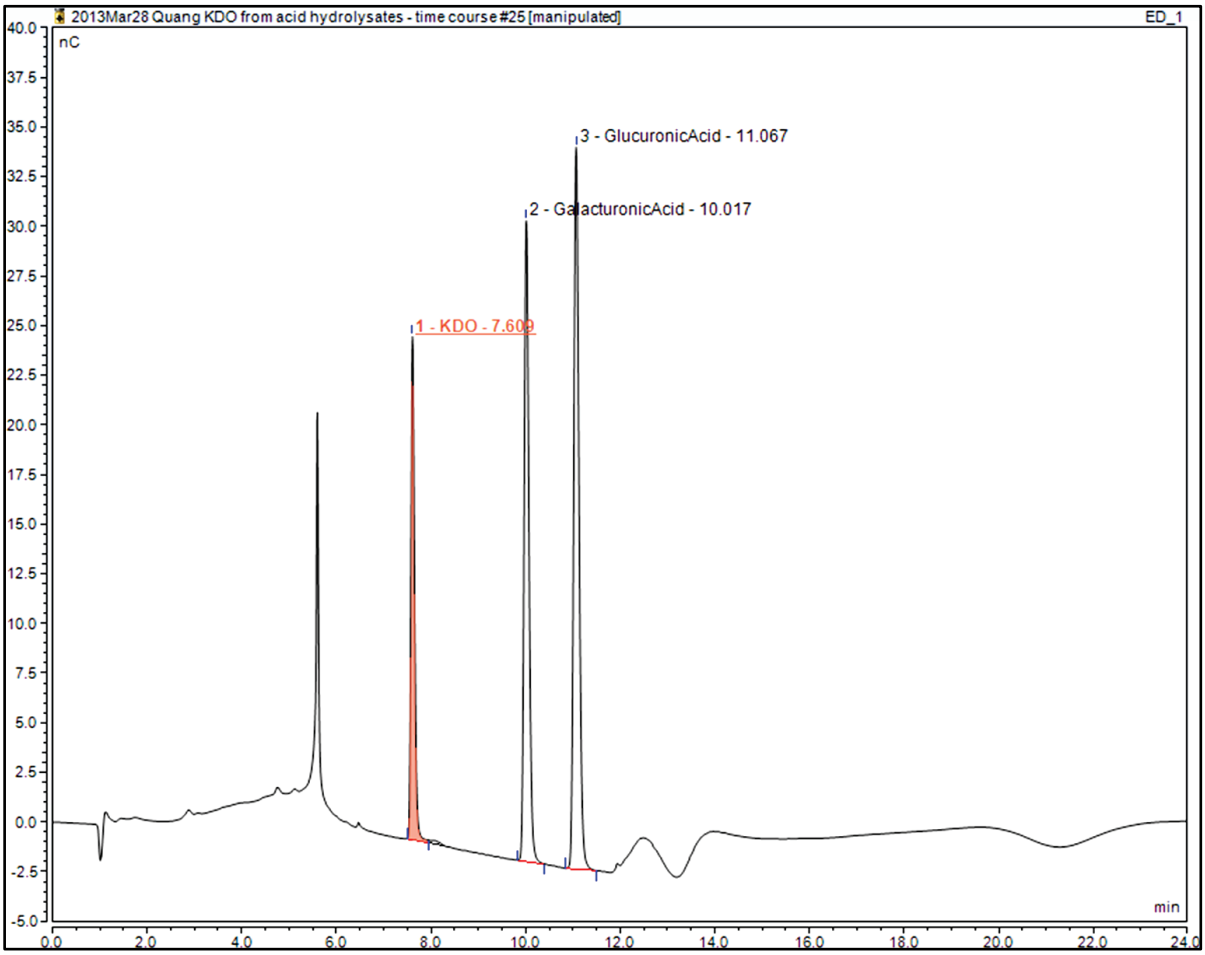


**Figure 50: Example elution profile of HPAEC standards**
Kdo external standard mixture under pulsed amperometric detection (PAD), included galacturonic acid and glucuronic acid.

## A.9 Calibration curves for fermentation IEC analysis

**Figure 51: Typical fermentation calibration curves on Rezex RFQ Fast Acid H+ (8%)**

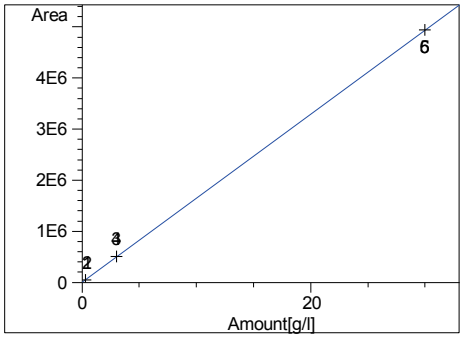


glucose at exp. RT: 2.125
RID1 A, Refractive Index Signal
Correlation: 1.00000
Residual Std. Dev.: 4783.48876
Formula: y = mx + b
m: 164676.38272
b: 3641.84661
x: Amount
y: Height

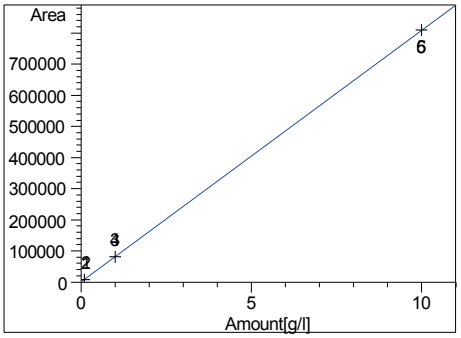


lactic acid at exp. RT: 2.838
RID1 A, Refractive Index Signal
Correlation: 1.00000
Residual Std. Dev.: 699.78925
Formula: y = mx + b
m: 81009.73910
b: 159.13477
x: Amount
y: Height

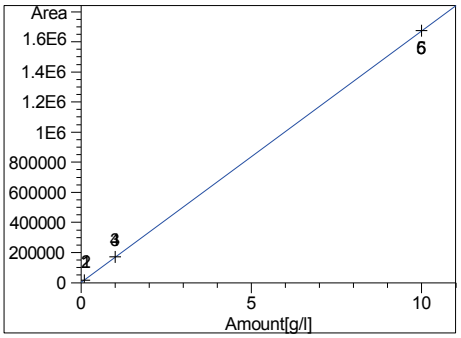


glycerol at exp. RT: 3.048
RID1 A, Refractive Index Signal
Correlation: 1.00000
Residual Std. Dev.: 2267.78842
Formula: y = mx + b
m: 167376.55562
b: 1480.01387
x: Amount
y: Height

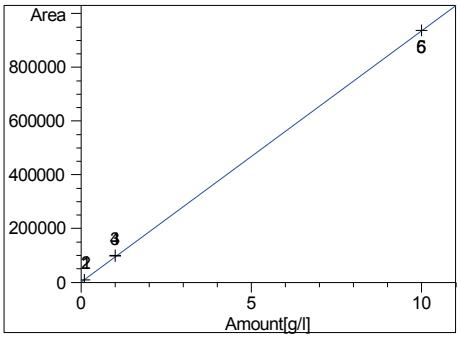


acetic acid at exp. RT: 3.289
RID1 A, Refractive Index Signal
Correlation: 0.99998
Residual Std. Dev.: 2744.62680
Formula: y = mx + b
m: 93621.71391
b: 1435.77651
x: Amount
y: Height

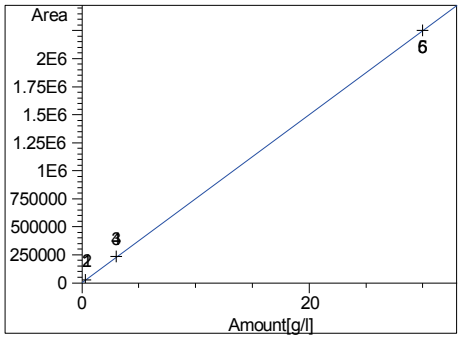


ethanol at exp. RT: 4.733
RID1 A, Refractive Index Signal
Correlation: 0.99999
Residual Std. Dev.: 3807.74696
Formula: y = mx + b
m: 74948.09546
b: 4336.71887
x: Amount
y: Height

**Figure 52: Typical fermentation calibration curves on HPX-87H ROA H+ (8%)**

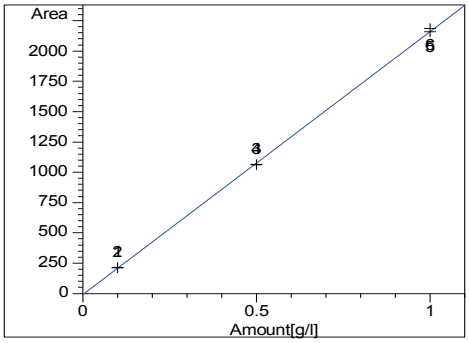


citric at exp. RT: 9.256
DAD1 C, Sig=210,8 Ref=off
Correlation: 0.99989
Residual Std. Dev.: 14.59506
Formula: y = mx + b
m: 2173.36581
b: -8.74588
x: Amount[g/l]
y: Area

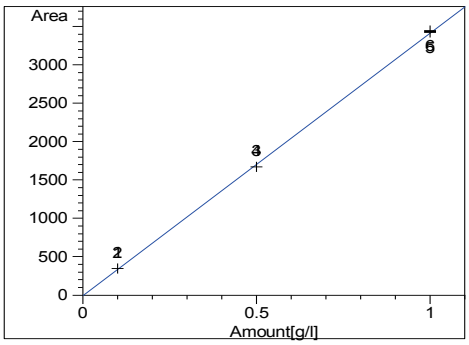


tartaric at exp. RT: 9.821
DAD1 C, Sig=210,8 Ref=off
Correlation: 0.99986
Residual Std. Dev.: 26.46626
Formula: y = mx + b
m: 3430.07101
b: -9.97815
x: Amount[g/l]
y: Area

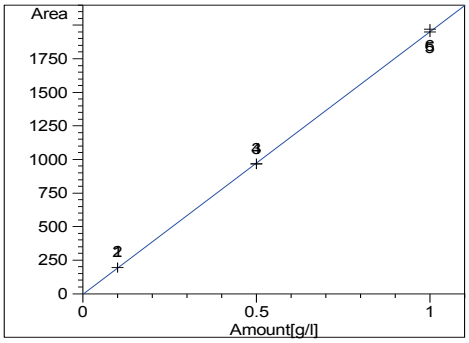


malic at exp. RT: 11.118
DAD1 C, Sig=210,8 Ref=off
Correlation: 0.99994
Residual Std. Dev.: 9.62397
Formula: y = mx + b
m: 1959.33084
b: -4.32050
x: Amount[g/l]
y: Area

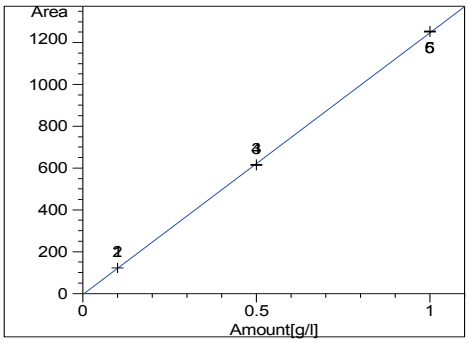


succinic at exp. RT: 13.837
DAD1 C, Sig=210,8 Ref=off
Correlation: 0.99995
Residual Std. Dev.: 5.83113
Formula: y = mx + b
m: 1254.41116
b: -4.82175
x: Amount[g/l]
y: Area

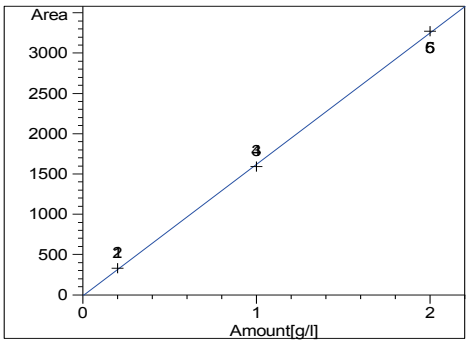


lactic at exp. RT: 14.926
DAD1 C, Sig=210,8 Ref=off
Correlation: 0.99988
Residual Std. Dev.: 23.74528
Formula: y = mx + b
m: 1634.04208
b: -10.41705
x: Amount[g/l]
y: Area

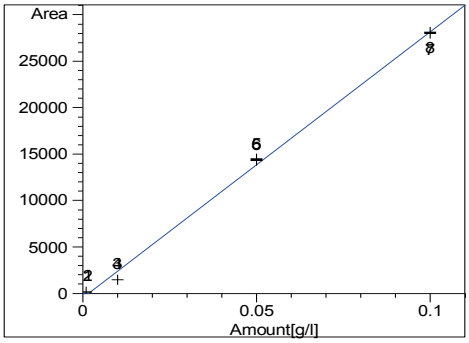


fumaric at exp. RT: 15.474
DAD1 C, Sig=210,8 Ref=off
Correlation: 0.99877
Residual Std. Dev.: 629.66252
Formula: y = mx + b
m: 286972.83903
b: -473.16989
x: Amount[g/l]
y: Area

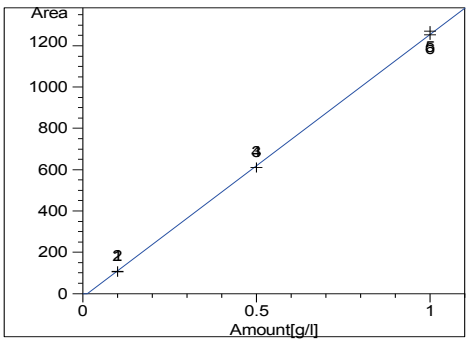


acetic at exp. RT: 17.923
DAD1 C, Sig=210,8 Ref=off
Correlation: 0.99981
Residual Std. Dev.: 11.56528
Formula: y = mx + b
m: 1273.92287
b: -16.43662
x: Amount[g/l]
y: Area

## A.10 Elution profile for fermentation standards

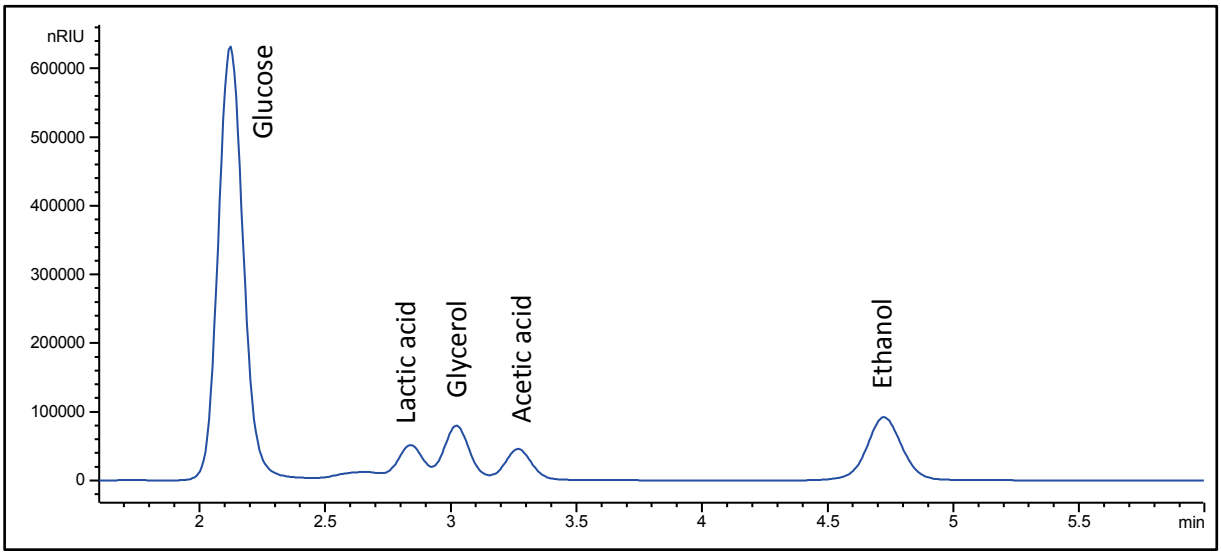


**Figure 53: Example elution profile of IEC glucose-ethanol standards**
Fermentation external standard 1× mixture on a Rezex RFQ Fast Acid H+ (8%) column under refractive index detection (RID).

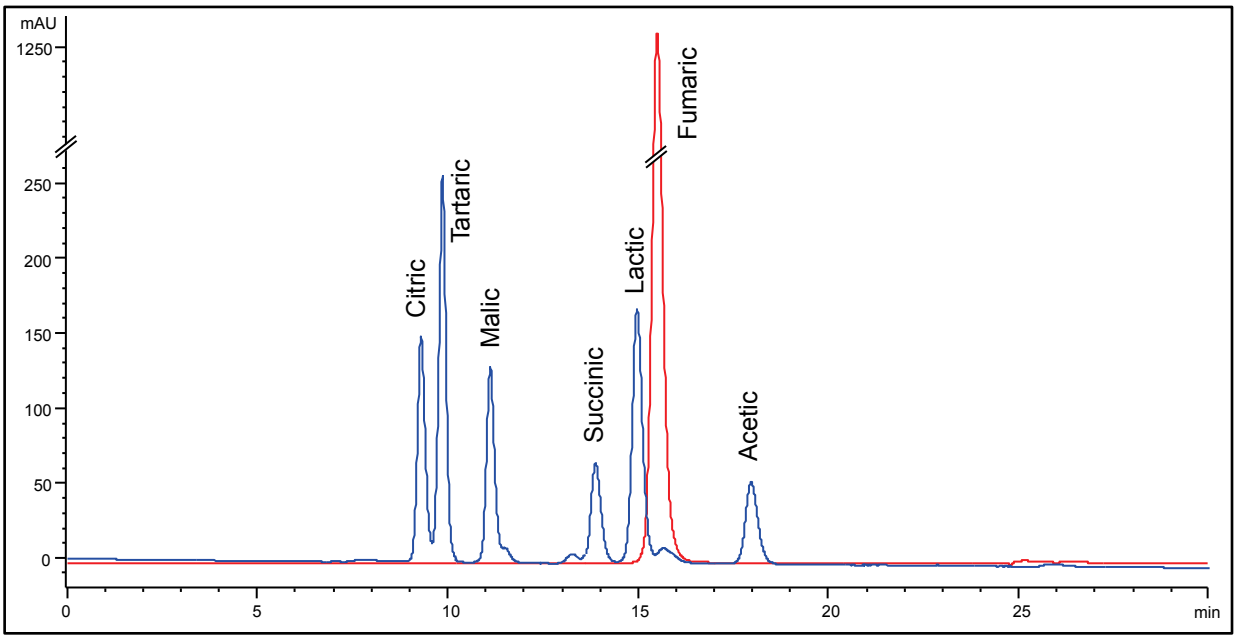


**Figure 54: Example elution profile of IEC fumaric acid and ROA standards**
Fermentation organic acid external standard 1× mixture on a HPX-87H ROA H+ (8%) column under 210 nm diode array detection (DAD).

# Appendix B

# Published review paper

As part of this Project, the following appended review article and corresponding corrigendum were published in the Journal of Biomass and Bioenergy.

## B.1 Bioethanol from microalgae (Corrigendum to review paper)

BIOMASS AND BIOENERGY 58 (2013) 406-407

Available online at www.sciencedirect.com

ScienceDirect

http://www.elsevier.com/locate/biombioe

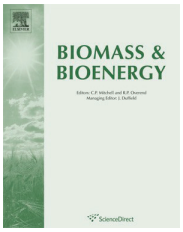


**Corrigendum**

# Corrigendum to "Microalgal biomass for bioethanol fermentation: Implications for hypersaline systems with an industrial focus" [Biomass Bioenergy 46 (2012) 79–88]

*Quang C. Doan* [a,c,*], *Navid R. Moheimani* [b], *Alison J. Mastrangelo* [c], *David M. Lewis* [a,c]

[a] Microalgae Engineering Research Group, University of Adelaide, Adelaide, SA 5005, Australia
[b] Algae R&D Center, School of Biological Sciences and Biotechnology, Murdoch University, Murdoch, WA 6150, Australia
[c] School of Chemical Engineering, University of Adelaide, Adelaide, SA 5005, Australia

The authors regret that a calculation error of $10^3$ was made in the conversion of annual biomass production values from $t \cdot ha^{-1}$ to the SI unit $Mg \cdot km^{-2}$ used in this review. For instance, annual biomass production values given as 7.3 Mg $km^{-2}$ should be 7.3 x $10^3$ Mg $km^{-2}$. This error occurs in Table 4 and in the review narrative where biomass production has been discussed. The error does not affect the relative comparisons made nor change overall conclusions of the review, yet, may mislead readers on this particular underestimated productivity parameter for the biomass sources discussed. A corrected Table 4 has been included in this corrigendum. The authors would like to apologise for any inconvenience caused.

DOI of original article: http://dx.doi.org/10.1016/j.biombioe.2012.08.022.
* Corresponding author. Microalgae Engineering Research Group, University of Adelaide, Adelaide, SA 5005, Australia.
E-mail address: quang.doan@adelaide.edu.au (Q.C. Doan).

http://dx.doi.org/10.1016/j.biombioe.2013.10.026

Table 4 – Comparison of potential yields from hypothetical large scale marine microalgal farms to reported yield from sugarcane energy crop.

| Biomass | Available sugar or starch ($w_B$) | Lipid ($w_B$) | Annual biomass production (Mg km$^{-2}$) | Annual potential ethanol conversion (dm$^3$ km$^{-2}$) | Productivity of ethanol production (dm$^3$ Mg$^{-1}$) | Additional lipid production (dm$^3$ Mg$^{-1}$) |
|---|---|---|---|---|---|---|
| Sugarcane | 0.118[c] | – | 7.75 x 10$^3$[c] | 5.89 x 10$^5$ | 76[c] | – |
| Dunaliella tertiolecta[a] | 0.104[d] | 0.15 | 7.3 x 10$^3$[g] | 4.89 x 10$^5$ | 67[h] | 167 |
| Isochrysis galbana[a] | 0.099[d] | 0.23 | 7.3 x 10$^3$[g] | 4.63 x 10$^5$ | 63[h] | 256 |
| Tetraselmis chui[a] | 0.102[d] | 0.17 | 7.3 x 10$^3$[g] | 4.80 x 10$^5$ | 66[h] | 189 |
| Nannochloris atomus[a] | 0.154[d] | 0.21 | 7.3 x 10$^3$[g] | 7.25 x 10$^5$ | 99[h] | 233 |
| Chlorella vulgaris[b] | 0.37[e] | 0.078[f] | 7.3 x 10$^3$[g] | 1.73 x 10$^6$ | 238[h] | 87 |

[a] Hypothetical scenario where microalgae species has been selected for lipid content. Carbohydrate and lipid data used from Brown (1991) [76].

[b] Hypothetical scenario where microalgae species has been selected for carbohydrate content.

[c] Annual production data for sugarcane energy crops from Brazil in 2008 [18]. Available sugar from sugarcane is calculated based on reported biomass and ethanol productivity data [2] using theoretical maximum mass fraction yield of 0.54.

[d] Glucose calculated from reported carbohydrate and monosaccharide quantities provided in Brown (1991) [76].

[e] Starch content used from the reported marine Chlorella vulgaris strain IAM C-534 from Hirano et al. (1997) [24].

[f] Lipid content used from a reported marine Chlorella vulgaris Liu et al. (2008) [77].

[g] Calculated based on daily average biomass productivity of 20 g m$^{-2}$ afdw for microalgae grown in open pond systems [17].

[h] Ethanol productivities calculated based on theoretical maximum mass fraction yield of 0.51 achieved from reported quantities of either glucose or total starch.

## Acknowledgment

This research was supported under Australian Research Council's Linkage Projects funding scheme (project LP100200616). The views expressed herein are those of the authors and are not necessarily those of the Australian Research Council.

References

[17] Borowitzka M, Moheimani N. Sustainable biofuels from algae. Mitigation and Adaptation Strategies for Global Change. 07 December 2010. http://dx.doi.org/10.1007/s11027-010-9271-9.

[18] Gauder M, Graeff-Hönninger S, Claupein W. The impact of a growing bioethanol industry on food production in Brazil. Appl Energ 2011;88:672–9.

[24] Hirano A, Ueda R, Hirayama S, Ogushi Y. CO2 fixation and ethanol production with microalgal photosynthesis and intracellular anaerobic fermentation. Energy 1997;22:137–42.

[76] Brown MR. The amino-acid and sugar composition of 16 species of microalgae used in mariculture. J Exp Mar Biol Ecol 1991;145:79–99.

[77] Liu ZY, Wang GC, Zhou BC. Effect of iron on growth and lipid accumulation in Chlorella vulgaris. Bioresour Technol 2008;99:4717–22.

# B.2 Bioethanol from microalgae (Review paper)

BIOMASS AND BIOENERGY 46 (2012) 79-88

Available online at www.sciencedirect.com

SciVerse ScienceDirect

http://www.elsevier.com/locate/biombioe


Review

## Microalgal biomass for bioethanol fermentation: Implications for hypersaline systems with an industrial focus

*Quang C. Doan* [a,c,*], *Navid R. Moheimani* [b], *Alison J. Mastrangelo* [c], *David M. Lewis* [a]

[a] Microalgal Engineering Research Group, School of Chemical Engineering, University of Adelaide, North Terrace, Adelaide, SA 5005, Australia

[b] Algae R&D Center, School of Biological Sciences and Biotechnology, Murdoch University, Murdoch, WA 6150, Australia

[c] School of Chemical Engineering, University of Adelaide, Adelaide, SA 5005, Australia

ARTICLE INFO

Article history:
Received 12 January 2012
Received in revised form
9 May 2012
Accepted 29 August 2012
Available online 29 September 2012

Keywords:
Bioethanol
Fermentation
Microalgae
Hypersaline
Sustainability
Industry

ABSTRACT

The potential of microalgae biomass as a feedstock for bioethanol fermentation has been widely considered in recent years. Yet, to date, only a modest level of research has been reported in this area. In all likelihood, the generation of a sustainable, sufficient level of biomass for biofuel production will need to be undertaken in saline water, and potentially under hypersaline conditions, to circumvent reliance on fresh water. However, the processing challenges associated with the fermentation of hypersaline biomass have yet to be adequately addressed. This review examines developments thus far for producing bioethanol from microalgae, indicating alternative means by which hypersaline microalgal biomass may be utilised, and provides a framework in which the industrial potential for sourcing such biomass should be considered.



## 1. Introduction

Over the last decade, the value of developing alternative sources for renewable liquid transportation fuels has increasingly been recognised. Key drivers for renewable energy have been the concern over global climate change associated with green house gas (GHG) emissions [1], as well as the speculation regarding energy security based on assessments that the world has already reached peak oil production [2]. To address the effective future mitigation of GHG emissions, the International Energy Agency (IEA) forecasted a 450 Scenario in their 2009 World Energy Outlook (WEO). This forecast, in which atmospheric GHG would be stabilised at a volume fraction of 450 mmol $mol^{-1}$ carbon dioxide equivalent ($CO_2$·eq), estimated that by 2030 the world demand for transport biofuels will be 11.64 EJ and supply 9.2% of total global transport fuels. This is equivalent to an annual production growth of 9.6% from a 1.43 EJ global biofuel output in 2007 [3]. Two important transport

Abbreviations: afdw, ash free dry weight; dw, dry weight; GHG, green house gas; PBR, photobioreactor; $CO_2$·eq, carbon dioxide equivalent; $w_B$, mass fraction of B (mass of substance B divided by the mass of the mixture): $w_B = m_B/m$.

* Corresponding author. Microalgal Engineering Research Group, School of Chemical Engineering, University of Adelaide, North Terrace, Adelaide, SA 5005, Australia. Tel.: +61 8 8303 6118; fax: +61 8 8303 4373.
E-mail address: quang.doan@adelaide.edu.au (Q.C. Doan).

0961-9534/$ – see front matter © 2012 Elsevier Ltd. All rights reserved.
http://dx.doi.org/10.1016/j.biombioe.2012.08.022

biofuels are bioethanol and biodiesel. Of these, bioethanol is currently produced in the largest volumes; for example, the bioethanol component of worldwide biofuel production in 2007 was 1.06 EJ, equivalent to 5.0 x $10^{10}$ $dm^3$ [4]. In the automotive industry, bioethanol has emerged as the primary alternative renewable transport fuel to supplement and potentially replace gasoline [5], and is, additionally, under consideration as a low-blend additive to diesel [6,7].

Bioethanol derived from photosynthetic organisms can mitigate the impact of GHG emissions through photoautotrophic conversion of atmospheric carbon dioxide to useful biomass. However, first generation bioethanol made from starch-rich agricultural produce have received widespread criticism for being unsustainable and socially irresponsible [8]. These concerns have led to development of second generation bioethanol from more sustainable feedstocks, such as cellulosic biomass [9]. Even so, proponents for the impact of global land use change (LUC) continue to question the overall benefit that biofuels, such as current bioethanol and biodiesel, derived from land vegetation will have on net global GHG emissions [10]. Furthermore, there remains uncertainty as to how future governmental policies on biofuels might be impacted with regard to the consequences of indirect land use change (iLUC) and its associated costs [11].

The potential for producing third generation bioethanol from alternative biomass such as microalgae and macroalgae has generated significant interest. A comprehensive recent review of this topic by John et al. (2011) [12] acknowledged a need for high salt tolerant microalgal species to improve utilisation of seawater. Marine or hypersaline algal species are desirable as sustainable sources of biomass; however, the fundamental aspect of hypersalinity inherent with such biomass is under-emphasised and has not been addressed in the majority of research reported in this area. Microalgae and macroalgae are often considered together when compared to terrestrial sources of biomass, yet they each present very different processing challenges from farming, production and conversion. Marine microalgae targeted for biofuels could be harvested from open or closed mass culturing systems, and most likely operated under hypersaline conditions to conserve water. Additionally, for both practical and economical reasons, marine microalgae as viable biofuel feedstocks cannot be completely dewatered and washed; hence concentrates of harvested marine microalgal biomass would carry significant quantities of saline or hypersaline water. In contrast, marine macroalgae would commonly be harvested from their natural coastal environment, whether wild or farmed, and can be more easily dewatered and washed.

There has been significant recent progress in the fermentation of marine macroalgal biomass for biofuel production. For instance, an important breakthrough microbial platform has been engineered in Escherichia coli for simultaneous saccharification and fermentation (SSF) of alginate, and enhanced assimilation of mannitol and glucose to bioethanol from the brown macroalga Saccharina japonica [13]. Additionally, there is now considerable research and commercial interest in developing marine macroalgae as a feedstock for biobutanol production through acetone butanol ethanol (ABE) fermentation with Clostridia spp. [14,15]. The conversion of marine macroalgal biomass to bioethanol and biobutanol warrants review to assess the implications of recent developments; particularly for macroalgal biomass conversion to biobutanol which has a higher energy density and better gasoline engine compatibility than bioethanol [16]. However, the review reported here will focus primarily on marine microalgae as a feedstock for bioethanol in order to highlight the importance of hypersaline systems for consideration.

While the attention of many research groups has focused towards utilising marine microalgal biomass for sustainable energy supplies, there has been minimal research and development on biofuel production under hypersaline conditions. In many parts of the world where arable land and fresh water resources are limited due to marginal climate conditions or demands associated with population growth, hypersaline processes will likely be required for sustainable commercial biofuel production from microalgae, particularly at the scale needed to supplement or supply the world's insatiable appetite for liquid transportation fuels [17]. The concerns around sustainable use of land and fresh water resources can be obviated through the development of marine based systems for producing biofuels. Photosynthetic marine microalgal production systems are well suited to this purpose as the microalgae can be cultured using seawater in arid locations that have no agricultural value. Microalgae are resilient organisms and include many culturable species rich in lipids and carbohydrates. They grow rapidly and are able to produce a daily average 20 g $m^{-2}$ ash free dry weight (afdw) biomass in open raceway pond systems, making them ideal biomass feedstock for producing biofuels [17]. This average microalgal biomass productivity is equivalent to an annual yield of 7.3 Mg $km^{-2}$ and is comparable to that of sugarcane crops, which have been reported at between 7.0 Mg $km^{-2}$ to 7.7 Mg $km^{-2}$; the largest energy crop harvested for bioethanol [5,18]. Indeed, it is anticipated that microalgae will be an important biomass for third generation biofuels. Although almost all of the reported research on microalgal liquid biofuels is focused on the production of lipid for biodiesel [19], the economic feasibility of generating biodiesel from a microalgal biomass feedstock may depend on the development of energy co-products such as methane, hydrogen, ethanol, butanol and aviation fuel [20].

In the early 1980s, it was recognised that microalgae such as the genus Dunaliella had potential as a rich, renewable biomass for use in the fermentative production of butanol and ethanol [21]. Furthermore, the increased global pressure on the resource sector to produce fuel from renewable and environmentally sustainable sources has led to ongoing research in methods to produce ethanol from microalgae since the late 1990s [12,22–27]. As a result, a modest body of knowledge now exists that demonstrates the feasibility of two main approaches for producing ethanol from microalgae. One area gaining significant interest is the anaerobic fermentation of the microalgal biomass by solventogenic microorganisms, which can utilise and convert the microalgal carbohydrates to ethanol. Another field of research has demonstrated the direct synthesis of ethanol as a metabolite in strains of both naturally occurring and engineered microalgae. Some such processes are currently under commercial development [28,29], although bioethanol made from microalgae is not yet available on the market.

The main focus of this review is on the potential for fermentative production of bioethanol from marine and hypersaline microalgal biomass, as well as assessing developments in the general area of microalgal ethanol reported thus far and proposing industrially and environmentally relevant process considerations for future research. As cultivation of marine microalgae in seawater introduces a minimum salinity of 35 g $dm^{-3}$ to the harvested biomass, particular emphasis is placed on the need for developing appropriate systems to operate under hypersaline conditions in order to minimise the environmental impact at commercial scale, thus achieving a sustainable biomass supply.

## 2. Fermentable substrates in microalgae

Commercially available ethanol biofuel is converted from fermentation of sugar-rich agricultural crops, with 80% sourced from corn and sugarcane [4], and demonstration cellulosic ethanol refineries are also now in operation [4,30–33]. The carbohydrates of microalgae have been studied since the mid-1900s [34–39]. While early studies did not focus on the fermentation potential of microalgal biomass, they did establish that many of today's commercially important microalgal groups, such as the chlorophyta green algae, contained starch-type storage carbohydrates similar to those found in vascular higher plants currently used as substrates for ethanol production [5]. The key storage carbohydrates of the main algal groups, which include unicellular microalgae and the cyanobacteria blue-green algae, are compared in Table 1. Structurally, microalgal starch grains consist of amylose and branched amylopectin homopolysaccharides much like those of higher plants [40], however, only green algae accumulated starch in the same way within the chloroplast through the assimilation of adenosine diphosphate (ADP) glucose. The floridean starch of red algae, as with similar cytosolic starch found in the cytoplasm and periplast of other algae groups (Table 1), is synthesised from uridine diphosphate (UDP) glucose much like glycogen from heterotrophic eukaryotes [41]. Other granular storage polysaccharides from this group of microorganisms include the α-1,4-glucan cyanophycean starch of cyanobacteria and the morphologically diverse paramylon, a β-1,3-polyglucan stored in the cytoplasm of euglenoids and chlorarachniophyta [42]. Additionally, the reserve polysaccharide chrysolaminaran in microalgae of the taxa heterokontophyta and haptophyta is soluble and stored in a cytoplasmic vacuole.

Aside from the polyglucan storage products there is a diverse range of carbohydrates associated with both cellular structure and osmoregulatory function across different species of microalgae. For instance among chlorophytes, the cell wall of some *Chlorella* spp. comprises of α-cellulose and hemicelluloses [43], whereas the more primitive *Chlamydomonas* spp. cell wall has hydroxyproline glycosides consisting of glucose, galactose and arabinose [44]. Different again, the chlorophyte *Tetraselmis* spp. present 2-keto sugar acids as their major cell wall carbohydrate [45]. In species such as *Botryococcus braunii* a large proportion of reported monosaccharides are secreted into the extracellular environment of the microalgae as exopolysaccharides [46]. The accumulation of sugar solutes can also provide an important osmoregulatory function in the salt tolerance of microalgae. Osmoregulation in the green halophilic alga *Dunaliella* occurs through the synthesis and degradation intracellular glycerol in response to the salinity conditions of its external environment [47]. In the euryhaline cyanobacteria, fresh water species are able to tolerate marginal hypersalinity of up to 45 g $dm^{-3}$ sodium chloride (NaCl) through accumulation of the disaccharides sucrose and trehalose, and those species typically from marine or hypersaline environments that synthesise the compatible solute glucosylglycerol have shown halotolerance in the range of 60 g $dm^{-3}$ to 100 g $dm^{-3}$ NaCl [48]. Given the degree of carbohydrate diversity amongst microalgae, there remains a common group of monosaccharides that have been reported across different genera. These are summarised in Table 2 and in most cases, the reported monosaccharides from microalgae have generally been extracted from whole cells and are thus likely to represent both structural and physiological carbohydrates; additionally, their distribution between microalgae division, genera and species is diverse.

The total carbohydrate content of microalgae has been reported at mass fractions of up to 0.5 to 0.6 dry weight (dw) and includes both starch and monosaccharides derived from structural carbohydrates, such as mannose, galactose and arabinose [27,49,50]. However, the carbohydrate yield from biomass is dependent on both the selected microalgae and the

Table 1 – The diversity of main storage carbohydrates of algae groups.

| Division | Storage carbohydrate | Composition |
|---|---|---|
| Cyanophyta (=Cyanobacteria), "Blue-green algae" | Cyanophycean starch | α-1,4 polyglucan |
| Prochlorophyta (=Chloroxybacteria) | Cyanophycean starch | α-1,4 polyglucan |
| Glaucophyta | Starch (in cytosol) | α-1,4 polyglucan; α-1,6 branches |
| Rhodophyta, "Red algae" | Floridean starch (in cytosol) | α-1,4 polyglucan; α-1,6 branches |
| Cryptophyta | Starch (in periplast) | α-1,4 polyglucan; α-1,6 branches |
| Heterokontophyta | Chrysolaminaran (in vacuole) | β-1,3 polyglucan; β-1,6 branches |
| Dinophyta | Starch (in cytosol) | α-1,4 polyglucan; α-1,6 branches |
| Haptophyta (=Prymnesiophyta) | Chrysolaminaran (in vacuole) | β-1,3 polyglucan; β-1,6 branches |
| Euglenophyta | Paramylon (in cytosol) | β-1,3 polyglucan |
| Chlorarachniophyta | Paramylon (in cytosol) | β-1,3 polyglucan |
| Chlorophyta, "Green Algae" | Starch (in chloroplast) | α-1,4 polyglucan; α-1,6 branches |

Referenced from [40,41,78–81].

Table 2 – Reported monosaccharide species commonly found in microalgal biomass.

| Carbohydrate group | Monosaccharide | Selected references |
|---|---|---|
| Pentose sugar | Xylose; ribose; fructose; arabinose | [37,44,46,48,76,82–86] |
| Hexose sugar | Mannose; gulose; glucose; galactose | [37,38,44,46,48, 76,82–86] |
| 6-Deoxyhexose sugar | Rhamnose; fucose | [37,46,76,82–86] |
| Sugar acid | Galacturonic acid | [82,84–86] |
| Sugar alcohol | Glycerol | [21,47,48] |

cultivation conditions utilised. In one study, the total carbohydrate yields from *Dunaliella primolecta* were reported at a mass fraction of 0.65 dw, when grown under nitrogen-deficient conditions [51]. Furthermore, the study demonstrated that such conditions could lead to a five-fold increase in the carbohydrate yields from both *D. primolecta* and *Tetraselmis suecica*, and suggested potential applications in instances where carbohydrate rich biomass may be required for conversion to ethanol. It should be noted, however, that these improved carbohydrate levels were at the cost of reduced photosynthetic efficiencies and total biomass dw yields decreased 0.5-fold and 0.65-fold below the respective nitrogen-sufficient estimates. Nonetheless, a recent study outlined a two-stage cultivation of fresh water *Chlorella vulgaris* in which the biomass yields were optimised prior to nitrogen and iron deprivation, resulting in both improved biomass and high intracellular carbohydrate yields; in fact, intracellular starch levels reached up to a mass fraction of 0.41 dw, an amount almost 2-fold higher than those previously reported in other strains of *Chlorella* spp. [52].

Amongst the storage, structural and physiological carbohydrates present in microalgae the types and quantities of basic monosaccharide components are potentially very suitable for conversion into ethanol. However, for optimal utilisation of such diverse carbohydrates new ethanologenic microorganisms may be required, although to date, the majority of studies in this area have utilised the standard strains of *Saccharomyces cerevisiae* (Table 3) with only a few that have assessed ethanologenic or solventogenic bacterial strains such as *Clostridium pasteurianum* [21] and recombinant *E. coli* [53]. Certainly, the emerging processes for second generation bioethanol from cellulosic type biomass have demonstrated a need to identify or engineer alternative microorganisms that are able to utilised a variety of monosaccharides other than the hexose sugar glucose [31]. Furthermore, to exploit biomass derived from marine microalgae cultivated in saline or hypersaline water, the identification of appropriate ethanologenic microorganisms that are halotolerant or halophilic may be necessary to facilitate industrial processing under conceivably hypersaline conditions.

## 3. Extraction of fermentable substrates

The structural carbohydrates of microalgal biomass consist of diverse monosaccharides. Although these have been analytically characterised, they are often components of complex cell walls in many marine microalgal species and may not easily be extracted or utilised. The conversion of microalgal sugars to bioethanol will depend on both the efficiency of their extraction, and the capacity of any chosen ethanologenic microorganism to utilise them. The extraction of fermentable sugars from microalgal biomass has been addressed by two groups in particular, using hydrothermal acid pretreatment with biomass from both *Chlamydomonas reinhardtii* UTEX 90 and *Chlorococcum humicola* [22,27]. Using another approach, other researchers focused on enzymatic pretreatment of

Table 3 – Reported bioethanol yields from fermentation of microalgal biomass. Ethanol yields have been calculated from data reported in each study.

| Microalga | Pretreatment(s) | Fermenting microorganism | $w_B$ ethanol from total dw biomass | Ref. |
|---|---|---|---|---|
| *Dunaliella* sp | Glucoamylase[b] | *Saccharomyces cerevisiae* IAM 4140 | 0.011 | [26] |
| *Chlorella vulgaris* IAMC-534[f] | α-Amylase & glucoamylase | *Saccharomyces cerevisiae* IFO 039 | 0.123 | [24] |
| *Chlamydomonas reinhardtii* UTEX 90 | Dilute acid/heat | *Saccharomyces cerevisiae* S288C | 0.292 | [27] |
| *Chlamydomonas reinhardtii* UTEX 90 | α-Amylase[c] | *Saccharomyces cerevisiae* S288C | 0.235 | [49] |
| *Chlorococcum* sp. | (No pretreatment) | *Saccharomyces bayanus* | 0.383 | [23] |
| *Chlorococcum humicola* | Dilute acid/heat | *Saccharomyces cerevisiae* | 0.520[a] | [22] |
| *Chlorella vulgaris*[f] | Dilute acid/heat, cellulase[d] & cellobiase[e] | *Escherichia coli* SJL2526 | 0.400[a] | [53] |

a Calculated yield that is above stoichiometric limit for sugar-to-ethanol conversion; based on report ethanol concentrations produced relative to percentage of carbohydrates biomass feedstock.
b Glucozym AF6 (Amano Pharmacy Co. Ltd.).
c Termamyl (Novozymes A/S).
d Celluclast (Novozymes A/S).
e Novozymes 188 (Novozymes A/S).
f Both have been reported as marine strains of C. vulgaris.

washed microalgal biomass with terrestrial cellulase, glucoamylase or α-amylase [24,26,49,54], though research by Matsumoto et al. (2003) [50] suggests that these enzymatic processes may be inherently limited or at the least incomplete. In their work, this team demonstrated the feasibility of converting saline biomass from a total of 76 different marine microalgae to reduced sugars by saccharification with a marine amylase-producing bacterium, Pseudoalterimonas undina NKMB 0074. They reported poor hydrolysis to reduced sugars due to low amylase production by the bacterium, but interestingly observed that under saline conditions terrestrial amylase and glucoamylase were completely inhibited and as such would be unsuited to industrial application for hydrolysing carbohydrates from unwashed marine biomass [50].

There is an expanding body of knowledge on halophilic enzymes and microorganisms that have the potential to effectively treat marine biomass. A recent review of applications for halophilic microorganisms concluded that the industrial demand for salt-tolerant enzymes is limited [55], though continued development of processes to generate biofuels from marine microalgae may provide future opportunities for such applications, for example, in the hydrolysis of hypersaline biomass. Potentially useful salt-tolerant enzymes have been isolated from a diverse population of marine and hypersaline microorganisms. The studies on many such salt-tolerant hydrolytic enzymes, including a number of halophilic amylases, from halophilic archaea and bacteria have been reviewed by Ventosa et al. (2005) [56]. Other examples include the marine Streptomyces sp. D1 which produces a moderately halophilic a-amylase [57], and a highly stable but salt dependent halophilic a-amylase isolated from Haloarcula hispanica [58]. Also, a glucoamylase able to hydrolyse both α-1,4 and α-1,6-glycosidic linkages of starch amylose and amylopectin has been discovered in the marine yeast Aureobasidium pullulans N13d [59], and a potentially very useful thermophilic and halophilic amyloglucosidase has been identified in Halobacterium sodomense with optimal activity at temperatures between 66 °C and 76 °C and molarities of 1.4 mol $dm^{-3}$ to 3.9 mol $dm^{-3}$ NaCl [60]. Additionally, it has been reported that some halophilic a-amylases, such as those from Haloarcula sp. strain S-1 and a particular strain of Nesterenkonia sp., are more tolerant to organic solvents than terrestrial amylases [61,62]. Such enzymes may be especially suitable for hydrolysis of carbohydrates from hypersaline biomass.

## 4. Fermentation of microalgal biomass

In comparison to the development efforts into other biomass sources such as lignocellulosic residues, a review of the literature has shown minimal progress made in the past 30 years towards fermenting bioethanol from renewable microalgal biomass. As a result, research in this area is really in its formative stage and a long way from yielding a commercially viable product. The genus Dunaliella, which accumulates high concentrations of intracellular glycerol in hypersaline environments as a means of osmotic stabilisation, was assessed by Nakas et al. (1983) as a potentially rich renewable biomass for use in fermentation schemes aimed at producing neutral solvents [21]. In this study, cultures of five Dunaliella species (Dunaliella tertiolecta, D. primolecta, Dunaliella parva, Dunaliella bardawil, and Dunaliella salina) were optimised for biomass glycerol content. A 300-fold concentrate of harvested biomass was successfully fermented to yield n-butanol, 1,3-propanediol and ethanol by the bacterium C. pasteurianum. This bacterium produced peak levels of solvent in 10 g $dm^{-3}$ NaCl but was totally inhibited in 30 g $dm^{-3}$ NaCl. The concentrated Dunaliella biomass preparation used had a salinity below 10 g $dm^{-3}$ but insufficient glycerol for solvent conversion to achieve yields comparable to those obtained utilising traditional substrates such as molasses or glucose. Despite its limited success, the study demonstrated that fermentation of microalgae biomass could indeed be realised. More importantly, Nakas et al. concluded that for large-scale applications the successful fermentation of a saline biomass would require either salt removal or the use of a solvent-producing halotolerant organism.

Since these early observations by Nakas et al. (1983) [21], minimal work on assessing halotolerant or halophilic organisms for fermentative production of ethanol has been reported. It would appear that many researchers have concluded that fermentation using yeast had been thoroughly investigated and, as such, have prioritised research around developing efficient technologies for biomass pretreatment [27]. A recent review of technological developments on the production of ethanol from microalgae alluded to the importance of using marine microalgae to avoid commodity competition for fresh water [12], but also presented fermentation as a ready option, simply involving the use of processes similar to those currently established employing appropriate yeast strains. This seems to be the dominant view taken by those currently investigating approaches to utilising microalgal biomass for conversion to ethanol. To circumvent the salinity issues presented by the fermentation of marine biomass, the majority of studies undertaken to date have used microalgae grown in low saline medium or, alternatively, have implemented a wash step for salt removal.

Bioethanol has been produced using biomass substrates from the freshwater microalga C. reinhardtii UTEX 90 [27,49], the marine microalgae Chlorococcum sp., C. humicola and Dunaliella sp. [22,23,26]., and reported marine strains of C. vulgaris, such as C. vulgaris IAM C-534 [24,53]. The reported ethanol yields from these studies (Table 3) demonstrate varying levels of success across the different processes assessed. Shirai et al. (1998) [26] had limited success fermenting biomass from a Dunaliella sp. which had been hydrolysed with a commercial glucoamylase, achieving ethanol yields of 0.011 dw biomass. In contrast, a study by Harun et al. (2010) [23], which assessed both whole cell and lipid-extracted Chlorococcum sp. biomass in the absence of hydrolytic pretreatment, reported ethanol yields of up to 0.383 dw biomass. This study is of particular interest as it suggests that a lipid-extraction process may facilitate the release of fermentable sugars from microalgal biomass for conversion to ethanol. The yield differences observed in these various studies can be attributed to the available levels of fermentable sugars from the selected microalgae and to the effective ethanol conversion rate in the processes used. These reported studies are important in demonstrating a proof of concept for efficient conversion of marine microalgal

carbohydrates to ethanol; furthermore, they highlight a need for sufficient extraction of fermentable carbohydrates from any microalgae biomass used to be matched with optimal process conditions and microorganisms for fermentation.

The limited available studies on conversion of microalgal biomass to ethanol emphasises a need for further verification of published studies, especially where ethanol yields above what would be considered stoichiometric limits have been reported (Table 3). Under ideal conditions, a theoretical stoichiometric ethanol yield of 0.51 is produced from typical yeast fermentation, where 1 mol of glucose yields 2 mol each of ethanol and carbon dioxide [5]. Considering the complexity of microalgal carbohydrates, it is unlikely that all carbohydrate groups would be efficiently utilised, particularly when using S. cerevisiae. Additionally, substrate to product mass balances should account for other dry weight components in the microalgae such as lipids and proteins that cannot be converted to ethanol. For instance, a reported ethanol yield of up to 0.52 dw from C. humicola biomass appears to exceed twice the stoichiometric maximum of 0.224 expected based on the reported total mass fraction of 0.438 dw input of carbohydrate and starch [22]. Likewise, it was reported that an E. coli SJL2526 fermentation of C. vulgaris biomass yielded ethanol at 0.40 dw from feedstock containing a mass fraction of 0.27 dw total sugars; a quantity which appears to be almost 3-fold higher than stoichiometric limits [53]. New studies to ratify existing data are essential before assessments can be made regarding the actual net energy return from current reported processes.

The knowledgebase required for process scale-up of bioethanol fermentation using marine microalgal biomass is incomplete. In particular, the issue of hypersalinity within the marine biomass has been overlooked which, in turn, has led to the seemingly prevalent opinion that the fermentable sugars from the biomass of marine microalgae can be easily converted to ethanol using existing processes. A trend in many existing studies has been to wash saline microalgal biomass feedstocks with deionised water for salt removal and improved compatibility with the selected downstream processes. For example, such a process generated reduced salt conditions which then facilitated the use of commercial terrestrial α-amylases for investigations with harvested biomass from two C. vulgaris strains and a Dunaliella sp. [24,26,53]. Ultimately, when considering industrial scale marine microalgae production, methods such as desalting with fresh water are unlikely to be viable, and practical process solutions to deal with hypersalinity will be a key factor for successful commercial implementation. In this type of setting, terrestrial hydrolytic enzymes and halosensitive ethanologenic microorganisms such as some S. cerevisiae and E. coli may prove to be ineffective.

## 5. Direct ethanol synthesis in microalgae

A lateral development path for producing ethanol from microalgae has been pursued by a number of research groups. Rather than harvesting microalgal biomass as a fermentation substrate, these researchers have selected or engineered microalgae that can directly produce ethanol as a secreted metabolite. In nature, some microalgae and cyanobacterium undergo self-fermentation through utilisation of their intracellular starch in dark and light anaerobic environments. Under these conditions, the production of ethanol has been reported in the C. reinhardtii strains F-60 and UTEX2247, Chlamydomonas sp. YA-SH-1, Chlorococcum littorale and Cyanothece PCC 7822 [24,25,63e66]. However, anaerobic self-fermentation via the Embden–Meyerhof–Parnas (EMP) metabolic pathway in naturally occurring microalgae produces much lower levels of ethanol in comparison to reported yields from yeast fermentations. For example, in a dark fermentation process, C. littorale produced an ethanol yield of 0.021 dw biomass with a conversion ratio of 0.27 [65], whereas lipid-extracted Chlorococcum sp. biomass, when used as a substrate for yeast fermentation, allowed for a more efficient conversion of available sugars with an ethanol yield of 0.383 dw biomass [23]. Furthermore, unless axenic microalgal cultures are used in dark fermentation systems, any ethanol secreted at such low titres may provide a nutrient source of carbon for contaminant heterotrophic organisms, thus limiting process efficiency [67].

In order to be practical, processes using microalgae under dark fermentation to produce ethanol require the selection of strains capable of high ethanologenic productivity. More productive dark fermentation studies have been reported utilising the marine microalgae C. reinhardtii UTEX2247 and Chlamydomonas sp. YA-SH-1 with respective ethanol yields of 0.08 and 0.154 dw biomass [24,25]. These studies required the maintenance of a viable microalgal culture for dark fermentation after harvesting by centrifugation, and form the basis for a US patent, which also lays claims for its utilisation with the genera Chlamydomonas, Chlorella, Spirulina, Oscillatoria and Microcystis [28]. However, aside from the need to maintain axenic cultures, there may be limitations for processes based on dark fermentation relating to intracellular substrate usage and starch-to-ethanol conversion efficiencies. Such metabolic limits were observed in an investigation of 37 cyanobacterial strains by Heyer and Krumbein (1991) [66], who concluded that the rates of dark fermentation were minimal and geared towards cell maintenance; most metabolites like ethanol were produced at much lower levels than what would be acceptable for fuel production. In regard to substrate availability, the ethanol producer can only utilise its intracellular supply. In fact, the data presented in the studies by Hirano et al. (1997) [24] and Hirayama et al. (1998) [25] suggests that conversion of carbohydrate reserves to ethanol ceases well before substrate exhaustion. In contrast, a fermentation system where exogenous substrate is provided to encourage growth and production can be more readily optimised through process design to yield higher producer densities and product titres.

A recent review of algal-based ethanol processes concluded that future developments should focus on the metabolic engineering of ethanol-producing microalgal strains and the design of appropriate photobioreactor (PBR) systems [12]. Early research in this area produced limited results when a fresh water cyanobacteria, Synechococcus sp. strain PCC 7942, was metabolically engineered to produce ethanol under oxygenic photoautotrophic conditions and gave yields much lower than those generally obtained during commercial production of ethanol by yeast fermentations [68]. Despite the early limitations in this approach to producing ethanol, commercial development in this area is ongoing; in fact, Algenol Biofuels

Inc. claim to have developed a commercially applicable process using a genetically modified (GM) strain of ethanol-producing autotrophic cyanobacteria [29,69,70] in a non-conventional PBR system. An industrial scale up of typical closed PBR designs currently in use for cultivating microalgae would incur prohibitively high infrastructure costs in construction, operation and maintenance [71], therefore, the viability of PBR systems for industry depends on significant improvements on plant design, operation and construction materials [72]. The Algenol Biofuels Inc. patented process utilises a new PBR design to minimise downstream processing by allowing for direct, continuous ethanol collection from evaporative condensate of their ethanologenic cultures.

## 6. Industrial outlook towards sustainable biomass

In 2007, an estimated arable land area of 43,000 $km^2$ was used in Brazil to cultivate sugarcane crops for the production of $2.5 \times 10^{10}$ $dm^3$ of bioethanol, or $5.81 \times 10^5$ $dm^3$ $km^{-2}$ [18], with the majority of bagasse from this feedstock being utilised for process heat [73]. Furthermore, it has been proposed that if discarded sugarcane trash was instead collected and used to supplement process heat generation, then 50% of the bagasse could be made available as feedstock for cellulosic bioethanol production and potentially account for an additional $4.0 \times 10^5$ $m^3$ $km^{-2}$ of bioethanol [73]. The net benefit of this improved biomass usage would be a 0.41-fold reduction in the required land area for producing 0.69-fold more bioethanol, yet even so, the total yearly production would be insufficient for the challenging biofuel targets set under the 2009 WEO's 450 Scenario. If sugarcane bioethanol remained as Brazil's primary biofuel and production was to increase at the IEA's required annual rate of 9.6% upto 2030, Brazil would still need to expand the cultivation of biofuel crops over a further 4-fold of the existing arable land area allocated for this purpose. A study by Gauder et al. (2011) [18] provided data to suggest that, in balance with domestic food production needs, Brazil may have sufficient arable land to sustainably expand its bioethanol capacity to $7.67 \times 10^7$ $m^3$ by 2020, which is within 94% of the production growth rate required under the 450 Scenario for this period. However, the world's population is expected to exceed 9 billion people by 2050 [74], and responsible use of arable land on a global level should be an important consideration. Indeed, it has been suggested that future population growth will have a considerably greater impact on land and water resources for food production than will other factors such as economic or technical developments, and that the global capacity for food production may be significantly limited by government policies which drive increased bioenergy usage [75].

The land use for commercial scale biofuel crop cultivation is well beyond the capacity of any current microalgal based system; in fact, the largest commercial microalgae open pond system is currently only 7.5 $km^2$ [17]. Nonetheless, biomass productivities by unit area per annum from saline or hypersaline microalgal open pond farms can be comparable to those of commercial biofuel crops such as sugarcane (Table 4), and hence, such farms could supply feedstock towards bioenergy production without competing with food production for arable land and drinking water. However, to date, there have been no reports on the biomass productivity of marine microalgae selected for carbohydrate enrichment and cultured over long-term growth studies in large scale open ponds. Additionally, the microalgal biomass described in many of the laboratory scale studies for ethanol fermentation contained significantly higher compositions of fermentable sugars than those currently assessed for lipid production in large scale open pond systems. Therefore, to compare potential biofuel yields from marine microalgal biomass against data from commercial sugarcane bioethanol production [18], a set of hypothetical large scale open pond farms have been constructed, as shown in Table 4. The compositional carbohydrate and lipid data for the microalgae

Table 4 – Comparison of potential yields from hypothetical large scale marine microalgal farms to reported yield from sugarcane energy crop.

| Biomass | Available sugar or starch ($w_B$) | Lipid ($w_B$) | Annual biomass production (Mg $km^{-2}$) | Annual potential ethanol conversion ($dm^3$ $km^{-2}$) | Productivity of ethanol production ($dm^3$ $Mg^{-1}$) | Additional lipid production ($dm^3$ $Mg^{-1}$) |
|---|---|---|---|---|---|---|
| Sugarcane | 0.118[c] | – | 7.75[c] | $5.89 \times 10^5$ | 76[c] | – |
| Dunaliella tertiolecta[a] | 0.104[d] | 0.15 | 7.3[g] | $4.89 \times 10^5$ | 67[h] | 167 |
| Isochrysis galbana[a] | 0.099[d] | 0.23 | 7.3[g] | $4.63 \times 10^5$ | 63[h] | 256 |
| Tetraselmis chui[a] | 0.102[d] | 0.17 | 7.3[g] | $4.80 \times 10^5$ | 66[h] | 189 |
| Nannochloris atomus[a] | 0.154[d] | 0.21 | 7.3[g] | $7.25 \times 10^5$ | 99[h] | 233 |
| Chlorella vulgaris[b] | 0.37[e] | 0.078[f] | 7.3[g] | $1.73 \times 10^6$ | 238[h] | 87 |

a Hypothetical scenario where microalgae species has been selected for lipid content. Carbohydrate and lipid data used from Brown (1991) [76].

b Hypothetical scenario where microalgae species has been selected for carbohydrate content.

c Annual production data for sugarcane energy crops from Brazil in 2008 [18]. Available sugar from sugarcane is calculated based on reported biomass and ethanol productivity data [18] using theoretical maximum mass fraction yield of 0.54.

d Glucose calculated from reported carbohydrate and monosaccharide quantities provided in Brown (1991) [76].

e Starch content used from the reported marine Chlorella vulgaris strain IAM C-534 from Hirano et al. (1997) [24].

f Lipid content used from a reported marine Chlorella vulgaris Liu et al. (2008) [77].

g Calculated based on daily average biomass productivity of 20 g $m^{-2}$ afdw for microalgae grown in open pond systems [17].

h Ethanol productivities calculated based on theoretical maximum mass fraction yield of 0.51 achieved from reported quantities of either glucose or total starch.

presented was extracted from the literature [24,76,77], and an assumption made that realistic average daily biomass productivities of 20 g $m^{-2}$ afdw could be achieved [17] in cultures of the marine microalgae selected. Furthermore, it was assumed that the reported cellular glucose or starch content in the microalgae would be fully converted to ethanol and, for the purposes of this example, any unresolved process limitations in relation to biomass harvesting and hypersaline fermentation systems were ignored. The biomass productivity of marine microalgae in open pond farms compares well against the yearly 7.75 Mg $km^{-2}$ production of Brazilian sugarcane crops, which averages to a daily 21 g $m^{-2}$. Only glucose and starch content were considered as fermentable carbohydrates in the microalgae assessed, yet even so, the potential ethanol yield from *D. tertiolecta*, *Isochrysis galbana* and *Tetraselmis chui* biomass was, on average, 86% of the reported yield from sugarcane. The glucose composition in these species would be considered as typical of microalgae at an approximate mass fraction of 0.10 dw, and *Nannochloris atomus* biomass, with a mass fraction of 0.154 dw of glucose, demonstrated the potential to yield 30% more ethanol per weight of biomass than sugarcane. These four species are perhaps representative of the saline and marine microalgae that could be considered in lipid production for bioenergy, yet would still provide residual biomass suitable for ethanol fermentation yields able to match that of terrestrial sugarcane crops. Conversely, if a microalga was to be selected for production of fermentable sugars, for example the marine strain of *C. vulgaris* IAM-C534 with a starch mass fraction of 0.37 dw of biomass, the potential ethanol yield could, in theory, be over three-fold higher than what could be produced from sugarcane while still yielding a significant proportion of lipid for other bioenergy products such as biodiesel.

## 7. Conclusion

In today's environmental and economic climate, ethanol has emerged as an important liquid transportation biofuel. The potential of marine or saline microalgal biomass to be cultivated as a sustainable substrate feedstock in ethanol fermentation is evident; however, there are still many technical challenges in both the early development and scale up stages. There has only been a modest level of investigation into the fermentation of marine microalgal biomass, and significant scope exists for improvement, particularly in the area of process sustainability. A consideration of the desired industrial outcomes should guide early development research objectives. For instance, hypersalinity should be a key factor in process design and optimisation, given that seawater is the most feasible and sustainable environment in which to produce microalgal biomass for bioenergy. Additionally, the cultivation of saline microalgae over thousands of square kilometres of land with annual productivities equivalent to 7.3 Mg $km^{-2}$ should direct downstream processing away from environmentally costly steps such as the desalting of saline biomass.

The limited number of reports in the published literature suggests that few research groups have addressed the issue of process hypersalinity. Yet there are clear advantages to developing a process for treating and fermenting hypersaline biomass, particularly in view of the extensive ongoing global development of marine microalgal systems for producing lipids for biofuels. Whether the end biomass is sourced from open raceway ponds or closed PBR systems there is likely to be an abundant supply of potentially fermentable lipid-extracted residue marine biomass for conversion to ethanol if a sustainable process can be developed. Even microalgal biomass with minimal fermentable sugar mass fractions of approximately 0.10 dw could be utilised to produce significant yields of bioethanol. However, in many instances, existing fermentation research may not be applicable for use with a sustainable marine or hypersaline biomass. Further investigation into halotolerant and halophilic enzymatic hydrolysis would address the need for more appropriate biochemical pretreatment of hypersaline biomass for extraction of fermentable sugars. Priority should also be given to developing improved microbial systems for effective ethanologenic or solventogenic conversion of hypersaline biomass, as a hypersaline fermentation system reduces the requirement for fresh water during production. Non-agricultural feedstock like marine microalgae may provide a solution to sustainable biomass supply.

This review does not cover the economic feasibility of producing bioethanol from hypersaline microalgal biomass. Nor has it assessed the comparative costs with existing processes that use agricultural crops. Additionally, the process engineering challenges associated with a hypersaline process have not been reviewed. Although the sole focus has been on bioethanol as the end product, the principle consideration for use of a hypersaline biomass remains the same regardless of the eventual end product. Indeed, there is likely significant value in other energy products such as butanol that may be similarly converted.

## REFERENCES

[1] Australian Academy of Science. The science of climate change: questions and answers. Canberra, ACT: Australian Academy of Science; 2010.
[2] Aleklett K, Höök M, Jakobsson K, Lardelli M, Snowden S, Söderbergh B. The peak of the oil age – analyzing the world oil production reference scenario in world energy outlook 2008. Energy Policy 2010;38:1398–414.
[3] International Energy Agency. World energy outlook. Paris, France: OECD Publishing; 2009.
[4] Sims R, Taylor M, Saddler J, Mabee W. From 1st- to 2nd-generation biofuel technologies: an overview of current industry and RD&D activities. Int Energ Agency 2008.
[5] Balat M, Balat H. Recent trends in global production and utilization of bio-ethanol fuel. Appl Energ 2009;86:2273–82.
[6] Pidol L, Lecointe B, Starck L, Jeuland N. Ethanol-biodiesel-diesel fuel blends: performances and emissions in conventional diesel and advanced low temperature combustions. Fuel 2012;93:329.
[7] Sayin C. Engine performance and exhaust gas emissions of methanol and ethanol–diesel blends. Fuel 2010;89:3410–5.
[8] Moore A. Biofuels are dead: long live biofuels(?) – part one. New Biotechnol 2008;25:6–12.
[9] Moore A. Biofuels are dead: long live biofuels(?) – part two. New Biotechnol 2008;25:96–100.
[10] Hill JD, Fargione JE, Plevin RJ. The ecological impact of biofuels. Annu Rev Ecol Evol Syst 2010;41:351–77.

[11] Kocoloski M, Matthews HS, Griffin WM. Indirect land use change and biofuel policy. Environ Res Lett 2009;4.
[12] John RP, Anisha GS, Nampoothiri KM, Pandey A. Micro and macroalgal biomass: a renewable source for bioethanol. Bioresour Technol 2011;102:186–93.
[13] Wargacki AJ, Leonard E, Win MN, Regitsky DD, Santos CNS, Kim PB, et al. An engineered microbial platform for direct biofuel production from brown macroalgae. Science 2012;335:308–13.
[14] Potts T, Du J, Paul M, May P, Beitle R, Hestekin J. The production of butanol from Jamaica Bay macro algae. Environ Prog Sustainable Energy 2012;31:29–36.
[15] Huesemann MH, Kuo L-J, Urquhart L, Gill GA, Roesijadi G. Acetone-butanol fermentation of marine macroalgae. Bioresour Technol 2012;108:305–9.
[16] Dürre P. Fermentative butanol production. Ann N Y Acad Sci 2008;1125:353–62.
[17] Borowitzka M, Moheimani N. Sustainable biofuels from algae. Mitig Adapt Strat Global Change. 07 December 2010. http://dx.doi.org/10.1007/s11027-010-9271-9.
[18] Gauder M, Graeff-Ho¨ nninger S, Claupein W. The impact of a growing bioethanol industry on food production in Brazil. Appl Energ 2011;88:672–9.
[19] Fon Sing S, Isdepsky A, Borowitzka M, Moheimani N. Production of biofuels from microalgae. Mitigation Adaptation Strateg Glob Change. 26 April 2011. http://dx.doi.org/10.1007/s11027-011-9294-x.
[20] Stephens E, Ross IL, King Z, Mussgnug JH, Kruse O, Posten C, et al. An economic and technical evaluation of microalgal biofuels. Nat Biotechnol 2010;28:126–8.
[21] Nakas JP, Schaedle M, Parkinson CM, Coonley CE, Tanenbaum SW. System development for linked-fermentation production of solvents from algal biomass. Appl Environ Microbiol 1983;46:1017–23.
[22] Harun R, Danquah MK. Influence of acid pre-treatment on microalgal biomass for bioethanol production. Process Biochem 2011;46:304–9.
[23] Harun R, Danquah MK, Forde GM. Microalgal biomass as a fermentation feedstock for bioethanol production. J Chem Technol Biot 2010;85:199–203.
[24] Hirano A, Ueda R, Hirayama S, Ogushi Y. $CO_2$ fixation and ethanol production with microalgal photosynthesis and intracellular anaerobic fermentation. Energy 1997;22:137–42.
[25] Hirayama S, Ueda R, Ogushi Y, Hirano A, Samejima Y, Hon-Nami K, et al. Ethanol production from carbon dioxide by fermentative microalgae. Adv Chem Converse Mitig Carbon Dioxide 1998;114:657–60.
[26] Shirai F, Kunii K, Sato C, Teramoto Y, Mizuki E, Murao S, et al. Cultivation of microalgae in the solution from the desalting process of soy sauce waste treatment and utilization of the algal biomass for ethanol fermentation. World J Microb Biot 1998;14:839–42.
[27] Nguyen MT, Choi SP, Lee J, Lee JH, Sim SJ. Hydrothermal acid pretreatment of Chlamydomonas reinhardtii biomass for ethanol production. J Microbiol Biotech 2009;19:161–6.
[28] Ueda R, Hirayama S, Sugata K, Nakayama H. Process for the production of ethanol from microalgae. United States Patent. 26 November 1996. United States. 5578472. Mitsubishi Jukogyo Kabushiki Kaisha (Tokyo, JP).
[29] Woods PR, Smith CR, Kramer D, Enke H, Baier K, Duhring U, et al. Genetically modified cyanobacteria for the production of ethanol, 18. United States: Patent Application Publication; March 2010. US 2010/0068776 A1. Algenol Biofuels, Inc. (Baltimore, MD, US).
[30] Jones DL. Potential air emission impacts of cellulosic ethanol production at seven demonstration refineries in the United States. J Air Waste Manage Assoc 2010;60:1118–43.
[31] Lin Y, Tanaka S. Ethanol fermentation from biomass resources: current state and prospects. Appl Microbiol Biotechnol 2006;69:627–42.
[32] Sivakumar G, Vail DR, Xu J, Burner DM, Lay Jr JO, Ge X, et al. Bioethanol and biodiesel: alternative liquid fuels for future generations. Eng Life Sci 2010;10:8–18.
[33] Wyman CE. Biomass ethanol: technical progress, opportunities, and commercial challenges. Annu Rev Energ Env 1999;24:189–226.
[34] Archibald AR, Hirst EL, Ryley JF, Manners DJ. Studies on the metabolism of the protozoa. Part VIII. The molecular structure of a starch-type polysaccharide from Chilomonas paramecium. J Chem Soc 1960:556–60.
[35] Eddy BP, Fleming ID, Manners DJ. α-1:4-Glucosans. Part IX. The molecular structure of a starch-type polysaccharide from Dunaliella bioculata. J Chem Soc 1958:2827–30.
[36] Hirst E, Manners DJ, Pennie IR. α-(1-4)-D-Glucans Part XXI. Molecular structure of starch-type polysaccharides from Haematococcus pluvialis and Tetraselmis carteriiformis. Carbohyd Res 1972;22:5–11.
[37] Olaitan SA, Northcote DH. Polysaccharides of Chlorella pyrenoidosa. Biochem J 1962;82:509–19.
[38] Suzuki H. Starch-type polysaccharide and mannitol in Platymonas. Phytochemistry 1974;13:1159–60.
[39] Wilkinson IA, Stacey M, Bourne EJ. The composition of the polysaccharide synthesised by Polytomella coeca. J Chem Soc 1950:2694–8.
[40] Ball SG. The Intricate pathway of starch Biosynthesis and degradation in the Monocellular alga Chlamydomonas reinhardtii. Aust J Chem 2002;55:49–59.
[41] Dauvillée D, Deschamps P, Ral J-P, Plancke C, Putaux J-L, Devassine J, et al. Genetic dissection of floridean starch synthesis in the cytosol of the model dinoflagellate Crypthecodinium cohnii. Proc Natl Acad Sci 2009;106:21126–30.
[42] Monfils AK, Triemer RE, Bellairs EF. Characterization of paramylon morphological diversity in photosynthetic euglenoids (Euglenales, Euglenophyta). Phycologia 2011;50:156–69.
[43] Northcote DH, Goulding KJ, Horne RW. The chemical composition and structure of the cell wall of Chlorella pyrenoidosa. Biochem J 1958;70:391–7.
[44] Miller DH, Lamport DTA, Miller M. Hydroxyproline heterooligosaceharides in Chlamydomonas. Science 1972;176:918–20.
[45] Becker D, Kamerling JP, Becker B, Melkonian M. 2-Keto-sugar acids in green flagellates: a chemical marker for Prasinophycean scales. J Phycol 1991;27:498–504.
[46] Allard B. Carbohydrate composition and characterization of sugars from the green microalga Botryococcus braunii. Phytochemistry 1990;29:1875–8.
[47] Ben-Amotz A, Avron M. Role of glycerol in osmotic regulation of halophilic alga Dunaliella parva. Plant Physiol 1973;51:875–8.
[48] Mackay MA, Norton RS, Borowitzla LJ. Organic osmoregulatory solutes in cyanobacteria. J Gen Microbiol 1984;130:2177–91.
[49] Choi SP, Nguyen MT, Sim SJ. Enzymatic pretreatment of Chlamydomonas reinhardtii biomass for ethanol production. Bioresour Technol 2010;101:5330–6.
[50] Matsumoto M, Yokouchi H, Suzuki N, Ohata H, Matsunaga T. Saccharification of marine microalgae using marine bacteria for ethanol production. Appl Biochem Biotechnol 2003;105:247–54.
[51] Thomas WH, Seibert DLR, Alden M, Neori A, Eldridge P. Yields, photosynthetic efficiencies and proximate composition of dense marine microalgal cultures. II. Dunaliella primolecta and Tetraselmis suecica experiments. Biomass London 1984;5:211–25.
[52] Dragone G, Fernandes BD, Abreu AP, Vicente AA, Teixeira JA. Nutrient limitation as a strategy for increasing starch accumulation in microalgae. Appl Energ 2011;88:3331–5.
[53] Lee S, Oh Y, Kim D, Kwon D, Lee C, Lee J. Converting carbohydrates extracted from marine algae into ethanol

using various ethanolic Escherichia coli strains. Appl Biochem Biotechnol 2011;164:878–88.
[54] Chen JY, Hung TC, Fu CC, Wu WT, Su CH. Hydrolysis of microalgae cell walls for production of reducing sugar and lipid extraction. Bioresour Technol 2010;101:8750–4.
[55] Oren A. Industrial and environmental applications of halophilic microorganisms. Environ Technol 2010;31:825–34.
[56] Ventosa A, Martín S, Sánchez-Porro C, Mellado E. Halophilic archaea and bacteria as a source of extracellular hydrolytic enzymes. In: Adaptation to Life at high salt concentrations in archaea, bacteria, and Eukarya. Dordrecht: Springer Netherlands; 2005. 337–354.
[57] Chakraborty S, Khopade A, Kokare C, Mahadik K, Chopade B. Isolation and characterization of novel α-amylase from marine Streptomyces sp. D1. J Mol Catal B-Enzym 2008;58:17–23.
[58] Vasisht N, Bolhuis A, Hutcheon GW. Characterisation of a highly stable α-amylase from the halophilic archaeon Haloarcula hispanica. Extremophiles 2005;9:487–95.
[59] Duan X, Sheng J, Wang L, Chi Z, Li H, Wu L. Glucoamylase production by the marine yeast Aureobasidium pullulans N13d and hydrolysis of potato starch granules by the enzyme. Process Biochem 2006;42:462–5.
[60] Oren A. A thermophilic amyloglucosidase from Halobacterium sodomense, a halophilic bacterium from the Dead Sea. Curr Microbiol 1983;8:225–30.
[61] Fukushima T, Mizuki T, Echigo A, Inoue A, Usami R. Organic solvent tolerance of halophilic α-amylase from a Haloarchaeon, Haloarcula sp. strain S-1. Extremophiles 2005;9:85–9.
[62] Shafiei M, Ziaee AA, Amoozegar MA. Purification and characterization of an organic-solvent-tolerant halophilic α-amylase from the moderately halophilic Nesterenkonia sp. strain F. J Ind Microbiol Biotechnol 2011;38:275–81.
[63] Gfeller RP, Gibbs M. Fermentative metabolism of Chlamydomonas reinhardtii: I. analysis of fermentative products from starch in dark and light. Plant Physiol 1984;75:212–8.
[64] van der Oost J, Bulthuis BA, Feitz S, Krab K, Kraayenhof R. Fermentation metabolism of the unicellular cyanobacterium Cyanothece PCC 7822. Arch Microbiol 1989;152:415–9.
[65] Ueno Y, Kurano N, Miyachi S. Ethanol production by dark fermentation in the marine green alga, Chlorococcum littorale. J Ferment Bioeng 1998;86:38–43.
[66] Heyer H, Krumbein WE. Excretion of fermentation products in dark and anaerobically incubated cyanobacteria. Arch Microbiol 1991;155:284–7.
[67] Puig S, Coma M, van Loosdrecht MCM, Colprim J, Balaguer MD. Biological nutrient removal in a sequencing batch reactor using ethanol as carbon source. J Chem Technol Biot 2007;82:898–904.
[68] Deng MD, Coleman JR. Ethanol synthesis by genetic engineering in cyanobacteria. Appl Environ Microbiol 1999; 65:523–8.
[69] Duhring U, Enke H, Kramer D, Smith CR, Woods PR, Baier K, et al. Genetically modified photoautotrophic ethanol producing host cells, method for producing the host cells, constructs for the transformation of the host cells, method for testing a photoautotrophic strain for a desired growth property and method of producing ethanol using the host cells, 25. United States: Patent Application Publication; November 2010. US 2010/0297736 A1. Algenol Biofuels, Inc. (Bonita Springs, FL, US).
[70] Woods PR, Legere E, Moll B, Unamunzaga C, Mantecon E. Closed photobioreactor system for continued daily in situ production, separation, collection, and removal of ethanol from genetically enhanced photosynthetic organisms. United States Patent. 23 March 2010. United States. US 7682821 B2. Algenol Biofuels Switzerland GmbH (Zug, CH).
[71] Borowitzka MA. Commercial production of microalgae: ponds, tanks, tubes and fermenters. 1–3 ed. Elsevier; 1999. p. 313–21.
[72] Davis R, Aden A, Pienkos PT. Techno-economic analysis of autotrophic microalgae for fuel production. Appl Energ 2011; 88:3524–31.
[73] Soccol CR, Vandenberghe LPdS, Medeiros ABP, Karp SG, Buckeridge M, Ramos LP, et al. Bioethanol from lignocelluloses: status and perspectives in Brazil. Bioresour Technol 2010;101:4820–5.
[74] Nations United. World population prospects: the 2006 revision. New York, NY: Department of Economic & Social Affairs; 2007.
[75] Schneider UA, Havlík P, Schmid E, Valin H, Mosnier A, Obersteiner M, et al. Impacts of population growth, economic development, and technical change on global food production and consumption. Agr Syst 2011;104:204–15.
[76] Brown MR. The amino-acid and sugar composition of 16 species of microalgae used in mariculture. J Exp Mar Biol Ecol 1991;145:79–99.
[77] Liu ZY, Wang GC, Zhou BC. Effect of iron on growth and lipid accumulation in Chlorella vulgaris. Bioresour Technol 2008;99: 4717–22.
[78] Bold HC, Wynne MJ. Introduction to the algae: structure and reproduction. Englewood Cliffs, N.J: Prentice-Hall; 1985.
[79] Barsanti L, Gualtieri P. Algae: anatomy, biochemistry, and biotechnology. 1 ed. CRC Press; 2006.
[80] Størseth TR, Hansen K, Reitan KI, Skjermo J. Structural characterization of β-D-(1→3)-glucans from different growth phases of the marine diatoms Chaetoceros mülleri and Thalassiosira weissflogii. Carbohyd Res 2005;340:1159–64.
[81] Hirokawa Y, Fujiwara S, Suzuki M, Akiyama T, Sakamoto M, Kobayashi S, et al. Structural and physiological studies on the storage β-polyglucan of haptophyte Pleurochrysis haptonemofera. Planta 2008;227:589–99.
[82] Becker B, Hård K, Melkonian M, Kamerling JP, Vliegenthart JFG. Identification of 3-deoxy-manno-2-octulosonic acid, 3-deoxy-5-O-methyl-manno-2-octulosonic acid and 3-deoxy-lyxo-2-heptulosaric acid in the cell wall (theca) of the green alga Tetraselmis striata Butcher (Prasinophyceae). Eur J Biochem 1989;182:153–60.
[83] Blumreisinger M, Meindl D, Loos E. Cell wall composition of Chlorococcal algae. Phytochemistry 1983;22:1603–4.
[84] Chiovitti A, Higgins MJ, Harper RE, Wetherbee R, Bacic A. The complex polysaccharides of the raphid diatom Pinnularia viridis (Bacillariophyceae). J Phycol 2003;39:543–54.
[85] Dai J, Wu Y, Chen SW, Zhu S, Yin HP, Wang M, et al. Sugar compositional determination of polysaccharides from Dunaliella salina by modified RP-HPLC method of precolumn derivatization with 1-phenyl-3-methyl-5-pyrazolone. Carbohyd Polym 2010;82:629–35.
[86] Gooday GW. Biochemical and autoradiographic study of role of golgi bodies in thecal formation in Platymonas tetrathele. J Exp Bot 1971;22:959–71.

# References


Abedinifar, S, Karimi, K, Khanahmadi, M & Taherzadeh, MJ (2009), 'Ethanol production by Mucor indicus and Rhizopus oryzae from rice straw by separate hydrolysis and fermentation', *Biomass and Bioenergy*, vol. 33, no. 5, pp. 828-833.

Aikawa, S, Joseph, A, Yamada, R, Izumi, Y, Yamagishi, T, Matsuda, F, Kawai, H, Chang, J-S, Hasunuma, T & Kondo, A (2013), 'Direct conversion of Spirulina to ethanol without pretreatment or enzymatic hydrolysis processes', *Energy & Environmental Science*, vol. 6, no. 6, pp. 1844-1849.

Aleklett, K, Höök, M, Jakobsson, K, Lardelli, M, Snowden, S & Söderbergh, B (2010), 'The peak of the Oil Age - analyzing the world oil production Reference Scenario in World Energy Outlook 2008', *Energy Policy*, vol. 38, no. 3, pp. 1398-1414.

Allard, B (1990), 'Carbohydrate composition and characterization of sugars from the green microalga *Botryococcus braunii*', *Phytochemistry*, vol. 29, no. 6, pp. 1875-1878.

Alvira, P, Tomás-Pejó, E, Ballesteros, M & Negro, MJ (2010), 'Pretreatment technologies for an efficient bioethanol production process based on enzymatic hydrolysis: A review', *Bioresource Technology*, vol. 101, no. 13, pp. 4851-4861.

American Society for Testing and Materials International (2013), *Standard practice for the preparation of substitute ocean water,* (D1141-98(2008)), American Society for Testing and Materials International, Philadelphia, PA.

Ammor, M (2007), 'Recent Advances in the Use of Intrinsic Fluorescence for Bacterial Identification and Characterization', *Journal of Fluorescence*, vol. 17, no. 5, pp. 455-459.

Andersen, RA (2005), *Algal culturing techniques*, Academic Press.

Archibald, AR, Hirst, EL, Ryley, JF & Manners, DJ (1960), 'Studies on the metabolism of the protozoa. Part VIII. The molecular structure of a starch-type polysaccharide from *Chilomonas paramecium*', *Journal of the Chemical Society*, pp. 556-560.

Arora, M, Anil, AC, Delany, J, Rajarajan, N, Emami, K & Mesbahi, E (2012), 'Carbohydrate-degrading bacteria closely associated with Tetraselmis indica: influence on algal growth', *Aquatic Biology*, vol. 15, no. 1, pp. 61-71.

Australian Academy of Science (2010), *The science of climate change: questions and answers*, Australian Academy of Science, Canberra, ACT.

Balat, M & Balat, H (2009), 'Recent trends in global production and utilization of bio-ethanol fuel', *Applied Energy*, vol. 86, no. 11, pp. 2273-2282.

Ball, SG (2002), 'The Intricate Pathway of Starch Biosynthesis and Degradation in the Monocellular Alga *Chlamydomonas reinhardtii*', *Australian Journal of Chemistry*, vol. 55, no. 2, pp. 49-59.

Barsanti, L, Coltelli, P, Evangelista, V, Frassanito, AM, Passarelli, V, Vesentini, N & Gualtieri, P 2008, 'The World of Algae', Springer Netherlands, Dordrecht, pp. 1-15.

Barsanti, L & Gualtieri, P (2006), *Algae: anatomy, biochemistry, and biotechnology*, 1 edn, CRC Press.

Becker, B, Hård, K, Melkonian, M, Kamerling, JP & Vliegenthart, JFG (1989), 'Identification of 3-deoxy-*manno*-2-octulosonic acid, 3-deoxy-5-*O*-methyl-*manno*-2-octulosonic acid and 3-deoxy-*lyxo*-2-heptulosaric acid in the cell wall (theca) of the green alga *Tetraselmis striata* Butcher (Prasinophyceae)', *European Journal of Biochemistry*, vol. 182, no. 1, pp. 153-160.

Becker, B, Melkonian, M & Kamerling, JP (1998), 'The cell wall (theca) of *Tetraselmis striata* (Chlorophyta): Macromolecular composition and structural elements of the complex polysaccharides', *Journal of Phycology*, vol. 34, pp. 779-787.

Becker, D, Kamerling, JP, Becker, B & Melkonian, M (1991), '2-Keto-sugar acids in green flagellates: a chemical marker for Prasinophycean scales', *Journal of Phycology*, vol. 27, no. 4, pp. 498-504.

BeMiller, JN, Whistler, RL & Shaw, DH (1993), *Methods in Carbohydrate Chemistry, Lipopolysaccharides, Separation and Analysis, Glycosylated Polymers*, Wiley.

Ben-Amotz, A & Avron, M (1973), 'Role of glycerol in osmotic regulation of halophilic alga *Dunaliella parva*', *Plant Physiology*, vol. 51, no. 5, pp. 875-878.

Bidwell, J & Spotte, S (1985), 'Artificial seawaters, formulas and methods. Jones and Barlett Publishers', *Inc. Boston*.

Blomberg, A & Adler, L 1992, 'Physiology of Osmotolerance in Fungi1', in AH Rose (ed.), *Advances in Microbial Physiology*, vol. Volume 33, Academic Press, pp. 145-212.

Blumreisinger, M, Meindl, D & Loos, E (1983), 'Cell wall composition of Chlorococcal algae', *Phytochemistry*, vol. 22, no. 7, pp. 1603-1604.

Bold, HC & Wynne, MJ (1985), *Introduction to the algae: structure and reproduction*, Prentice-Hall, Englewood Cliffs, N.J.

Bondioli, P, Della Bella, L, Rivolta, G, Chini Zittelli, G, Bassi, N, Rodolfi, L, Casini, D, Prussi, M, Chiaramonti, D & Tredici, MR (2012), 'Oil production by the marine microalgae *Nannochloropsis* sp. F&M-M24 and *Tetraselmis suecica* F&M-M33', *Bioresource Technology*, vol. 114, no. 0, pp. 567-572.

Borowitzka, M & Moheimani, N (2013), 'Sustainable biofuels from algae', *Mitigation and Adaptation Strategies for Global Change*, vol. 18, no. 1, pp. 13-25.

Borowitzka, MA (1999), 'Commercial production of microalgae: ponds, tanks, tubes and fermenters', vol. 70, pp. 313-321.

Brancoli, P, Ferreira, JA, Bolton, K & Taherzadeh, MJ (2017), 'Changes in carbon footprint when integrating production of filamentous fungi in 1st generation ethanol plants', *Bioresource Technology*.

Brennan, L & Owende, P (2010), 'Biofuels from microalgae-A review of technologies for production, processing, and extractions of biofuels and co-products', *Renewable & Sustainable Energy Reviews*, vol. 14, no. 2, pp. 557-577.

Brown, MR (1991), 'The amino-acid and sugar composition of 16 species of microalgae used in mariculture', *Journal of Experimental Marine Biology and Ecology*, vol. 145, no. 1, pp. 79-99.

Brown, MR & Jeffrey, SW (1992), 'Biochemical-composition of microalgae from the green algal classes Chlorophyceae and Prasinophyceae. 1. Amino-acids, sugars and pigments', *Journal of Experimental Marine Biology and Ecology*, vol. 161, no. 1, pp. 91-113.

Bureau of Meteorology (2018), *Daily global solar exposure - Karratha Aero*, Australia Government, accessed [18 August 2018], <http://www.bom.gov.au/jsp/ncc/cdio/weatherData/av?p_display_type=dailyDataFile&p_nccObsCode=193&p_stn_num=004083&p_c=-3468085&p_startYear=2012>.

Butinar, L, Zalar, P, Frisvad, JC & Gunde-Cimerman, N (2005), 'The genus Eurotium– members of indigenous fungal community in hypersaline waters of salterns', *FEMS Microbiology Ecology*, vol. 51, no. 2, pp. 155-166.

Canet, A, Benaiges, MD, Valero, F & Adlercreutz, P (2017), 'Exploring substrate specificities of a recombinant Rhizopus oryzae lipase in biodiesel synthesis', *New Biotechnology*, vol. 39, no. Part A, pp. 59-67.

Cantabrana, I, Perise, R & Hernández, I (2015), 'Uses of Rhizopus oryzae in the kitchen', *International Journal of Gastronomy and Food Science*, vol. 2, no. 2, pp. 103-111.

Chakraborty, S, Khopade, A, Kokare, C, Mahadik, K & Chopade, B (2008), 'Isolation and characterization of novel *α*-amylase from marine *Streptomyces* sp. D1', *Journal of Molecular Catalysis B: Enzymatic*, vol. 58, pp. 17-23.

Chen, JY, Hung, TC, Fu, CC, Wu, WT & Su, CH (2010), 'Hydrolysis of microalgae cell walls for production of reducing sugar and lipid extraction', *Bioresource Technology*, vol. 101, no. 22, pp. 8750-8754.

Chernova, NI & Kiseleva, SV (2017), 'Microalgae biofuels: Induction of lipid synthesis for biodiesel production and biomass residues into hydrogen conversion', *International Journal of Hydrogen Energy*, vol. 42, no. 5, pp. 2861-2867.

Cherry, JR & Fidantsef, AL (2003), 'Directed evolution of industrial enzymes: an update', *Current Opinion in Biotechnology*, vol. 14, no. 4, pp. 438-443.

Chiovitti, A, Higgins, MJ, Harper, RE, Wetherbee, R & Bacic, A (2003), 'The complex polysaccharides of the raphid diatom *Pinnularia viridis* (Bacillariophyceae)', *Journal of Phycology*, vol. 39, no. 3, pp. 543-554.

Chisti, Y (2007), 'Biodiesel from microalgae', *Biotechnology Advances*, vol. 25, no. 3, pp. 294-306.

Choi, SP, Nguyen, MT & Sim, SJ (2010), 'Enzymatic pretreatment of *Chlamydomonas reinhardtii* biomass for ethanol production', *Bioresource Technology*, vol. 101, no. 14, pp. 5330-5336.

Christensen, T, Woeldike, H, Boel, E, Mortensen, SB, Hjortshoej, K, Thim, L & Hansen, MT (1988), 'High level expression of recombinant genes in Aspergillus oryzae', *Nature Biotechnology*, vol. 6, no. 12, p. 1419.

Comino, P, Shelat, K, Collins, H, Lahnstein, J & Gidley, MJ (2013), 'Separation and Purification of Soluble Polymers and Cell Wall Fractions from Wheat, Rye and Hull less Barley Endosperm Flours for Structure-Nutrition Studies', *Journal of Agricultural and Food Chemistry*, vol. 61, no. 49, pp. 12111-12122.

Dai, J, Wu, Y, Chen, SW, Zhu, S, Yin, HP, Wang, M & Tang, J (2010), 'Sugar compositional determination of polysaccharides from *Dunaliella salina* by modified RP-HPLC method of precolumn derivatization with 1-phenyl-3-methyl-5-pyrazolone', *Carbohydrate Polymers*, vol. 82, no. 3, pp. 629-635.

Dalterio, RA, Nelson, WH, Britt, D, Sperry, JF, Tanguay, JF & Suib, SL (1987), 'The Steady-State and Decay Characteristics of Primary Fluorescence From Live Bacteria', *Applied Spectroscopy*, vol. 41, no. 2, pp. 234-241.

Dauvillée, D, Deschamps, P, Ral, J-P, Plancke, C, Putaux, J-L, Devassine, J, Durand-Terrasson, A, Devin, A & Ball, SG (2009), 'Genetic dissection of floridean starch synthesis in the cytosol of the model dinoflagellate *Crypthecodinium cohnii*', *Proceedings of the National Academy of Sciences*, vol. 106, no. 50, pp. 21126-21130.

Davis, R, Aden, A & Pienkos, PT (2011), 'Techno-economic analysis of autotrophic microalgae for fuel production', *Applied Energy*, vol. 88, no. 10, pp. 3524-3531.

Day, JG, Thomas, NJ, Achilles-Day, UE & Leakey, RJ (2012), 'Early detection of protozoan grazers in algal biofuel cultures', *Bioresource Technology*, vol. 114, pp. 715-719.

Deng, MD & Coleman, JR (1999), 'Ethanol synthesis by genetic engineering in cyanobacteria', *Applied and Environmental Microbiology*, vol. 65, no. 2, pp. 523-528.

Doan, QC, Moheimani, NR, Mastrangelo, AJ & Lewis, DM (2012), 'Microalgal biomass for bioethanol fermentation: Implications for hypersaline systems with an industrial focus', *Biomass and Bioenergy*, vol. 46, pp. 79-88.

Doan, QC, Moheimani, NR, Mastrangelo, AJ & Lewis, DM (2013), 'Corrigendum to “Microalgal biomass for bioethanol fermentation: Implications for hypersaline systems with an industrial focus” [Biomass Bioenergy 46 (2012) 79–88]', *Biomass and Bioenergy*, vol. 58, pp. 406-407.

Doddema, H & Vogels, G (1978), 'Improved identification of methanogenic bacteria by fluorescence microscopy', *Applied and Environmental Microbiology*, vol. 36, no. 5, pp. 752-754.

Domozych, DS, Ciancia, M, Fangel, JU, Mikkelsen, MD, Ulvskov, P & Willats, WGT (2012), 'The cell walls of green algae: a journey through evolution and diversity', *Frontiers in plant science*, vol. 3.

Domozych, DS, Stewart, KD & Mattox, KR (1981), 'Development of the cell wall in *Tetraselmis*: role of the Golgi apparatus and extracellular wall assembly', *Journal of Cell Science*, vol. 52, no. 1, pp. 351-371.

Dörsam, S, Fesseler, J, Gorte, O, Hahn, T, Zibek, S, Syldatk, C & Ochsenreither, K (2017), 'Sustainable carbon sources for microbial organic acid production with filamentous fungi', *Biotechnology for Biofuels*, vol. 10, no. 1, p. 242.

Dragone, G, Fernandes, BD, Abreu, AP, Vicente, AA & Teixeira, JA (2011), 'Nutrient limitation as a strategy for increasing starch accumulation in microalgae', *Applied Energy*, vol. 88, no. 10, pp. 3331-3335.

Duan, X, Sheng, J, Wang, L, Chi, Z, Li, H & Wu, L (2006), 'Glucoamylase production by the marine yeast *Aureobasidium pullulans* N13d and hydrolysis of potato starch granules by the enzyme', *Process Biochemistry*, vol. 42, no. 3, pp. 462-465.

Dubois, M, Gilles, KA, Hamilton, JK, Rebers, PA & Smith, F (1956), 'Colorimetric method for determination of sugars and related substances', *Analytical Chemistry*, vol. 28, no. 3, pp. 350-356.

Duhring, U, Enke, H, Kramer, D, Smith, CR, Woods, PR, Baier, K & Oesterhelt, C (2010), *Genetically modified photoautotrophic ethanol producing host cells, method for producing the host cells, constructs for the transformation of the host cells, method for testing a photoautotrophic strain for a desired growth property and method of producing ethanol using the host cells*, Algenol Biofuels, Inc. (Bonita Springs, FL, US), US 2010/0297736 A1, United States.

Dürre, P (2008), 'Fermentative Butanol Production', *Annals of the New York Academy of Sciences*, vol. 1125, no. 1, pp. 353-362.

Eaton, AD, Clesceri, LS, Greenberg, AE & Franson, MAH (1998), *Standard methods for the examination of water and wastewater*, 4500-NC Persulfate method, vol. 1268, American Public Health Association, Washington, DC.

Eddy, BP, Fleming, ID & Manners, DJ (1958), '$\alpha$-1:4-Glucosans. Part IX. The molecular structure of a starch-type polysaccharide from *Dunaliella bioculata*', *Journal of the Chemical Society*, pp. 2827-2830.

Edge, PA & Ricketts, TR (1977), 'Effect of nitrogen refeeding on carbohydrate content into nitrogen-starved cells of *Platymonas striata* Butcher', *Planta*, vol. 136, no. 2, pp. 159-162.

El-Kady, IA, Moubasher, MH & Eman Mostafa, M (1994), 'Glycerol production by two filamentous fungi grown at different ionic and nonionic osmotics and cheese whey', *Folia Microbiologica*, vol. 39, no. 3, pp. 203-207.

Evans, S, Hansen, RW, Stone, HM & Schneegurt, MA (2013), 'Isolation and Characterization of Halotolerant Soil Fungi from the Great Salt Plains of Oklahoma (USA)', *Cryptogamie, Mycologie*, vol. 34, no. 4, pp. 329-341.

FazeliNejad, S, Ferreira, JA, Brandberg, T, Lennartsson, PR & Taherzadeh, MJ (2016), 'Fungal protein and ethanol from lignocelluloses using Rhizopus pellets under simultaneous saccharification, filtration and fermentation (SSFF)', *Biofuel Research Journal*, vol. 3, no. 1, pp. 372-378.

Fiedurek, J (1998), 'Effect of osmotic stress on glucose oxidase production and secretion by Aspergillus niger', *Journal of Basic Microbiology*, vol. 38, no. 2, pp. 107-112.

Fon Sing, S (2010), 'Strain selection and outdoor cultivation of halophilic microalgae with potential for large-scale biodiesel production', PhD Thesis thesis, Murdoch University.

Fon Sing, S & Borowitzka, MA (2015), 'Isolation and screening of euryhaline *Tetraselmis* spp. suitable for large-scale outdoor culture in hypersaline media for biofuels', *Journal of Applied Phycology*, pp. 1-14.

Fon Sing, S, Isdepsky, A, Borowitzka, M & Moheimani, N (2011), 'Production of biofuels from microalgae', *Mitigation and Adaptation Strategies for Global Change*, 26 April 2011, pp. 1-26, DOI 10.1007/s11027-011-9294-x, <http://dx.doi.org/10.1007/s11027-011-9294-x>.

Fon Sing, S, Isdepsky, A, Borowitzka, MA & Lewis, DM (2014), 'Pilot-scale continuous recycling of growth medium for the mass culture of a halotolerant Tetraselmis sp. in raceway ponds under

increasing salinity: a novel protocol for commercial microalgal biomass production', *Bioresource Technology*, vol. 161, pp. 47-54.

Food & Drug Administration (2017), *Code of Federal Regulations Title 21 Food and Drugs, Part 173 Secondary direct food additives permitted in food for human consumption, Subpart B Enzyme preparations and microorganisms, Section 173.130 Carbohydrase derived from Rhizopus oryzae*, U.S. Department of Health & Human Services, accessed [01 April 2017], <https://www.accessdata.fda.gov/scripts/cdrh/cfdocs/cfcfr/CFRSearch.cfm?fr=173.130>.

Fukushima, T, Mizuki, T, Echigo, A, Inoue, A & Usami, R (2005), 'Organic solvent tolerance of halophilic *α*-amylase from a Haloarchaeon, *Haloarcula* sp. strain S-1', *Extremophiles*, vol. 9, no. 1, pp. 85-89.

Gauder, M, Graeff-Hönninger, S & Claupein, W (2011), 'The impact of a growing bioethanol industry on food production in Brazil', *Applied Energy*, vol. 88, no. 3, pp. 672-679.

Gfeller, RP & Gibbs, M (1984), 'Fermentative metabolism of *Chlamydomonas reinhardtii*: I. analysis of fermentative products from starch in dark and light', *Plant Physiology*, vol. 75, no. 1, pp. 212-218.

Ghosh, B & Ray, RR (2011), 'Current commercial perspective of Rhizopus oryzae: a review', *J Appl Sci*, vol. 11, pp. 2470-2486.

Gong, C-s, Maun, CM & Tsao, GT (1981), 'Direct fermentation of cellulose to ethanol by a cellulolytic filamentous fungus, Monilia sp', *Biotechnology Letters*, vol. 3, no. 2, pp. 77-82.

González-Fernández, C & Ballesteros, M (2012), 'Linking microalgae and cyanobacteria culture conditions and key-enzymes for carbohydrate accumulation', *Biotechnology Advances*, vol. 30, no. 6, pp. 1655-1661.

Gooday, GW (1971a), 'Biochemical and autoradiographic study of role of golgi bodies in thecal formation in *Platymonas tetrathele*', *Journal of Experimental Botany*, vol. 22, no. 73, pp. 959-971.

Gooday, GW (1971b), 'Control by light of starch degradation and cell-wall biosynthesis in Platymonas tetrathele', *The Biochemical journal*, vol. 123, no. 2, p. 3P.

Guillard, RR & Ryther, JH (1962), 'Studies of marine planktonic diatoms: I. *Cyclotella nana Hustedt*, and *Detonula confervacea* (Cleve) *Gran*', *Canadian journal of microbiology*, vol. 8, no. 2, pp. 229-239.

Gunde-Cimerman, N & Zalar, P (2014), 'Extremely Halotolerant and Halophilic Fungi Inhabit Brine in Solar Salterns Around the Globe', *Food Technology & Biotechnology*, vol. 52, no. 2, pp. 170-179.

Hahn-Hägerdal, B, Galbe, M, Gorwa-Grauslund, MF, Lidén, G & Zacchi, G (2006), 'Bio-ethanol – the fuel of tomorrow from the residues of today', *Trends in Biotechnology*, vol. 24, no. 12, pp. 549-556.

Han, W, Clarke, W & Pratt, S (2014), 'Composting of waste algae: A review', *Waste Management*, vol. 34, no. 7, pp. 1148-1155.

Hare, J (2008), 'Sabouraud agar for fungal growth protocols'.

Harun, R & Danquah, MK (2011), 'Influence of acid pre-treatment on microalgal biomass for bioethanol production', *Process Biochemistry*, vol. 46, no. 1, pp. 304-309.

Harun, R, Danquah, MK & Forde, GM (2010), 'Microalgal biomass as a fermentation feedstock for bioethanol production', *Journal of Chemical Technology and Biotechnology*, vol. 85, no. 2, pp. 199-203.

Heyer, H & Krumbein, WE (1991), 'Excretion of fermentation products in dark and anaerobically incubated cyanobacteria', *Archives of Microbiology*, vol. 155, no. 3, pp. 284-287.

Hill, JD, Fargione, JE & Plevin, RJ (2010), 'The ecological impact of biofuels', *Annual Review of Ecology, Evolution, and Systematics*, vol. 41, pp. 351-377.

Hirano, A, Ueda, R, Hirayama, S & Ogushi, Y (1997), '$CO_2$ fixation and ethanol production with microalgal photosynthesis and intracellular anaerobic fermentation', *Energy*, vol. 22, no. 2/3, pp. 137-142.

Hirayama, S, Ueda, R, Ogushi, Y, Hirano, A, Samejima, Y, Hon-Nami, K & Kunito, S (1998), 'Ethanol production from carbon dioxide by fermentative microalgae', *Advances in Chemical Conversions for Mitigating Carbon Dioxide*, vol. 114, pp. 657-660.

Hirokawa, Y, Fujiwara, S, Suzuki, M, Akiyama, T, Sakamoto, M, Kobayashi, S & Tsuzuki, M (2008), 'Structural and physiological studies on the storage β-polyglucan of haptophyte *Pleurochrysis haptonemofera*', *Planta*, vol. 227, no. 3, pp. 589-599.

Hirst, E, Manners, DJ & Pennie, IR (1972), '*α*-(1-4)-D-Glucans. Part XXI. Molecular structure of starch-type polysaccharides from *Haematococcus pluvialis* and *Tetraselmis carteriiformis*', *Carbohydrate Research*, vol. 22, no. 1, pp. 5-11.

Ho, S-H, Huang, S-W, Chen, C-Y, Hasunuma, T, Kondo, A & Chang, J-S (2013), 'Bioethanol production using carbohydrate-rich microalgae biomass as feedstock', *Bioresource Technology*, vol. 135, no. 0, pp. 191-198.

Hoekman, SK & Broch, A (2017), 'Environmental implications of higher ethanol production and use in the U.S.: A literature review. Part II – Biodiversity, land use change, GHG emissions, and sustainability', *Renewable and Sustainable Energy Reviews*.

Hoekman, SK, Broch, A & Liu, X (2017), 'Environmental implications of higher ethanol production and use in the U.S.: A literature review. Part I – Impacts on water, soil, and air quality', *Renewable and Sustainable Energy Reviews*.

Huesemann, MH, Kuo, L-J, Urquhart, L, Gill, GA & Roesijadi, G (2012), 'Acetone-butanol fermentation of marine macroalgae', *Bioresource Technology*, vol. 108, no. 0, pp. 305-309.

International Energy Agency (2009), *World energy outlook 2009*, OECD Publishing, Paris, France.

International Energy Agency (2017), *Tracking Clean Engery Progress 2017*, OECD Publishing, Paris, France.

International Energy Agency (2018a), *ETP 2017 data visualisation*, Organisation for Economic Co-operation and Development, International Energy Agency, accessed [22/04/2018], <https://www.iea.org/etp/explore/>.

International Energy Agency (2018b), *Scenarios and projections*, Organisation for Economic Co-operation and Development, International Energy Agency, accessed [22/04/2018], <http://www.iea.org/publications/scenariosandprojections/>.

International Energy Agency (2018c), *Transport*, Organisation for Economic Co-operation and Development, International Energy Agency, accessed [22/04/2018], <https://www.iea.org/topics/transport/>.

Isdepsky, A (2015), 'Saline microalgae for biofuels Outdoor culture from small-scale to pilot scale', PhD thesis, Murdoch University, <http://researchrepository.murdoch.edu.au/id/eprint/26095/>.

Iwai, M, Yokono, M, Inada, N & Minagawa, J (2010), 'Live-cell imaging of photosystem II antenna dissociation during state transitions', *Proceedings of the National Academy of Sciences*, vol. 107, no. 5, pp. 2337-2342.

John, RP, Anisha, GS, Nampoothiri, KM & Pandey, A (2011), 'Micro and macroalgal biomass: a renewable source for bioethanol', *Bioresource Technology*, vol. 102, pp. 186-193.

Jones, DL (2010), 'Potential air emission impacts of cellulosic ethanol production at seven demonstration refineries in the United States', *Journal of the Air & Waste Management Association*, vol. 60, pp. 1118-1143.

Jørgensen, H, Kristensen, JB & Felby, C (2007), 'Enzymatic conversion of lignocellulose into fermentable sugars: challenges and opportunities', *Biofuels, Bioproducts and Biorefining*, vol. 1, no. 2, pp. 119-134.

Karimi, K, Emtiazi, G & Taherzadeh, MJ (2006), 'Ethanol production from dilute-acid pretreated rice straw by simultaneous saccharification and fermentation with< i> Mucor indicus</i>,< i> Rhizopus oryzae</i>, and< i> Saccharomyces cerevisiae</i>', *Enzyme and Microbial Technology*, vol. 40, no. 1, pp. 138-144.

Kermanshahi-pour, A, Sommer, TJ, Anastas, PT & Zimmerman, JB (2014), 'Enzymatic and acid hydrolysis of *Tetraselmis suecica* for polysaccharide characterization', *Bioresource Technology*, vol. 173, no. 0, pp. 415-421.

Kiang, J, Szu, SC, Wang, L-X, Tang, M & Lee, YC (1997), 'Determination of 2-keto-3-deoxyoctulosonic acid (KDO) with high-performance anion-exchange chromatography (HPAEC): survey of stability of KDO and optimal hydrolytic conditions', *Analytical Biochemistry*, vol. 245, no. 1, pp. 97-101.

Kirk, O, Borchert, TV & Fuglsang, CC (2002), 'Industrial enzyme applications', *Current Opinion in Biotechnology*, vol. 13, no. 4, pp. 345-351.

Kirst, G (1990), 'Salinity Tolerance Of Eukaryotic Marine Algae', *Annual Review of Plant Physiology and Plant Molecular Biology*, vol. 41, no. 1, pp. 21-53.

Kocoloski, M, Matthews, HS & Griffin, WM (2009), 'Indirect land use change and biofuel policy', *Environmental Research Letters*, vol. 4, no. 034008.

Kolaei, EA, Cenatus, C, Tweddell, RJ & Avis, TJ (2013), 'Antifungal activity of aluminium-containing salts against the development of carrot cavity spot and potato dry rot', *Annals of Applied Biology*, vol. 163, no. 2, pp. 311-317.

Lane, DJ, van Eyk, PJ, Ashman, PJ, Kwong, CW, de Nys, R, Roberts, DA, Cole, AJ & Lewis, DM (2015), 'Release of cl, s, p, k, and na during thermal conversion of algal biomass', *ENERGY & FUELS*, vol. 29, no. 4, pp. 2542-2554.

Laws, EA & Berning, JL (1991), 'A study of the energetics and economics of microalgal mass culture with the marine chlorophyte *Tetraselmis suecica*: Implications for use of power plant stack gases', *Biotechnology and Bioengineering*, vol. 37, no. 10, p. 936.

Lee, A, Lewis, D, Kalaitzidis, T & Ashman, P (2016), 'Technical issues in the large-scale hydrothermal liquefaction of microalgal biomass to biocrude', *Current Opinion in Biotechnology*, vol. 38, pp. 85-89.

Lee, S, Oh, Y, Kim, D, Kwon, D, Lee, C & Lee, J (2011), 'Converting carbohydrates extracted from marine algae into ethanol using various ethanolic *Escherichia coli* strains', *Applied Biochemistry and Biotechnology*, vol. 164, no. 6, pp. 878-888.

Lennartsson, PR, Taherzadeh, MJ & Edebo, L 2014, 'Rhizopus', in CABL Tortorello (ed.), *Encyclopedia of Food Microbiology (Second Edition)*, Academic Press, Oxford, pp. 284-290.

Lennox, ES (1955), 'Transduction of linked genetic characters of the host by bacteriophage P1', *Virology*, vol. 1, no. 2, pp. 190-206.

Lewin, R (1958), 'The cell walls of Platymonas', *Journal of General Microbiology*, vol. 19, no. 1, pp. 87-90.

Lewis, LA & McCourt, RM (2004), 'Green algae and the origin of land plants', *American Journal of Botany*, vol. 91, no. 10, pp. 1535-1556.

Lide, DR (2010), *CRC handbook of chemistry and physics*, 90th edn, CRC press.

Lidén, G (2017), 'Carboxylic Acid Production', Multidisciplinary Digital Publishing Institute.

Lin, Y & Tanaka, S (2006), 'Ethanol fermentation from biomass resources: current state and prospects', *Applied Microbiology and Biotechnology*, vol. 69, no. 6, pp. 627-642.

Liu, H, Zhao, S, Jin, Y, Yue, X, Deng, L, Wang, F & Tan, T (2017), 'Production of fumaric acid by immobilized Rhizopus arrhizus RH 7-13-9# on loofah fiber in a stirred-tank reactor', *Bioresource Technology*, vol. 244, no. Part 1, pp. 929-933.

Liu, ZY, Wang, GC & Zhou, BC (2008), 'Effect of iron on growth and lipid accumulation in *Chlorella vulgaris*', *Bioresource Technology*, vol. 99, no. 11, pp. 4717-4722.

Londoño-Hernández, L, Ramírez-Toro, C, Ruiz, HA, Ascacio-Valdés, JA, Aguilar-Gonzalez, MA, Rodríguez-Herrera, R & Aguilar, CN (2017), 'Rhizopus oryzae – Ancient microbial resource with importance in modern food industry', *International Journal of Food Microbiology*, vol. 257, no. Supplement C, pp. 110-127.

Lourenço, SO, Marquez, UML, Mancini-Filho, J, Barbarino, E & Aidar, E (1997), 'Changes in biochemical profile of *Tetraselmis gracilis* I. Comparison of two culture media', *Aquaculture*, vol. 148, no. 2–3, pp. 153-168.

Mackay, MA, Norton, RS & Borowitzla, LJ (1984), 'Organic osmoregulatory solutes in cyanobacteria', *Journal of General Microbiology*, vol. 130, no. 9, pp. 2177-2191.

Masuko, T, Minami, A, Iwasaki, N, Majima, T, Nishimura, S-I & Lee, YC (2005), 'Carbohydrate analysis by a phenol–sulfuric acid method in microplate format', *Analytical Biochemistry*, vol. 339, no. 1, pp. 69-72.

Mathews, CK (1990), *Biochemistry*, ed. KE Van Holde, Benjamin/Cummings Pub. Co., Redwood City, Calif.

Matsumoto, M, Yokouchi, H, Suzuki, N, Ohata, H & Matsunaga, T (2003), 'Saccharification of marine microalgae using marine bacteria for ethanol production', *Applied Biochemistry and Biotechnology*, vol. 105, no. 1, pp. 247-254.

Megazyme (2018), *Total Starch Assay Kit (AA/AMG)*, Megazyme, accessed [17/04/2018], <https://secure.megazyme.com/Total-Starch-Assay-Kit>.

Melkonian, M (1979), 'An ultrastructural study of the flagellate *Tetraselmis cordiformis* Stein (*Chlorophyceae*) with emphasis on the flagellar apparatus', *Protoplasma*, vol. 98, no. 1-2, pp. 139-151.

Melkonian, M, Becker, B & Becker, D (1991), 'Scale formation in algae', *Journal of Electron Microscopy Technique*, vol. 17, no. 2, pp. 165-178.

Mert, HH & Dizbay, M (1977), 'The effect of osmotic pressure and salinity of the medium on the growth and sporulation of Aspergillus niger and Paecilomyces lilacinum species', *Mycopathologia*, vol. 61, no. 2, pp. 125-127.

Milano, J, Ong, HC, Masjuki, HH, Chong, WT, Lam, MK, Loh, PK & Vellayan, V (2016), 'Microalgae biofuels as an alternative to fossil fuel for power generation', *Renewable and Sustainable Energy Reviews*, vol. 58, pp. 180-197.

Millati, R, Edebo, L & Taherzadeh, MJ (2005), 'Performance of Rhizopus, Rhizomucor, and Mucor in ethanol production from glucose, xylose, and wood hydrolyzates', *Enzyme and Microbial Technology*, vol. 36, no. 2–3, pp. 294-300.

Miller, DH, Lamport, DTA & Miller, M (1972), 'Hydroxyproline heterooligosaceharides in *Chlamydomonas*', *Science*, vol. 176, no. 4037, pp. 918-920.

Miranda, J, Passarinho, PC & Gouveia, L (2012), 'Bioethanol production from Scenedesmus obliquus sugars: the influence of photobioreactors and culture conditions on biomass production', *Applied Microbiology and Biotechnology*, vol. 96, no. 2, pp. 555-564.

Moheimani, N, Borowitzka, M, Isdepsky, A & Sing, S 2013, 'Standard Methods for Measuring Growth of Algae and Their Composition', in MA Borowitzka & NR Moheimani (eds), *Algae for Biofuels and Energy*, vol. 5, Springer Netherlands, pp. 265-284.

Molina, E, Martínez, E, Sańchez, S, García, F & Contreras, A (1991), 'The influence of temperature and the initial N:P ratio on the growth of microalgae *Tetraselmis* sp.', *Process Biochemistry*, vol. 26, no. 3, pp. 183-187.

Monfils, AK, Triemer, RE & Bellairs, EF (2011), 'Characterization of paramylon morphological diversity in photosynthetic euglenoids (Euglenales, Euglenophyta)', *Phycologia*, vol. 50, no. 2, pp. 156-169.

Moore, A (2008a), 'Biofuels are dead: long live biofuels(?) - part one', *New Biotechnology*, vol. 25, no. 1, pp. 6-12.

Moore, A (2008b), 'Biofuels are dead: long live biofuels(?) - part two', *New Biotechnology*, vol. 25, no. 2/3, pp. 96-100.

Morita, H, Fukuda, T, Kawakita, H, Mamitsuka, K, Shiozawa, M, Uezu, K & Komaki, I (2004), 'Effects of Some Metal Ions on the Production of an Antibacterial Substance by <I>Rhizopus</I> sp. MKU 24', *Biocontrol Science*, vol. 9, no. 4, pp. 111-115.

Müller-Loennies, S, Lindner, B & Brade, H (2003), 'Structural Analysis of Oligosaccharides from Lipopolysaccharide (LPS) of Escherichia coli K12 Strain W3100 Reveals a Link between Inner and Outer Core LPS Biosynthesis', *Journal of Biological Chemistry*, vol. 278, no. 36, pp. 34090-34101.

Nair, RB, Kabir, MM, Lennartsson, PR, Taherzadeh, MJ & Horváth, IS (2017a), 'Integrated Process for Ethanol, Biogas, and Edible Filamentous Fungi-Based Animal Feed Production from Dilute Phosphoric Acid-Pretreated Wheat Straw', *Applied Biochemistry and Biotechnology*.

Nair, RB, Lundin, M, Lennartsson, PR & Taherzadeh, MJ (2017b), 'Optimizing dilute phosphoric acid pretreatment of wheat straw in the laboratory and in a demonstration plant for ethanol and edible fungal biomass production using Neurospora intermedia', *Journal of Chemical Technology & Biotechnology*, vol. 92, no. 6, pp. 1256-1265.

Nakas, JP, Schaedle, M, Parkinson, CM, Coonley, CE & Tanenbaum, SW (1983), 'System development for linked-fermentation production of solvents from algal biomass', *Applied and Environmental Microbiology*, vol. 46, no. 5, pp. 1017-1023.

Naude, A & Nicol, W (2017), 'Fumaric acid fermentation with immobilised Rhizopus oryzae: Quantifying time-dependent variations in catabolic flux', *Process Biochemistry*, vol. 56, no. Supplement C, pp. 8-20.

Nguyen, MT, Choi, SP, Lee, J, Lee, JH & Sim, SJ (2009), 'Hydrothermal acid pretreatment of *Chlamydomonas reinhardtii* biomass for ethanol production', *Journal of Microbiology and Biotechnology*, vol. 19, no. 2, pp. 161-166.

Norris, R, Hori, T & Chihara, M (1980), 'Revision of the genus *Tetraselmis* (Class Prasinophyceae)', *Journal of Plant Research*, vol. 93, no. 4, pp. 317-339.

Northcote, DH, Goulding, KJ & Horne, RW (1958), 'The chemical composition and structure of the cell wall of *Chlorella pyrenoidosa*', *Biochemical Journal*, vol. 70, no. 3, pp. 391-397.

Oda, Y, Yajima, Y, Kinoshita, M & Ohnishi, M (2003), 'Differences of Rhizopus oryzae strains in organic acid synthesis and fatty acid composition', *Food Microbiology*, vol. 20, no. 3, pp. 371-375.

Okauchi, M & Kawamura, K (1997), 'Optimum medium for large-scale culture of Tetraselmis tetrathele', *Hydrobiologia*, vol. 358, no. 1, pp. 217-222.

Olaitan, SA & Northcote, DH (1962), 'Polysaccharides of *Chlorella pyrenoidosa*', *Biochemical Journal*, vol. 82, no. 3, pp. 509-519.

Oren, A (1983), 'A thermophilic amyloglucosidase from *Halobacterium sodomense*, a halophilic bacterium from the Dead Sea', *Current Microbiology*, vol. 8, no. 4, pp. 225-230.

Oren, A (2010), 'Industrial and environmental applications of halophilic microorganisms', *Environmental Technology*, vol. 31, no. 8, pp. 825-834.

Özer Uyar, GE & Uyar, B (2016), 'Effect of NaCl and KCl salts on growth and lactic acid production of Rhizopus Oryzae', *GIDA/The Journal of Food*, vol. 41, no. 5, pp. 299-304.

Parke, M & Manton, I (1965), 'Preliminary observations on fine structure of *Prasinocladus marinus*', *Journal of the Marine Biological Association of the United Kingdom*, vol. 45, no. 2, pp. 525-536.

Pena, MS, Hansen, MS & Stocks, SM (2012), 'A systematic approach for scaling Aspergillus niger industrial fermentation processes', *New Biotechnology*, vol. 29, p. S13.

Pidol, L, Lecointe, B, Starck, L & Jeuland, N (2012), 'Ethanol-biodiesel-Diesel fuel blends: Performances and emissions in conventional Diesel and advanced Low Temperature Combustions', *Fuel*, vol. 93, no. Journal Article, p. 329.

Pimtong, V, Ounaeb, S, Thitiprasert, S, Tolieng, V, Sooksai, S, Boonsombat, R, Tanasupawat, S, Assabumrungrat, S & Thongchul, N (2017), 'Enhanced effectiveness of Rhizopus oryzae by immobilization in a static bed fermentor for l-lactic acid production', *Process Biochemistry*, vol. 52, no. Supplement C, pp. 44-52.

Potts, T, Du, J, Paul, M, May, P, Beitle, R & Hestekin, J (2012), 'The production of butanol from Jamaica Bay macro algae', *Environmental Progress & Sustainable Energy*, vol. 31, no. 1, pp. 29-36.

Puig, S, Coma, M, van Loosdrecht, MCM, Colprim, J & Balaguer, MD (2007), 'Biological nutrient removal in a sequencing batch reactor using ethanol as carbon source', *Journal of Chemical Technology and Biotechnology*, vol. 82, no. 10, pp. 898-904.

Raes, E, Isdepsky, A, Muylaert, K, Borowitzka, M & Moheimani, N (2013), 'Comparison of growth of Tetraselmis in a tubular photobioreactor (Biocoil) and a raceway pond', *Journal of Applied Phycology*, pp. 1-9.

Rosowski, JR (1992), 'Specificity of bacterial attachment sites on the filamentous diatom Navicula confervacea (Bacillariophyceae)', *Canadian journal of microbiology*, vol. 38, no. 7, pp. 676-686.

Sawayama, S, Minowa, T & Yokoyama, SY (1999), 'Possibility of renewable energy production and CO2 mitigation by thermochemical liquefaction of microalgae', *Biomass and Bioenergy*, vol. 17, no. 1, pp. 33-39.

Sawayama, S & Tsukahara, K (2005), 'Liquid fuel production using microalgae', *Journal of the Japan Petroleum Institute*, vol. 48, no. 5, pp. 251-259.

Sayin, C (2010), 'Engine performance and exhaust gas emissions of methanol and ethanol–diesel blends', *Fuel*, vol. 89, no. 11, pp. 3410-3415.

Schenk, P, Thomas-Hall, S, Stephens, E, Marx, U, Mussgnug, J, Posten, C, Kruse, O & Hankamer, B (2008), 'Second Generation Biofuels: High-Efficiency Microalgae for Biodiesel Production', *BioEnergy Research*, vol. 1, no. 1, pp. 20-43.

Schneider, UA, Havlík, P, Schmid, E, Valin, H, Mosnier, A, Obersteiner, M, Böttcher, H, Skalský, R, Balkovic, J, Sauer, T & Fritz, S (2011), 'Impacts of population growth, economic development, and

technical change on global food production and consumption', *Agricultural Systems*, vol. 104, no. 2, pp. 204-215.

Shafiei, M, Ziaee, AA & Amoozegar, MA (2011), 'Purification and characterization of an organic-solvent-tolerant halophilic *α*-amylase from the moderately halophilic *Nesterenkonia* sp. strain F', *Journal of Industrial Microbiology & Biotechnology*, vol. 38, no. 2, pp. 275-281.

Sharypova, LA, Chataigné, G, Fraysse, N, Becker, A & Poinsot, V (2006), 'Overproduction and increased molecular weight account for the symbiotic activity of the rkpZ-modified K polysaccharide from Sinorhizobium meliloti Rm1021', *Glycobiology*, vol. 16, no. 12, pp. 1181-1193.

Shirai, F, Kunii, K, Sato, C, Teramoto, Y, Mizuki, E, Murao, S & Nakayama, S (1998), 'Cultivation of microalgae in the solution from the desalting process of soy sauce waste treatment and utilization of the algal biomass for ethanol fermentation', *World Journal of Microbiology and Biotechnology*, vol. 14, no. 6, pp. 839-842.

Shokrkar, H, Ebrahimi, S & Zamani, M (2017), 'Bioethanol production from acidic and enzymatic hydrolysates of mixed microalgae culture', *Fuel*, vol. 200, pp. 380-386.

Sims, R, Taylor, M, Saddler, J & Mabee, W (2008), *From 1st- to 2nd-generation biofuel technologies: an overview of curent industry and RD&D activities*, International Energy Agency.

Sivakumar, G, Vail, DR, Xu, J, Burner, DM, Lay Jr, JO, Ge, X & Weathers, PJ (2010), 'Bioethanol and biodiesel: alternative liquid fuels for future generations', *Engineering in Life Sciences*, vol. 10, no. 1, pp. 8-18.

Skory, CD, Freer, SN & Bothast, RJ (1997), 'Screening for ethanol-producing filamentous fungi', *Biotechnology Letters*, vol. 19, no. 3, pp. 203-206.

Soccol, CR, Vandenberghe, LPdS, Medeiros, ABP, Karp, SG, Buckeridge, M, Ramos, LP, Pitarelo, AP, Ferreira-Leitão, V, Gottschalk, LMF, Ferrara, MA, Silva Bon, EPd, Moraes, LMPd, Araújo, JdA & Torres, FAG (2010), 'Bioethanol from lignocelluloses: status and perspectives in Brazil', *Bioresource Technology*, vol. 101, no. 13, pp. 4820-4825.

Spotte, S (1979), *Fish and invertebrate culture: water management in closed systems*, John Wiley and sons.

Stephens, E, Ross, IL, King, Z, Mussgnug, JH, Kruse, O, Posten, C, Borowitzka, MA & Hankamer, B (2010), 'An economic and technical evaluation of microalgal biofuels', *Nature Biotechnology*, vol. 28, no. 2, pp. 126-128.

Størseth, TR, Hansen, K, Reitan, KI & Skjermo, J (2005), 'Structural characterization of β-D-(1→3)-glucans from different growth phases of the marine diatoms *Chaetoceros mülleri* and *Thalassiosira weissflogii*', *Carbohydrate Research*, vol. 340, no. 6, pp. 1159-1164.

Strizh, IG, Popova, LG & Balnokin, YV (2004), 'Physiological Aspects of Adaptation of the Marine Microalga Tetraselmis (Platymonas) viridis to Various Medium Salinity', *Russian Journal of Plant Physiology*, vol. 51, no. 2, pp. 176-182.

Suzuki, H (1974), 'Starch-type polysaccharide and mannitol in *Platymonas*', *Phytochemistry*, vol. 13, no. 7, pp. 1159-1160.

Taher, H, Al-Zuhair, S, Al-Marzouqi, AH, Haik, Y & Farid, MM (2011), 'A Review of Enzymatic Transesterification of Microalgal Oil-Based Biodiesel Using Supercritical Technology', *Enzyme Research*, vol. 2011, p. 25.

Taherzadeh, MJ, Fox, M, Hjorth, H & Edebo, L (2003), 'Production of mycelium biomass and ethanol from paper pulp sulfite liquor by< i> Rhizopus oryzae</i>', *Bioresource Technology*, vol. 88, no. 3, pp. 167-177.

Taherzadeh, MJ & Karimi, K (2007), 'Acid-based hydrolysis processes for ethanol from lignocellulosic materials: a review', *BioResources*, vol. 2, no. 3, pp. 472-499.

Thomas, WH, Seibert, DLR, Alden, M, Neori, A & Eldridge, P (1984), 'Yields, photosynthetic efficiencies and proximate composition of dense marine microalgal cultures. II. *Dunaliella primolecta* and *Tetraselmis suecica* experiments', *Biomass London*, vol. 5, pp. 211-225.

Thongchul, N, Navankasattusas, S & Yang, S-T (2010), 'Production of lactic acid and ethanol by Rhizopus oryzae integrated with cassava pulp hydrolysis', *Bioprocess and Biosystems Engineering*, vol. 33, no. 3, pp. 407-416.

Treco, DA & Lundblad, V 2001, 'Preparation of Yeast Media', *Current Protocols in Molecular Biology*, John Wiley & Sons, Inc.

Ueda, R, Hirayama, S, Sugata, K & Nakayama, H (1996), *Process for the production of ethanol from microalgae*, Mitsubishi Jukogyo Kabushiki Kaisha (Tokyo, JP), 08/310769, 5578472, United States.

Ueno, Y, Kurano, N & Miyachi, S (1998), 'Ethanol production by dark fermentation in the marine green alga, *Chlorococcum littorale*', *Journal of Fermentation and Bioengineering*, vol. 86, no. 1, pp. 38-43.

Uju, Wijayanta, AT, Goto, M & Kamiya, N (2015), 'Great potency of seaweed waste biomass from the carrageenan industry for bioethanol production by peracetic acid–ionic liquid pretreatment', *Biomass and Bioenergy*, vol. 81, pp. 63-69.

United Nations (2007), *World population prospects: the 2006 revision*, Department of Economic & Social Affairs, New York, accessed [15 February], <http://www.un.org/esa/population/publications/wpp2006/wpp2006.htm>.

Utting, SD (1985), 'Influence of nitrogen availability on the biochemical composition of three unicellular marine algae of commercial importance', *Aquacultural Engineering*, vol. 4, no. 3, pp. 175-190.

van der Oost, J, Bulthuis, BA, Feitz, S, Krab, K & Kraayenhof, R (1989), 'Fermentation metabolism of the unicellular cyanobacterium *Cyanothece* PCC 7822', *Archives of Microbiology*, vol. 152, no. 5, pp. 415-419.

Varga, E, Klinke, HB, Réczey, K & Thomsen, AB (2004), 'High solid simultaneous saccharification and fermentation of wet oxidized corn stover to ethanol', *Biotechnology and Bioengineering*, vol. 88, no. 5, pp. 567-574.

Vasisht, N, Bolhuis, A & Hutcheon, GW (2005), 'Characterisation of a highly stable *α*-amylase from the halophilic archaeon *Haloarcula hispanica*', *Extremophiles*, vol. 9, no. 6, pp. 487-495.

Ventosa, A, Martín, S, Sánchez-Porro, C & Mellado, E 2005, 'Halophilic archaea and bacteria as a source of extracellular hydrolytic enzymes', *Adaptation to Life at High Salt Concentrations in Archaea, Bacteria, and Eukarya*, vol. 9, Springer Netherlands, Dordrecht, pp. 337-354.

Ward, A & Lewis, D (2015), 'Pre-treatment options for halophytic microalgae and associated methane production', *Bioresource Technology*, vol. 177, pp. 410-413.

Ward, AJ, Lewis, DM & Green, FB (2014), 'Anaerobic digestion of algae biomass: A review', *Algal Research*, vol. 5, no. 0, pp. 204-214.

Wargacki, AJ, Leonard, E, Win, MN, Regitsky, DD, Santos, CNS, Kim, PB, Cooper, SR, Raisner, RM, Herman, A, Sivitz, AB, Lakshmanaswamy, A, Kashiyama, Y, Baker, D & Yoshikuni, Y (2012), 'An engineered microbial platform for direct biofuel production from brown macroalgae', *Science*, vol. 335, no. 6066, pp. 308-313.

Wesoff, E (2017), *Hard Lessons From the Great Algae Biofuel Bubble*, Greentech Media, accessed [28/04/2018], <https://www.greentechmedia.com/articles/read/lessons-from-the-great-algae-biofuel-bubble>.

Wilkinson, IA, Stacey, M & Bourne, EJ (1950), 'The composition of the polysaccharide synthesised by *Polytomella coeca*', *Journal of the Chemical Society*, pp. 2694-2698.

Woods, PR, Legere, E, Moll, B, Unamunzaga, C & Mantecon, E (2010a), *Closed photobioreactor system for continued daily in situ production, separation, collection, and removal of ethanol from genetically enhanced photosynthetic organisms*, Algenol Biofuels Switzerland GmbH (Zug, CH), 11/929503 US 7682821 B2, United States.

Woods, PR, Smith, CR, Kramer, D, Enke, H, Baier, K, Duhring, U, Ziegler, K, Lockau, W, Grundel, M, Coleman, J & Oesterhelt, C (2010b), *Genetically modified cyanobacteria for the production of ethanol*, Algenol Biofuels, Inc. (Baltimore, MD, US) US 2010/0068776 A1, United States.

Wucherpfennig, T, Hestler, T & Krull, R (2011), 'Morphology engineering - Osmolality and its effect on Aspergillus niger morphology and productivity', *Microbial Cell Factories*, vol. 10, no. 1, p. 58.

Wyman, CE (1999), 'Biomass ethanol: technical progress, opportunities, and commercial challenges', *Annual Review of Energy and the Environment*, vol. 24, pp. 189-226.

Wynne, D & Rhee, G-Y (1986), 'Effects of light intensity and quality on the relative N and P requirement (the optimum N:P ratio) of marine planktonic algae', *Journal of Plankton Research*, vol. 8, no. 1, pp. 91-103.

Yamamoto, FM & Rokushika, S (2004), 'Study of pH dependence using molecular modeling in reversed-phase liquid chromatography of 1-phenyl-3-methyl-5-pyrazolone derivatives of aldose', *Analytica Chimica Acta*, vol. 501, no. 2, pp. 143-149.

Yao, C-H, Ai, J-N, Cao, X-P & Xue, S (2013a), 'Characterization of cell growth and starch production in the marine green microalga Tetraselmis subcordiformis under extracellular phosphorus-deprived and sequentially phosphorus-replete conditions', *Applied Microbiology and Biotechnology*, pp. 1-12.

Yao, C-H, Ai, J-N, Cao, X-P & Xue, S (2013b), 'Salinity manipulation as an effective method for enhanced starch production in the marine microalga Tetraselmis subcordiformis', *Bioresource Technology*, vol. 146, no. 0, pp. 663-671.

Yao, C, Ai, J, Cao, X, Xue, S & Zhang, W (2012), 'Enhancing starch production of a marine green microalga Tetraselmis subcordiformis through nutrient limitation', *Bioresource Technology*, vol. 118, no. 0, pp. 438-444.

York, WS, Darvill, AG, McNeil, M & Albersheim, P (1985), '3-deoxy-d-manno-2-octulosonic acid (KDO) is a component of rhamnogalacturonan II, a pectic polysaccharide in the primary cell walls of plants', *Carbohydrate Research*, vol. 138, no. 1, pp. 109-126.

Zhang, K, Zhang, B & Yang, ST (2013), 'Production of citric, itaconic, fumaric, and malic acids in filamentous fungal fermentations', *Bioprocessing Technologies in Biorefinery for Sustainable Production of Fuels, Chemicals, and Polymers*, pp. 375-398.